2014

Mercury Distributions and Cycling in the North Atlantic and Eastern Tropical Pacific Oceans

Katlin L. Bowman
Wright State University

MERCURY DISTRIBUTIONS AND CYCLING IN THE NORTH ATLANTIC AND EASTERN TROPICAL PACIFIC OCEANS

A dissertation submitted in partial fulfillment of the requirements for the degree of Doctor of Philosophy

By

KATLIN L. BOWMAN
B.S., Wright State University, 2010

2014
WRIGHT STATE UNIVERSITY

WRIGHT STATE UNIVERSITY

GRADUATE SCHOOL

December 5, 2014

I HEREBY RECOMMEND THAT THE DISSERTATION PREPARED UNDER MY SUPERVISION BY Katlin Bowman ENTITLED **Mercury distributions and cycling in the North Atlantic and Eastern Tropical Pacific Oceans** BE ACCEPTED IN PARTIAL FULFILLMENT OF THE REQUIREMENTS FOR THE DEGREE OF Doctor of Philosophy.

_____

Chad Hammerschmidt, Ph.D.
Dissertation Director

_____

Donald Cipollini, Ph.D.
Director, ES Ph.D. Program

_____

Robert E.W. Fyffe, Ph.D.
VP for Research and
Dean of the Graduate School

Committee on Final Examination

_____

Carl Lamborg, Ph.D.

_____

William Fitzgerald, Ph.D.

_____

Steven Higgins, Ph.D.

_____ _____

Christopher Barton, Ph.D. Sarah Tebbens, Ph.D

ABSTRACT

Bowman, Katlin Ph.D., Environmental Sciences Ph.D. Program, Wright State University, 2014. Mercury distributions and cycling in the North Pacific and Eastern Tropical Pacific Oceans.

The distribution of mercury (Hg) in the ocean is complex as a result of in situ chemical transformations and inputs from natural and anthropogenic sources. Within the ocean, inorganic Hg is methylated to monomethylmercury (MMHg), which bioaccumulates and biomagnifies in marine food webs and poses a health risk to humans who eat fish. The biogeochemistry of Hg in the ocean has been studied for decades, however, recently improved sampling and analytical techniques have allowed for an enhanced understanding of global distributions of different Hg species. This dissertation uses a newly developed method for the analysis of MMHg that improves detection limits 10-fold over previous methods and allows for separation and analysis of dissolved gaseous dimethylmercury (DMHg) in the same sample. Filtered total Hg (HgT), MMHg, DMHg, and elemental Hg (Hg^0) were measured in high vertical and horizontal resolution in the water column of the North Atlantic (GA03) and eastern tropical South Pacific (GP16) Oceans, using vetted methods for the trace-metal clean sampling and analysis of Hg through the U.S. GEOTRACES program. Total Hg and MMHg were also measured in suspended particles across both sections. A wide range of oceanographic features important to Hg chemistry were sampled including oligotrophic waters in the Atlantic, productive upwelling waters in the Pacific, hydrothermal vent plumes, and deep and

intermediate water masses of varying ages and source regions. The subsurface distribution of Hg^0 was connected to the nitrogen cycle, with nutrient-like vertical distributions, similar to nitrate, in the Atlantic basin and increasing Hg^0 concentrations with denitrification in the Pacific. Filtered total Hg exhibited both scavenged- and nutrient-type vertical distributions in the Atlantic and nutrient-type distributions in the Pacific. Elevated concentrations of HgT were observed in a hydrothermal vent plume stemming from the Mid-Atlantic Ridge; however, Hg was not increased in a plume extending from the East Pacific Rise. Total Hg concentrations increased from younger to older Pacific deep waters but were anomalously high in Atlantic deep waters subducted within the past 200 y due to anthropogenic inputs. Young deep water impacted by anthropogenic Hg in the Atlantic contained 1.4× more methylated Hg (MMHg + DMHg) on average compared to unimpacted deep water in the Pacific. Dimethylmercury was often the dominant form of methylated Hg in deep water and concentrations of both MMHg and DMHg increased in aging Pacific deep water. Vertically stratified maxima of MMHg and DMHg were observed often near the subsurface chlorophyll maximum and frequently in low-oxygen thermocline waters where MMHg concentrations were 2× greater than DMHg. Methylated Hg was weakly positively correlated with apparent oxygen utilization, however, methylated Hg concentrations decreased with greater oxygen consumption. Concentrations of MMHg and DMHg were similar between Atlantic thermocline waters affected by anthropogenic Hg inputs and thermocline waters underlying the highly productive upwelling region in the eastern Pacific, despite substantial differences in oxygen concentrations. Analytical separation of methylated Hg species revealed unique and independent distributions of MMHg and DMHg. Data from

both cruise sections suggests that MMHg and DMHg are produced throughout the water column in oxygenated subsurface waters, low-oxygen thermocline waters, and likely in deep water masses. Comparison of oceanic sections following thermohaline circulation revealed the impact of anthropogenic Hg inputs with increased concentrations of HgT, MMHg, and DMHg in young (< 200 y) deep and subsurface Atlantic waters.

TABLE OF CONTENTS

LIST OF FIGURES

LIST OF TABLES

ACKNOWLEDGEMENTS

I would like to thank my advisor, Chad, for hiring me when I was 19-years-old to work as an undergraduate research technician, a part-time job that turned into a 7 year stay. I was able to learn and grow as a scientist through your trust and faith in me and I will always appreciate your mentorship. I thank Bill and Carl for adopting me into Team Hg; you have been insightful and enthusiastic mentors and a pleasure to work with. Wright State's Department of Earth and Environmental Sciences has taken care of me for over 8 years and for that I am grateful. I also thank the Environmental Science Ph.D. program and all of my committee members at Wright State for their time and commitment.

I thank my parents for their continued support and for fostering my interest in science at a young age. They helped me compete in 8 science fairs as a kid – my dad drove me around to streams and lakes during the winter and busted through ice with a sledge hammer so I could collect water samples. My mom proofread every single report and project board, and even let me ship plastic tubes of live ants to the house (my brother later knocked over the ant farm and those "live ants" stuck around longer than expected). Dan Vargo, Jodi Tayor, and Ray Wagner from Columbiana High School were also great supporters of my science fair efforts, and educators that go above and beyond their job descriptions.

I thank my siblings, past and present lab mates, and close friends for always making me laugh and keeping me grounded.

This dissertation would not have been possible without the U.S. GEOTRACES program and financial support from the U.S. National Science Foundation (Chemical Oceanography Division of Ocean Sciences; OCE-0928191, OCE-1132480, OCE-1232979). My work has benefited greatly from the collaborative efforts of dozens of scientists who have provided samples, high quality data, and thoughtful discussion. I also thank the captains and crews and of the R/V *Knorr* and R/V *Thompson* for making this work possible.

"Do not let your fire go out, spark by irreplaceable spark in the hopeless swamps of the not-quite, the not-yet, and the not-at-all. Do not let the hero in your soul perish in lonely frustration for the life you deserved and have never been able to reach. The world you desire can be won. It exists…it is real…it is possible…it's yours."
-Ayn Rand

Dedicated to Jeanne Dusi

1. INTRODUCTION

1.1. Mercury biogeochemistry

Mercury (Hg) enters the environment through natural sources such as weathering of mineral deposits and volcanic outgassing, and anthropogenic sources, mainly the combustion of coal and other fossil fuels for energy production (Fitzgerald et al., 2007). The ocean receives Hg inputs primarily from atmospheric deposition, although riverine discharge, remobilization from sediments, groundwater discharge, and submarine hydrothermal vents can be important (Mason et al., 2012; Amos et al., 2014). An estimated two thirds of Hg in the atmosphere is anthropogenic and man-made emissions are projected to increase during the next century (Fitzgerald et al., 1998; Pirrone, et al., 2010; Hammerschmidt, 2011; Kocman et al., 2013). Anthropogenic emissions have added 290 ± 80 million moles of Hg to the global ocean with two-thirds residing in thermocline waters where in situ chemical transformations may be most active (Lamborg et al., 2014).

The biogeochemistry of Hg in the ocean is controlled by biological and chemical processes that influence its transport, fate, and chemical speciation (Fig. 1). Elemental Hg (Hg^0) in the atmosphere is oxidized to Hg^{2+} and deposited to the surface ocean in either wet or dry deposition (Holmes et al., 2009; Mason et al., 2001). In the mixed layer, reduction processes transform some of the Hg^{2+} back to Hg^0, which often results in supersaturation and evasion back to the atmosphere (Andersson et al., 2011). Hg^{2+} can be either reduced throughout the water column, complexed with dissolved and particulate ligands, or methylated to methylmercury (CH_3Hg^+, MMHg) and dimethylmercury ($(CH_3)_2Hg$, DMHg). Dimethylmercury is thought to be a relatively short-lived gas and

found mainly in cold, deep waters (Mason et al., 1995). Monomethylmercury is a bioaccumulative, toxic species of Hg found in marine sediments and throughout the water column (Mason et al., 2012); MMHg biomagnifies in marine food webs and is known to affect cardiovascular, endocrine, and neurological systems, posing a health threat to humans who eat fish and piscivorous wildlife (Zahir et al., 2005; Scheuhammer et al., 2007; Sunderland, 2007; Bose-O'Reilly et al., 2010; Karimi et al., 2012).

The formation and relationship between MMHg and DMHg in seawater is poorly understood; the two species may be produced either independently or through a series of methyl-group transfer reactions. Monomethylmercury production is hypothesized to occur through abiotic pathways in surface water and rainwater (Celo et al., 2006; Hammerschmidt et al., 2007), however, microbial production is thought to be the dominant source in sediments (Benoit et al., 2003). In sediments, Hg methylation occurs under anoxic conditions through the activity of sulfate- and iron-reducing bacteria, and possibly methanogens (King et al., 2000; Kerin et al., 2006; Hamelin et al., 2011; Graham et al., 2012). Incubation studies have observed production of DMHg and MMHg in seawater under both oxic and low-oxygen conditions (Lehnherr et al., 2011; Monperrus et al., 2007). Genomic studies have identified specific genes associated with Hg reduction (*merA*) and methylation (*hgcAB*), however, the abundance of these genes in marine systems has yet to be explored (Barkay and Wagner-Döbler, 2005; Parks et al., 2013; Gilmour et al., 2013). Biotic and abiotic processes also decompose methylated Hg (Barkay et al., 2003; Zhang and Hsu-Kim, 2010); therefore the oceanic distributions of MMHg and DMHg likely reflect a steady-state condition between competing methylation and demethylation reactions.

1.2. Human exposure to Hg and associated health risks

Mercury became widely recognized as an environmental toxin during the 1950s and 1960s when waste from the Chisso Company in Minamata, Japan, was discharged into Minamata Bay. Monomethylmercury in the waste biomagnified within the food web, subsequently poisoning wildlife and humans who consumed locally harvested seafood. Thousands of people suffered from severe neurological and developmental impairments in what is known as one of the worst environmental disasters in history (NIMD, 2013). Today the threat of Hg pollution is more subtle; mass poisoning events similar to Minamata are now unheard of, however, humans are still exposed to MMHg through the consumption of fish and a majority of those fish are harvested from the ocean (Mahaffey, 2004; Sunderland, 2007; Višnjevec et al., 2014; FAO, 2014). Exposure to MMHg in utero has been associated with impaired neurological development in children (Mahaffey et al., 2011). An estimated 10% of U.S. women of child-bearing age have blood MMHg levels high enough to increase these risks in their unborn children (Mahaffey et al., 2009). Adults exposed to high doses of MMHg also can experience neurological as well as cardiovascular impairments (Edna et al., 2003; Auger et al., 2005; Stern et al., 2005; Mergler et al., 2007).

Fish is a nutritionally valuable food source that supplies the global population with 15–20% of animal protein needs and contains omega-3 fatty acids important for brain growth and development (Mahaffey et al., 2011; FAO, 2014). Anthropogenic inputs have increased concentrations of inorganic Hg in the ocean and industrial emissions are expected to continue rising this century (Streets et al., 2009; Hammerschmidt, 2011; Lamborg et al., 2014). Additional emissions will continue to increase loadings of Hg to

the ocean, which could exacerbate exposures of humans and wildlife. It is therefore important to understand Hg biogeochemistry in marine systems to better assess how future emission scenarios will affect the ocean and, by extension, humans who eat seafood.

1.3. Oceanic distribution of Hg

There are two published data sets for Hg in the Atlantic Ocean, one in subpolar North Atlantic waters near regions of deep water formation (Mason et al., 1995) and the other in the western South Atlantic (Mason & Sullivan 1999). These studies reported average HgT concentrations around 2 pM in unfiltered samples with up to 57% as Hg^0 in the mixed layer. Monomethylmercury concentrations were below detection limit (<50 fM) and DMHg was found mainly in deep waters, where it was thought to be produced during deep water formation (Mason et al., 1995). More data exist for the Pacific Ocean, where HgT concentrations are reported to be closer to 1 pM, however, a majority of this data is limited to the upper 1000 m of the water column (Mason and Fitzgerald 1993; Laurier et al., 2004; Sunderland et al., 2009; Hammerschmidt and Bowman, 2012).

Historical data suggest that vertical profiles of HgT have either a scavenged- or nutrient-type distribution, with Hg removal from surface waters through either bioaccumulation or adsorption to sinking particles and released at intermediate depths through remineralization processes (Mason et al., 2012). In deep water, total Hg is generally homogenous with depth and concentrations below the thermocline reflect the drawdown of atmospheric Hg during water mass formation and release of Hg from sinking biological material (Lamborg et al., 2014).

Insufficient detection limits and the analytical challenge of separating MMHg and DMHg have inhibited our understanding of methylated Hg in the ocean (many studies report $MeHg_T$, the summation of MMHg and DMHg concentrations). Regardless of these challenges, a general vertical trend has been observed in multiple ocean basins; methylated Hg is low in surface waters due to removal processes (photodecomposition and adsorption of MMHg, atmospheric evasion of DMHg), with maxima in low-oxygen regions of the water column and homogenous concentrations in deep water (Mason et al, 2012). In situ production is hypothesized to be the primary source of methylated Hg maxima in oxygen minimum zones (OMZs). Remineralization of organic matter in OMZs releases inorganic Hg and organic substrate to fuel heterotrophic microbes that may produce MMHg and DMHg within the water column. Significant correlations between methylated Hg and either dissolved oxygen, apparent oxygen utilization, or organic carbon remineralization rate have been observed in the Mediterranean Sea, South Atlantic, North Pacific and Southern Oceans (Mason and Fitzgerald, 1991; Mason and Sullivan, 1999; Kirk et al., 2008; Sunderland et al., 2009; Heimbürger et al., 2010; Cossa et al., 2011; Lehnherr et al., 2011).

The dominant form of methylated Hg and lifetimes of MMHg and DMHg in the ocean are uncertain. In the Atlantic and equatorial Pacific Oceans, DMHg was the dominant methylated species while MMHg concentrations were 2–4× greater than DMHg in the North Pacific (Mason et al., 1995; Mason and Sullivan, 1999; Hammerschmidt and Bowman, 2012). Mechanistic studies in polar marine waters also have found greater rate constants for the production of MMHg from isotopically labeled Hg(II) compared to DMHg production (Lehnherr et al., 2011). The estimated lifetime of DMHg in oceanic

waters is <50 y while no estimates for MMHg exist (Mason and Fitzgerald, 1993; Mason and Sullivan 1999). The importance of external sources verses in situ production and the time needed to reach steady state between production and loss in deep waters needs to be examined in order to constrain estimates of methylated Hg in the ocean.

1.4. Specific aims

By participating in two U.S. GEOTRACES zonal sections, I generated high-resolution, full-depth profiles of Hg species in the North Atlantic and eastern tropical South Pacific Oceans. Low-level (femtomolar) MMHg measurements in seawater were made with a new method that allows for separation and analysis of DMHg from the same sample (Chapter 2; Bowman and Hammerschmidt, 2010). Filtered and particulate HgT and MMHg and dissolved gaseous Hg^0 and DMHg were measured during the zonal sections of the North Atlantic (Chapter 3; Bowman et al., 2014) and eastern Pacific Ocean (Chapter 4). My objective was to use these two oceanic data sets to improve understanding of the distribution and behavior of Hg in the ocean. Chapter 5 compares the distribution of MMHg and DMHg between similar and contrasting oceanographic features of the Atlantic and Pacific Oceans.

GEOTRACES is an international program with a central goal of quantifying fluxes and processes of key trace elements and their isotopes in the global ocean (geotraces.org). By participating in GEOTRACES cruises I had access to trace metal, nutrient, and radioisotope data that assisted in my interpretation of Hg distributions in regard to the oceanographic processes taking place in both basins. Each section

encompassed a variety of either unique or prominent oceanographic features, outlined below.

1.4.1 North Atlantic zonal transect key features

- Deep water masses formed in the subpolar North Atlantic (North Atlantic Deep Water, NADW) and Southern Ocean (Antarctic Bottom Water, AABW). NADW across this section ranged in age from ~90 y to ~200 y.
- Intermediate waters from the subpolar North Atlantic (Irminger Sea Water), Southern Ocean (Antarctic Intermediate Water), and Mediterranean Sea (Mediterranean Overflow Water).
- Broad continental shelf in the western (North America) and eastern basins (Europe & Africa).
- Oligotrophic surface water in the Sargasso Sea and more productive waters near the coast of Africa where an OMZ is pronounced.
- A buoyant hydrothermal vent plume over the Mid-Atlantic Ridge.
- Atmospheric inputs from industrial (North America and Europe) and natural (Saharan dust) sources.

1.4.2 Eastern Pacific zonal transect key features

- Deep water among the oldest in the ocean (Pacific Deep Water and Modified Pacific Deep Water), as well as deep water more recently subducted from the Antarctic Circumpolar Current (Lower Circumpolar Deep Water).

- Intermediate water from the Southern Ocean (Antarctic Intermediate Water) and mode waters from the Southwestern Pacific (South Pacific Subtropical Mode Water) and Antarctic Circumpolar Current (Subantarctic Mode Water).
- A narrow continental margin and subduction zone (Peru trench, ~5500 m).
- Highly productive surface waters resulting from upwelling near the Peru margin that create a suboxic (2–10 μmol kg^{-1} O_2) oxygen minimum zone. Oligotrophic waters west of the upwelling zone.
- A buoyant hydrothermal vent plume extending west from the East Pacific Rise located between 2000–3000 m depth.

1.5. Hypotheses

I had the following hypotheses related to the distributions and behavior of Hg species in the ocean:

1) Release from sinking particles will increase Hg concentrations in deep water over time, however, deep water downwelled within the last 100–200 y may contain more Hg than older waters due to anthropogenic inputs.
2) MMHg, DMHg, and Hg^0 produced in continental margin sediments will be mobilized to overlying water in both basins. Efflux from deep-sea sediments will not be a significant source.
3) Vertical maxima of MMHg and DMHg will be found in the OMZ, with greater concentrations in OMZs under more productive waters where microorganisms suspected of producing methylated-Hg thrive under low-oxygen conditions generated by remineralization processes.

4) Dissolved Hg^0 in deep water masses will decrease with age as a result of dark oxidation reactions. Distributions of Hg^0 will correlate with nitrite, suggesting Hg resistance (*merA*) in nitrifying bacteria.
5) Input of hydrothermal fluids in the Atlantic and Pacific will be a significant source of Hg to deep waters in both basins.
6) Because Hg methylation has been observed in both oxic and low-oxygen seawater, MMHg and DMHg will not have a significant correlation with apparent oxygen utilization.
7) MMHg may correlate with Fe(II) and cobalt; Fe-reducing bacteria have been shown to produce MMHg in culture (Kerin et al., 2006) and production of vitamin B-12 (cobalt dependent) via the acetyl Co-A pathway releases excess methyl groups that may contribute to MMHg production (Choi et al., 1994; Ekstrom et al., 2003).
8) DMHg will be the dominant form of methylated-Hg in deep water, but the MMHg:DMHg molar ratio in surface and intermediate waters will be >1.

References

Amos, H.M., Jacob, D.J., Kocman, D., Horowitz, H.M., Zhang, Y., Dutkiewicz, S., et al. 2014. Global biogeochemical implications of mercury discharges from rivers and sediment burial. Environ. Sci. Technol. 48, 9514–9522.

Andersson, M.E., Sommar, J., Gårdfeldt, K., Jutterström, S. 2011. Air-sea exchange of volatile mercury in the North Atlantic Ocean. Mar. Chem. 125, 1–7.

Auger, N., Kofman, O., Kosatsky, T., Armstrong, B. 2005. Low-level methylmercury exposure as a risk factor for neurologic abnormalities in adults. Neurotoxicology. 26, 149–157.

Barkay, T., Miller, S. M. & Summers, A. O. 2003. Bacterial mercury resistance from atoms to ecosystems. FEMS Microbiol. Rev. 27, 355–384.

Barkay, T., Wagner-Döbler, I. 2005. Microbial transformations of mercury: Potentials, challenges, and achievements in controlling mercury toxicity in the environment. Adv. Appl. Microbiol. DOI: 10.1016/S0065-2164(05)57001-1.

Benoit, J. M., C. C. Gilmour, A. Heyes, R. P. Mason, and C. L. Miller. 2003. Geochemical and biological controls over methylmercury production and degradation in aquatic systems, p. 262–297. *In* Y. Cai and O. C. Braids [eds.], Biogeochemistry of environmentally important trace metals. American Chemical Society.

Bose-O'Reilly, S., McCarty, K.M., Steckling, N., Lettmeier, B. 2010. Mercury exposure and children's health. Curr. Probl. Pediatr. Adolesc. Health Care 40, 186–215.

Bowman, K.L., Hammerschmidt, C.R. 2011. Extraction of monomethylmercury from seawater for low-femtomolar determination. Limnol. Oceanor-Meth. 9, 121–128.

Bowman, K.L., Hammerschmidt, C.R., Lamborg, C.H., Swarr, G. 2014. Mercury in the North Atlantic Ocean: The U.S. GEOTRACES zonal and meridional sections. Deep-Sea Res. II. DOI: 10.1016/j.dsr2.2014.07.004.

Celo, V., Lean, D. R. S & Scott, S. L. 2006. Abiotic methylation of mercury in the aquatic environments. Sci. Tot. Environ. 368, 126–137.

Choi, S., Chase, T. Jr., Bartha, R. 1994. Metabolic pathways leading to mercury methylation in Desulfovibrio desulfuricans. Appl. Environ. Microbio. 60: 4072-4077.

Cossa, D., Heimbürger, L.-E., Lannuzel, D., Rintoul, S.R., Butler, E.C.V., Bowie, A.R., et al. 2011. Mercury in the Southern Ocean. Geochim. Cosmochim. Ac. 75, 4037–4052.

Edna, Y., Joaquim, V., Lynn, G., Illeane, P., Ellen, S. 2003. Low level methylmercury exposure affects neuropsychological function in adults. Environ. Health. 2, 8.

Ekstrom, E.B., Morel, F.M.M., Benoit, J.M. 2003. Mercury methylation independent of the acetyl-coenzyme A pathway in sulfate-reducing bacteria. App. Environ. Microbiol. 69: 5414-5422.

(FAO) Food and Agricultural Organization of the United Nations, 2014. The state of world fisheries and aquaculture. <www.fao.org/publications>.

Fitzgerald, W.F., Engstrom, D.R., Mason, R.P., Nater, E.A. 1998. The case from atmospheric mercury contamination in remote areas. Environ. Sci. Technol. 32, 1–7.

Fitzgerald, W.F., Lamborg, C.H., Hammerschmidt, C.R. 2007. Marine biogeochemical cycling of mercury. Chem. Rev. 107, 641–662.

Graham A. M., Bullock, A. L., Maizel, A. C., Elias, D. A. & Gilmour, C. C. 2012. Detailed assessment of the kinetics of Hg-cell association, Hg methylation, and methylmercury degradation in several Desulfovibrio species. Appl. Environ. Microbiol. 78, 7337–7346.

Gilmour, C.C., Podar, M., Bullock, A.L., Graham, A.M., Brown, S.D., Somenahally, A.C., et al. 2013. Mercury methylation by novel microorganisms from new environments. Environ. Sci Technol. 47, 11810–11820.

Hamelin, S., Amyot, M., Barkay, T., Wang, Y. P. & Planas, D. 2011. Methanogens: principal methylators of mercury in lake periphyton. Environ. Sci. Technol. 45, 7693–7700.

Hammerschmidt, C.R., Lamborg, C.H., Fitzgerald, W.F. 2007. Aqueous phase methylation as a potential source of methylmercury in wet deposition. Atmos. Environ. 41, 1663–1668.

Hammerschmidt, C.R. 2011. Mercury and carbon dioxide relationships: Uncoupling a toxic relationship. Environ. Toxicol. Chem. 30, 2640–2646.

Hammerschmidt, C.R., Bowman, K.L. 2012. Vertical methylmercury distribution in the subtropical North Pacific Ocean. Mar. Chem. 132, 2640-2646.

Heimbürger, L.-E., Cossa, D., Marty, J.-C., Migon, C., Averty, B., Dufour, A., Ras, J. 2010. Methyl mercury distributions in relation to the presence of nano- and picophytoplankton in an oceanic water column (Ligurian Sea, North-western Mediterranean). Geochim. Cosmochim. Acta 74, 5549–5559.

Holmes, C.D., Jacob, D.J., Yang, X. 2006. Global lifetime of elemental mercury against oxidation by atomic bromine in the free troposphere. Geophys. Res. Lett. 33, doi:10.1029/2006GL027176

Holmes, C.D., Jacob, D.J., Mason, R.P., Jaffe, D.A. 2009. Sources and deposition of reactive gaseous mercury in the marine atmosphere. Atmos. Environ. 43, 2278–2285.

Karimi, R., Fitzgerald, T.P., Fisher, N.S. 2012. A quantitative synthesis of mercury in commercial seafood and implications for exposure in the United States. Environ. Health Perspect. 120, 1512–1519.

Kerin, E. J., Gilmour, C.C., Roden, R., Suzuki, M.T., Coates, J.D., Mason, R.P. 2006. Mercury methylation by dissimilatory iron-reducing bacteria. Appl.Environ. Microbiol. 72, 7919–7921.

King, J. K., Kostka, J. E., Frischer, M. E. & Saunders, F. M. 2000. Sulfate-reducing bacteria methylate mercury at variable rates in pure culture and in marine sediments. Appl. Environ. Microbiol. 66, 2430–2437.

Kirk, J.L., St. Louis, V.L., Hintelmann, H., Lehnherr, I., Else, B., Poissant, L. 2008. Methylated mercury species in marine waters of the Canadian High and Sub Arctic. Environ. Sci. Technol. 42, 8367–8373.

Kocman, D., Horvat, M., Pirrone, N., Cinnirella, S. 2013. Contribution of contaminated sites to the global mercury budget. Environ. Res. http://dx.doi.org/10.1016/j.envres.2012.12.011.

Lamborg, C.H., W.F. Fitzgerald, A.W.H. Damman, J.M. Benoit, P.H. Balcom, and D.R. Engstrom. 2002. Modern and historic atmospheric mercury fluxes in both hemispheres: global and regional mercury cycling implications. Global Biogeochem. Cycles 16:1104-1114.

Lamborg, C.H., Hammerschmidt, C.R., Bowman, K.L., Swarr, G.J., Munson, K.M., Ohnemus, D.C., et al. 2014. A global ocean inventory of anthropogenic mercury based on water column measurements. Nature. DOI:10.1038/nature13563.

Laurier, F.J.G., Mason, R.P., Gill, G.A., Whalin, L. 2004. Mercury distributions in the North Pacific Ocean – 20 years of observations. Mar. Chem. 90, 3-19.

Lehnherr, I., St. Louis, V.L., Hintelmann, H., Kirk, J.L. 2011. Methylation of inorganic mercury in polar marine waters. Nat. Geosci. 4, 298–302.

Lindberg, S., Bullock, R., Ebinghaus, R., Engstrom, D., Feng, X., Fitzgerald, W et al. 2007. A synthesis of progress and uncertainties in attributing the sources of mercury in deposition. Ambio. 36, 19–32.

Mahaffey, K.R. 2004. Fish and shellfish as dietary sources of methylmercury and the ω-3 fatty acids, eicosahexaenoic acid and docosahexaenoic acid: risks and benefits. Environ. Res. 95, 414–428.

Mahaffey, K.R., Clickner, R.P., Jeffries, R.A. 2009. Adult women's blood mercury concentrations vary regionally in the United States: association with patterns of fish consumption (NHANES 1999–2004). Environ. Helath Perspect. 117, 47–53.

Mahaffey, K.R., Sunderland, E.M., Chan, H.M., Choi, A.L., Grandjean, P., Mariën, K., et al. 2011. Balancing the benefits of n-3 polyunsaturated fatty acids and the risks of methylmercury exposure from fish consumption. Nutr. Rev. 69, 493–508.

Mason, R.P, Fitzgerald, W.F. 1991. Mercury speciation in open ocean waters. Water Air Soil Poll. 56, 779–798.

Mason, R.P, Fitzgerald, W.F. 1993. The distribution and biogeochemical cycling of mercury in the equatorial Pacific Ocean. Deep-Sea Res. I 40, 1897–1924.

Mason, R.P., Rolfhus, K.R., Fitzgerald, W.F. 1995. Methylated and elemental mercury cycling in surface and deep ocean waters of the North Atlantic. Water Air Soil Pollut. 80, 665–677.

Mason, R.P., Sullivan, K.A. 1999. The distribution and speciation of mercury in the South and equatorial Atlantic. Deep-Sea Res. II 46, 937–956.

Mason, R.P., Lawson, N.M., Sheu, G.-R. 2001. Mercury in the Atlantic Ocean: factors controlling air-sea exchange of mercury and its distribution in the upper waters. Deep-Sea Res. II 48, 2829–2853.

Mason, R.P., Choi, A.L., Fitzgerald, W.F., Hammerschmidt, C.R., Lamborg, C.H., Soerensen, A.L., Sunderland, E.M. 2012. Mercury biogeochemical cycling in the ocean and policy implications. Environ. Res. 119, 101–117.

Mergler, D., Anderson, H.A., Chan, L.H.M., Mahaffey, K.R., Murray, M., Sakamoto, M., Stern, A.H. 2007. Methylmercury exposure and health effects in humans: A worldwide concern. Ambio. 36, 3–11.

Monperrus, M., Tessier, E., Amouroux, D., Leynaert, A., Huonnic, P., Donard, O.F.X. 2007. Mercury methylation, demethylation and reduction rates in coastal and marine surface waters of the Mediterranean Sea. Mar. Chem. 107, 49–63.

(NIMD) National Institute for Minamata Disease. 2013. Minamata Disease Q&A. Japan Ministry of the Environment. http://www.nimd.go.jp/english/.

Parks, J. M., A. Johs, M. Podar, R. Bridou, R. A. Hurt, S. D. Smith, et al. 2013. The Genetic Basis for Bacterial Mercury Methylation. Science, 10.1126/science.1230667.

Pirrone, N., Cinnirella, S., Feng, X., Finkelman, R.B., Friedli, H.R., Leaner, J., et al. 2010. Global mercury emissions to the atmosphere from anthropogenic and natural sources. Atmos. Chem. Phys. 10, 5951–5964.

Scheuhammer, A.M., Meyer, M.W., Sandheinrich, M.B., Murray, M.W. 2007. Effects of environmental methylmercury on the health of wild birds, mammals, and fish. Ambio. 36, 12–18.

Stern, A.H. 2005. A review of the studies of the cardiovascular health effects of methylmercury with consideration of their suitability for risk assessment. Environ. Res. 98, 133–142.

Streets, D. G., Q. Zhang and Y. Wu. 2009. Projections of Global Mercury Emissions in 2050. Environ. Sci. Technol. 43, 2983-2988.

Sunderland, E. M. 2007. Mercury exposure from domestic and imported estuarine and marine fish in the U.S. seafood market. Environ. Health Perspect. 115, 235–242.

Sunderland, E.M., Krabbenhoft, D.P., Moreau, J.W., Strode, S.A., Landing, W.A. 2009. Mercury sources, distribution, and bioavailability in the North Pacific Ocean: Insights from data and models. Global Biogeochem. Cycles 23, GB2010.

Višnjevec, A.M., Kocman, D., Horvat. M. 2014. Human mercury exposure and effects in Europe. Environ. Toxicol. Chem. 33, 1259–1270.

Zahir, F., Rizwi, S.J., Haq, S.K., Khan, R.H. 2005. Low dose mercury toxicity and human health. Environ. Toxicol. Pharmacol. 20, 351–360.

Zhang, T. & Hsu-Kim, H. 2010. Photolytic degradation of methylmercury enhanced by binding to natural organic ligands. Nature Geosci. 3, 473–476.

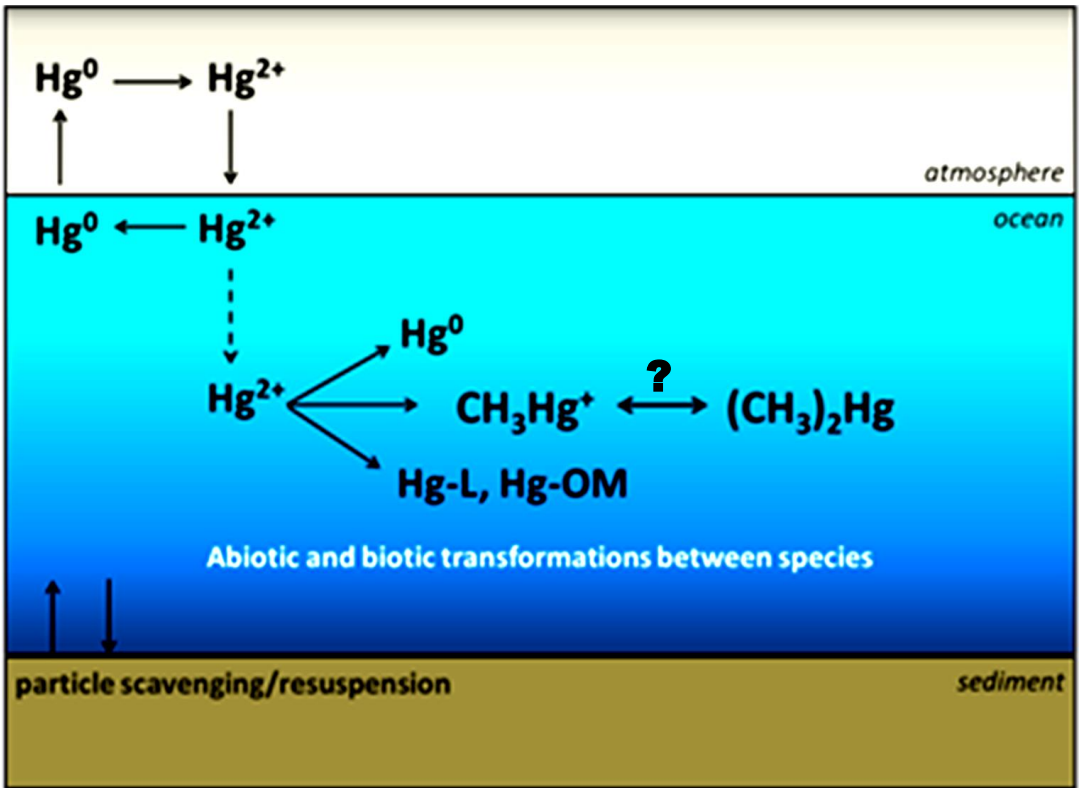

Figure 1.1. Mercury biogeochemistry in the ocean.

2. EXTRACTION OF MONOMETHYLMERCURY FROM SEAWATER FOR LOW-FEMTOMOLAR DETERMINATION

Bowman, K.L., Hammerschmidt, C.R. 2011. Extraction of monomethylmercury from seawater for low-femtomolar determination. Limnol. Oceanogr.: Methods, 9, 121–128.

Abstract

Humans are exposed to toxic monomethylmercury (MMHg) principally by the consumption of marine fish. However, and due in part to analytical limitations, little is known about the distribution, sources, and biogeochemical cycling of MMHg in the ocean, where aqueous concentrations are in the femtomolar range and often less than current limits of detection. Here, we present a simple method for extraction and analysis of MMHg in seawater that has a detection limit of about 2 fM for a 2-L sample, which is a 10-fold improvement over current approaches. The technique, which is readily adaptable to a shipboard laboratory, involves purging and quantification of dimethylmercury (DMHg) from an unaltered 2-L water sample followed by acidification to 1% with H_2SO_4 for > 6 h, pH neutralization, derivatization of MMHg in the seawater matrix with an ethylating agent, and purge-and-trap analysis with gas-chromatographic cold-vapor atomic fluorescence spectrometry. The method was developed and validated with analyses of seawater from the North Atlantic and Pacific Oceans, in addition to two fresh waters. This technique can be used to quantify, differentiate, and develop an improved understanding of the biogeochemistries of MMHg and DMHg in the ocean.

2.1. Introduction

Monomethylmercury (MMHg) is the highly toxic form of mercury that accumulates in aquatic biota. MMHg is produced from complexes of inorganic Hg (Hg(II)) by microorganisms (Benoit et al., 2003), concentrated from water by phytoplankton (Mason et al., 1996), and subsequently biomagnified through successive dietary trophic transfers (Wiener et al., 2003), resulting in some fish having MMHg levels that may be harmful to piscivorous wildlife (Scheuhammer et al., 2007) and humans who eat fish (Mergler et al., 2007). Most of the fish consumed by humans are from the marine environment (U.S. EPA, 2002); however, and due in part to analytical limitations, little is known about the distribution, sources, and biogeochemical cycling of MMHg in the ocean, where aqueous concentrations are in the femtomolar range and often less than current limits of detection (Fitzgerald et al., 2007).

Most current methods for determination of MMHg involve extraction from natural solution, derivatization to a volatile compound, pre-concentration and separation of the derivative by gas chromatography (Bloom, 1989), and detection by either cold-vapor atomic fluorescence spectrometry (CVAFS; Bloom and Fitzgerald, 1988) or inductively coupled plasma mass spectrometry (ICPMS; Hintelmann and Evans, 1997). Aqueous distillation and solvent-solvent extraction with CH_2Cl_2 (Horvat et al., 1993), both of which include an acidification step, are techniques used commonly to separate MMHg from organic and inorganic constituents in natural waters that may interfere with the derivatization reaction, which is often by alkylation (Bloom, 1989) or hydride generation (Filippelli et al., 1992). These analytical separations also result in dimethylmercury (DMHg), if present, being decomposed to MMHg (Wood et al., 1968;

Black et al., 2009) and therefore artifactually bias measured levels of MMHg. With typical sample volumes of 0.1−0.2 L, method detection limits for aqueous MMHg are often between about 40 and 100 fM. While such limits of detection are sufficient for analysis of MMHg in most fresh (e.g., Hurley et al., 1995; St. Louis et al., 2005; Brigham et al., 2009) and coastal marine (e.g., Hammerschmidt and Fitzgerald, 2006; Kirk et al., 2008; Kotnik et al., 2007; Cossa et al., 2009) waters, they result often in MMHg being undetectable in open-ocean seawater (Fitzgerald to al., 2007) and thereby present a limitation to understanding the biogeochemistry of this toxic and bioaccumulative compound in the marine environment.

We have developed a simple technique for extraction and analysis of MMHg in seawater that lowers the detection limit to about 2 fM for a 2-L sample and isolates DMHg from MMHg. Instead of developing a more sensitive measurement technology, we sought to improve the detection limit for MMHg by increasing the volume of sample from which it is pre-concentrated, which requires an alternative to distillation and solvent extraction for sample pre-treatment. Prior studies have shown that MMHg in freshwaters may be determined quantitatively by direct ethylation with sodium tetraethylborate (e.g., Holz et al., 1999; Rolfhus et al., 2003; Hammerschmidt and Fitzgerald, 2010). It has been suggested, however, that direct ethylation of MMHg is ineffective for seawater because chloride interferes with the reaction (Bloom, 1989). Our initial tests of this assumption proved similar: MMHg could be recovered by direct ethylation, albeit not completely (50−80% recovery of known additions). Hence, we conducted a suite of laboratory experiments to optimize a direct ethylation technique with the goal of quantitatively recovering MMHg from seawater. We found that acidification of seawater

to 1% with concentrated H_2SO_4, after removal of gaseous DMHg by purging, results in MMHg being sufficiently labile for quantitative derivatization directly in the seawater matrix. This technique was developed and validated with experimental laboratory and shipboard analyses of seawater from the North Atlantic and Pacific Oceans, in addition to two fresh waters.

2.2. Materials and procedures

2.2.1 Water

Seawater for laboratory tests was obtained from an open-ocean location in the northwest Atlantic Ocean (38° 43' N, 70 °W) in August 2008. Surface water from the Atlantic (salinity = 33.27; dissolved organic carbon = 85 µM) was sampled with a trace-metal clean rosette at 10 m depth, capsule filtered (0.45 µm; Meissner Alpha, polyethylene membrane) promptly after collection, and stored in a 50-L polyethylene carboy. No DMHg was detected (< 2 fM). Seawater was sampled similarly from various depths of the North Pacific Ocean (30 °N, 140 °W), capsule filtered (0.2 µm; Pall AcroPak-200, polyethersulfone membrane) directly from rosette bottles, and used for shipboard analytical tests during the U.S. GEOTRACES Intercalibration cruise in May 2009.

2.2.2 Methylmercury quantification

MMHg was determined by gas-chromatographic CVAFS (Bloom, 1989) with a Hg speciation analyzer that we have described previously (Tseng et al., 2004). In laboratory and shipboard tests, a known volume of aqueous sample (0.2–2 L) was introduced to a gas-liquid separator (GLS). For 0.2-L samples, the GLS was a 0.5-L glass side-arm flask that was in-line with the Hg speciation analyzer (Tseng et al., 2004).

The GLS for 2-L samples during the North Pacific cruise was a 2-L FEP Teflon bottle capped with a multi-port cap and impinger (Omnifit Q-series; Danbury, CT), which is off-line of the Hg speciation analyzer. The pH of samples was adjusted to 4.9 with 4 M acetate buffer and an aliquot of ice-cold 1% (wt:vol) sodium tetraethylborate (NaTEB; Strem Chemical, Newburyport, MA) added as the derivatization reagent (U.S. EPA, 2001). The volume of added NaTEB was 0.1−0.2% of the sample. NaTEB reacts with MMHg and Hg(II) to produce methylethylmercury (MeEtHg, the MMHg derivative) and diethylmercury (the Hg(II) derivative), which are gases and can be purged quantitatively from solution. NaTEB was allowed to react with sample Hg in a closed GLS before purging derivatives from solution with N_2 through a fine-pore glass or ceramic frit located at the bottom of the GLS. The N_2 was ultra-high purity (grade 5.0) and cleaned of Hg by passage through Au-coated glass beads and Tenax TA resin (23% graphitized carbon, 20/35 mesh, Alltech) prior to the GLS. Optimal duration of the derivatization reaction and N_2 purging conditions were investigated and described below in the assessment.

Effluent gas from the GLS, containing sample MeEtHg, passed through a Teflon column (10 cm long, 3.2 mm ID) packed with reagent-grade soda lime (~20 mesh) and then a glass column (10 cm long, 3.2 mm ID) packed with Tenax TA. Soda lime removes water vapor/aerosols and neutralizes any acidity in the gas stream, whereas Tenax sequesters volatile methylmercury species. Soda lime columns were prepared daily and replaced upon wetting, which was typically after purging either one 2-L sample or 10−20 0.2-L samples. Newly prepared Tenax columns were conditioned with multiple loadings and subsequent desorption of MeEtHg prior to use for trapping sample Hg; this

pretreatment improves peak resolution. In a stream of Ar carrier (ultra-high purity and passed over Au and Tenax; 0.09 L min^{-1}), volatile Hg species were desorbed thermally from the Tenax, separated with an isothermal gas chromatographic column (60 °C, 30 cm long, 3.2 mm ID, packed with 60/80 mesh Chromosorb WAW-DMSC coated with 15% OV-3; Supelco), pyrolyzed (500 °C) to Hg^0 upon elution from the chromatographic column, and Hg^0 detected by CVAFS (Tseng et al., 2004).

Determination of gaseous DMHg (Mason and Fitzgerald, 1993) was similar methodologically to that of MMHg, the only difference was that no chemical amendments were made to water prior to purging DMHg from solution with N_2 and trapping on Tenax. Because of its volatility and susceptibility to decomposition to MMHg upon water acidification (Black et al., 2009), DMHg must be purged from unacidified solutions promptly after sampling; otherwise, it is either lost or measured levels of MMHg may be biased artifactually. We did not purge DMHg from North Atlantic surface water in our laboratory tests because it was not present at detectable levels (< 2 fM).

2.2.3 Direct ethylation technique

We investigated the effect of different experimental conditions on recovery of MMHg from filtered seawater. Experimental samples were prepared by adding 400−500 femtomoles of MMHg, as CH_3HgCl, to either 0.2-L (laboratory tests) or 2.0-L (shipboard tests) aliquots of filtered seawater inside FEP Teflon bottles. MMHg amendments to seawater were about 10–100× greater than ambient levels, but were useful for optimizing analytical conditions and not enough to oversaturate Cl^- or organic ligands (Lamborg et al., 2003), the dominant complexing agents of MMHg in seawater (Fitzgerald et al.,

2007). The bottles were capped, solutions homogenized by hand shaking for several seconds, and stored in the dark (4–24 °C) for ≥ 24 h prior to any experimental treatment or analysis. This time period is sufficient for Hg(II) to equilibrate with natural ligands (Lamborg et al., 2003); therefore, added CH_3HgCl should have the same chemical speciation with dissolved and colloidal ligands as ambient MMHg. Tests to optimize recovery of MMHg from seawater by direct ethylation included the following variables: 1) pretreatment with different types and concentrations of mineral acids, 2) duration of sample pretreatment with acid, 3) duration of derivatization with NaTEB, and 4) N_2 purge volume of samples.

2.2.4 Quality control

Water samples were collected, manipulated, and analyzed with trace-metal clean procedures (Gill and Fitzgerald, 1985). All equipment and containers used for sample collection, storage, and analysis were cleaned rigorously with acid and rinsed with reagent-grade water (resistivity, > 18 MΩ-cm) prior to use. Sample MMHg was quantified after each Tenax column was calibrated individually with aliquots of an aqueous MMHg standard that was derivatized and purged from solution in the same GLS used for samples; each Tenax column typically had excellent linear calibration regressions ($r^2 \geq 0.99$) within the range of sample MMHg. Aqueous MMHg standards were standardized versus Hg^0 (Gill and Fitzgerald, 1987). Precision of MMHg determinations averaged 13% relative standard deviation (RSD) for 33 sets of laboratory test samples that were replicated procedurally in this study.

Although environmental samples are not prone to contamination with MMHg, determinations can be biased by contamination from analytical reagents, and there is a

potential for artifactual formation of MMHg from Hg(II) during analysis (Bloom et al., 1997; Hintelmann et al., 1997; Hammerschmidt and Fitzgerald, 2001). Analysis of procedural blanks is important for assessment of MMHg impurities introduced by reagents. Procedural blanks consisted of analytical reagents added to either reagent-grade water or previously ethylated and purged seawater (i.e., no remaining MMHg). With regard to a 2-L seawater sample acidified to 1% with H_2SO_4, this included 20 mL of 18 M H_2SO_4, 60 mL of 12 M KOH (for pH neutralization), about 30 mL of 4 M acetate buffer (pH adjustment to ~5), and 2 mL of 1% NaTEB. While these reagents add substantial Hg(II) to the matrix (> 500 fmoles for a 2-L sample), procedural blanks contained routinely about 5 fmoles (1 pg) of Hg, as MMHg, for a 2-L sample. Acetate buffer is the only reagent from which we have detected a contribution of MMHg, presumably from chemical methylation of contaminant Hg(II) in the sodium acetate. As an alternative to sodium acetate, we have found that preparation of acetate buffer from glacial acetic acid and KOH results often in an undetectable MMHg blank.

2.3. Assessment

2.3.1 Acid treatment

Treatment of natural waters with dilute concentrations of mineral acids promotes the release of MMHg from particles (e.g., Tseng et al., 1997; Hammerschmidt and Fitzgerald, 2001) and/or its reactivity to NaTEB (Hammerschmidt and Fitzgerald, 2010). Accordingly, we examined whether addition to seawater of either 12 M HCl (1 and 2% vol:vol), 16 M HNO_3 (1 and 2%), or 18 M H_2SO_4 (1%; all acids were Baker Instra-analyzed) increased recovery of MMHg from the matrix beyond the 50−80% recovery observed for untreated samples (n = 3 for each acid type/concentration). After treatment

with each acid for 24 h, sample acidity was neutralized by titration with 12 M KOH (ACS grade, Fisher); base is added directly to the sample bottle, as opposed to the GLS, so that the solution can be mixed to dissolve $Mg(OH)_2$ precipitate that forms during addition of base. Titrated samples were transferred within 15 min of neutralization to a GLS and analyzed as described above, with a 10-min reaction period for NaTEB and N_2 purging for 25 min at 0.15 L min^{-1} for a 0.2-L sample. Relative to samples with no acid treatment (mean ± 1 SD recovery of MMHg; 80 ± 3%), addition of HCl reduced precision and recovery of MMHg (1% HCl = 31 ± 18%, 2% HCl = 56 ± 20%), HNO_3 had no effect (1% HNO_3 = 83 ± 7%, 2% HNO_3 = 66 ± 24%), and 1% H_2SO_4 yielded quantitative results (100 ± 10%).

We examined whether concentrations of H_2SO_4 less than 1% were equally effective in promoting MMHg recovery from seawater, because acidification to 1% with H_2SO_4 requires relatively large volumes of acid, base, and buffer. Two-liter aliquots of North Pacific surface water (pre-purged of DMHg) and 0.2-L volumes of North Atlantic water were equilibrated for 24 h with 500 fmoles of added CH_3HgCl and then treated for 24 h with 18 M H_2SO_4 at concentrations ranging from 0 to 1% (vol:vol), after which the acid was titrated with KOH and samples analyzed as described above. While no correction for ambient MMHg was used for 0.2-L aliquots of North Atlantic surface water (ambient MMHg not detectable in this sample volume, < 20 fM), 17 fM (ambient level) was subtracted from measurements of North Pacific water to estimate recovery of known MMHg additions. N_2 purging rates were greater for 2-L samples (0.8 L min^{-1} for 40 min) than for 0.2-L aliquots (0.15 L min^{-1} for 20 min), but the same relative volume ratio of purge gas to water (15) was used for both. For both sample volumes and types,

MMHg recovery was about 60−80% for samples treated with less than 0.6% H_2SO_4 and considerably greater at higher acidities, with 1% H_2SO_4 yielding complete recovery of MMHg (Figure 1). Therefore, we used 1% H_2SO_4 as the acid treatment for all subsequent MMHg extractions.

2.3.2 Duration of H_2SO_4 treatment

Initial tests of MMHg recovery as a function of acid type and concentration were conducted on samples treated with acid for 24 h at room temperature. The potential influence of acid-treatment time was investigated with 0.2-L aliquots of North Atlantic water amended with 500 fmoles of MMHg, treated with 2 mL of 18 M H_2SO_4 (i.e., 1% vol:vol), and stored acidified for 1, 6, 12, 24, 48, 72, and 168 h (n = 3 for each period). MMHg recovery was quantitative among all periods except the 1-h treatment (mean ± 1 SD recovery of MMHg); 1 h = 29 ± 2%, 6 h = 112 ± 20%, 12 h = 86 ± 12%, 24 h = 100 ± 10%, 48 h = 88 ± 14%; 72 h = 93 ± 10%, and 168 h = 95 ± 6%. These results indicate that acidification to 1% with 18 M H_2SO_4 for ≥ 6 h increases sufficiently the lability of MMHg in seawater for quantitative analysis, and also suggests that samples may be acidified for at least one week prior to analysis without any substantial loss or gain of MMHg.

2.3.3 Duration of derivatization period

Method development for direct ethylation analysis of MMHg in arctic lake waters indicated that a 10 min derivatization period prior to purging gave quantitative results (Hammerschmidt and Fitzgerald, 2010). Accordingly, tests of acid type, concentration, and treatment period (described above) were conducted with a 10-min NaTEB reaction period prior to purging solutions with N_2. The duration of NaTEB derivatization period

required for ethylation of MMHg in seawater was examined with 0.2-L aliquots of MMHg-amended water from the North Atlantic. Samples were acidified to 1% with 18 M H_2SO_4 for 24 h, neutralized with KOH, buffered, and allowed to react with added NaTEB for 0, 5, 10, and 20 min prior to N_2 purging (0.15 L min^{-1} for 20 min). Recovery of MMHg from solution (mean ± 1 SD; n = 3 for each period) was complete among all tested reaction periods, averaging 90 ± 11% for 0 min, 88 ± 8% for 5 min, 100 ± 2% for 10 min, and 85 ± 14% for 20 min. Quantitative recovery from the 0-min reaction period suggests that NaTEB effectively ethylates MMHg during the 20-min purging step and that a pre-purge reaction period is not needed.

2.3.4 N_2 purge volume

The volume of N_2 required to purge MeEtHg quantitatively from solution was investigated with multiple 2-L samples of filtered water from the mixed layer of the North Pacific (no detectable DMHg). Seawater was amended with 500 fmoles of MMHg, allowed to equilibrate for 24 h, acidified with 18 M H_2SO_4 to 1% for 12 h, and analyzed as described above. The only difference was that samples were purged with N_2 at 0.8 and 1.2 L min^{-1}, at room temperature, for periods ranging between 10 and 60 min. Differences in N_2 purge rates and times permitted analysis of MeEtHg recovery versus gas volume purged through the water between two different rates (Figure 2). Regression analysis of the results indicated that >95% recovery of MMHg was achieved by purging 2-L samples with 30 L of N_2, which is 15× the water volume, at either rate. Moreover, and following the methods of Andersson and colleagues (2008), results from the gas recovery curve can be used to estimate a dimensionless Henry's law constant (H) of about 0.2 for MeEtHg, under the conditions of this test. This value compares favorably

to that of DMHg (H = 0.31 at 25 °C; Lindqvist and Rodhe, 1985). We also have found that compressed air, generated from a compressor pump and cleaned of Hg species by passage through Au-coated beads, is equally as effective as N_2 for purging MeEtHg from solution. This is an important consideration for extended oceanographic cruises where the ship's storage capacity for compressed gas cylinders may be limited.

2.3.5 MMHg determination in freshwater

The utility of pre-treatment with 1% H_2SO_4 and direct ethylation also was investigated for fresh waters. Surface water was collected from two sources in southwest Ohio that have relatively high pH, dissolved organic carbon, and MMHg; Crystal Lake (Clark County; pH = 7.65, DOC = 2100 µM, ambient MMHg = 1550 fM) and the Little Miami River (Greene County; pH = 8.50, DOC = 500 µM, MMHg = 70 fM). As in tests with seawater, added CH_3HgCl (500 fmoles) was allowed to equilibrate with ambient ligands in 0.2-L aliquots of filtered water (0.2 µm) for 24 h prior to treatment with 1% H_2SO_4 for 24 h and subsequent analysis. We also examined the recovery of added MMHg from unfiltered Little Miami River water (total suspended solids = 6 mg L^{-1}) acidified to 1% with H_2SO_4. Recovery of added MMHg from filtered water was quantitative for both sources: 91 ± 7% for Little Miami River (n = 9) and 98 ± 12% for Crystal Lake (n = 3). Recovery of added MMHg from unfiltered river water averaged 101 ± 22% (n = 6). Hence, this extraction technique appears to be applicable to filtered and unfiltered fresh waters, in addition to seawater.

2.3.6 Sulfide

Water used in all of our experiments had between 50 and 300 µM oxygen and presumably very little sulfide. MMHg has a high affinity for sulfide, about 10^9 greater

than that for Cl^- (Dyrssen and Wedborg, 1991). Because stratified estuaries, some marginal seas, and portions of the ocean have considerable levels of sulfide, we investigated whether sample treatment with H_2SO_4 could result in quantitative recovery of MMHg from sulfidic water. For this experiment, aliquots of North Atlantic surface water were deoxygenated by purging with N_2, amended with S^{2-} to 20 µM and MMHg to 1250 fM, and allowed to equilibrate in closed bottles for 24 h prior to treatment with 1% H_2SO_4 for 24 h and subsequent analysis. Importantly, no MMHg was recovered from water amended with sulfide (n = 5). We found, however, that purging of acidified (1% H_2SO_4), sulfidic seawater with air (about 15× water volume) prior to KOH addition allowed for quantitative recovery of MMHg (91 ± 8%, n = 3). This step presumably removed sulfide by either purging H_2S from solution or by reaction with oxygen. Thus, removal of sulfide by purging with air appears to be a technique that can be applied to samples suspected of having increased levels of the ligand.

2.3.7 Tenax

Tenax resin was used to trap gaseous methylmercury species in this study. Tenax, in contrast to Carbotrap resin, was selected because we observed it to sequester less water vapor, which can cause auto-fluorescence during CVAFS analysis. We also found Tenax to suitably remove MeEtHg from gas streams. The trapping efficiency of Tenax was investigated by loading either 100 or 2500 fmoles of MeEtHg, from water at the same gas purging rates used above, onto Tenax analytical traps that were immediately upstream of a breakthrough trap (also Tenax). For comparison, the same test was performed with Carbotrap in the primary position and Tenax breakthrough traps. In the 100-fmole test, no MeEtHg was detected on breakthrough traps downstream of either the Tenax or

Carbotrap analytical traps (n = 3 each). This quantity of MeEtHg in a 2-L water sample equates to 50 fM and is within the range of levels observed in the North Pacific (below). At the extreme, loadings of 2500 fmoles of MeEtHg also did not break through Carbotrap whereas 6.2 ± 2.4% passed the Tenax analytical trap and was sequestered on the breakthrough trap (n = 3 each). Although this degree of trap loading is uncommon for natural seawater, a 6% negative bias is within typical ranges of analytical uncertainty at such low concentrations.

2.3.8 Shipboard analyses of MMHg in North Pacific water

The above described analytical technique was applied to measurement of MMHg and DMHg in seawater during the 2009 U.S. GEOTRACES Intercalibration cruise (Table 1). After purging of DMHg, MMHg was determined in duplicate 2-L aliquots of filtered water from the upper 800 m of the water column, where concentrations ranged from 17 to 33 fM. Precision of duplicate analyses averaged 15% relative difference (range = 5–24%, n = 6). Recovery of known MMHg additions (100 fmoles) from sample matrixes averaged 90% (range = 83–92%, n = 8). The detection limit for MMHg was about 2 fM, estimated as 3× the standard deviation of reagent blank concentrations.

2.3.9 Shipboard analyses of DMHg in North Pacific water

A useful advantage of the described direct ethylation technique is that it allows determination of DMHg in the same water sample, particularly when purging off-line in 2-L bottles (Table 1). That is, and prior to acidification for MMHg analysis, 2-L samples (unamended with chemical regent) can be purged with N_2 and evolved DMHg trapped on a resin for analysis. After stripping DMHg, the same sample is acidified to 1% with 18 M H_2SO_4 and analyzed for MMHg as described above. DMHg is a dissolved gas and

measured typically in unfiltered water decanted from rosette to sample bottles with a laminar flow through tubing. However, seawater collected as part of the U.S. GEOTRACES program is typically passed through an in-line capsule filter while decanting into sample bottles.

To test whether filtration affects levels of dissolved gaseous DMHg, we compared measured concentrations between 2-L aliquots of unfiltered water and that filtered through a pre-rinsed capsule (0.2 µm; Pall AcroPak-200, polyethersulfone membrane) and silicone tubing as it was decanted from the rosette bottle. Unfiltered water was collected similarly but without filtration. Water was sampled from three different depths (300−800 m) in the North Pacific Ocean. DMHg in filtered:unfiltered water was 10:11 fM (300 m depth), 9:11 fM (300 m duplicate), 19:14 fM (600 m), and 14:11 fM (800 m). DMHg in unfiltered and filtered water at 300 m depth compared well between duplicate samples and, among all four samples, DMHg levels in filtered water did not differ significantly from unfiltered aliquots (paired *t*-test, $p = 0.43$). While the number of samples tested is few, these results suggest that DMHg is not lost when samples are filtered carefully.

Prior research has indicated that DMHg can diffuse out of sample water through Teflon bottles, with about 10% loss within 24 h of collection (Parker and Bloom, 2005), although it is stable in glass bottles for at least 10 h (Black et al., 2009). DMHg losses could occur between sampling and analysis, particularly when the Teflon bottle (i.e., GLS) is pressurized with N_2 during purging. All water samples from the North Pacific were purged of DMHg within about 1–2 h of sampling. To evaluate whether substantial losses might occur during such a period prior to purging, 2-L aliquots of seawater were

amended with 500 fmoles of MeEtHg and measured for MeEtHg content after 1–2 h storage, in the dark at room temperature. MeEtHg was added in lieu of DMHg because 1) of laboratory safety concerns associated with concentrated solutions of DMHg and 2) both gases have similarly low solubility in water, as noted above. Recovery of MeEtHg from seawater after 1–2 h of storage in FEP Teflon was 97 ± 14% (n = 4). We also examined whether MeEtHg is lost during purging by comparing 2-L bottles made of either FEP or borosilicate glass (no storage period). Recovery of 250 fmoles of MeEtHg from FEP Teflon bottles (101 ± 7%, n = 5) was comparable to that from glass bottles (101 ± 22%, n = 6). This finding is consistent with the good recovery of known MMHg additions purged from 2-L North Pacific waters in FEP bottles (mean = 90 ± 2%, n = 8), which suggests substantial quantities of volatile methylmercury species do not escape the bottle during purging. Hence, while gas-impermeable glass may be a superior bottle material for DMHg sampling and analysis (Parker and Bloom, 2005), FEP appears to be a suitable alternative if DMHg is purged promptly after sample collection.

It also has been suggested that Tenax is inferior to Carbotrap for trapping DMHg (Bloom et al., 2005). While we did not test breakthrough of DMHg, we infer that Tenax sequesters DMHg as efficiently as it does MeEtHg, based on their similar physicochemistry. This is supported by the relatively good agreement among replicate samples of filtered seawater from depth in the North Pacific. Precision of DMHg determinations averaged 15% RSD (range = 4–25% RSD) among 14 sets of samples that contained between 6–19 fM DMHg. Such good agreement would not be expected if random losses of analyte occurred as a result of either breakthrough, filtration, or diffusion through bottle material. The detection limit for DMHg is about 2 fM, estimated

as 3× the standard deviation of three replicate measurements of low-DMHg water (2 fM) from 125 m depth in the North Pacific.

2.4. Discussion

Purging of DMHg prior to seawater acidification and MMHg analysis permits separate quantification of both mercury species. This is in contrast to methodologies used in many prior investigations, including our own (e.g., Hammerschmidt and Fitzgerald, 2006), where filtered or unfiltered water is often acidified for storage or during analysis, and determined concentrations of "methylmercury" are either assumed wrongly to be representative of MMHg only or recognized to include both MMHg and DMHg. It is long known that acidification causes demethylation of DMHg to MMHg (Wood et al., 1968). Either interpretation is problematic because if DMHg were a substantial fraction of the methylated Hg, then the measured concentration of "methylmercury" is biased and little progress is made toward better understanding the biogeochemistry of MMHg, a bioaccumulative solute, versus DMHg, a non-bioaccumulative gas. Differentiation between MMHg and DMHg is particularly important for sub-surface marine waters, in which levels of DMHg may be comparable to, or greater than, MMHg (Fitzgerald et al., 2007). Hence, this methodology presents a useful tool for quantifying, differentiating, and developing an improved understanding of the different, but likely interrelated, concentrations and biogeochemistries of MMHg and DMHg in the ocean.

The biogeochemistry of toxic and bioaccumulative MMHg in seawater is vastly understudied given its toxicological significance to both humans and wildlife. While there is a large and growing knowledge of MMHg in freshwater systems, very little is

known about the sources and cycling of methylmercury species in the ocean. This is due, in part, to the concentration of MMHg in open-ocean seawater often being less than contemporary limits of detection. Here, we have developed and outlined the basis of a method, which we are certain to see improved, that readily allows quantification of MMHg in seawater at levels of 2 fM or greater, a 10-fold improvement on current limits of detection. Moreover, and critically, this technique allows the separation and determination of DMHg from the same aliquot of seawater and thereby neither biases determined levels of MMHg nor confounds interpretation of MMHg and DMHg cycling.

Acknowledgment

We thank the scientific parties, captains, and crews of the R/V *Endeavor* (EN-452) and R/V *Knorr* (KN-198-5) for help with seawater sampling. This research was supported by the U.S. National Science Foundation (OCE-0825108).

References

Andersson, M. E., K. Gårdfeldt, I. Wängberg, and D. Strömberg. 2008. Determination of Henry's law constant for elemental mercury. Chemosphere 73:587–592 [doi: 10.1016/j.chemosphere.2008.05.067].

Benoit, J. M., C. C. Gilmour, A. Heyes, R. P. Mason, and C. L. Miller. 2003. Geochemical and biological controls over methylmercury production and degradation in aquatic systems, p. 262–297. *In* Y. Cai and O. C. Braids [eds.], Biogeochemistry of environmentally important trace metals. American Chemical Society.

Black, F. J., C. H. Conaway, and A. R. Flegal. 2009. Stability of dimethyl mercury in seawater and its conversion to monomethyl mercury. Environ. Sci. Technol. 43:4056–4062 [doi: 10.1021/es9001218].

Bloom, N. S., and W. F. Fitzgerald. 1988. Determination of volatile mercury species at the picogram level by low-temperature gas chromatography with cold-vapor atomic fluorescence detection. Anal. Chim. Acta. 208:151−161 [doi: 10.1016/S0003-2670(00)80743-6].

Bloom, N. 1989. Determination of picogram levels of methylmercury by aqueous phase ethylation, followed by cryogenic gas-chromatography with cold vapor atomic fluorescence detection. Can. J. Fish. Aquat. Sci. 46:1131−1140 [doi: 10.1139/f89-147].

Bloom, N. S., J. A. Colman, and L. Barber. 1997. Artifact formation of methyl mercury during aqueous distillation and alternative techniques for the extraction of methyl

mercury from environmental samples. Fresenius J. Anal. Chem. 358:371−377 [doi: 10.1007/s002160050432].

Bloom, N. S., A. K. Grout, and E. M. Prestbo. 2005. Development and complete validation of a method for the determination of dimethyl mercury in air and other media. Anal. Chim. Acta 546:92–101 [doi: 10.1016/j.aca.2005.04.087].

Brigham, M. E., D. A. Wentz, G. R. Aiken, and D. P. Krabbenhoft. 2009. Mercury cycling in stream ecosystems. 1. Water column chemistry and transport. Environ. Sci. Technol. 43:2720–2725 [doi: 10.1021/es802694n].

Cossa, D., B. Averty, and N. Pirrone. 2009. The origin of methylmercury in open Mediterranean waters. Limnol. Oceanogr. 54:837–844.

Dyrssen, D., and M. Wedborg. 1991. The sulphur-mercury(II) system in natural waters. Water Air Soil Pollut. 56:507−519 [doi: 10.1007/BF00342295].

Filippelli, M., F. Baldi, F. E. Brinckman, and G. J. Olson. 1992. Methylmercury determination as volatile methylmercury hydride by purge and trap gas chromatography in line with Fourier transform infrared spectroscopy. Environ. Sci. Technol. 26:1457−1460 [doi: 10.1021/es00031a025].

Fitzgerald, W. F., C. H. Lamborg, and C. R. Hammerschmidt. 2007. Marine biogeochemical cycling of mercury. Chem. Rev. 107:641–662 [doi: 10.1021/cr050353m].

Gill, G. A., and W. F. Fitzgerald. 1985. Mercury sampling of open ocean waters at the picomolar level. Deep Sea Res. A 32:287–297 [doi: 10.1016/0198-0149(85)90080-9].

Gill, G. A., and W. F. Fitzgerald. 1987. Picomolar mercury measurements in seawater and other materials using stannous chloride and two-stage amalgamation with gas phase detection. Mar. Chem. 20:227–243 [doi: 10.1016/0304-4203(87)90074-0].

Hammerschmidt, C. R., and W. F. Fitzgerald. 2001. Formation of artifact methylmercury during extraction from a sediment reference material. Anal. Chem. 73:5930−5936 [doi: 10.1021/ac010721w].

Hammerschmidt, C. R., and W. F. Fitzgerald. 2006. Methylmercury cycling in sediments on the continental shelf of southern New England. Geochim. Cosmochim. Acta 70:918−930 [doi: 10.1016/j.gca.2005.10.020].

Hammerschmidt, C. R., and W. F. Fitzgerald. 2010. Iron-mediated photochemical decomposition of methylmercury in an arctic Alaskan lake. Environ. Sci. Technol. 44:6138–6143 [doi: 10.1021/es1006934].

Hintelmann, H., and R. D. Evans. 1997. Application of stable isotopes in environmental tracer studies–Measurement of monomethylmercury (CH_3Hg^+) by isotope dilution ICP-MS and detection of species transformation. Fresenius J. Anal. Chem. 358:378–385 [doi: 10.1007/s002160050433].

Hintelmann, H., R. Falter, G. Ilgen, and R. D. Evans. 1997. Determination of artifactual formation of monomethylmercury (CH_3Hg^+) in environmental samples using stable Hg^{2+} isotopes with ICP-MS detection: Calculation of contents applying species specific isotope dilution. Fresenius J. Anal. Chem. 358:363−370 [doi: 10.1007/s002160050431].

Holz, J., J. Kreutzmann, R.-D. Wilken, and R. Falter. 1999. Methylmercury monitoring

in rainwater samples using in situ ethylation in combination with GC-AFS and GC-ICP-MS techniques. Appl. Organometal. Chem. 13:789–794 [doi: 10.1002/(SICI)1099-0739(199910)13:10<789::AID-AOC908>3.0.CO;2-N].

Horvat, M., N. S. Bloom, and L. Liang. 1993. Comparison of distillation with other current isolation methods for the determination of methyl mercury compounds in low level environmental samples. Part II. Water. Anal. Chim. Acta 282:153−168 [doi: 10.1016/0003-2670(93)80364-Q].

Hurley, J. P., J. M. Benoit, C. L. Babiarz, M. M. Shafer, A. W. Andren, J. R. Sullivan, R. Hammond, and D. A. Webb. 1995. Influences of watershed characteristics on mercury levels in Wisconsin rivers. Environ. Sci. Technol. 29:1867−1875 [doi: 10.1021/es00007a026].

Kirk, J. L., V. L. St. Louis, H. Hintelmann, I. Lehnherr, B. Else, and L. Poissant. 2008. Methylated mercury species in marine waters of the Canadian High and sub Arctic. Environ. Sci. Technol. 42:8367−8373 [doi: 10.1021/es801635m].

Kotnik, J., M. Horvat, E. Tessier, N. Ogrinc, M. Monperrus, D. Amouroux, V. Fajon, D. Gibičar, S. Žižek, F. Sprovieri, and N. Pirrone. 2007. Mercury speciation in surface and deep waters of the Mediterranean Sea. Mar. Chem. 107:13–30 [doi: 10.1016/j.marchem.2007.02.012].

Lamborg, C. H., C.-M. Tseng, W. F. Fitzgerald, P. H. Balcom, and C. R. Hammerschmidt. 2003. Determination of the mercury complexation characteristics of dissolved organic matter in natural waters with “reducible Hg” titrations. Environ. Sci. Technol. 37:3316−3322[doi: 10.1021/es0264394].

Lindqvist, O., and H. Rodhe. 1985. Atmospheric mercury: A review. Tellus Ser. B 37:136−159 [doi: 10.1111/j.1600-0889.1985.tb00062.x].

Mason, R. P, and W. F. Fitzgerald. 1993. The distribution and biogeochemical cycling of mercury in the equatorial Pacific Ocean. Deep-Sea Res. I 40:1897−1924 [doi: 10.1016/0967-0637(93)90037-4].

Mason, R. P., J. R. Reinfelder, and F. M. M. Morel. 1996. Uptake, toxicity, and trophic transfer of mercury in a coastal diatom. Environ. Sci. Technol. 30:1835−1845 [doi: 10.1021/es950373d].

Mergler, D., H. A. Anderson, L. H. M. Chan, K. R. Mahaffey, M. Murray, M. Sakamoto, and A. H. Stern. 2007. Methylmercury exposure and health effects in humans: A worldwide concern. Ambio 36:3−11 [doi: 10.1579/0044-7447(2007)36[3:MEAHEI]2.0.CO;2].

Parker, J. L., and N. S. Bloom. 2005. Preservation and storage techniques for low-level aqueous mercury speciation. Sci. Total Environ. 337:253–263 [doi: 10.1016/j.scitotenv.2004.07.006].

Rolfhus, K. R., H. E. Sakamoto, L. B. Cleckner, R. W. Stoor, C. L. Babiarz, R. C. Back, H. Manolopoulos, and J. P. Hurley. 2003. Distribution and fluxes of total and methylmercury in Lake Superior. Environ. Sci. Technol. 37: 865−872 [doi: 10.1021/es026065e].

Scheuhammer, A. M., M. W. Meyer, M. B. Sandheinrich, and M. W. Murray. 2007. Effects of environmental methylmercury on the health of wild birds, mammals, and fish. Ambio 36:12−18 [doi: 10.1579/0044-7447(2007)36[12:EOEMOT]2.0.CO;2].

St. Louis, V. L., M. J. Sharp, A. Steffen, A. May, J. Barker, J. L. Kirk, D. J. A. Kelly, S. E. Arnott, B. Keatley, and J. P. Smol. 2005. Some sources and sinks of monomethyl and inorganic mercury on Ellesmere Island in the Canadian High Arctic. Environ. Sci. Technol. 39:2686−2701 [doi: 10.1021/es049326o].

Tseng, C.-M., A. de Diego, F. M. Martin, and O. F. X. Donard. 1997. Rapid and quantitative microwave-assisted recovery of methylmercury from standard reference sediments. J. Anal. At. Spectrom. 12:629−635 [doi: 10.1039/A700832E].

Tseng, C.-M., C. R. Hammerschmidt, and W. F. Fitzgerald. 2004. Determination of methylmercury in environmental matrixes by on-line flow injection and atomic fluorescence spectrometry. *Anal. Chem.* 76:7131−7136 [doi: 10.1021/ac049118e].

U.S. Environmental Protection Agency. 2001. Method 1630: Methyl mercury in water by distillation, aqueous ethylation, purge and trap, and CVAFS. EPA-821-R-01-020. U.S. Environmental Protection Agency, Washington, DC.

U.S. Environmental Protection Agency. 2002. Estimated per capita fish consumption in the United States, August 2002. EPA-821-C-02-003. U.S. Environmental Protection Agency, Washington, DC.

Wiener, J. G., D. P. Krabbenhoft, G. H. Heinz, and A. M. Scheuhammer. 2003. Ecotoxicology of mercury, p. 409–463. *In* D. J. Hoffman, B. A. Rattner, and G. A. Burton, Jr. [eds.], Handbook of ecotoxicology. Lewis.

Wood, J. M., F. S. Kennedy, and C. G. Rosen. 1968. Synthesis of methyl-mercury

compounds by extracts of a methanogenic bacterium. Nature 220:173−174 [doi: 10.1038/220173a0].

Table 2.1. Methodological sequence for quantitatively extracting DMHg and MMHg (as methylethylmercury, MeEtHg) from a 2-L sample of water.

Analytical step	Sample water manipulation
DMHg purge	Purge with N_2 for 40 min at 0.8 L min^{-1}, trap DMHg on Tenax downstream of soda lime column
DMHg determination	No manipulation; analyze trapped DMHg by CVAFS
Acidification	Add 20 mL of 18 M H_2SO_4, shake, and store in the dark at 4–25 °C for ≥ 6 h
pH adjustment	Add 60 mL of 12 M KOH and 30 mL of 4 M acetate buffer
MMHg derivatization	Add 2 mL of 1% (wt:vol) NaTEB
MMHg purge	Purge with N_2 (or Hg-free air) for 40 min at 0.8 L min^{-1}, trap MeEtHg on Tenax downstream of soda lime column
MMHg determination	No manipulation; analyze trapped MeEtHg by CVAFS

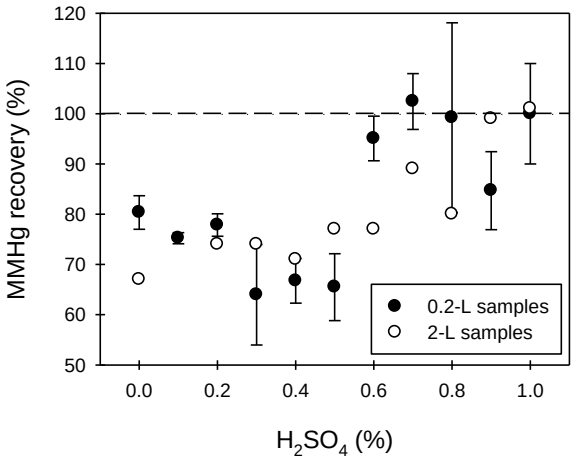

Figure 2.1. Recovery of added MMHg (500 fmoles) from 0.2-L samples of North Atlantic surface water and 2-L aliquots of North Pacific surface water acidified to 0−1% with 18 M H_2SO_4 for 24 h prior to analysis. N_2 purging was at 0.15 L min^{-1} (× 25 min) for 0.2-L aliquots and 0.8 L min^{-1} (× 60 min) for 2-L samples. Error bars are the difference among duplicate samples (North Atlantic only). Dashed line is 100% recovery.

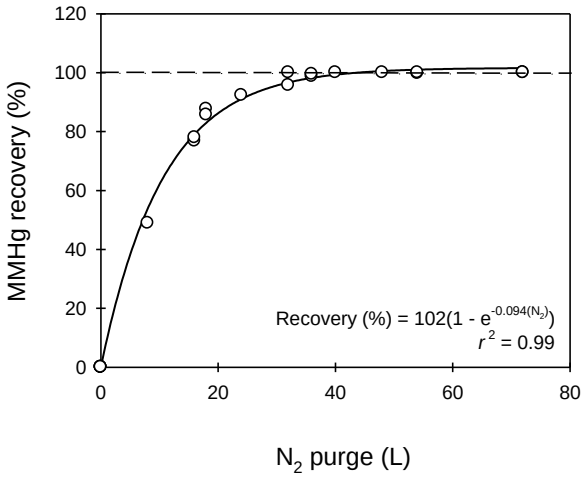

Figure 2.2. Recovery of MMHg (as methylethylmercury) from 2-L samples of filtered seawater purged with various volumes of N_2. Tests were conducted with multiple samples at N_2 purge rates of 0.8 and 1.2 L min^{-1}. Dashed line is 100% recovery.

3. MERCURY IN THE NORTH ATLANTIC OCEAN: THE U.S. GEOTRACES ZONAL AND MERIDIONAL SECTIONS

Bowman, K.L., Hammerschmidt, C.R., Lamborg, C.H., Swarr, G. 2014. Mercury in the North Atlantic Ocean: The U.S. GEOTRACES zonal and meridional sections. Deep-Sea Res.II, DOI: 10.1016/j.dsr2.2014.07.004.

Abstract

Mercury (Hg) in the ocean undergoes many chemical transformations, including *in situ* production of monomethylmercury (MMHg), the form that biomagnifies in marine food webs. Because the ocean is a primary and dynamic reservoir of Hg cycling at earth's surface and the principal source of human MMHg exposures through seafood, it is important to understand the distribution of Hg and its chemical species in marine environments. We examined total Hg, elemental Hg (Hg^0), MMHg, and dimethylmercury (DMHg) with fully resolved high-resolution profiles during the U.S. GEOTRACES zonal and meridional sections of the North Atlantic Ocean (GEOTRACES GA03). Total Hg in filtered water had both scavenged- and nutrient-type vertical distributions, whereas concentrations of DMHg, Hg^0, and filtered MMHg were increased in the oxygen deficient zone of the permanent thermocline across the basin, relative to water above and often below. Total Hg and MMHg on suspended particles accounted for less than 10% of total concentrations. The TAG hydrothermal vent on the Mid-Atlantic Ridge (MAR) was a source of total Hg and MMHg to nearby waters with apparent scavenging and Hg transformation occurring in the buoyant plume. Uniquely, we observed significant horizontal segregation of filtered total Hg and MMHg, DMHg, and Hg^0 in North Atlantic Deep Water (NADW) between younger water on the western and older water on the eastern side of the MAR. Relative to eastern NADW, Hg concentrations in western NADW were greater, on average, by 1.14× for filtered total Hg, 1.6× for Hg^0, 2.5× for filtered MMHg, and 2.6× for DMHg. Total Hg enrichment in deep water of the western basin may have resulted from downwelling of anthropogenic Hg during NADW formation. Enrichment of MMHg, DMHg, and Hg^0 in western basin NADW may be

explained by either greater Hg substrate availability or greater methylation and reduction potentials in younger deep waters.

3.1. Introduction

Mercury (Hg) is a ubiquitous environmental contaminant that originates from natural and anthropogenic sources (Fitzgerald et al., 2007). Direct atmospheric deposition is the primary source of Hg to the ocean whereas riverine discharge, mobilization from sediments, groundwater, and submarine hydrothermal inputs contribute lesser amounts (Mason et al., 2012). The majority of atmospheric Hg emissions are anthropogenic (Fitzgerald et al., 1998; Amos et al., 2013) and emissions are hypothesized to increase during the next century (Hammerschmidt, 2011; Kocman et al., 2013; Pirrone et al., 2010; Streets et al., 2009). Because the ocean is a primary and dynamic reservoir of Hg cycling at earth's surface and the principal source of human Hg exposures through seafood (Mason et al., 2012), it is important to understand the distribution of Hg and its chemical species in marine environments.

Mercury exists as four primary chemical species in seawater: mercuric ion (Hg(II)) and monomethylmercury (MMHg, CH_3Hg^+) in complexes with inorganic and organic ligands as well as elemental Hg (Hg^0) and dimethylmercury (DMHg, $(CH_3)_2Hg$), which are dissolved gases. Each of these species are hypothesized to be linked through the Hg(II) pool (Fitzgerald et al., 2007). For example, Hg(II) may be either reduced to Hg^0 or transformed to MMHg and DMHg by biological and abiotic mechanisms (Monperrus et al., 2007; Whalin et al., 2007; Lehnherr et al., 2011). Hg(II) reduction occurs to such an extent that Hg^0 in estuarine and marine surface waters are usually supersaturated with respect to the atmosphere, leading to evasion (Andersson et al., 2011). Moreover, *in situ* methylation of Hg(II) is an important source of MMHg and DMHg in many marine ecosystems (Balcom et

al., 2004; Hammerschmidt and Fitzgerald, 2006a; Sunderland et al., 2009; Hollweg et al., 2010; Cossa et al., 2011). MMHg is the bioaccumulative species of Hg that is present throughout the marine water column (Hammerschmidt and Bowman, 2012; Heimbürger et al., 2010; Mason et al., 2012). Harmful to humans and piscivorous wildlife, MMHg can interfere with neurological, cardiovascular, and endocrine systems (Bose-O'Reilly et al., 2010; Scheuhammer et al., 2007; Zahir et al., 2005). In the United States and Europe, consumption of marine fish is the primary route of human exposure to MMHg (Sunderland, 2007; Višnjevec et al., 2014).

We investigated the speciation and distribution of Hg in the North Atlantic Ocean during the U.S. GEOTRACES zonal and meridional sections in Fall 2010 and Fall 2011 (GEOTRACES GA03; Figure 1). These cruise tracks included multiple oceanographic features that may influence the biogeochemical cycling of Hg species: 1) a broad continental shelf on the western margin, 2) oligotrophic surface waters in the Sargasso Sea, 3) the Mid-Atlantic Ridge with active hydrothermal venting, 4) relatively productive surface waters along the eastern margin as a result of upwelling and Saharan dust inputs, 5) multiple deep and intermediate water masses (Figure 2), and 6) age differences of North Atlantic Deep Water (NADW) between the western and eastern sides of the Mid-Atlantic Ridge. We measured high-resolution vertical profiles of Hg^0, DMHg, MMHg, and total Hg in filtered water at 32 stations across the North Atlantic as well as particulate total Hg and MMHg at 22 stations to assemble the most comprehensive and resolved distribution of Hg species in any ocean basin. Here, we provide the first descriptive presentation of our speciation results.

3.2. Materials and Methods

3.2.1 Sample collection

Seawater was sampled with 12-L Teflon-coated Go-Flo bottles attached to a dedicated trace-metal clean rosette that was deployed with a plastic-coated hydrowire (Cutter and Bruland, 2012). Twenty full-depth stations (24–36 depths) and 12 "demi" stations (12 depths each in upper 1000 m) were sampled and analyzed for Hg species in filtered water. Go-Flo bottles were promptly transferred to a clean laboratory van where seawater was filtered without agitation through pre-rinsed capsules (0.2 μm Pall AcroPak-200) into 2-L Teflon bottles for determination of DMHg, Hg^0, and MMHg. An additional 0.2-L aliquot of filtered seawater was collected into 0.25-L borosilicate glass bottles for measurement of total Hg. Each sample bottle, which was cleaned rigorously with vetted methods (Hammerschmidt et al., 2011), was rinsed 3× with sample water (about 10% bottle volume) before filling.

Suspended particles (1–51 μm) were sampled from 16 depths at 22 stations onto quartz fiber filters (Whatman QMA) with McLane *in situ* pumps (Bishop et al., 2012). Filters were subsampled in a clean laboratory into 25-mm diameter punches and stored frozen until Hg analysis at Wright State University. The volume of seawater passed through each 25-mm filter subsample ranged from about 25 to 100 L.

3.2.2. Mercury analysis

Hg species in filtered seawater were extracted and quantified on board the research vessel inside a clean laboratory van, which was separate from other GEOTRACES laboratories to prevent potential sample contamination from Hg^0 release to the air from mercury electrodes used by other researchers. Within 2 h of water sampling

and filtration, gaseous Hg^0 and DMHg were extracted from 2-L samples by purging with Hg-free N_2 (30 L total at 0.8 L min^{-1}; Bowman and Hammerschmidt, 2011). The sample bottles were fitted with multi-port caps (Omnifit Q-series; Danbury, CT) that allowed influent N_2 to flow through fritted glass impingers while effluent gas exited through a series of three collection traps connected by Teflon fittings. The first trap contained reagent-grade soda lime to help remove water vapor/aerosols generated from purging, the second contained Tenax TA to concentrate DMHg, and the third contained Au-coated glass beads to collect Hg^0 (Lamborg et al., 2012). This extraction and trapping approach allows for DMHg and Hg^0 to be determined independently as opposed to trapping both species on Au as generic dissolved gaseous mercury (DGM). It also allows for species-specific differentiation of DMHg and MMHg, which are more commonly determined as total methylated mercury (ΣCH_3Hg) after sample acidification (Mason et al., 2012). DMHg was quantified after thermal desorption from Tenax by gas chromatographic cold vapor atomic fluorescence spectrometry (GC-CVAFS, Bloom, 1989; Bowman and Hammerschmidt, 2011) and Hg^0 by dual Au-amalgamation CVAFS (Bloom and Fitzgerald, 1988). Each Au-trap for analysis of Hg^0 was calibrated at every other station after direct loading with a known quantity of Hg^0 vapor. Procedural precision of Hg^0 determinations averaged 10 ± 6 relative percent difference (RPD; n = 5 pairs) between duplicate samples. Tenax traps for DMHg analysis were calibrated frequently between stations with known additions of methylethylmercury, a volatile derivative of MMHg. Procedural precision of DMHg analyses averaged 16 ± 18 RPD between 16 pairs of samples. The number of duplicate samples for DMHg, Hg^0, and MMHg analysis was low relative to the total number of samples because water budgets for the Go-Flo bottles

were extremely limited, particularly for an extra 2-L of water. Method detection limits were 0.01 pM for Hg^0 and 0.002 pM for DMHg.

After quantitatively stripping Hg^0 and DMHg from solution, water samples were transferred to 2-L polycarbonate bottles and acidified to 1% with trace-metal grade H_2SO_4 for MMHg determination (Bowman and Hammerschmidt, 2011). After 12–24 h, sample acidity was neutralized with 12 M KOH, pH adjusted to 5 with 4 M acetate buffer, and ethylated with sodium tetraethylborate (NaTEB). Low-Hg acetate buffer was prepared from acetic acid and KOH, as opposed to acetic acid and sodium acetate because the sodium salt can contain significant amounts of total Hg and MMHg. Sample bottles were fitted with multi-port caps and purged with air (30 L total at 0.8 L min^{-1}) that was cleaned of Hg by passing over Au and Carbotrap. Effluent gas from the bottles passed through soda lime before methylethylmercury was concentrated on Tenax. MMHg was quantified by GC-CVAFS (Bloom, 1989; Bowman and Hammerschmidt, 2011). Recovery of known additions of MMHg from seawater averaged 105 ± 6% (n = 3) and procedural precision averaged 13 ± 13 RPD between 14 pairs of duplicate samples. Individual Tenax traps were calibrated frequently between stations with aliquots of an aqueous MMHgCl standard; the standard was calibrated versus digested TORT-2 reference material (lobster hepatopancreas, National Research Council of Canada) every two weeks.

Total Hg in filtered seawater was measured within 48 h of sampling from 0.2-L aliquots separate from those used for Hg^0 and organo-Hg species. Water was oxidized with BrCl solution (0.1% by volume) for >12 h and pre-reduced with NH_2OH immediately prior to analysis. Oxidized Hg species were reduced to Hg^0 with $SnCl_2$,

purged from solution with custom-made UConn Bubblers (Lamborg et al., 2012), and quantified by dual Au-amalgamation CVAFS (Bloom and Fitzgerald, 1988; Fitzgerald and Gill, 1979), after calibration with aqueous Hg(II) standards that were traceable to the U.S. National Institute of Standards and Technology (NIST). The method detection limit for total Hg in filtered seawater was 0.02 pM. Recovery of known additions of aqueous Hg(II) averaged 99 ± 5% (n = 12) and near-weekly measurements of total Hg in BCR-579 (Total Mercury in Coastal Seawater, European Commission) averaged 10.3 ± 0.6 pmol/kg (n = 5), which was within the certified range of 9.5 ± 2.5 pmol/kg. Procedural precision of total Hg measurements in filtered seawater averaged 5 ± 5 RPD between 18 pairs of samples.

Filter punches containing suspended particulate matter were stored frozen (≤ −20°C) until analysis at Wright State University within two to three months of sampling. Mercury was leached from filters with high-purity 2 N HNO_3 for 4 h in a 60 ^{o}C water bath (Hammerschmidt and Fitzgerald, 2006b). Aliquots of digestate were analyzed for MMHg by flow-injection GC-CVAFS (Tseng et al., 2004) after calibration with procedural MMHg standards digested similarly in 2 N HNO_3. MMHg standards for analysis of particulate MMHg were calibrated against aqueous Hg(II) solutions traceable to the U.S. NIST. Particulate total Hg was determined from the same digestates used for MMHg analysis. Aliquots of digestates were oxidized with BrCl, pre-reduced with NH_2OH, reduced with $SnCl_2$, and analyzed by dual Au-amalgamation CVAFS (Hammerschmidt and Fitzgerald, 2006b). The method detection limit for particulate MMHg was 0.002 pM and that for total Hg was 0.03 pM. Due to low analyte concentrations and limited sample volumes, analytical precision of particulate Hg

determinations was assessed only during analysis of total Hg: precision of analytical replicates averaged 3 ± 3 RPD (n = 18).

Trace-metal clean procedures were followed throughout sample collection and processing. Collection and filtration methods, sample bottle materials and cleaning techniques, and analytical methods were evaluated rigorously during the U.S. GEOTRACES Intercalibration cruises in the Atlantic and Pacific Oceans, prior to the North Atlantic sections (Bowman and Hammerschmidt, 2011; Hammerschmidt et al., 2011; Bishop et al., 2012; Lamborg et al., 2012; Cutter and Bruland, 2012).

3.3. Results and Discussion

3.3.1 Physical oceanography of the basin

The zonal and meridional sections traversed multiple water masses in North Atlantic Ocean (Figure 2). The largest water mass in the North Atlantic is NADW, which occupies the water column from about 1500 to 4000 m depth. The dominant flow of newly formed NADW is from the Labrador and Norwegian Seas into the western basin of the North Atlantic. Not until the Romanche Fracture Zone, south of the equator, does some NADW return northward and ventilate the abyss on the eastern side of the Mid-Atlantic Ridge. This path of deep water flow results in NADW of the western basin (~90 y old near Bermuda) having a radiocarbon age about 150 y younger than the eastern basin (~240 y old; Broecker et al., 1991). These age differences of NADW between the eastern and western basin are related to the speciation and concentration of Hg in NADW, as discussed below and elsewhere (Lamborg et al., accepted).

3.3.2 Total Hg

Among all stations and depths in the North Atlantic, total Hg in filtered water ranged from 0.09 to 1.9 pM (Table 1), excluding waters sampled from the TAG hydrothermal plume on the Mid-Atlantic Ridge (Station 16), which is discussed in section 3.6. The mean concentration of filtered total Hg in our study (0.89 ± 0.30 pM) is less than half of that determined from other locations in the North (Mason et al., 1998) and Equatorial and South Atlantic (Mason and Sullivan, 1999) about two decades earlier. Lower concentrations in the current study may be attributed to decreased atmospheric inputs of Hg to the North Atlantic during the past 20 years (Ebinghaus et al., 2011). Alternatively, the difference may reflect on-going improvements in clean techniques for sampling and analysis of Hg in seawater, particularly as a result of testing and development during the U.S. GEOTRACES Intercalibration (Hammerschmidt et al., 2011; Lamborg et al., 2012).

Total Hg in filtered water had both scavenged- and nutrient-type vertical distributions in the North Atlantic (Figure 3a). The concentration of filtered total Hg in the upper 100 m of the water column averaged 0.65 ± 0.32 pM (n = 103) among all stations during both meridional and zonal sections and were much less than levels in deeper water. Relative to surface water, concentrations of filtered total Hg were increased in the oxygen deficient zone (ODZ), extending from east to west across the North Atlantic (Figure 3a), consistent with release of Hg from sinking particles during remineralization. Strong scavenging of total Hg from surface waters was evident in the eastern Atlantic, where dust deposition and upwelling promote biological productivity and either bioaccumulation or scavenging of Hg from solution.

Horizontal segregation of filtered total Hg was evident in NADW, excluding the hydrothermal plume on the Mid-Atlantic Ridge that had concentrations of filtered total Hg up to 13 pM. We have hypothesized that Hg slowly accumulates in deep waters of the ocean as a result of soft-tissue remineralization at depth, resulting in older deep waters (e.g., North Pacific) having greater concentrations than younger deep water (e.g., North Atlantic; Hammerschmidt and Bowman, 2012; Lamborg et al., accepted). In contrast, younger NADW in the western North Atlantic (Stations 1–15, zonal transect) has a mean concentration of filtered total Hg (1.04 ± 0.17 pM, n = 65) that is about 15% greater than that in approximately 150-y older NADW in the eastern basin (mean = 0.91 ± 0.23 pM, n = 68; Mann-Whitney rank sum, $p < 0.001$), disregarding the TAG hydrothermal station on the Mid-Atlantic Ridge (Station 16). Greater concentrations of filtered total Hg in younger NADW of the western basin compared to the eastern North Atlantic may be attributed to younger NADW having downwelled anthropogenic Hg during deep water formation (Lamborg et al., accepted). Such a source would be in addition to the natural and anthropogenic Hg that is added to deep waters on both sides of the Mid-Atlantic Ridge as a result of particle scavenging and remineralization. In water deeper than 4000 m, which is a combination of NADW and Antarctic Bottom Water (AABW; Jenkins et al., in review), concentrations of filtered total Hg (1.3 ± 0.1 pM) were greater than those in NADW and comparable to concentrations in AABW in the Southern Ocean (1.4 ± 0.4 pM; Cossa et al., 2011). The similarity of concentrations between the deepest waters of the North Atlantic and those in young AABW suggests that Hg is not effectively scavenged from deep waters on time scales <300 years. Ineffective scavenging may result from either an attenuated particle flux at depth (Antia et al., 2001) or Hg existing

predominantly as either complexes (e.g., Hg-organic ligands; Fitzgerald et al., 2007) or redox species (Hg^0, described below) that are less relative to particles. With the exception of zonal Stations 2, 3, and 6 on the northwest continental margin, filtered total Hg was not more concentrated in water overlying the sediment interface, suggesting that diffusion and advection of dissolved and colloidal Hg from deep-sea sediments is not an important source to the ocean.

Total Hg in suspended particles accounted for less than 10% of Hg in the water column of the North Atlantic, with much greater concentrations in surface waters than at depth (Figure 3b). The vertical distribution of particulate total Hg is consistent with that of particulate organic matter in the North Atlantic (Antia et al., 2001). The mean concentration of particulate total Hg along the U.S. GEOTRACES sections (Table 1; 0.038 ± 0.039 pM) is similar to that determined by Mason and colleagues (1998) in surface waters of the North Atlantic between 50 and 70 °N (0.035 ± 0.02 pM). Similar concentrations of particulate total Hg between this study and that of Mason and co-workers (1998) further suggest that concentrations of filtered total Hg determined in the previous study may be artificially high, unless there has been a significant change in particle-water partitioning of Hg in the North Atlantic during the past 20 years. Elevated concentrations of total Hg on suspended particles (but not in filtered water) were observed in benthic nephloid layers at meridional Station 9 in the eastern Atlantic and zonal Stations 4, 8, and 10 in the western Atlantic (Figure 3b). Particles enriched with metal-oxides apparently scavenge Hg in the TAG hydrothermal plume, which is discussed in section 3.6.

3.3.3 Elemental Hg

Elemental Hg has a complex vertical and horizontal distribution across the North Atlantic (Figure 4). Elemental Hg is the product of both photochemical and biological mechanisms that reduce Hg(II) substrates (Costa and Liss, 1999; Rolfhus and Fitzgerald, 2004; Poulain et al., 2007) as well as biological and photochemical demethylation of methylated Hg (Mason and Fitzgerald, 1993; Lehnherr et al., 2011), with both biological reduction and demethylation potentially mediated by the *mer*-operon (Barkay et al., 2003). Concentrations of Hg^0 varied nearly 100-fold within the North Atlantic (Table 1), with levels in thermocline and deep waters typically exceeding those in the upper 100 m of the water column (mean = 0.15 ± 0.12 pM, n = 109). Levels of Hg^0 in the mixed layer of the North Atlantic at our sampling locations between 17 and 40 °N are much less than those measured between 50 and 70 °N (0.65 ± 0.39 pM; Mason et al., 1998). Elemental Hg at the sea surface, sampled underway at 2 m depth with a towed fish, averaged 0.05 ± 0.03 pM (n = 24).

Vertical profiles of Hg^0 had a distinct nutrient-type distribution that closely followed that of total filtered Hg and nitrate in the western North Atlantic (zonal Stations 1-12 and 14), as shown for Station 12 (Figure 5a). This was unexpected as nutrient-type profiles of Hg^0 had not previously been documented, also photochemical and microbial reduction of Hg(II) in surface waters can lead to super-saturation of Hg^0 with respect to the atmosphere (Andersson et al., 2011), suggesting maximum rather than minimum concentrations could be found at the surface. In the western basin, Hg^0 concentrations increased with depth from the surface, were greatest in the ODZ, and relatively homogenous at greater depths. In contrast, at stations in the eastern North Atlantic (zonal

Stations 16-24, and meridional Stations 11-12), Hg^0 was maximum in the ODZ with much lower concentrations in sub-thermocline waters (Figure 5b). Both Hg^0 concentrations and the fraction of filtered total Hg as Hg^0 in NADW differed significantly between the western and eastern North Atlantic (Mann-Whitney rank sum, *p*-values < 0.001). The mean concentration of Hg^0 in western NADW (0.42 ± 0.09 pM, *n* = 66) was nearly twice that of eastern NADW (0.26 ± 0.10 pM, *n* = 72). Likewise, the fraction of filtered total Hg as Hg^0 in NADW also was greater in the western (42 ± 8%, *n* = 63) than eastern basin (30 ± 15% *n* = 59).

One potential explanation for the horizontal segregation of Hg^0 in NADW is that Hg^0 is downwelled during NADW formation in the Labrador and Norwegian Seas and slowly oxidized as the water ages. A study of Hg in the sub-polar North Atlantic near locations of NADW formation found that Hg^0 was produced in the mixed layer and conserved as the water mass was formed and sank to depth (Mason et al., 1998). Concentrations of Hg^0 in NADW in the western North Atlantic (0.42 ± 0.09 pM) are not different from those in surface waters of the Norwegian Sea (0.35 ± 0.18 pM; Mason et al., 1998) and support this hypothesis. However, a more recent study found concentrations of DGM (> 90% as Hg^0 in surface water; Mason et al., 1998) were 0.1 pM or less in surface waters of the Labrador Sea (Andersson et al., 2008), which is a source region for NADW formation and contradicts this hypothesis. Measurements of Hg^0 in NADW along a meridional section of the western North Atlantic, ideally between the equator and Labrador and Norwegian Seas, would help validate whether Hg^0 is conserved during the first century of deep water flow.

Alternatively, Hg^0 concentrations in deep water may represent a balance between *in situ* reduction and oxidation reactions. While photochemical processes are thought to be the primary mechanism of Hg reduction in the surface ocean (Rolfhus and Fitzgerald, 2004), the concentration maximum of Hg^0 that extends across the Atlantic in the ODZ is indicative of a dark reaction leading to its formation at depth, likely coincident with organic matter remineralization. By extension, it is reasonable to speculate that Hg^0 in deep water masses also is formed by either an abiotic or microbial reduction process. The difference of Hg^0 concentrations in NADW between the western and eastern basins of the North Atlantic may be due to differences in either Hg reactivity or activity of reductants, including microbes, in the water. Biological reduction of Hg can be mediated by microbes containing *mer*-operon encoded proteins (Barkay et al., 2003). While the evolutionary time frame of the *mer*-operon has not been identified, it is plausible that increasing Hg in the environment during the past 150 years has exerted selective pressure on the *mer* operon (Boyd and Barkay, 2012). Accordingly, older NADW may contain less Hg^0 due to lower efficiency of microbial Hg reduction, compared to younger NADW generated during the last 100 years when anthropogenic Hg emissions were increasing. In contrast, the *mer* operon may have a much slower evolutionary time scale and the difference in Hg^0 between older eastern and younger western NADW may result from exhaustion of reducible forms of Hg after >100 y. Based on the distribution and relatively low concentrations of MMHg and DMHg across the transect, reductive demethylation cannot explain the difference in Hg^0 concentrations between basins.

3.3.4 Monomethylmercury

Monomethylmercury in filtered water ranged from <0.002 (detection limit) to 0.60 pM in the North Atlantic Ocean (Table 1). The typical vertical distribution of filtered MMHg at most stations in the North Atlantic was relatively low concentrations in the upper 100 m (0.06 ± 0.05 pM, n = 70), a subsurface maximum in the ODZ, and lower concentrations in water below the thermocline (Figure 6a), which is consistent with vertical distributions observed in other ocean basins (Mason and Fitzgerald, 1993; Mason and Sullivan, 1999; Sunderland et al., 2009; Cossa et al., 2009, 2011; Hammerschmidt and Bowman, 2012). Although Hg is methylated in the mixed layer (Lehnherr et al., 2011), relatively low concentrations of MMHg there can be attributed to bioaccumulation and photochemical and microbial decomposition (Monperrus et al., 2007; Lehnherr et al., 2011; Black et al., 2012; Hammerschmidt and Bowman, 2012). As observed for filtered total Hg and Hg^0, filtered MMHg concentrations in NADW were significantly greater in the western (0.15 ± 0.12 pM, n = 31) than eastern basin (0.06 ± 0.06 pM, n = 64; Mann-Whitney rank sum, $p < 0.001$), although there was more intra-basin variability of MMHg concentrations than for the other two Hg species. This comparison of MMHg concentrations in NADW neglects results from Station 16 on the Mid-Atlantic Ridge that has hydrothermal inputs. Some of the variability and greater mean concentration of filtered MMHg in NADW of the western North Atlantic can be attributed to increased concentrations near the slopes of the northwest Atlantic and Bermuda, which may result from benthic production and mobilization to overlying water (Hollweg et al., 2010). Aside from these locations, deep ocean sediments do not appear to be an important source of MMHg to the water column of the North Atlantic, as also hypothesized for

other ocean basins (Heimbürger et al., 2010; Cossa et al., 2011; Hammerschmidt and Bowman, 2012). Similar to filtered total Hg, filtered MMHg in AABW (0.18 ± 0.08 pM) was increased relative to NADW.

The primary influence on MMHg cycling in the eastern North Atlantic is strong particle scavenging (Figure 6). Scavenging in the eastern Atlantic is evident from both the very low concentrations of filtered MMHg and relatively high levels of particulate MMHg in the mixed layer and permanent thermocline (Figure 6b). Increased particulate MMHg concentrations near the African coast, which are unlike those in the rest of the North Atlantic, are the result of high dust deposition and coastal upwelling that fuel primary production. Given that suspended material had exceedingly low concentrations of MMHg (mean = 0.0007 ± 0.001 pM) and that sinking particles have similar, if not lower, concentrations of MMHg than suspended particles (Lamborg et al, 2009), we would expect release of surface-formed MMHg from sinking particles during remineralization to have little influence on levels of filtered MMHg in the thermocline. Such is the case in the far eastern North Atlantic, where there is no connection between particulate and filtered MMHg. On average, suspended particles contained less than 1% of total MMHg in the water column.

Subsurface maxima of filtered MMHg were observed in the ODZ across the North Atlantic. Maxima of methylated Hg in ODZs, or oxygen minimum zones, have been widely attributed to *in situ* production fueled by microbial remineralization of organic matter (Cossa et al., 1994, 2009; Mason & Fitzgerald, 1993; Mason and Sullivan, 1999; Sunderland et al., 2009; Heimbürger et al., 2010; Hammerschmidt and Bowman, 2012). Multiple sectional oceanographic studies have observed positive associations

between concentrations of methylated Hg and either apparent oxygen utilization (AOU; Mason and Sullivan, 1999; Cossa et al., 1994, 2009, 2011; Kirk et al., 2008; Heimbürger et al., 2010; Lehnherr et al., 2011) or organic carbon remineralization rate (Sunderland et al., 2009), which could be interpreted to suggest that production of methylated Hg in the marine water column is limited by microbial methylation potential more than it is by Hg(II) availability. However, we observed no correlation between filtered MMHg concentration and either the concentration of dissolved O_2 ($p = 0.15$) or AOU ($p = 0.42$) across these far ranging sections of the North Atlantic. This suggests that lower oxygen concentrations and the microbial community, potentially including anaerobes, in the ODZ are not unique in their ability to produce MMHg, which is consistent with results from process studies. Incubation tests with waters from the eastern equatorial Pacific Ocean and Arabian Sea imply that Hg(II) methylation is not particularly active in oxygen minimum zones and anaerobic microorganisms are not important methylators of Hg in the marine water column (Malcolm et al., 2010). Moreover, rates of Hg methylation were similar between the oxic mixed layer, near the subsurface chlorophyll maximum, and oxygen minimum zone at multiple locations in the Canadian Arctic Archipelago (Lehnherr et al., 2011). Thus, an alternative hypothesis for the maxima of MMHg in the ODZ is that MMHg may be produced throughout the marine water column and is less susceptible to decomposition and scavenging in the ODZ than it is at other depths. While the functional identities of microorganisms that demethylate MMHg are largely unknown, a slower rate of decomposition in the ODZ is consistent with the inhibitory effect of low O_2 concentrations on rates of aerobic metabolism as well as the rarity of *mer* genes in anaerobic microbes (Barkay et al., 2010).

Secondary maxima of filtered MMHg also were observed at depths shallower than the ODZ and near the chlorophyll and oxygen maxima at zonal Stations 16–22 in the eastern North Atlantic Ocean (Figure 7). Maxima of filtered MMHg (~0.2–0.6 pM) were observed between 100–200 m at these stations and within about 80 m depth of the in situ fluorescence and associated O_2 maxima. Increased MMHg concentrations immediately below the euphotic zone can be interpreted to indicate production in surface waters and may result from enhanced microbial respiration of organic carbon (Heimbürger et al., 2010).

3.3.5 Dimethylmercury

The distribution of DMHg in the North Atlantic is similar to that of MMHg and Hg^0 (Figure 8). Like MMHg, concentrations of DMHg in the upper 100 m were extremely low, increased in the ODZ, and were relatively homogeneous with depth. Low concentrations of DMHg in the mixed layer are a result of its evasion to the atmosphere (Black et al., 2009). Also similar to MMHg, concentrations of DMHg in NADW were considerably greater in the western North Atlantic (mean = 0.18 ± 0.12 pM, n = 48) than on the east side of the Mid-Atlantic Ridge (mean = 0.07 ± 0.04 pM, n = 23; Mann-Whitney rank sum, $p < 0.001$), excluding results from Station 16 above the ridge. Water deeper than 4000 m, a combination of AABW and NADW, contained 0.18 ± 0.12 pM of DMHg (n = 16), a mean concentration similar to that in western NADW. The average concentration of ΣCH_3Hg, calculated as the sum of MMHg and DMHg, in AABW was 0.37 ± 0.08 pM at stations between 20 and 30 °N, and comparable to, if not slightly less than, ΣCH_3Hg levels measured in AABW in the Southern Ocean (0.52 ± 0.11 pM; Cossa et al., 2011).

Dimethylmercury can be the dominant form of methylated Hg in the open ocean (Mason and Fitzgerald, 1993; Mason et al., 1995; Mason and Sullivan, 1999). For surface waters in which DMHg was detectable, the filtered MMHg:DMHg molar ratio was large and highly variable in the upper 100 m of the water column (18 ± 25). In contrast, MMHg:DMHg averaged 1.6 ± 1.8 in North Atlantic water deeper than 1000 m. The filtered MMHg:DMHg ratio for sub-thermocline waters in the North Atlantic is similar to that in North Pacific Deep and Bottom Waters (> 1500 m), which averaged 1.9 ± 0.4 (Hammerschmidt and Bowman, 2012), and suggests that MMHg is dominant form of methylated Hg in deep waters. DMHg has been posited to be the immediate product of microbial methylation, with MMHg resulting from its decomposition (Mason and Fitzgerald, 1993; Mason et al., 1995; Mason and Sullivan, 1999). However, results from a recent process study suggest that the rate of MMHg formation from Hg(II) is about three orders of magnitude greater than production of DMHg from Hg(II) in seawater (Lehnherr et al., 2011), suggesting that DMHg may be formed primarily by methylation of MMHg.

Unlike Hg^0 in NADW, which may have been downwelled during deep water formation, DMHg in the water mass was likely formed in situ during thermohaline flow. DMHg concentrations in the mixed layer of the Labrador and Norwegian Seas were either undetectable or less than 0.02 pM (Mason et al., 1998). On the basis of oceanographic measurements and modeling, Mason and Fitzgerald (1993) hypothesized that DMHg accumulates slowly in seawater because its rate of formation and decomposition are of the same order of magnitude. They later observed that DMHg in recently formed NADW increased with age and depth of the water, from about 0.03 pM

in the upper water column to 0.13 ± 0.08 pM at depth at stations between 50 and 60 °N (Mason et al., 1998). Our results for DMHg in NADW in the western Atlantic (0.18 ± 0.12 pM) are consistent with this hypothesis and suggest that concentrations may have increased during southward transit between 50 and 60 °N to between 25 and 40 °N in the current study. However, the lower concentrations of DMHg in NADW of the eastern compared to the western basin are inconsistent with the hypothesis. Indeed, levels of both DMHg and filtered MMHg were significantly lower in older eastern than younger western NADW. The mean concentration of DMHg in western NADW was 2.6-fold greater than that in the eastern basin and the average level of MMHg in the west was 2.5-fold greater than in eastern NADW. The similarity of these enrichment factors indicates that concentrations of filtered MMHg and DMHg are proportional in NADW on both sides of the Mid-Atlantic Ridge. However, the difference between these enrichment factors and that of filtered total Hg in NADW (1.14-fold greater in the west), suggests that older NADW has less of a methylation potential for Hg than younger deep water in the west. This is supported by the mean fraction of total Hg as MMHg in filtered water being significantly greater in western NADW (14 ± 11%) than in eastern NADW (7 ± 8%; Mann-Whitney rank sum, $p < 0.01$). A difference in the average percentage of filtered total Hg as ΣCH_3Hg in NADW also existed between the western (33 ± 16%) and eastern (23 ± 14%) North Atlantic but the difference was not significant at $\alpha = 0.05$ (*t*-test, $p = 0.08$).

3.3.6 TAG hydrothermal vent plume

Seawater and suspended particles were sampled from a plume at the TAG submarine hydrothermal vent mound located on the east wall of the Mid-Atlantic Ridge

(Station 16, 26.14 °N, 44.83 °W; Rona et al., 1986). The buoyant plume was located between 3200 and 3400 m depth and identified during sampling with a transmissometer. Previous studies of vent systems in the Pacific Ocean have found a wide range of total Hg concentrations in hydrothermal vent fluids (4–11,000 pM; Lamborg et al., 2006; Crespo-Medina et al., 2009) although little is known about Hg in vent systems of the Atlantic Ocean (Demina et al., 2012).

Mercury is emitted from the TAG hydrothermal vent and Hg species are scavenged and transformed in the plume (Figures 3 and 9). The maximum concentration of filtered total Hg in the plume was 13 pM at 3400 m depth, more than 10× greater than levels in surrounding NADW (Figure 9a). The speciation of Hg at the filtered total Hg maximum (3400 m depth) was 8% as Hg^0, 3% as filtered MMHg, and less than 0.2% as DMHg, with particulate Hg comprising less than 2% of the total Hg. This speciation is in contrast to vent fluids sampled at the Gorda Ridge in the Pacific Ocean where nearly all Hg was present as MMHg (Lamborg et al., 2006). At shallower depths in the plume (3200–3330 m), filtered total Hg decreased to 0.90 ± 0.04 pM, concentrations less than those in NADW above the plume (1.15 pM), and Hg^0 decreased to 0.13 ± 0.06 pM and as low as 0.05 pM at 3250 m (Figure 9a), a concentration 8-fold less than in NADW above the plume and 20-fold greater than at 3400 m. The decline of filtered total Hg between the bottom and interior of the plume can be attributed to scavenging. Metal oxides are formed within the plume and concentrations of particulate total Hg follow those of particulate Fe oxides, with 27% of the total at 3300 m depth being associated with particles (Figure 9b). Because Hg^0 is not particle reactive, its loss from the core of the hydrothermal plume may result from oxidation reactions.

The TAG hydrothermal vent also was a localized source of MMHg, but not DMHg, to the deep North Atlantic (Figure 9). MMHg was enriched in the hydrothermal plume relative to waters above and below. In contrast to total Hg that was reactive to particle scavenging, more than 99.5% of MMHg in the plume was in the filtered phase, resulting in MMHg accounting for 42 ± 24% of filtered total Hg in the plume at depths other than the filtered total Hg maximum at 3400 m. Particle-water partitioning coefficients of MMHg are typically an order of magnitude less than those of Hg(II) in oxic seawater (Balcom et al., 2008). The apparent absence of any DMHg enrichment in the hydrothermal plume is consistent with DMHg being less stable at higher temperatures (Mason and Sullivan, 1999) and lower pH (Wood et al., 1968; Beijer and Jernelöv, 1979) that would expected in the vent. While the source of MMHg in submarine hydrothermal fluids is unknown and may be either biological or abiotic (Lamborg et al., 2006), the two gene clusters associated with bacterial Hg methylation (Parks et al., 2013) have been identified in at least one species of hydrothermal vent bacteria, *Deferrisoma camini* (Slobodkina et al., 2012).

3.4. Summary

The U.S. GEOTRACES zonal and meridional sections of the North Atlantic Ocean have allowed for the first fully resolved high-resolution examination of Hg speciation within this ocean basin. We found that total Hg, MMHg, Hg^0, and DMHg in water of the North Atlantic are vertically segregated as a function of bioaccumulation, scavenging, remineralization, and transformation reactions in the water column. A hydrothermal vent on the Mid-Atlantic Ridge was confirmed to be a source of total Hg and MMHg to deep water, as suggested by previous studies of vent fluids elsewhere. Our

most significant and unexpected discovery was the horizontal segregation of Hg and its chemical species in NADW between the western and eastern North Atlantic. While greater concentrations of filtered total Hg in younger NADW of the western basin compared to the eastern North Atlantic may be attributed to younger NADW having downwelled anthropogenic Hg during deep water formation (Lamborg et al., accepted), the reason for horizontal enrichment of Hg^0, MMHg, and DMHg in western NADW is unknown. We speculate that younger NADW has a greater methylation and reduction potential than older waters in the mass. Both a meridional section of the western North Atlantic as well as process-based investigations are needed to better understand the enrichment of Hg^0, MMHg, and DMHg in western NADW.

Acknowledgements

We thank our U.S. GEOTRACES colleagues, especially co-chief scientists Greg Cutter, Ed Boyle, and Bob Anderson. Jessica Fitzsimmons, Peter Morton, Randie Bundy, Rachel Shelley, and Anna Aguilar-Islas helped sample and filter water. Phoebe Lam and Dan Ohnemus sampled suspended particles and provided particulate Fe data for the hydrothermal plume. This research was supported by the U.S. National Science Foundation Chemical Oceanography Program.

References

Andersson, M.E., Sommar, J., Gårdfeldt, K., Jutterström, S. 2011. Air-sea exchange of volatile mercury in the North Atlantic Ocean. Mar. Chem. 125, 1–7.

Barkay, T., Miller, S.M., Summers, A.O. 2003. Bacterial mercury resistance from atoms to ecosystems. FEMS Microbiol. Rev. 27, 355–384.

Bishop, J.K.B., Lam, P.J., Wood, T.J. 2012. Getting good particles: Accurate sampling of particles by large volume in-situ filtration. Limnol. Oceanogr.: Methods 10, 681–710.

Bloom, N.S. 1989. Determination of pictogram levels of methylmercury by aqueous phase ethylation, followed by cryogenic gas chromatography, with cold vapour atomic fluorescence detection. Can. J. Fish. Aquat. Sci. 46, 1131–1140.

Bloom, N.S., Fitzgerald, W.F. 1988. Determination of volatile mercury species at the picogram level by low-temperature gas chromatography with cold-vapor atomic fluorescence detection. Anal. Chim. Acta. 208, 151–161.

Blum, J.D., Popp, B.N., Drazen, J.C., Choy, C.A., Johnson, M.W. 2013. Methylmercury production below the mixed layer in the North Pacific Ocean. Nat. Geosci. 6, 879–884.

Bose-O'Reilly, S., McCarty, K.M., Steckling, N., Lettmeier, B. 2010. Mercury exposure and children's health. Curr. Probl. Pediatr. Adolesc. Health Care 40, 186–215.

Bowman, K.L., Hammerschmidt, C.R. 2011. Extraction of monomethylmercury from seawater for low-femtomolar determination. Limnol. Oceanor-Meth. 9, 121–128.

Boyd, E.S., Barkay, T. 2012. The mercury resistance operon: from an origin in a geothermal environment to an efficient detoxification machine. 3, 349.

Broecker, W.S., Blanton, S., Smethie, W., Ostlund, G. 1991. Radiocarbon decay and oxygen utilization in the deep Atlantic Ocean. Global Biogeochem. Cycles 5, 87–117.

Cossa, D., Elbaz-Poulichet, F., Nieto, J.M. 2001. Mercury in the Tinto-Odiel Estuarine System (Gulf of Cádiz, Spain): Sources and dispersion. Aquat. Geochem. 7, 1–12.

Cossa, D., Heimbürger, L.-E., Lannuzel, D., Rintoul, S.R., Butler, E.C.V., Bowie, A.R., Averty, B., Watson, R.J., Remenyi, T. 2011. Mercury in the Southern Ocean. Geochim. Cosmochim. Ac. 75, 4037–4052.

Cossa, D., Martin, J-M., Takayanagi, K., Sanjuan, J. 1997. The distribution and cycling of mercury species in the western Mediterranean. Deep-Sea Res. II 44, 721–740.

Costa, A.M., Mil-Homens, M., Lebreiro, S.M., Richter, T.O., de Stigter, H., Boer, W., Trancoso, M.A., Melo, Z., Mouro, F., Mateus, M., Canário, J., Branco, V., Caetano, M. 2011. Origin and transport of trace metals deposited in the canyons off Lisboa and adjacent slopes (Portuguese Margin) in the last century. Mar. Geol. 282, 169–177.

Crespo-Medina, M., Chatziefthimiou, A.D., Bloom, N.S., Luther III, G.W., Wright, D.D., Reinfelder, J.R., Vetriani, C., Barkay, T. 2009. Adaptation of chemosynthetic microorganisms to elevated mercury concentrations in deep-sea hydrothermal vents. Limnol. Oceanogr. 54, 41–49.

Cutter, G.A., Bruland, K.W. 2012. Rapid and noncontaminating sampling system for trace elements in global ocean surveys. Limnol. Oceanogr-Meth. 10, 425–430.

Demina, L.L., Holm, N.G., Galkin, S.V., Lein, A.Y. 2012. Some features of the trace metal biogeochemistry in the deep-sea hydrothermal vent fields (Menez Gwen, Rainbow, Broken Spur at the MAR and 9°50'N at the EPR): A synthesis. J. Marine Syst. http://dx.doi.org/10.1016/j.marsys.2012.09.005.

England, M.H. 1995. The age of water and ventilation timescales in a global ocean model. J. Phys. Oceanogr. 25, 2756–2777.

FAO (Food and Agriculture Organization of the United Nations). 2012. The state of world fisheries and aquaculture 2012. FOA Fisheries and Agriculture Department. http://www.fao.org/docrep/016/i2727e/i2727e.pdf.

Figueres, G., Martin, J.M., Meybeck, M., Seyler, P. 1985. A comparative study of mercury contamination in the Tagus Estuary (Portugal) and major French esutaries (Gironde, Loire, Rhône). Estuarine Coastal Shelf Sci. 20, 183–203.

Fitzgerald, W.F., Engstrom, D.R., Mason, R.P., Nater, E.A. 1998. The case from atmospheric mercury contamination in remote areas. Environ. Sci. Technol. 32, 1–7.

Fitzgerald, W.F., Gill, G.A. 1979. Subnanogram determination of mercury by two-stage gold amalgamation applied to atmospheric analysis. Anal. Chem. 51, 1714–1720.

Fitzgerald, W.F., Lamborg, C.H., Hammerschmidt, C.R. 2007. Marine biogeochemical cycling of mercury. Chem. Rev. 107, 641–662.

Hammerschmidt, C.R. 2011. Mercury and carbon dioxide relationships: Uncoupling a toxic relationship. Environ. Toxicol. Chem. 30, 2640–2646.

Hammerschmidt, C.R., Bowman, K.L. 2012. Vertical methylmercury distribution in the subtropical North Pacific Ocean. Mar. Chem. 132–133, 77–82.

Hammerschmidt, C.R., Bowman, K.L., Tabatchnick, M.D., Lamborg, C.H. 2011. Storage bottle material and cleaning for determination of total mercury in seawater. Limnol. Oceanor-Meth. 9, 426–431.

Hammerschmidt, C.R., Fitzgerald, W.F. 2006. Bioaccumulation and trophic transfer of methylmercury in Long Island Sound. Arch. Environ. Contam. Toxicol. 51, 416–424.

Hammerschmidt, C.R., Fitzgerald, W.F. 2010. Iron-mediated photochemical decomposition of methylmercury in an artic Alaskan lake. Environ. Sci. Technol. 44, 6138–6143.

Heimbüger, L.-E., Cossa, D., Marty, J.-C., Migon, C., Averty, B., Dufour, A., Ras, J. 2010. Methyl mercury distributions in relation to the presence of nano- and picophytoplankton in an oceanic water column (Ligurian Sea, North-western Mediterranean). Geochim. Cosmochim. Acta 74, 5549–5559.

Holmes, C.D., Jacob, D.J., Mason, R.P., Jaffe, D.A. 2009. Sources and deposition of reactive gaseous mercury in the marine atmosphere. Atmos. Environ. 43, 2278–2285.

Kerin, E.J., Gilmour, C.C., Roden, E., Suzuki, M.T., Coates, J.D., Mason, R.P. 2006. Mercury methylation by dissimilatory iron-reducing bacteria. Appl. Environ. Microb. 72, 7919– 7921.

Kocman, D., Horvat, M., Pirrone, N., Cinnirella, S. 2013. Contribution of contaminated sites to the global mercury budget. Environ. Res. http://dx.doi.org/10.1016/j.envres.2012.12.011.

Lamborg, C.H., Fitzgerald, W.F., Damman, A.W.H., Benoit, J.M., Balcom, P.H., Engstrom, D.R. 2002. Modern and historic atmospheric mercury fluxes in both hemispheres: Global and regional mercury cycling implications. Global Biogeochem. Cycles 16, 1104, http://dx.doi.org/10.1029/2001GB001847.

Lamborg, C.H., Hammerschmidt, C.R., Gill, G.A., Mason, R.P., Gichuki, S. 2012. An intercomparison of procedures for the determination of total mercury in seawater and recommendations regarding mercury speciation during GEOTRACES cruises. Limnol. Oceanor-Meth. 10, 90–100.

Lamborg, C.H., Von Damm K.L., Fitzgerald, W.F., Hammerschmidt, C.R., Zierenberg, R. 2006. Mercury and monomethylmercury in fluids from Sea Cliff submarine hydrothermal field, Gorda Ridge. Geophys. Res. Lett. 33, L17606, doi:10.1029/2006GL026321.

Lehnherr, I., St. Louis, V.L., Hintelmann, H., Kirk, J.L. 2011. Methylation of inorganic mercury in polar marine waters. Nat. Geosci. 4, 298–302.

Malcom, E.G., Schaefer, J.K., Ekstrom, E.B., Tuit, C.B., Jayakumar, A., Park, H., Ward, B.B., Morel, F.M.M. 2010. Mercury methylation in oxygen deficient zones of the oceans: No evidence for the predominance of anaerobes. Mar. Chem. 122, 11–19.

Mason, R.P., Choi, A.L., Fitzgerald, W.F., Hammerschmidt, C.R., Lamborg, C.H., Soerensen, A.L., Sunderland, E.M. 2012. Mercury biogeochemical cycling in the ocean and policy implications. Environ. Res. 119, 101–117.

Mason, R.P, Fitzgerald, W.F. 1993. The distribution and biogeochemical cycling of mercury in the equatorial Pacific Ocean. Deep-Sea Res. I 40, 1897–1924.

Mason, R.P., Lawson, N.M., Sheu, G.-R. 2001. Mercury in the Atlantic Ocean: factors controlling air-sea exchange of mercury and its distribution in the upper waters. Deep-Sea Res. II 48, 2829–2853.

Mason, R.P., Rolfhus, K.R., Fitzgerald, W.F. 1995. Methylated and elemental mercury cycling in surface and deep ocean waters of the North Atlantic. Water Air Soil Pollut. 80, 665–677.

Mason, R.P., Rolfhus, K.R., Fitzgerald, W.F. 1998. Mercury in the North Atlantic. Mar. Chem. 61, 37–53.

Mason, R.P., Sheu, G.-R. 2002. Role of the ocean in the global mercury cycle. Global Biogeochem. Cycles 16, doi: 10.1029/2001GB001440.

Mason, R.P., Sullivan, K.A. 1999. The distribution and speciation of mercury in the South and equatorial Atlantic. Deep-Sea Res. II 46, 937–956.

Mieiro, C.L., Pato, P., Pereira, E., Mirante, F., Coutinho, J.A.P., Pinheiro, L.M., Magalhães, V.H., Duarte, A.C. 2007. Total mercury in sediments from mud volcanoes in Gulf of Cadiz. Mar. Pollut. Bull. 54, 1523–1558.

Mil-Homens, M., Blum, J., Canário, J., Caetano, M., Costa, A.M., Lebreiro, S.M., Trancoso, M., et al. 2013. Tracing anthropogenic Hg and Pb input using stable Hg and Pb isotope ratios in sediments of the central Portuguese Margin. Chem. Geol. 336, 62–71.

Monperrus, M., Tessier, E., Amouroux, D., Leynaert, A., Huonnic, P., Donard, O.F.X. 2007. Mercury methylation, demethylation and reduction rates in coastal and marine surface waters of the Mediterranean Sea. Mar. Chem. 107, 49–63.

NOAA (National Oceanic and Atmospheric Administration). Table of Global Hydrothermal Vents. http://www.pmel.noaa.gov/vents/PlumeStudies/global-vents/global-vents-text.html.

Parks, J.M., Johs, A., Podar, M., Bridou, R., Hurt Jr., R.A., Smith, S.D., et al. 2013. The genetic basis for bacterial mercury methylation. Science 339, 1332–1335.

Pascale, P.B., Hollinsworth, J.L., Hintelmann, H. 2013. Evaluation and optimization of solid adsorbents for the sampling of gaseous methylated mercury species. Anal. Chim. Acta 786, 61–69.

Pirrone, N., Cinnirella, S., Feng, X., Finkelman, R.B., Friedli, H.R., Leaner, J., et al. 2010. Global mercury emissions to the atmosphere from anthropogenic and natural sources. Atmos. Chem. Phys. 10, 5951–5964.

Rona, P.A., Klinkhammer, G., Nelsen, T.A., Trefry, J.H., Elderfield, H. 1986. Black smokers, massive sulfides and vent biota at the Mid-Atlantic Ridge. Nature 321, 33–37.

Sánchez-García, L., de Andrés, J.-R., Martin-Rubí, J.-A. 2010. Geochemical signature in off-shore sediments from the Gulf of Cádiz inner shelf: Sources and spatial variability of major and trace elements. J. Mar. Syst. 80, 191–202.

Scheuhammer, A.M., Meyer, M.W., Sandheinrich, M.B., Murray, M.W. 2007. Effects of environmental methylmercury on the health of wild birds, mammals, and fish. Ambio. 36, 12–18.

Schmidt, S. 2006. Impact of the Mediterranean Outflow Water on particle dynamics in intermediate waters of the Northeast Atlantic, as revealed by ^{234}Th and ^{228}Th. Mar. Chem. 100, 289–298.

Slobodkina, G.B., Reysenbach, A.-L., Panteleeva, A.N., Kostrikina, N.A., Wagner, I.D., Bonch-Osmolovskaya, E.A., Slobodkin, A.I. 2012. *Deferrisoma camini* gen. nov., sp. nov., a moderately thermophilic, dissimilatory iron (III)-reducing bacterium from a deep-sea hydrothermal vent that forms a distinct phylogenetic branch in the *Deltaproteobacteria*. Int. J. Syst. Evol. Micr. 62, 2463.

Smethie, W.M. Jr., Fine, R.A., Putzka, A., Jones, E.P. 2000. Tracing the flow of North Atlantic Deep Water using chlorofluorocarbons. J. Geophys. Res. 105, 297–323.

Streets, D.G., Zhang, W., Wu, Ye. 2009. Projections of global mercury emissions in 2050. Environ. Sci. Technol. 43, 2983–2988.

Sunderland, E. M. 2007. Mercury exposure from domestic and imported estuarine and marine fish in the U.S. seafood market. Environ. Health Perspect. 115, 235–242.

Sunderland, E.M., Krabbenhoft, D.P., Moreau, J.W., Strode, S.A., Landing, W.A. 2009. Mercury sources, distribution, and bioavailability in the North Pacific Ocean: Insights from data and models. Global Biogeochem. Cycles 23, GB2010.

Tseng, C.-M., Hammerschmidt, C.R., Fitzgerald, W.F. 2004. Determination of methylmercury in environmental matrixes by on-line flow injection and atomic fluorescence spectrometry. Anal. Chem. 76, 7131–7136.

Vetriani, C., Chew, Y.S., Miller, S.M., Yagi, J., Coombs, J., Lutz, R.A., Barkay, T. 2005. Mercury adaptation among bacteria from a deep-sea hydrothermal vent. Appl. Environ. Microb. 71, 220–226.

Zahir, F., Rizwi, S.J., Haq, S.K., Khan, R.H. 2005. Low dose mercury toxicity and human health. Environ. Toxicol. Pharmacol. 20, 351–360.

Zhang, T., Hsu-Kim, H. 2010. Photolytic degradation of methylmercury enhanced by binding to natural organic ligands. Nat. Geosci. 3, 473–476.

Table 3.1. Summary of concentrations and speciation of Hg across the transect. Average and range values are listed in pM units and include data from all 32 stations at all depths. For suspended particulate MMHg, the percentage as HgT refers only to the suspended particulate phase.

Hg species	Average ± stdev	Range	% of HgT	n
HgT[a]	0.90 ± 0.36	0.040 – 3.0	N/A	647
Hg^0	0.32 ± 0.17	0.012 – 1.0	35 ± 16	625
DMHg	0.095 ± 0.10	>DL – 0.65	10 ± 11	427
MMHg	0.095 ± 0.098	>DL – 0.60	11 ± 11	432
Particulate HgT	0.038 ± 0.039	>DL – 0.38	N/A	322
Particulate MMHg	0.00069 ± 0.0013	>DL – 0.010	4 ± 7	255

[a]Data from the TAG hydrothermal vent plume at station 16 was not included in HgT average and range.

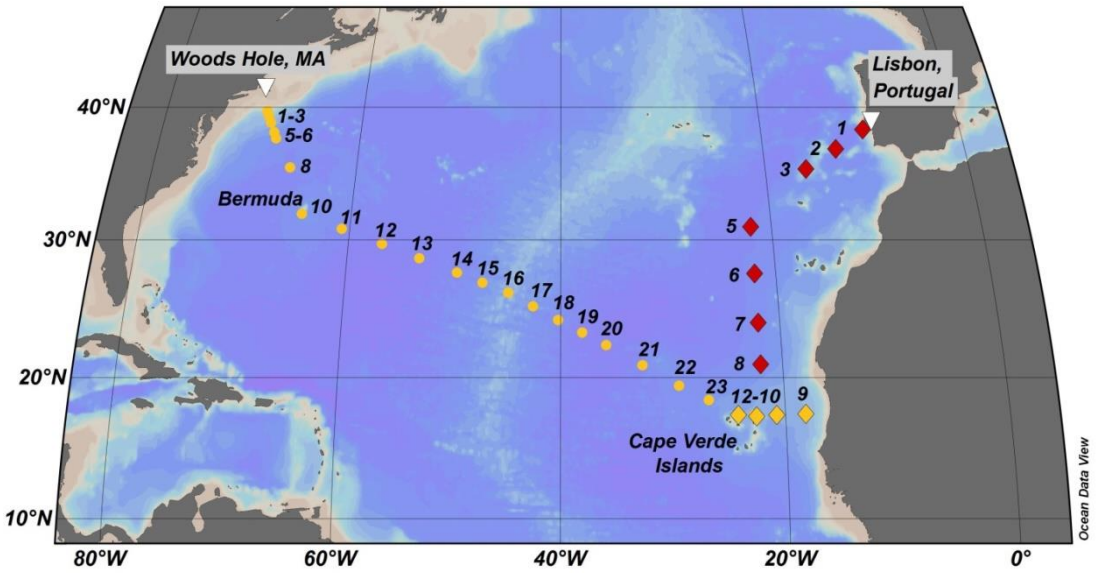

Figure 3.1. GEOTRACES GA03 water sampling stations during the meridional (red) and zonal (yellow) transects of the North Atlantic Ocean. Stations occupied in 2010 are represented by diamonds, and stations occupied in 2011 are represented by circles.

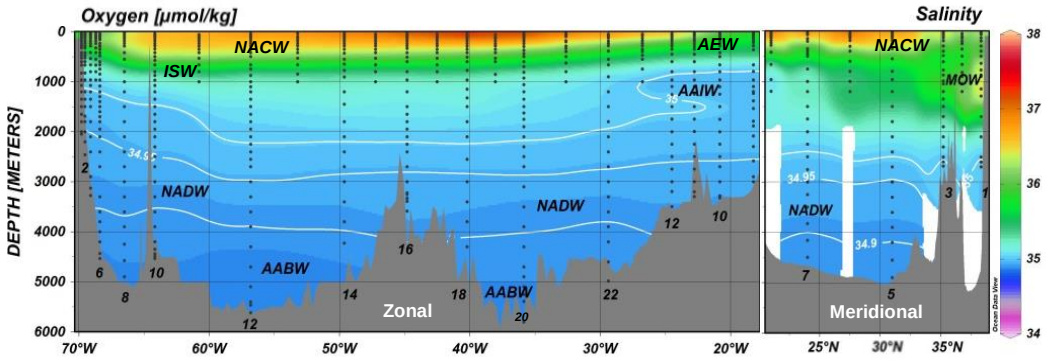

Figure 3.2. Water masses in the North Atlantic along the GEOTRACES GA03 transect, superimposed on the salinity distribution. Surface waters are mainly North Atlantic Central Water (NACW) with Atlantic Equatorial Water (AEW) at the southernmost extent of the cruise near the Cape Verde Islands. Intermediate waters include Irminger Sea Water (ISW) in the west, Antarctic Intermediate Water (AAIW) in the central basin, and Mediterranean Overflow Water (MOW) in the east. North Atlantic Deep Water (NADW) is between 1500 and ~4000 m. Water deeper than 4000 m is a mixture of NADW and Antarctic Bottom Water (AABW) with the fraction as AABW increasing below 5000 m (Jenkins et al., in review). Sampling points are shown as black dots and station numbers are listed intermittently throughout the grey bathymetric section.

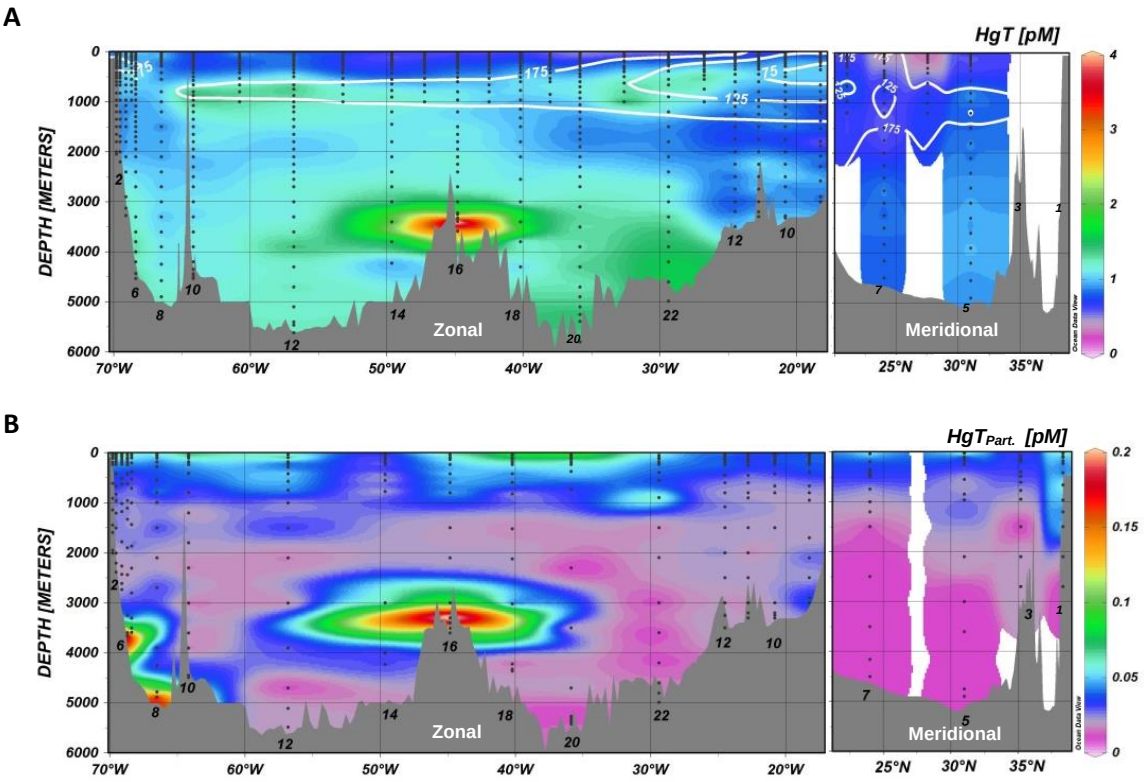

Figure 3.3. Distribution of total Hg concentrations (pM) in filtered water (panel A) and suspended particles (panel B) along GEOTRACES GA03 in the North Atlantic Ocean. Isobars of dissolved oxygen have concentration units of µmol/kg. Sampling points are shown as black dots and station numbers are listed intermittently throughout the grey bathymetric sections.

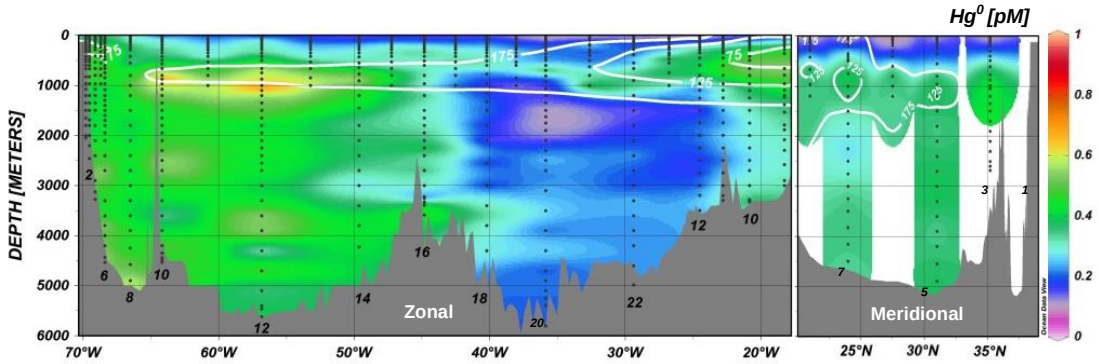

Figure 3.4. Distribution of Hg^0 (pM) along GEOTRACES GA03 in the North Atlantic Ocean. Isobars of dissolved oxygen have concentration units of μmol/kg. Sampling points are shown as black dots and station numbers are listed intermittently throughout the grey bathymetric section.

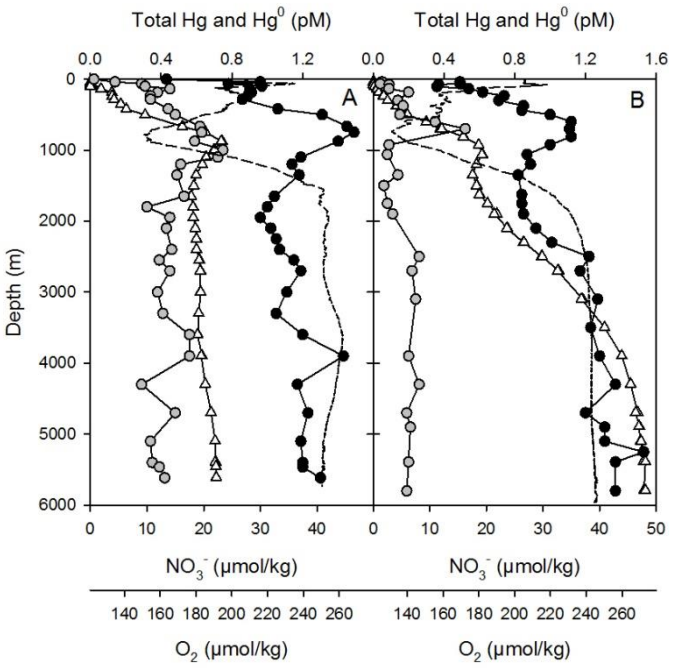

Figure 3.5. Vertical profiles of elemental Hg (grey circles), filtered total Hg (black circles), nitrate (open triangles), and dissolved oxygen (dashed line) at Stations 12 (panel A) and 20 (panel B) of GEOTRACES GA03 in the North Atlantic Ocean. Error bars are covered by figure symbols; relative percent difference was 4 ± 4 (n=5) for filtered HgT, and 0.3 ± 0.7 (n=72) for nitrate.

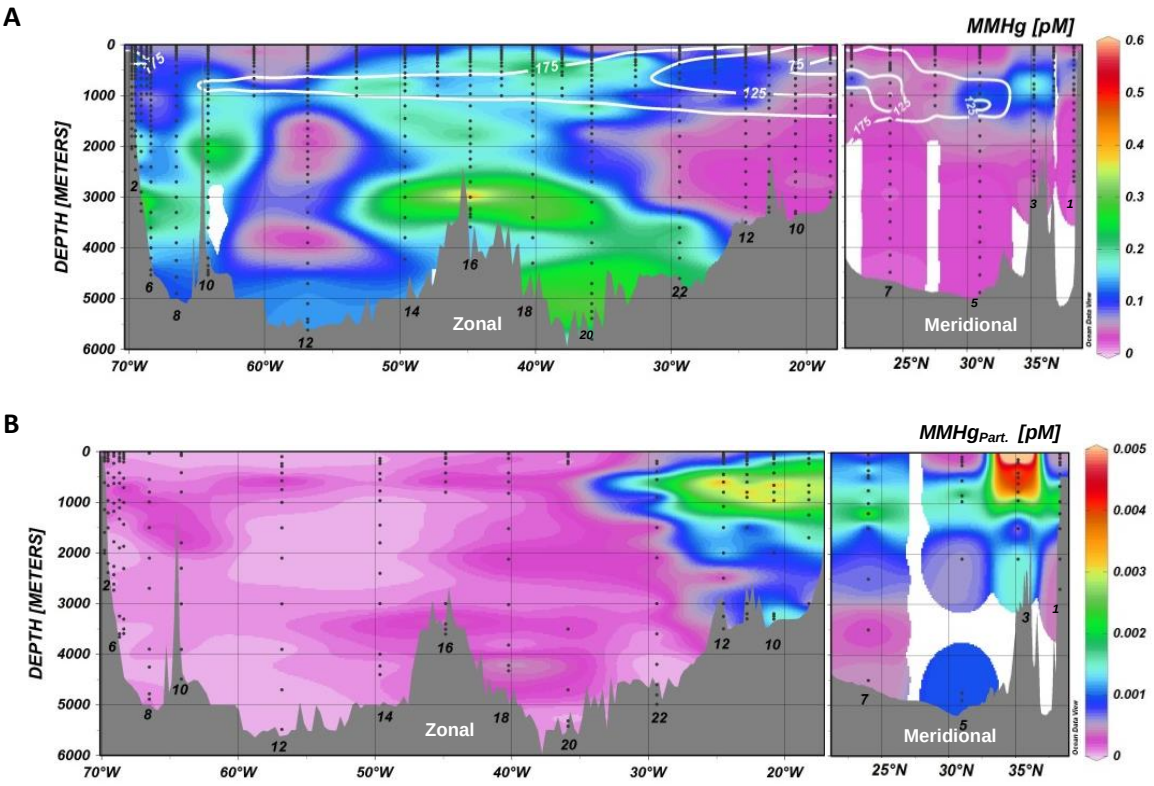

Figure 3.6. Distribution of MMHg concentrations (pM) in filtered water (panel A) and suspended particles (panel B) along GEOTRACES GA03 in the North Atlantic Ocean. Isobars of dissolved oxygen have concentration units of µmol/kg. Sampling points are shown as black dots and station numbers are listed intermittently throughout the grey bathymetric sections.

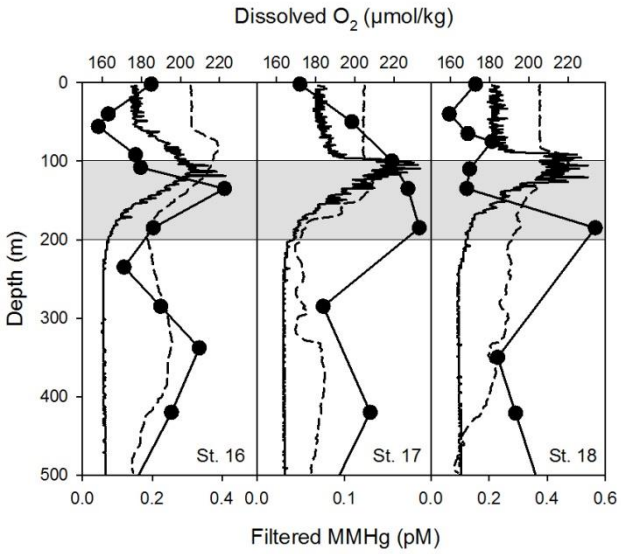

Figure 3.7. Profiles of filtered MMHg (closed circles), CTD fluorescence (solid line), and dissolved O_2 (dashed line) at zonal Stations 16–18 near the center of the North Atlantic Ocean. The grey area highlights MMHg maxima in oxic water between 100 and 200 m depth.

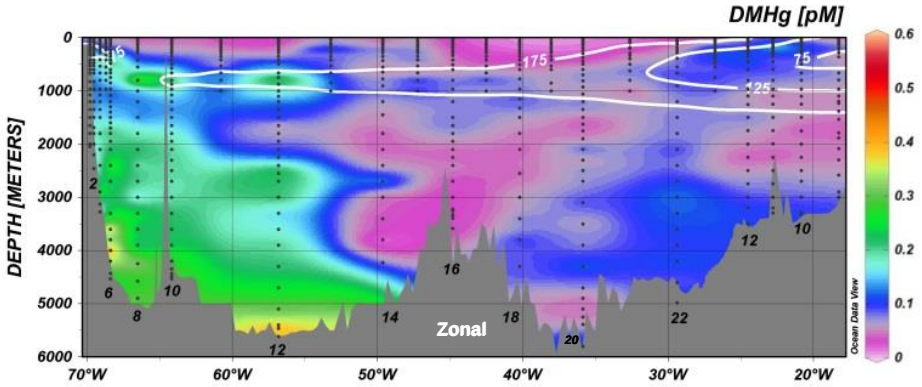

Figure 3.8. Distribution of DMHg concentrations (pM) along GEOTRACES GA03 in the North Atlantic Ocean. Isobars of dissolved oxygen have concentration units of µmol/kg. Sampling points are shown as black dots and station numbers are listed intermittently throughout the grey bathymetric section.

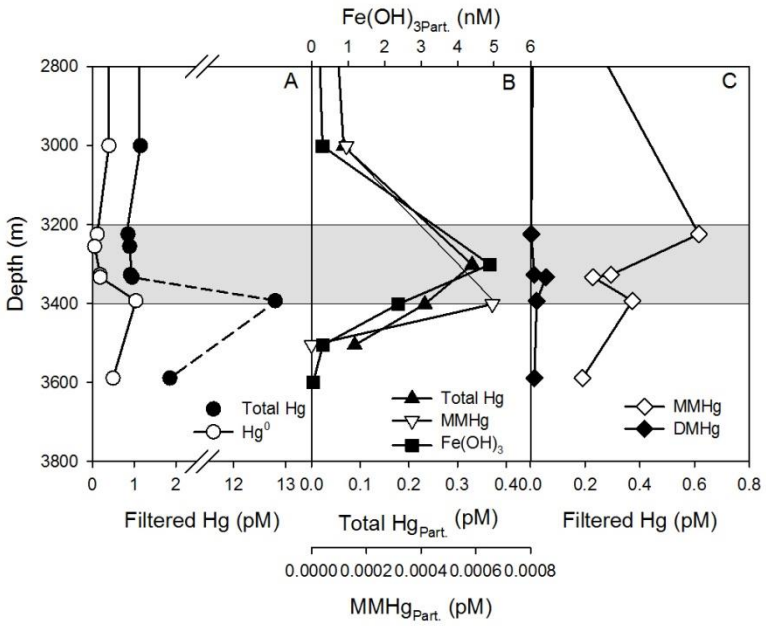

Figure 3.9. Mercury and iron speciation in the TAG hydrothermal vent plume (zonal Station 16). The grey area highlights the layer of the hydrothermal plume between 3200 and 3400 m depth.

Chapter 4: DISTRIBUTION OF MERCURY SPECIES ACROSS A ZONAL SECTION OF THE EASTERN TROPICAL PACIFIC OCEAN (U.S. GEOTRACES GP16)

Katlin L. Bowman[1], Chad R. Hammerschmidt[1], Carl H. Lamborg[2], Gretchen J. Swarr[3], Alison M. Agather[1]
(1) Wright State University, Dayton, OH
(2) University of California, Santa Cruz, CA
(3) Woods Hole Oceanographic Institution, Woods Hole, MA

Abstract

Mercury (Hg) in the ocean undergoes transformations in the water column including reduction to elemental Hg (Hg^0) and methylation to dimethylmercury ($(CH_3)_2Hg$, DMHg) and monomethylmercury (CH_3Hg^+, MMHg). Monomethylmercury is a neurotoxin that bioaccumulates in predatory fish species harvested for human consumption. I participated in the U.S. GETORACES section of the eastern tropical Pacific Ocean (GP16) to examine filtered and particulate total Hg (HgT) and MMHg, and dissolved gaseous Hg^0 and DMHg with high-resolution vertical profiles at 35 sampling stations. Total Hg had a nutrient-like vertical distribution with increasing concentrations in aging Pacific deep waters. Concentrations of filtered HgT, MMHg and DMHg also increased with age among deep water masses unaffected by anthropogenic Hg. Unlike in the Atlantic Ocean, a large hydrothermal plume stemming from the East Pacific Rise was not enriched with Hg relative to surrounding deep waters. Waters within 1000 m of abyssal sediments contained more HgT than expected from remineralization of sinking particles. Geothermal heating along the rise may increase the flux of Hg from sediments, accounting for the excess Hg. The behavior of HgT surrounding the East Pacific Rise may be unique to fast spreading centers in the ocean. In thermocline waters, elemental Hg was inversely correlated with N*, a proxy for denitrification, suggesting that denitrifying bacteria (pseudomonads, e.g.) may also be capable of Hg reduction. The cruise section

sampled productive waters near the Peru-Chile upwelling region that supports one of the world's largest fisheries and sustains an expansive suboxic oxygen minimum zone. All three Hg species and HgT were elevated within the upwelling region compared to non-upwelling stations. Thermocline waters had, on average, 2× more filtered MMHg than DMHg, however, concentrations of MMHg and DMHg were comparable in the upwelling region.

4.1. Introduction

Mercury (Hg) is emitted from natural (e.g., geogenic emissions, terrestrial and aquatic re-emissions) and anthropogenic sources (dominantly fossil fuel combustion) to the atmosphere, where it can remain for up to one year allowing for long-range transport and deposition to the global ocean (Lamborg et al., 2002; Holmes et al., 2006; Mason et al., 2012). Once deposited to seawater, Hg binds with inorganic and organic ligands and undergoes chemical transformations mediated by abiotic and microbial processes. Inorganic Hg can be reduced to elemental Hg (Hg^0) that is ubiquitous throughout the marine water column (Fitzgerald et al., 2007; Bowman et al., 2014). Inorganic Hg also can be methylated to either gaseous dimethylmercury ($(CH_3)_2Hg$, DMHg) or monomethylmercury (CH_3Hg^+, MMHg; Monperrus et al., 2007; Whalin et al., 2007; Lehnherr et al., 2011).

Monomethylmercury is a toxic, bioaccumulative form of Hg that biomagnifies in marine food webs and is most concentrated in predatory fish species (Karimi et al., 2012; Sunderland, 2007; Mason et al., 2012). Consumption of fish is the primary route of human exposure to MMHg and 70% of the global fish harvest comes from the ocean (Sunderland, 2007; Višnjevec et al., 2014; FAO, 2014). Fish are an important source of

omega-3 fatty acids that support healthy brain growth and development, MMHg, however, is antagonistic –maternal fish consumption has been linked to neurological deficits and decreased cognitive performance in developing children (Innis, 2008; Oken et al., 2008; Bose-O'Reilly et al., 2010). Adults exposed to high levels of MMHg also can experience neurological and cardiovascular impairments (Stern et al., 2005; Auger et al., 2005; Edna et al., 2003; Mergler et al., 2007). The marine biogeochemical cycling of Hg, therefore, has important implications for marine fish harvested from the ocean.

I investigated the distribution of total Hg, Hg^0, MMHg, and DMHg in the eastern tropical South Pacific Ocean, as part of the U.S. GEOTRACES expedition (GP16) in October–December 2013. The section included 35 high-resolution vertical profiles between Peru and Tahiti and tranversed the Peru-Chile upwelling region (Fig. 4.1), which supports one of the world's largest fisheries (FAO, 2014). Wind-driven upwelling along the Peru-Chile coast fuels high levels of primary production that subsequently contributes to the persistence of a suboxic oxygen minimum zone (OMZ; 2–10 μM O_2; Codispoti et al., 2005) in the thermocline (Fig. 4.2). In situ production of MMHg and DMHg in the ocean has been linked to processes in low-oxygen thermocline waters (Mason and Fitzgerald, 1991; Mason and Sullivan, 1999; Kirk et al., 2008; Sunderland et al., 2009; Heimbürger et al., 2010; Cossa et al., 2011; Lehnherr et al., 2011; Hammerschmidt and Bowman, 2012) so a relationship between MMHg, DMHg, and dissolved oxygen was examined over a strong productivity gradient from suboxic thermocline waters in the upwelling region to more oxygenated thermocline waters in the South Pacific gyre (Fig. 2). Other oceanographic features of the transect included 1) deep Pacific waters unaffected by anthropogenic Hg emissions (Lamborg et al., 2014), 2) a large buoyant

hydrothermal plume stemming from the East Pacific Rise (EPR), 3) waters once in contact with the Peru shelf, margin, and trench, and 4) intermediate and mixed layer waters originating from the Antarctic Circumpolar Current (ACC, Fig. 2).

4.2. Methods

4.2.1 Sample collection

Filtered water and suspended particles were collected and analyzed with vetted trace-metal clean techniques (Hammerschmidt et al., 2011; Bowman and Hammerschmidt, 2011; Bishop et al., 2012; Lamborg et al., 2012), similar to those described previously for the U.S. GEOTRACES North Atlantic sections (Bowman et al., 2014). Seawater was sampled at 18 full-depth stations (36 water depths at each station), four shelf stations (6–23 depths), and 13 demi stations (12 depths each in upper 1000 m) with 12-L Teflon-coated Go-Flo bottles attached to a trace-metal clean rosette (Cutter and Bruland, 2012). Go-Flo bottles were transferred from the rosette to a clean laboratory van where seawater was filtered through pre-rinsed capsules (0.2 μm Pall AcroPak-200) into 2-L Teflon bottles for determination of Hg^0, DMHg, and MMHg, and 0.25-L borosilicate glass bottles for determination of HgT. The water was filtered carefully so as to not degas volatile Hg species during transfer to the sample bottles (Bowman and Hammerschmidt, 2011). McLane in situ pumps (Bishop et al., 2012) were used to sample suspended particles (1–51 μm) onto quartz fiber filters from the 18 full-depth stations (16 depths each) and four shelf stations (5–8 depths). Filters were subsampled into 25-mm diameter punches (25–100 L of seawater filtered through each) that were frozen and transported to Wright State University for analysis of particulate MMHg and HgT.

4.2.2 Mercury analysis

Mercury species in filtered seawater were analyzed on board the research vessel in a dedicated laboratory van under clean conditions. Gaseous Hg^0 and DMHg were determined within ~2 h of sampling from 2-L water samples with a purge-and-trap method (Bowman and Hammerschmidt, 2011). Samples were purged with Hg-free N_2 (30 L total at 0.8 L min^{-1}), and effluent gas from the bottle was first passed through reagent-grade soda lime to remove water vapor and aerosols. Dimethylmercury was concentrated on Bond Elut resin (Agilent; Baya et al., 2013) and Hg^0 on a Au-trap downstream of the Bond Elut (Lamborg et al., 2012). Dimethylmercury was quantified by gas-chromatographic cold vapor atomic fluorescence spectrometry (GC-CVAFS; Tseng et al., 2004; Bowman and Hammerschmidt, 2011) and Hg^0 by dual Au-amalgamation CVAFS (Bloom and Fitzgerald, 1988) following thermal desorption from the traps. Each Au-trap was calibrated at every station after loading with a known quantity of Hg^0. Procedural precision (± SD) of Hg^0 determinations averaged 20 ± 15 relative percent difference (RPD) among 27 pairs of replicate samples. Bond Elut traps for DMHg analysis were calibrated every 2–3 stations with known additions of methylethylmercury, a volatile derivative of MMHg. Procedural precision of DMHg analyses averaged 27 ± 20 RPD (n = 17 pairs). Method detection limits were appropriate for open-ocean Hg measurements (0.01 pM for Hg^0 and 0.002 pM for DMHg). Bond Elut traps were replaced frequently (after 12–24 uses) when deterioration of the resin became apparent. Deteriorating Bond Elut traps have poor trapping efficiency and they generate a residue that coats the fluorescence cuvette, reducing analytical sensitivity.

Seawater purged of DMHg and Hg^0 was transferred to a 2-L polycarbonate bottle for MMHg analysis. Samples were acidified to 1% with trace-metal grade H_2SO_4 for 12–24 h, neutralized with 12 M KOH, adjusted to pH 5 with 4 M acetate buffer, amended with ascorbic acid (to 0.003 M), and derivatized with sodium tetraethylborate (NaTEB; Bowman and Hammerschmidt, 2011; Munson et al., 2014). Hg-free air was used to purge volatile methylethylmercury from samples (30 L total at 0.8 L min^{-1}) that was concentrated on Tenax after passing through reagent-grade soda lime. Monomethylmercury (as methylethylmercury) was quantified by GC-CVAFS (Tseng et al., 2004; Bowman and Hammerschmidt, 2011). Bond Elut was not a good alternative for MMHg determination in seawater; NaTEB derivatized other organic molecules in seawater with a similar volatility to methylethylmercury that were collected on Bond Elut, interfering with the MMHg chromatographic peak. Recovery of known additions of MMHg from seawater averaged 84 ± 12% (n = 3) and procedural precision averaged 35 ± 22 RPD (n = 6). Individual Tenax traps were calibrated every 2–3 stations with aliquots of an aqueous CH_3HgCl standard that was calibrated versus TORT-2 reference material (lobster hepatopancreas, National Research Council of Canada). Method detection limit for MMHg was 0.02 pM and approtiate for open-ocean measurements.

Total Hg was measured in 0.25-L filtered seawater samples within 48 h of sampling with a purge-and-trap method (Lamborg et al., 2012) and dual Au-amalgamation CVAFS detection (Bloom and Fitzgerald, 1988; Fitzgerald and Gill, 1979). Total Hg in seawater was calibrated against aqueous Hg(II) standards traceable to the U.S. National Institute of Standards and Technology. Procedural precision averaged 7

± 9 RPD (*n* = 29 pairs) and the method detection limit for HgT was 0.03 pM and appropriate for open-ocean measurements.

Mercury in suspended particles was leached from filter punches with 2 M HNO_3 for 4 h in a 60 °C water bath (Hammerschmidt and Fitzgerald, 2006; Bowman et al., 2014). MMHg in the digestates was quantified by flow-injection GC-CVAFS (Tseng et al., 2004) and analyses were calibrated with procedural standards. Standards of CH_3HgCl were calibrated against TORT-2 reference material, and the method detection limit for particle-associated MMHg in seawater was 0.002 pM. Recovery of known additions of MMHg from filter punches averaged 98 ± 20% (*n* = 7) and procedural precision averaged 16 ± 11 RPD (*n* = 16). Separate aliquots of digestate were oxidized and analyzed for HgT by dual Au-amalgamation CVAFS (Hammerschmidt and Fitzgerald, 2006). Procedural precision averaged 8 ± 8 RPD (*n* = 10) and the method detection limit for particulate HgT was 0.03 pM.

4.3. Results

4.3.1 Physical oceanography of the section

The section covered a large portion of the South Pacific gyre and traversed multiple water masses. Deep water masses that were sampled included Lower Circumpolar Deep Water (LCDW), Pacific Deep Water (PDW), and modified PDW (PDW_M; Fig. 4.2). Wind-driven upwelling south of the Antarctic Circumpolar Current (ACC) shoals and mixes deep water masses from the Indian, Pacific, and Atlantic Oceans. This mixture of deep water masses, referred to as Circumpolar Deep Water (CDW), is downwelled by convergence between the ACC and the Subantarctic Front, and spreads north into the Pacific Ocean (Rintoul et al., 2001; Kawabe and Fujio, 2010;

Talley et al., 2011). Density stratification divides CDW into two layers: 1) a deeper layer of LCDW that has greater density and dissolved oxygen due to entrainment of North Atlantic Deep Water (NADW), and 2) an upper layer (Upper Circumpolar Deep Water; UCDW) that is less dense and composed of mainly Indian Deep Water and PDW (Talley et al., 2011). UCDW and PDW are synonymous, and occupy the same depths and density range (Talley et al., 2011). Once UCDW reaches the North Pacific and circulates south, it becomes PDW; "younger" UCDW and "older" PDW are best differentiated by their silicate and oxygen concentrations. LCDW (θ = 0.2–0.8 °C, S = 34.7) was at depths >4000 m west of the EPR. The section contained mostly PDW (θ = 1.1–1.2 °C, S = 34.68–34.69) between 2000–4000 m and at depths >4000 m east of the EPR. PDW_M is formed in the North Pacific by deep upwelling of LCDW that mixes with PDW and flows south along the coast of South America (Kawabe and Fujio, 2010). East of the EPR, PDW_M is found between 2000–4000 m (Fig. 4.2).

Antarctic Intermediate Water (AAIW) forms north of the Subantarctic Front in the southeast Pacific, and was between 700 and 1000 m depth across the section (θ = 2–10 °C, S = 33.8–34.5; Siedler et al., 2003). Water between 1000–2000 m was too saline to be AAIW and too dilute to be classified as PDW and is therefore considered a mixture of the two water masses (Fig. 4.2). Equatorial surface and intermediate water masses were not encountered because the cruise track was too far south (10–15 °S). Surface waters included South Pacific Subtropical Mode Water overlying Subantarctic Mode Water (Talley et al., 2011). ENSO conditions were neutral during the sampling period (NOAA, 2014) and normal wind-driven coastal upwelling occurred at Stations 1–9 supporting a suboxic OMZ.

4.3.2 Total Hg

Filtered HgT had a nutrient-like distribution due to scavenging at the surface, remineralization in low-oxygen thermocline waters, and accumulation in aging deep waters during thermohaline flow (Fig. 4.3; Table 4.1). Mixed layer and thermocline waters in the Peru upwelling zone (Stations 1–9) were enriched in both particulate and filtered HgT compared to Stations 10–36, where there was no upwelling (Table 4.2). The upwelling zone contained waters brought to the surface from ~350 m depth, and this water may have contained Hg that was scavenged at the surface (post-deposition) and likely released during organic matter remineralization. Excess Hg in upwelling waters may also have originated from sediments on the Peru margin. At Stations 2 and 3 on the shelf, water deeper than 50 m was suboxic and concentrations of filtered HgT increased near the sediment-water interface, suggesting mobilization from the benthos (Fig. 4.4). Mercury remobilized from deposits on the margin was not distributed homogeneously through the water column; however, shelf waters (<200 m depth) contained uncharacteristically high concentrations of filtered HgT (1.3 ± 0.4 pM, n = 14) compared to other mixed layer waters in the Pacific Ocean (< 0.5 pM; Laurier et al., 2004; Bowman and Hammerschmidt, 2012; Munson, 2014). Total Hg in suspended particles was significantly greater along the Peru margin (Stations 1–5; 0.2 ± 0.1 pM, n = 47) compared to other stations (0.1 ± 0.1 pM, n = 290; Mann-Whitney Rank Sum p <0.0001; Fig. 3b). Greater concentrations of particulate Hg on the margin may result from increased mass of suspended particles (data available 2015; Phoebe Lam, personal communication), or different sediment-water partitioning of Hg near the continental margin.

Concentrations of filtered HgT increased with deep water mass age (Table 4.1), in contrast to AAIW which appeared to have decreasing Hg concentrations with greater age as it circulates through the South Pacific (Fig. 4.5). Radiocarbon and chloroflurocarbons measured across the section will be used to compile a detailed hydrographic synthesis including age approximations, and these results will be available in 2015/2016 (William Jenkins and Jim Happell, personal communication). Hydrographic properties (increasing silicate and decreasing oxygen concentrations) suggest that LCDW was the youngest deep water mass followed in increasingly greater age by PDW and PDW_M. PDW_M contains some "younger" LCDW; however, deep upwelling of LCDW can occur at latitudes up to 50 °N where the oldest PDW resides (Kawabe and Fujio, 2010; DeVries and Primeau, 2011; Gebbie and Huybers, 2012). PDW_M contained significantly more filtered HgT than younger PDW and LCDW (Kruskal-Wallis One Way ANOVA, $p < 0.05$). A trend of increasing HgT in progressively older deep waters in the Pacific is supported by concentration comparisons among deep waters in different ocean basins. For example, filtered HgT in relatively young deep water of the Southern Ocean (1.2 ± 0.3 pM unfiltered; Cossa et al., 2011) is less than that in increasing older deep waters of the Central Pacific (1.25–1.5 pM at 10 °S and 1.5–2.0 pM at 10 °N; Munson, 2014) and northeast Pacific (1.3 ± 0.3 pM; Hammerschmidt and Bowman, 2012). AAIW in the South Pacific has an anticyclonic circulation originating in the southeast (Talley et al., 2011), and oxygen concentrations decreased from east to west across the section (Fig. 4.5a). Filtered HgT also decreased significantly ($p = 0.01$) with station longitude from 80 to 150 °W (Fig. 4.5b) as AAIW aged.

Increased Hg concentrations in the bottom 1000 m of the water column may have been linked to geothermal heat beneath the ridge axis of the EPR. Decreasing potential temperature with increasing depth observed at stations west of the EPR crest (Stations 21–36) was consistent with other observations of deep water in the South Pacific where $\theta < 1.2$ °C at depths greater than 3500 m (Fig. 4.6; Kawabe and Fujio, 2010; Talley, 2007; Talley et al., 2011). Potential temperature was greater than expected at the same depths east of the EPR crest (Stations 1–17) and vertically homogenous rather than decreasing with depth. Filtered HgT was elevated in the bottom 1000 m of water at the stations east of the ridge crest and increased with depth up to 2 pM (Fig. 4.3a), 2-fold greater than average deep water concentrations (Table 4.1). Models based on radiocarbon measurements estimate that deep water in the southeastern Pacific is ~ 900 y old, therefore, any accumulated Hg should be from natural rather than anthropogenic sources (DeVries and Primeau, 2011; Gebbie and Huybers, 2012; Lamborg et al., 2014). Lamborg and colleagues (2014) found a ratio of filtered HgT to remineralized phosphorus (P_{remin}) of 1 pmol/μmol in deep Pacific waters unaffected by anthropogenic inputs, which accumulate Hg and P from decomposing biological material. At stations on the east side of the EPR, where geothermal heating was apparent, deep water within 1000 m of abyssal sediments had an average $Hg:P_{remin} > 1$, which suggests a source of filtered HgT to the water column other than organic matter remineralization. On the western ridge geothermal heating was not evident, however, $Hg:P_{remin.}$ was still greater than 1 pmol/μmol at most stations (Fig. 4.7). At the EPR in the North Pacific (9°50’N), unfiltered diffuse flow fluids contained 14–445 pM HgT (Crespo-Medina, 2009),

however, at Station 18 (15°S) directly above the EPR filtered and particulate HgT was not elevated and Hg:P_{remin} ≈ 1 (0.87 ± 0.18, n = 32).

Geothermal heating of deep water at 15 °S near the EPR has been observed previously (Thompson and Johnson, 1996) in addition to other locations along the EPR in the North and South Pacific Ocean (Detrick et al., 1974; Bender et al., 1985; Joyce et al., 1986; Crane et al., 1987). Upwelling mantle centered at the EPR crest can travel through shallow melt channels at the base of the crust and ascend through porous channels, moving heat to shallower depths within the crust along the rise (Key et al., 2013). In the North Atlantic and Pacific Oceans, where there was no geothermal heating, abyssal sediments were not a source of Hg to bottom waters (Laurier et al., 2004; Hammerschmidt and Bowman, 2012; Bowman et al., 2014). Efflux of Hg from sediments overlying geothermally heated crust has not been studied previously, however, it appears that warmer sediments overlying the EPR may be responsible for a noticeable flux of Hg to bottom waters. On the western side of the EPR, geothermal heating did not appear to impact bottom water temperatures, however, excess heat from geothermal sources can be as small as 0.05 °C (Talley et al., 2011), and may not have been measured precisely with the CTD thermocouple. Alternatively, sediments composed of mainly biological material on the eastern side of the EPR may contain and release more Hg compared to sediment on the western side of the EPR which is likely dominated by lithogenic material. While this is a new and unexpected source of Hg to the water column, concentrations in geothermally impacted waters (Hg:$P_{remin.}$ > 1) were not significantly different from surrounding PDW or PDW_M (Mann-Whitney Rank Sum p = 0.13 and p = 0.99, respectively).

4.3.3 Elemental Hg

Elemental Hg concentrations were low in old Pacific Ocean deep water masses compared to younger Atlantic waters (Fig.4.8; Bowman et al., 2014). Average concentrations were low in the mixed layer and AAIW compared to the thermocline where microbial processes reduce inorganic Hg during organic matter remineralization (Table 1; Monperrus et al., 2007; Whalin et al., 2007; Lehnherr et al., 2011). Mixed layer and thermocline waters in the upwelling region (Stations 1–9) had 5× more Hg^0 compared to stations where there was no upwelling (Stations 10–36; Table 4.2). On average, Hg^0 in deep water masses was 0.03–0.04 pM, an order of magnitude less than concentrations in young NADW in the North Atlantic (0.3–0.4 pM Hg^0; Bowman et al., 2104). Greater concentrations of Hg^0 in NADW may have contributed to higher levels of Hg^0 in PDW_M and LCDW, both of which contain some entrained NADW, compared to PDW (Kruskal-Wallis One Way ANOVA $p < 0.05$).

On the Peru shelf and slope, concentrations of Hg^0 did not increase at the sediment-water interface, however, concentrations were increased in suboxic bottom waters of the shelf (Stations 2–3; 0.1–0.3 pM Hg^0) relative to oxygenated bottom waters on the slope (Station 4; 0.04 pM Hg^0; Fig. 4.4). Elemental Hg in deep water near the Peru coast (Station 1) was elevated (> 0.1 pM) and more characteristic of shelf waters than adjacent PDW_M (Fig. 4.8). Based on these observations, reduction of inorganic Hg in sediments along the margin of South America could be a source of Hg^0 to PDW_M flowing southward along South America.

Denitrification exceeded nitrogen fixation (negative N*; Gruber and Sarmiento, 1997) in mixed layer and thermocline waters across the entire section, and concentrations

of Hg^0 were inversely correlated with N* (Fig. 4.9). Reduction of inorganic Hg by denitrifying bacteria has been observed in culture (Schaefer et al., 2002; Kritee et al., 2008), and Munson (2014) recently found a similar relationship between Hg^0 and N* at one location in the central tropical Pacific Ocean. In the more oligotrophic waters of the North Atlantic, nitrogen fixation was greater than denitrification (positive N*), and there was no correlation between Hg^0 and N*; instead, Hg^0 had a nutrient-like vertical distribution across most of the basin (Bowman et al., 2014). Different planktonic community structures between Fe-limited waters in the eastern South Pacific and N- and P-limited waters in the North Atlantic (Moore et al., 2013) may affect the distribution of the *mer* operon, which mediates Hg reduction, resulting in inter-basin differences in Hg^0 distribution.

4.3.4 DMHg and MMHg

Dimethylmercury concentrations increased with depth throughout the water column and both MMHg and DMHg concentrations were maximum in the thermocline (Table 4.1, Fig.4.10a,b). In the mixed layer, DMHg can evade to the atmosphere and MMHg can be demethylated either photochemically or microbially (Mason et al., 2012). The MMHg:DMHg molar ratio in the mixed layer was high and variable (12 ± 16, n = 24), but on average there was 3× more MMHg, which could be attributed to either a greater loss of DMHg compared to MMHg or an external source of MMHg such as rainwater (Hammerschmidt et al., 2007; Hammerschmidt et al., 2014).

Mixed layer and thermocline waters were enriched with filtered and particulate MMHg and gaseous DMHg in the upwelling zone compared to stations where there was no upwelling (Table 4.2), and proximity to shelf and slope sediments had a large

influence on the MMHg:DMHg molar ratio (Fig. 4.11). In thermocline waters where there was no upwelling (Stations 10–36), MMHg was more abundant that DMHg (MMHg:DMHg = 2 ± 3, n = 84; Mann-Whitney Rank Sum, p <0.001), and within the upwelling zone (Stations 1–9) concentrations of MMHg and DMHg were similar (MMHg:DMHg = 1.5 ± 1.3, n = 87; Mann-Whitney Rank Sum, p = 0.7). On the shelf and slope (Stations 2–4), filtered MMHg and DMHg increased near the sediment-water interface, and uniquely, DMHg concentrations were 1.5–2× greater than those of MMHg (Fig. 11). This is different than the continental shelf and slope in the North Atlantic where concentrations of filtered MMHg were greater than those of DMHg near the benthos (Fitzgerald et al., 2012). Higher concentrations of organic matter in sediments underlying the productive upwelling region may have scavenged MMHg from pore fluids and attenuated its flux to overlying water (Hammerschmidt et al., 2004), while gaseous DMHg would not be affected similarly. On the slope (Station 4), oxygenated bottom water contained concentrations of filtered MMHg and DMHg that were twice as high as bottom water on the shelf. Increased flux from oxygenated surface sediments due to bioturbation is not likely because concentrations of filtered HgT at the same station on the slope did not increase with proximity to the sediment-water interface (Section 3.2, Fig. 4.4; Hammerschmidt and Fitzgerald, 2008). High sulfide concentrations in anoxic sediments inhibit the bioavailability and subsequent methylation of inorganic Hg (Hammerschmidt et al., 2008). Accordingly, sulfide may have resulted in a lower flux of methylated Hg from the suboxic shelf compared to the oxygenated slope.

Accumulation of DMHg and MMHg in aging deep water, and net loss from intermediate water contributed to a decreasing concentration gradient from east to west

along the section (Fig. 4.10). Similar to filtered HgT (Fig. 4.5), concentrations of DMHg and MMHg decreased from east to west as AAIW (700–1000 m depth) became older, and linear regression analyses suggest a similar loss rate for both methylated species (Fig. 4.12). Because gaseous DMHg is not scavenged, similar loss rates suggest that demethylation rather than scavenging is responsible for decreasing concentrations with age and westward circulation of AAIW. These observations are consistent with high concentrations of methylated Hg measured in young AAIW in the Southern Ocean (0.4 ± 0.2 pM methylated Hg; Cossa et al., 2011) and even lower concentrations in older AAIW further west (155–175 °W) in the central Pacific at 10°S (DMHg < 0.075 pM, MMHg < 0.05 pM; Munson, 2014). Methylated Hg concentrations reported by Cossa and colleagues (2011) were measured in unfiltered water, however, MMHg in suspended particles is typically $\leq$ 1% of total MMHg in the water column (this study, Bowman et al., 2014) and inclusion of particles should have an undiscernible effect. Mason and Sullivan (1999) also observed decreasing DMHg concentrations with increasing age of AAIW from south to north in the South Atlantic Ocean. The MMHg:DMHg molar ratio in Pacific AAIW was 0.9 ± 0.9 (n = 46) and concentrations of DMHg were significantly greater than MMHg (Mann-Whitney Rank Sum, p = 0.004). Greater concentrations of DMHg than MMHg may result from increased solubility of DMHg in low-temperature waters.

In deep Pacific waters, concentrations of DMHg and MMHg, both independently and together as methylated Hg, increase with water mass age (Table 4.1; Kruskal-Wallis One Way ANOVA, $p < 0.05$). Dimethylmercury was significantly greater than MMHg in PDW and PDW_M (Mann-Whitney Rank Sum, $p < 0.001$ for PDW and $p = 0.03$ for

PDW_M). Monomethylmercury in suspended particles was too low (< 0.001 pM) to increase filtered MMHg through remineralization, suggesting in situ methylation increases MMHg in deep water masses. Munson (2014) reported similar concentrations of DMHg and MMHg at 10 °S in the Central Pacific, however, there are inconsistencies with other studies. Concentrations of methylated Hg were high in newly formed CDW in the Southern Ocean (0.5 ± 0.2 pM; Cossa et al., 2011), which would not support increasing concentrations with water mass age. Also, in the subtropical northeast Pacific, concentrations of DMHg were lower and those of MMHg higher than would be expected in younger PDW_M (Hammerschmidt and Bowman, 2012). Methylation dynamics in deep water masses have not been studied and more experimental and observational data is needed understand the behavior of methylated Hg in the deep ocean.

4.3.5 Oxygen relationships and methylated Hg

Correlations between methylated Hg and oxygen consumption have emphasized a dependence on organic carbon remineralization to sustain methylation of inorganic Hg (Mason et al., 2012). However, tests examining Hg methylation in seawater from the Canadian Archipelago found that methylation rates were unrelated to oxygen concentration (Lehnherr et al., 2011), and others have found maxima of methylated Hg near the oxygenated subsurface chlorophyll maximum (Heimbürger et al., 2010; Bowman et al., 2014). In thermocline waters of this section (100–700 m) of the eastern South Pacific, there were weak, but statistically significant, inverse correlations between concentrations of MMHg, DMHg, and dissolved oxygen (Fig. 4.13). Removing suboxic upwelling stations (Stations 1–9) did not affect either the strength or significance of these relationships. Concentrations of both DMHg and MMHg were typically low where

oxygen was elevated, but highly variable where oxygen concentrations approached zero. Suboxic thermocline waters at upwelling stations (Stations 1–9) had 1–2 maxima of MMHg and DMHg which contributed to a wide range of concentrations in low-oxygen waters (Fig. 4.13). Stations outside the upwelling zone (Stations 10–36) had only one vertical maxima of MMHg and DMHg within the thermocline.

Maxima of DMHg and MMHg observed were also in oxygenated waters near the subsurface chlorophyll maximum. Monomethylmercury maxima were observed near the subsurface chlorophyll maximum at most stations across the section and DMHg maxima were observed only near the subsurface chlorophyll maximum at upwelling stations (1–9). In suspended particles, concentrations of MMHg increased in parallel to filtered MMHg at the subsurface chlorophyll maximum and OMZ, suggesting that in situ production rather than release from particles was responsible for these maxima. Weak correlations with oxygen and maxima of methylated Hg in oxygenated waters in this section of the Pacific emphasizes the potential importance of aerobic microbial functional groups and their access to organic substrates and bioavailable forms of inorganic Hg to methylate Hg. Primary and secondary nitrite maxima were observed near the subsurface chlorophyll maximum and OMZ, similar to maxima of MMHg and DMHg; however, there was no significant correlation between either DMHg or MMHg and N* ($p = 0.5$ for DMHg, $p = 0.09$ for MMHg).

4.3.6 Hg in the EPR hydrothermal vent plume

Total Hg was not enriched in the buoyant hydrothermal plume that extends west from the EPR at 113–150 °W between 2000–3000 m (Fig.4.3). Some scavenging of HgT occurred at the base of the plume as evidenced by increased concentrations of particulate

HgT (Stations 18–21; Fig. 4.3b), however, scavenging did not affect filtered concentrations in deep water. Similar to a vent plume near the Mid-Atlantic Ridge, concentrations of MMHg increased and DMHg decreased slightly near the EPR (Fig.4.6; Bowman et al., 2014). The absence of increased Hg concentrations within the EPR plume was surprising because other trace metals (i.e., Al, Mn, Fe) were elevated above background PDW concentrations in the EPR plume (Resing et al., 2014) and filtered HgT was increased in the Mid-Atlantic Ridge hydrothermal plume (Bowman et al., 2014). Other studies of vent fluids and a hydrothermal plume have found increased and variable concentrations of HgT, ranging from 4 to 11,000 pM (Lamborg et al., 2006; Crespo-Medina, 2009; Bowman et al., 2014). Such high concentrations in vent fluids and the observation of geothermal Hg discussed in Section 3.2 suggests that Hg likely was enriched in EPR hydrothermal fluids, however, the Hg may have either precipitated, possibly as cinnabar, or been scavenged by metal oxides before ascending into the buoyant plume.

Hydrothermal vents at fast and slow spreading ridges may differ in their ability to release and disperse Hg. Focused-flow vent fluids (>350°C) sampled at 9 °N on the EPR had a dark color, presumably from precipitated metals, and contained 3,500–11,000 pM HgT (unfiltered; Crespo-Medina et al., 2009). At Gorda Ridge, a slower spreading center in the northeast Pacific, unfiltered fluids from a focused-flow vent were clear and contained substantially less HgT (4–10 pM; Lamborg et al., 2006). A similar concentration of HgT (13 pM) was measured in a plume near the Mid-Atlantic Ridge, also a slow spreading center (Bowman et al., 2014). Fast spreading centers are characterized by greater volumes of magma that create a thicker layer of basalt compared

to slow spreading centers. This results in a more shallow percolation of seawater near the ridge crest, and less contact with the upper mantle (Ligi et al., 2013). Different spreading rates and depths of seawater penetration could affect the chemical speciation, precipitation, and concentration of Hg released from hydrothermal vent systems.

4.4. Summary

Mercury released during particle remineralization and accumulated from contact with shelf sediments was brought to the upper water column (20–700 m) in the Peru upwelling region. Mixed layer and thermocline waters in the upwelling region contained significantly greater concentrations of MMHg and DMHg than in non-upwelling areas of the eastern South Pacific Ocean. Most (95%) of the fish harvested from the upwelling zone are anchovy, a low trophic level species containing low concentrations of MMHg (Karimi et al., 2012; FAO 2014). Accordingly, the feeding ecology and trophic status of anchovy may mitigate the risks imposed by elevated concentrations of methylated Hg in productive upwelling waters. Oscillating ENSO cycles and overfishing are a threat to anchovy in this region and implementing sustainable fishing practices could also help to remove MMHg from the base of the food web.

Sediments on the Peru shelf release DMHg in excess of MMHg to bottom waters. Outside of the upwelling zone concentrations of MMHg are greater than those of DMHg in thermocline waters, and concentrations of each are comparable within the upwelling zone. There was a weak correlation between oxygen and methylated Hg, however, concentrations of MMHg and DMHg found in suboxic thermocline waters were comparable to concentrations found in the oligotrophic North Atlantic Ocean where oxygen is >50 μmol kg^{-1} (Bowman et al., 2014). When multiple ocean basins are

considered, concentrations of MMHg and DMHg do not increase linearly with decreasing oxygen. This could result from scavenging and bioaccumulation in more productive waters, or limitations of microbial activity and bioavailable forms of inorganic Hg.

Elemental Hg was inversely related to N*, suggesting that denitrifiying bacteria in suboxic ocean waters may reduce inorganic Hg. Concentrations of HgT, MMHg, and DMHg decreased with westward distance and age of AAIW and increased with age in Pacific deep water masses unaffected by anthropogenic inputs. The buoyant hydrothermal vent plume stemming from the EPR was not enriched with Hg, however, geothermal heating along the rise may increase the flux of Hg from abyssal sediments.

Acknowledgements

I thank my U.S. GEOTRACES colleagues, especially co-chief scientists Chris German and James Moffett, and the captain and crew of the R/V *Thompson*. Cheryl Zurbrick, Claire Parker, Sara Rauschenberg, Rob Sherrell, Laura Richards, and Greg Cutter helped sample and filter water. Phoebe Lam and Dan Ohnemus sampled suspended particles. This research was supported by the U.S. National Science Foundation Chemical Oceanography Program.

References

Anderson, R.N., Hobart, M.A. 1976. The relation between heat flow, sediment thickness, and age in the Eastern Pacific. J. Geophys. Res. 81, 2968–2989.

Auger, N., Kofman, O., Kosatsky, T., Armstrong, B. 2005. Low-level methylmercury exposure as a risk factor for neurologic abnormalities in adults. Neurotoxicology. 26, 149–157.

Baya, P.A., Hollinsworth, J.L., Hintelmann, H. 2013. Evaluation and optimization of solid adsorbents for the sampling of gaseous methylated mercury species. Anal. Chim. Acta. 786, 61–69.

Bender, M.L., Hudson, A., Graham, D.W., Barnes, R.O., Leinen, M., Kahn, D. 1985. Diagenesis and convection reflected in pore water chemistry on the western flank of the East Pacific Rise, 20 degrees south. Earth Planet. Sci. Lett. 76, 71–83.

Bishop, J.K.B., Lam, P.J., Wood, T.J. 2012. Getting good particles: Accurate sampling of particles by large volume in-situ filtration. Limnol. Oceanogr.- Methods 10, 681–710.

Bloom, N.S., Fitzgerald, W.F. 1988. Determination of volatile mercury species at the picogram level by low-temperature gas chromatography with cold-vapor atomic fluorescence detection. Anal. Chim. Acta. 208, 151–161.

Bloom, N.S. 1989. Determination of pictogram levels of methylmercury by aqueous phase ethylation, followed by cryogenic gas chromatography, with cold vapour atomic fluorescence detection. Can. J. Fish. Aquat. Sci. 46, 1131–1140.

Bose-O'Reilly, S., McCarty, K.M., Steckling, N., Lettmeier, B. 2010. Mercury exposure and children's health. Curr. Probl. Pediatr. Adolesc. Health Care 40, 186–215.

Bowman, K.L., Hammerschmidt, C.R. 2011. Extraction of monomethylmercury from seawater for low-femtomolar determination. Limnol. Oceanogr.-Methods 9, 121–128.

Bowman, K.L., Hammerschmidt, C.R., Lamborg, C.H., Swarr, G. 2014. Mercury in the North Atlantic Ocean: The U.S. GEOTRACES zonal and meridional sections. Deep-Sea Res. II. DOI: 10.1016/j.dsr2.2014.07.004.

Codispoti, L.A., Yoshinari, T., Devol, A.H. 2005. Suboxic respiration in the oceanic water column, in *Respiration in the Aquatic Ecosystems,* edited by P. Del Giorgio and W. Peter, pp.225–247, Oxford Univ. Press, Oxford, U.K.

Cossa, D., Heimbürger, L.-E., Lannuzel, D., Rintoul, S.R., Butler, E.C.V., Bowie, A.R., et al. 2011. Mercury in the Southern Ocean. Geochim. Cosmochim. Acta 75, 4037–4052.

Crane, K., Aikman III., F., Foucher, J.-P. 1987. The distribution of geothermal fields along the East Pacific Rise from 13°10'N to 8°20'N: Implications for deep seated origins. Mar. Geophys. Res. 9, 211–236.

Crespo-Medina, M., Chatziefthimiou, A.D., Bloom, N.S., Luther III, G.W., Wright, D.D., Reinfelder, J.R., et al. 2009. Adaptation of chemosynthetic microorganisms to elevated mercury concentrations in deep-sea hydrothermal vents. Limnol. Oceanogr. 54, 41–49.

Cutter, G.A., Bruland, K.W. 2012. Rapid and noncontaminating sampling system for trace elements in global ocean surveys. Limnol. Oceanogr-Meth. 10, 425–430.

Detrick,R.S., Williams, D.L., Mudie, J.D., Sclater, J.G. 1974. The Galapagos Spreading Centre: Bottom-water temperatures and the significance of geothermal heating. Geophys. J. Roy. Astr. S. 38, 627–637.

DeVries, T., Primeau, F. 2011. Dynamically and observationally constratined estimates of water-mass distributions and ages in the global ocean. J. Phys. Oceanor. 41, 2381–2401.

Edna, Y., Joaquim, V., Lynn, G., Illeane, P., Ellen, S. 2003. Low level methylmercury exposure affects neuropsychological function in adults. Environ. Health. 2, 8.

Fitzgerald, W.F., Gill, G.A. 1979. Subnanogram determination of mercury by two-stage gold amalgamation applied to atmospheric analysis. Anal. Chem. 51, 1714–1720.

Fitzgerald, W.F., Hammerschmidt, C.R., Bowman, K.L., Balcom, P.H., O'Donnell, J. 2012. High Resolution distributions and fluxes of monomethyl and dimethyl mercury on the continental margin of the NW Atlantic. Abstract A0019 presented at 2012 Ocean Science Meeting, Salt Lake City, UT, 20-24 Feb.

Fitzgerald, W.F., Lamborg, C.H., Hammerschmidt, C.R. 2007. Marine biogeochemical cycling of mercury. Chem. Rev. 107, 641–662.

(FAO) Food and Agricultural Organization of the United Nations, 2014. The state of world fisheries and aquaculture. <www.fao.org/publications>.

Gebbie, G., Huybers, P. 2011. The mean age of ocean waters inferred from radiocarbon observations: sensitivity to surface sources and accounting for mixing histories. J. Phys. Oceanogr., 42, 291–305.

Gruber, N., Sarmiento, J.L. 1997. Global patterns of marine nitrogen fixation and denitrification. Global Biogeochem. Cycles 11, 235–266.

Hammerschmidt, C.R., Bowman, K.L. 2012. Vertical methylmercury distribution in the subtropical North Pacific Ocean. Mar. Chem. 132–133, 77–82.

Hammerschmidt, C.R., Bowman, K.L., Tabatchnick, M.D., Lamborg, C.H. 2011. Storage bottle material and cleaning for determination of total mercury in seawater. Limnol. Oceanogr.-Methods 9, 426–431.

Hammerschmidt, C.R., Fitzgerald, W.F. 2006. Bioaccumulation and trophic transfer of methylmercury in Long Island Sound. Arch. Environ. Contam. Toxicol. 51, 416–424.

Hammerschmidt, C.R., Fitzgerald, W.F., Lamborg, C.H., Balcom, P.H., Visscher, P.T. 2004. Biogeochemistry of methylmercury in sediments of Long Island Sound. Mar. Chem. 90, 31–52.

Hammerschmidt, C.R., Lamborg, C.H., Fitzgerald, W.F. 2007. Aqueous phase methylation as a potential source of methylmercury in wet deposition. Atmos. Environ. 41, 1663–1668.

Heimbürger, L.-E., Cossa, D., Marty, J.-C., Migon, C., Averty, B., Dufour, A., Ras, J. 2010. Methyl mercury distributions in relation to the prescence of nano- and

picophytoplankton in an oceanic water column (Ligurian Sea, North-western Mediterranean). Geochim. Cosmochim. Acta 74, 5549–5559.

Hammerschmidt, C.R., Swarr, G.J., Bowman, K.L., Lamborg, C.H., Shelley, R.U. 2014. U.S. GEOTRACES: Air-sea exchange of mercury along zonal transects of the North Atlantic and eastern tropical South Pacific Oceans. Abstract 13897 presented at 2014 Ocean Science Meeting, Honolulu, HI, 23-28 Feb.

Holmes, C.D., Jacob, D.J., Yang, X. 2006. Global lifetime of elemental mercury against oxidation by atomic bromine in the free troposphere. Geophys. Res. Lett. 33, L20808, doi: 10.1029/2006GL027176.

Innis, S.M., 2008. Dietary omega 3 fatty acids and the developing brain. Brain Res. 1237, 35–43.

Joyce, T.M., Warren, B.A., Talley, L.D. 1986. The geothermal heating of the abyssal sub-Arctic Pacific Ocean. Deep-Sea Res. 33:1003–1015.

Karimi, R., Fitzgerald, T.P., Fisher, N.S. 2012. A quantitative synthesis of mercury in commercial seafood and implications for exposure in the United States. Environ. Health Perspect. 120, 1512–1519.

Kawabe, M., Fujio, S. 2010. Pacific Ocean circulation based on observation. J. Oceanogr. 66, 38–9403.

Key, K., Constable, S., Liu, L., Pommier, A. 2013. Electrical image of passive mantle upwelling beneath the northern East Pacific Rise. Nature 495, 499–502.

Kirk, J.L., St. Louis, V.L., Hintelmann, H., Lehnherr, I., Else, B., Poissant, L. 2008. Methylated mercury species in marine waters of the Canadian High and Sub Arctic. Environ. Sci. Technol. 42, 8367–8373.

Kritee, K., Blum, J.D., Barkay, T. 2008. Mercury stable isotope fractionation during reduction of Hg(II) by different microbial pathways. Environ. Sci. Technol. 42, 9171–9177.

Lamborg, C.H., W.F. Fitzgerald, A.W.H. Damman, J.M. Benoit, P.H. Balcom, and D.R. Engstrom. 2002. Modern and historic atmospheric mercury fluxes in both hemispheres: global and regional mercury cycling implications. Global Biogeochem. Cycles 16:1104–1114.

Lamborg, C.H., Hammerschmidt, C.R., Bowman, K.L., Swarr, G.J., Munson, K.M., Ohnemus, D.C., et al. 2014. A global ocean inventory of anthropogenic mercury based on water column measurements. Nature 512, 65–68.

Lamborg, C.H., Hammerschmidt, C.R., Gill, G.A., Mason, R.P., Gichuki, S. 2012. An intercomparison of procedures for the determination of total mercury in seawater and recommendations regarding mercury speciation during GEOTRACES cruises. Limnol. Oceanogr-Methods 10, 90–100.

Lamborg, C.H., Von Damm K.L., Fitzgerald, W.F., Hammerschmidt, C.R., Zierenberg, R. 2006. Mercury and monomethylmercury in fluids from Sea Cliff submarine hydrothermal field, Gorda Ridge. Geophys. Res. Lett. 33, L17606.

Laurier, F.J.G., Mason, R.P., Gill, G.A., Whalin, L. 2004. Mercury distributions in the North Pacific Ocean–20 years of observations. Mar. Chem. 90, 3–19.

Lehnherr, I., St. Louis, V.L., Hintelmann, H., Kirk, J.L. 2011. Methylation of inorganic mercury in polar marine waters. Nat. Geosci. 4, 298–302.

Ligi, M., Bonatti, E., Cuffaro, M., Brunelli, D. 2013. Post-Mesozoic rapid increase of seawater Mg/Ca due to enhanced mantle-seawater interaction. Scientific Reports 3, 2752, doi: 10.1038/srep02752.

Mason, R.P., Choi, A.L., Fitzgerald, W.F., Hammerschmidt, C.R., Lamborg, C.H., Soerensen, A.L., Sunderland, E.M. 2012. Mercury biogeochemical cycling in the ocean and policy implications. Environ. Res. 119, 101–117.

Mason, R.P, Fitzgerald, W.F. 1991. Mercury speciation in open ocean waters. Water Air Soil Poll. 56, 779–798.

Mason, R.P., Sullivan, K.A. 1999. The distribution and speciation of mercury in the South and equatorial Atlantic, Deep-Sea Res. PT II. 46, 937–956.

Mergler, D., Anderson, H.A., Chan, L.H.M., Mahaffey, K.R., Murray, M., Sakamoto, M., Stern, A.H. 2007. Methylmercury exposure and health effects in humans: A worldwide concern. Ambio. 36, 3–11.

Monperrus, M., Tessier, E., Amouroux, D., Leynaert, A., Huonnic, P., Donard, O.F.X. 2007. Mercury methylation, demethylation and reduction rates in coastal and marine surface waters of the Mediterranean Sea. Mar. Chem. 107, 49–63.

Moore, C.M., Mills, M.M., Arrigo, K.R., Berman-Frank, I., Bopp, L., Boyd, P.W., Galbraith, E.D., … Ulloa, O. 2013. Processes and patterns of oceanic nutrient limitation. Nat. Geosci. 6, 701–710.

Munson, K. M. 2014. Transformations of mercury in the marine water column. (Doctoral dissertation). Retrieved from Massachusetts Institute of Technology Libraries. http://hdl.handle.net/1721.1/87513.

Munson, K.M., Babi, D., Lamborg, C.H. 2014. Determination of monomethylmercury from seawater with ascorbic acid-assisted direct ethylation. Limnol. Oceanogr.-Methods 12, 1–9.

(NOAA) National Oceanic and Atmospheric Administration. 2014. El Niño/Southern Oscillation (ENSO): Historical information. Center for Weather and Climate Prediction.

Oken, E., Radesky, J.S., Wright, R.O., Bellinger, D.C., Amarasiriwardena, C.J., Kleinman, K.P., Gillman, M.W. 2008. Maternal fish intake during pregnancy, blood mercury levels, and child cognition at age 3 years in a US cohort. Am. J. Epidemiol. 167, 117–11181.

Resing, J.A., Sedwick, P., Soht, B. 2014. GEOTRACES Eastern Pacific Zonal Transect: Shipboard iron, manganese, and aluminum. Abstract 16887 presented at 2014 Ocean Science Meeting, Honolulu, HI, 23-28 Feb.

Rintoul, S.R., Hughes, C.W., Olbers, D. 2001. The Antarctic Circumpolar Current system, in Ocean Circulation and Climate, edited by G. Siedler, pp.271–301, Elsevier, New York.

Schaefer, J.K., Letowski, J., Barkay, T. 2002. Mer-mediated resistance and volatilization of Hg(II) under anaerobic conditions. Geomicrobiol. J. 19, 87–102.

Siedler, G., Church, J., Gould, J. 2003. Ocean Circulation and Climate: Observing and Modelling the Global Ocean, Academic Press, AIP International Geophysics Series, Volume 77.

Stern, A.H. 2005. A review of the studies of the cardiovascular health effects of methylmercury with consideration of their suitability for risk assessment. Environ. Res. 98, 133–142.

Sunderland, E.M. 2007. Mercury exposure from domestic and imported estuarine and marine fish in the U.S. seafood market. Environ. Health Persect. 115, 235–242.

Sunderland, E.M., Krabbenhoft, D.P., Moreau, J.W., Strode, S.A., Landing, W.A. 2009. Mercury sources, distribution, and bioavailability in the North Pacific Ocean: Insights from data and models. Global Biogeochem. Cycles 23, GB2010.

Talley, L.D. 2007. Hydrographic Atlas of the World Ocean Circulation Experiment (WOCE). Volume 2: Pacific Ocean (eds. M. Sparrow, P. Chapman and J. Gould), International WOCE Project Office, Southampton, U.K., ISBN 0-904175-54-5.

Talley, L.D., Pickard, G.L., Emery, W.J., Swift, J.H. 2011. Descriptive Physical Oceanography: An Introduction (Sixth Edition), Elsevier, Boston, 560, pp.303–362.

Thompson, L., Johnson, G.C., 1996, Abyssal currents generated by diffusion and geothermal heating over rises. Deep-Sea Res. I. 43, 193–211.

Tseng, C.-M., Hammerschmidt, C.R., Fitzgerald, W.F. 2004. Determination of methylmercury in environmental matrixes by on-line flow injection and atomic fluorescence spectrometry. Anal. Chem. 76, 7131–7136.

Višnjevec, A.M., Kocman, D., Horvat. M. 2014. Human mercury exposure and effects in Europe. Environ. Toxicol. Chem. 33, 1259–1270.

Whalin, L., Kim, E.-H., Mason, R. 2007. Factors influencing the oxidation, reduction, methylation and demethylation of mercury species in coastal waters. Mar. Chem. 107, 278–294.

Table 4.1. Mean (± SD) concentrations of Hg species in filtered water from different water masses. All concentrations are pM and the number of concentration measurements are in parentheses. The average concentration of Hg^0 in PDW_M does not included elevated concentrations at Station 1 near the Peru margin.

Water mass	HgT	Hg^0	DMHg	MMHg
Mixed layer[a]	0.34 ± 0.35 *(117)*	0.041 ± 0.070 *(114)*	0.015 ± 0.041 *(100)*	0.056 ± 0.062 *(79)*
Thermocline[b]	0.62 ± 0.38 *(259)*	0.049 ± 0.066 *(246)*	0.060 ± 0.072 *(226)*	0.069 ± 0.061 *(185)*
AAIW	0.73 ± 0.18 *(75)*	0.029 ± 0.039 *(72)*	0.091 ± 0.069 *(64)*	0.058 ± 0.058 *(49)*
AAIW/PDW[c]	0.75 ± 0.32 *(71)*	0.035 ± 0.051 *(68)*	0.050 ± 0.036 *(64)*	0.071 ± 0.043 *(43)*
PDW_M	1.25 ± 0.23 *(55)*	0.042 ± 0.030 *(39)*	0.12 ± 0.068 *(56)*	0.089 ± 0.057 *(49)*
PDW	1.06 ± 0.28 *(261)*	0.029 ± 0.028 *(216)*	0.074 ± 0.068 *(208)*	0.049 ± 0.055 *(114)*
LCDW	0.96 ± 0.15 *(11)*	0.035 ± 0.016 *(11)*	0.017 ± 0.011 *(8)*	0.012 ± 0.0075 *(7)*

[a]20–100 m, [b]100-700 m, [c]>1000-2000 m

Table 4.2. Mean (± SD) concentrations of Hg species (pM) in the upper water column (20–700 m) at upwelling and non-upwelling stations. The number of concentration measurements is in parentheses.

Stations	$HgT_{Filt.}$	$Hg_{Part.}$	Hg^0	DMHg	$MMHg_{Filt.}$	$MMHg_{Part.}$
Upwelling St. 1–9	0.90 ± 0.42 *(105)*	0.12 ± 0.092 *(42)*	0.011 ± 0.096 *(103)*	0.075 ± 0.070 *(105)*	0.085 ± 0.066 *(103)*	0.0012 ± 0.0014 *(43)*
Non-upwelling St. 10–36	0.40 ± 0.27 *(254)*	0.052 ± 0.052 *(98)*	0.023 ± 0.026 *(273)*	0.032 ± 0.062 *(221)*	0.052 ± 0.055 *(161)*	0.0071 ± 0.0099 *(100)*

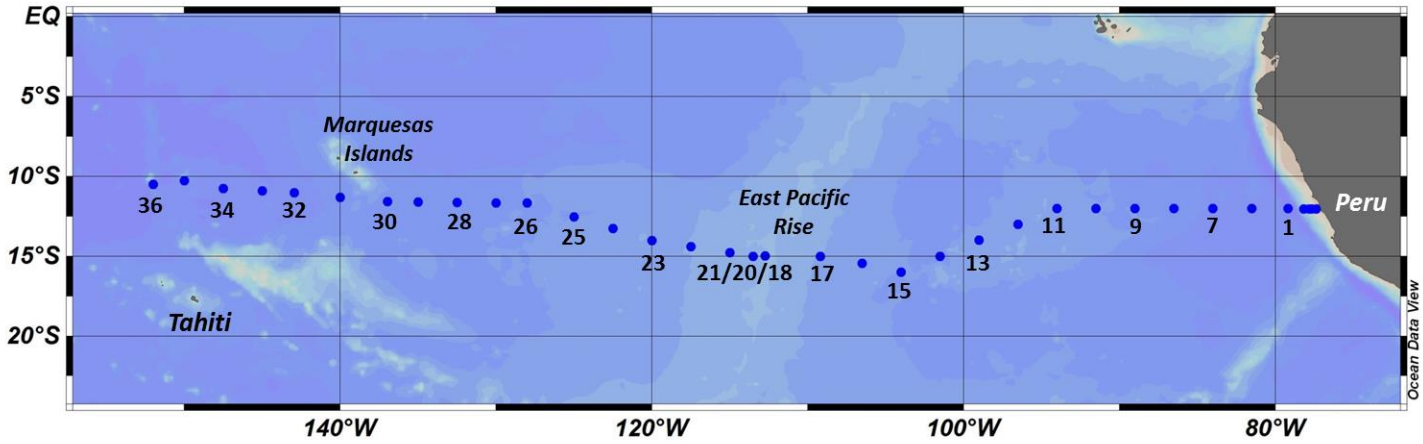

Figure 4.1. U.S. GEOTRACES GP16 water sampling stations in the eastern tropical South Pacific Ocean. Stations with identification numbers were sampled with full depth profiles, unlabeled stations were demi-stations (upper 1000 m) or shelf stations.

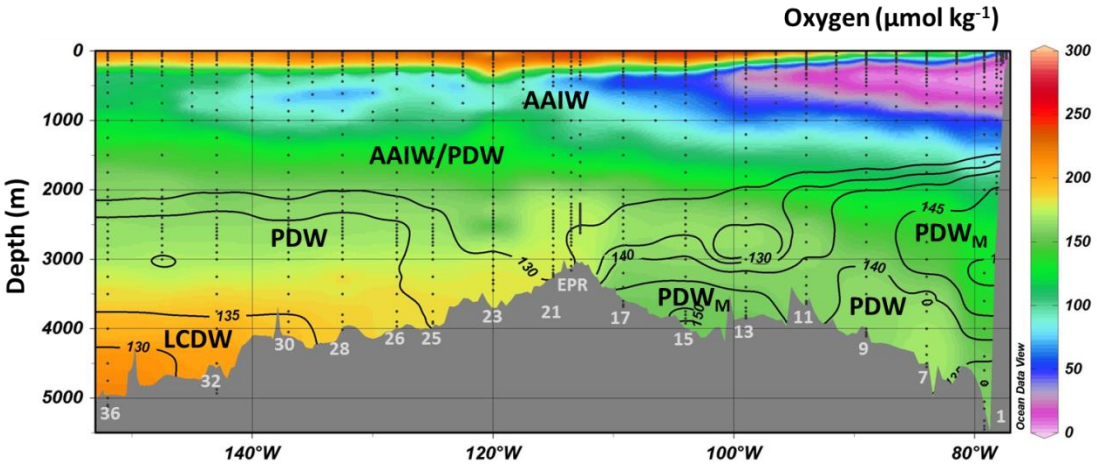

Figure 4.2. Oxygen concentrations are overlayed with silicate contours (µmol kg^{-1}) to identify water masses. Antarctic Intermediate Water (AAIW) is between 700–1000 m, AAIW mixes with Pacific Deep Water (PDW) from 1000–2000 m, PDW is found throughout the western and eastern portions of the transection >2000 m, Modified PDW (PDW_M) is found between 2000–4000 m east of the East Pacific Rise (EPR), and Lower Circumpolar Deep Water (LCDW) is found west of the EPR >4000 m (Kawabe and Fujio, 2010; Talley et al., 2011). Sampling points are shown as black dots and stations with full-depth profiling are identified numerically in the gray bathymetric section.

(A)

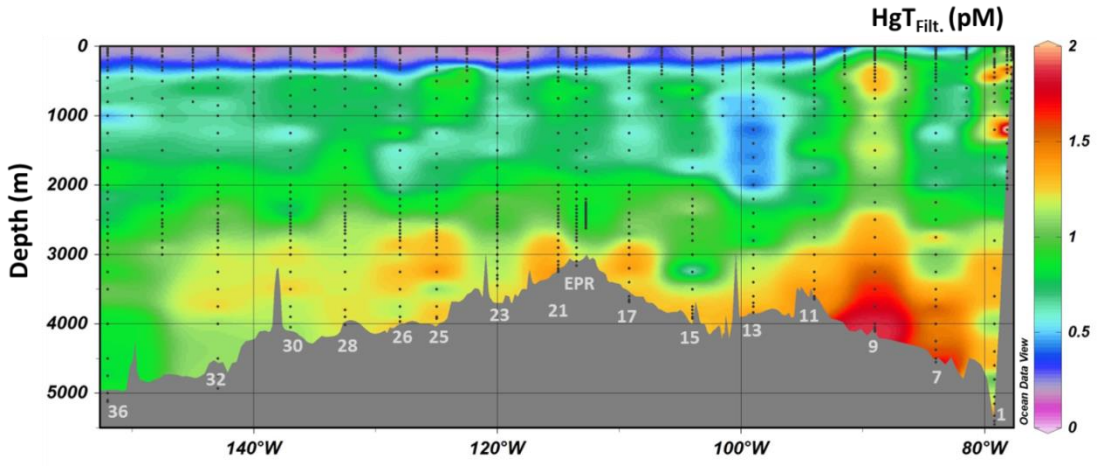

(B)

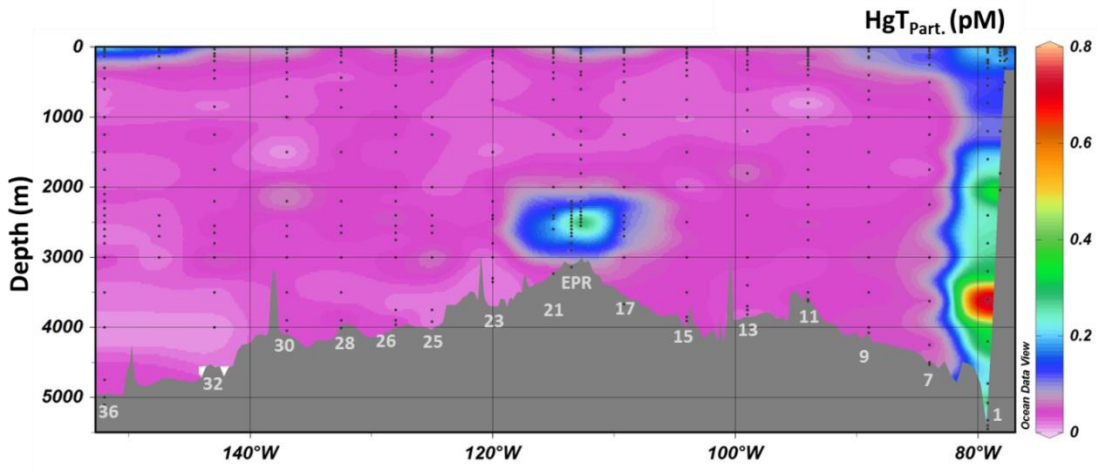

Figure 4.3. Concentrations of filtered (panel A) and suspended particulate (panel B) HgT in the eastern South Pacific Ocean. Sampling points are shown as black dots and full station numbers are listed throughout the gray bathymetric section.

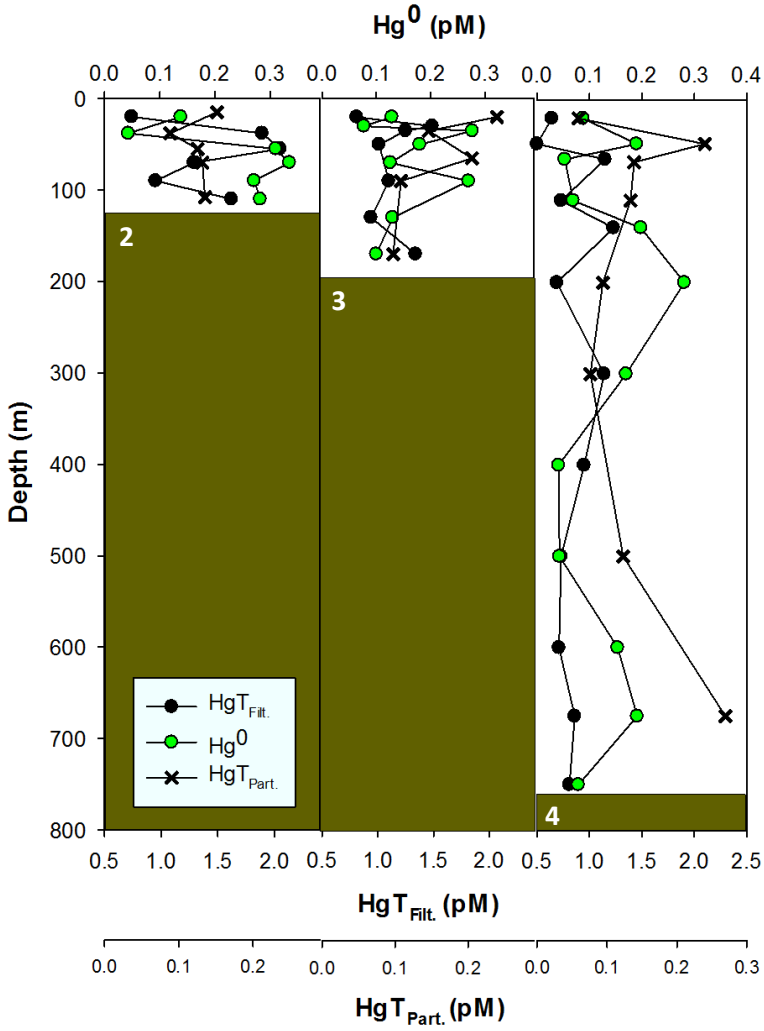

Figure 4.4. Filtered and particulate HgT and Hg^0 in the water column on the continental shelf (Stations 2–3) and slope (Station 4) near Peru.

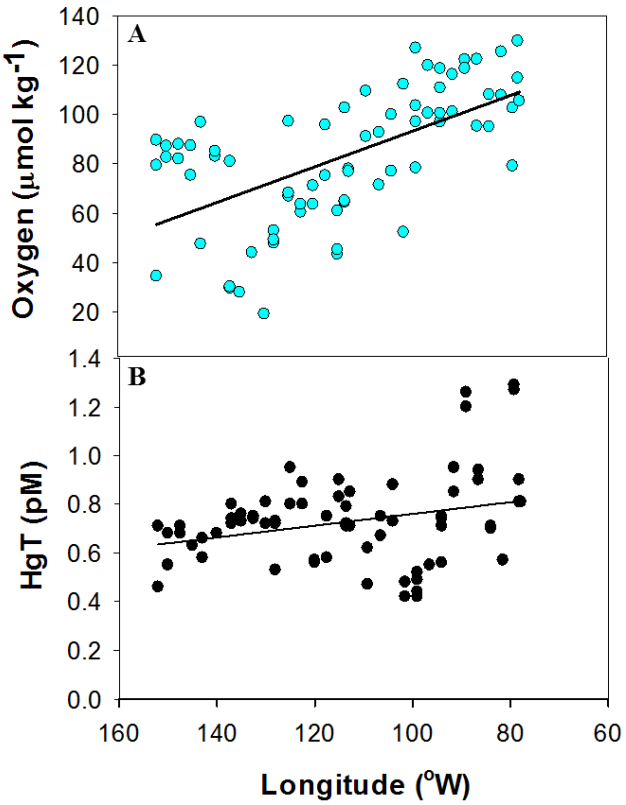

Figure 4.5. Oxygen concentrations decrease in AAIW (700–1000 m) from east to west across the transect (panel A). Filtered HgT (r^2 = 0.1, p = 0.01) decreases as AAIW ages moving west (panel B).

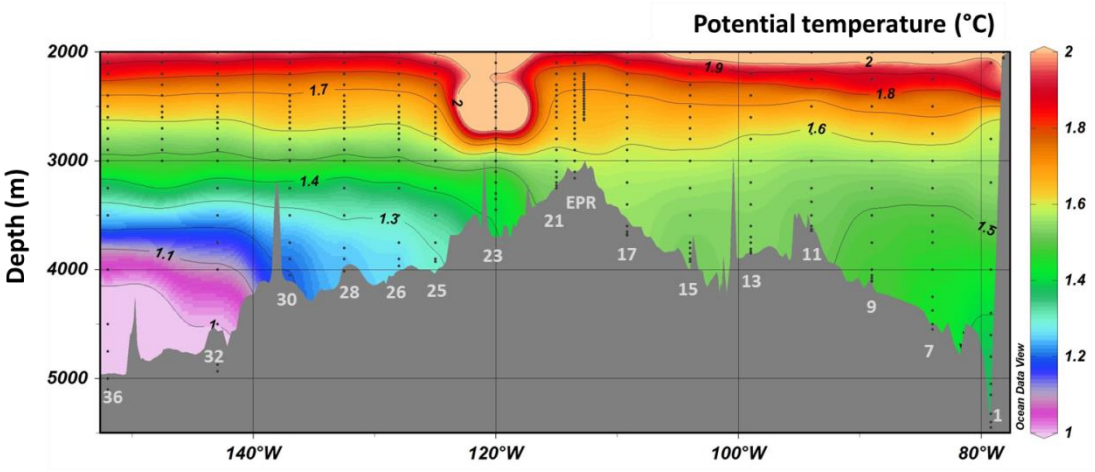

Figure 4.6. Potential temperature decreases with depth west of the EPR crest and remains constant with depth east of the crest due to geothermal heating along the rise.

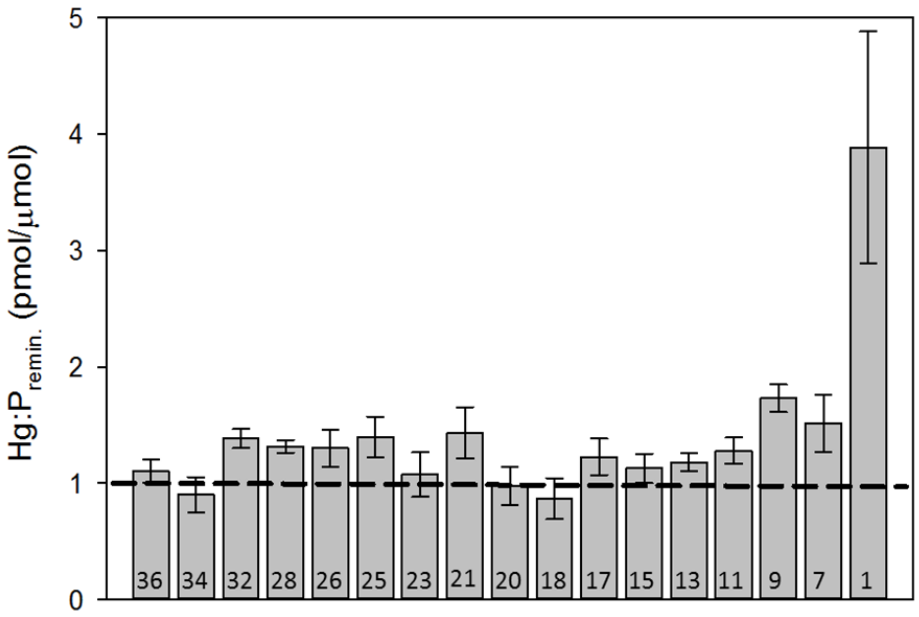

Figure 4.7. Mean (± SD) Hg:P_{remin} ratios in bottom water <1000 m from abyssal sediments. Station numbers are listed in the bars. The dashed line at Hg:P_{remin} = 1 represents the deep water ratio expected in waters that only accumulate Hg released from sinking biological material (Lamborg et al., 2014).

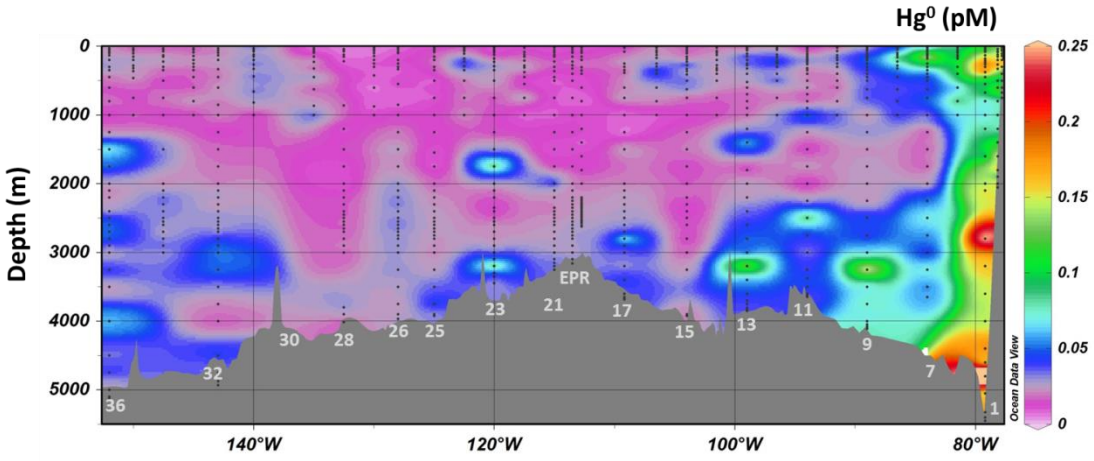

Figure 4.8. Elemental Hg distribution in eastern South Pacific Ocean. Sampling points are shown as black dots and full station numbers are listed throughout the gray bathymetric section.

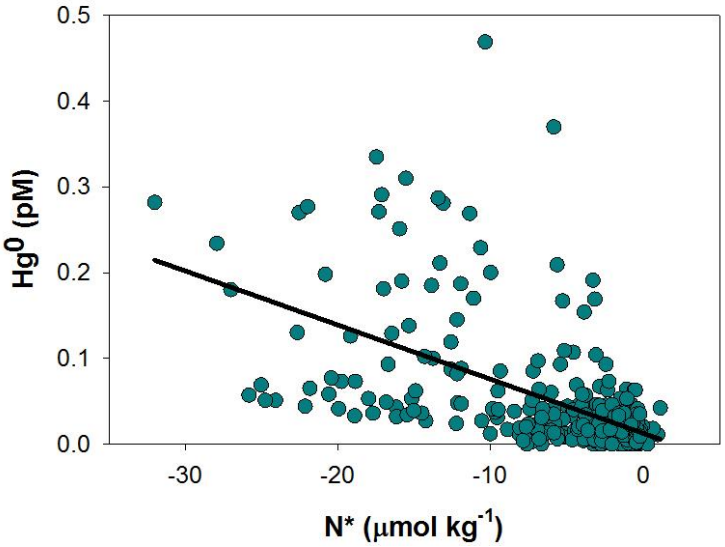

Figure 4.9. Elemental Hg (Hg^0) was inversely related to degree of denitrification in mixed layer and thermocline waters (20–700 m; $r^2 = 0.3$, $p < 0.001$). N* was calculated according to Gruber and Sarmiento (1991); $N^* = 0.87(NO_3 - 16PO_4 + 2.95)$.

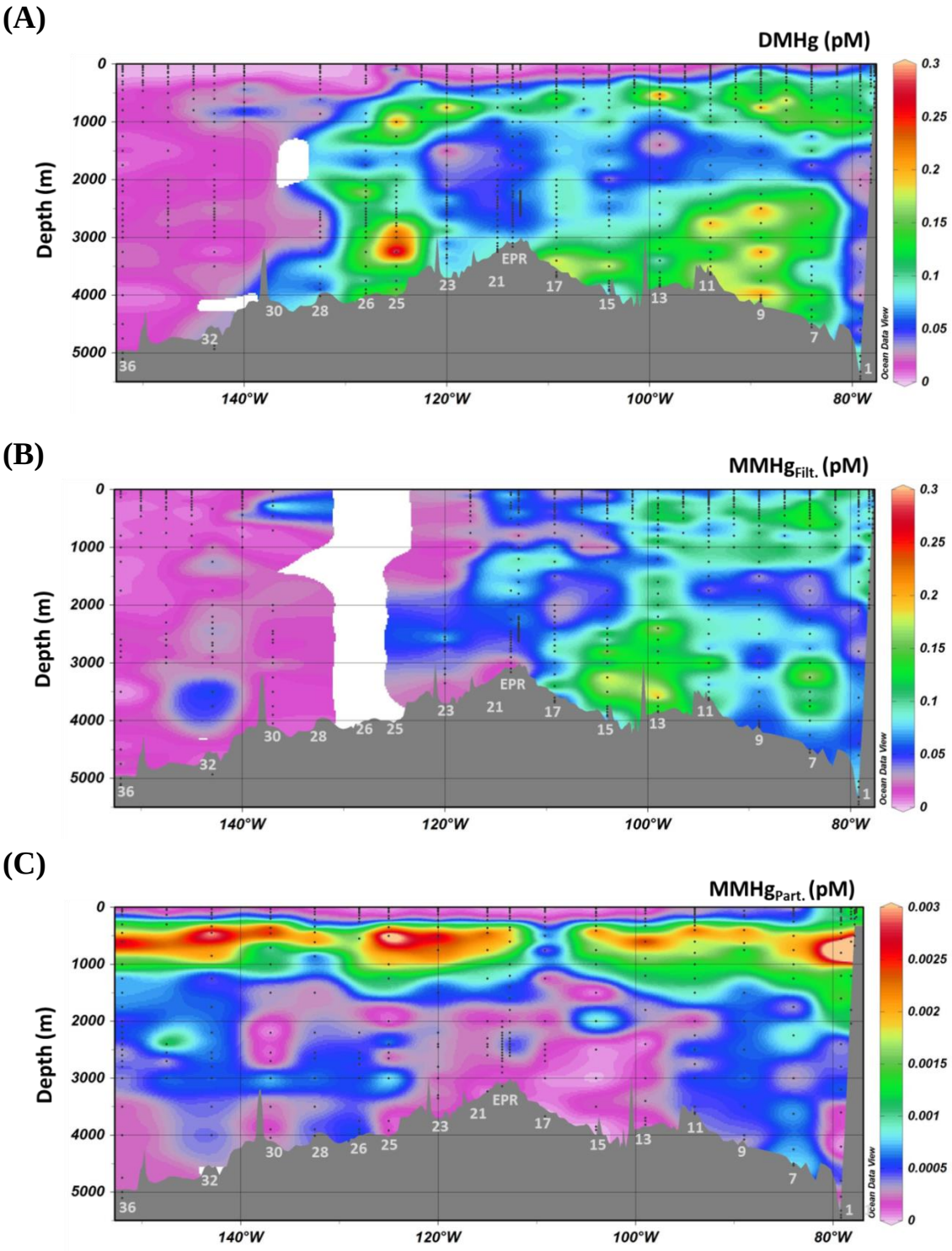

Figure 4.10. Concentrations of DMHg (panel A), filtered MMHg (panel B), and suspended particulate MMHg (panel C). Sampling points are shown as black dots and full station numbers are listed throughout the gray bathymetric section.

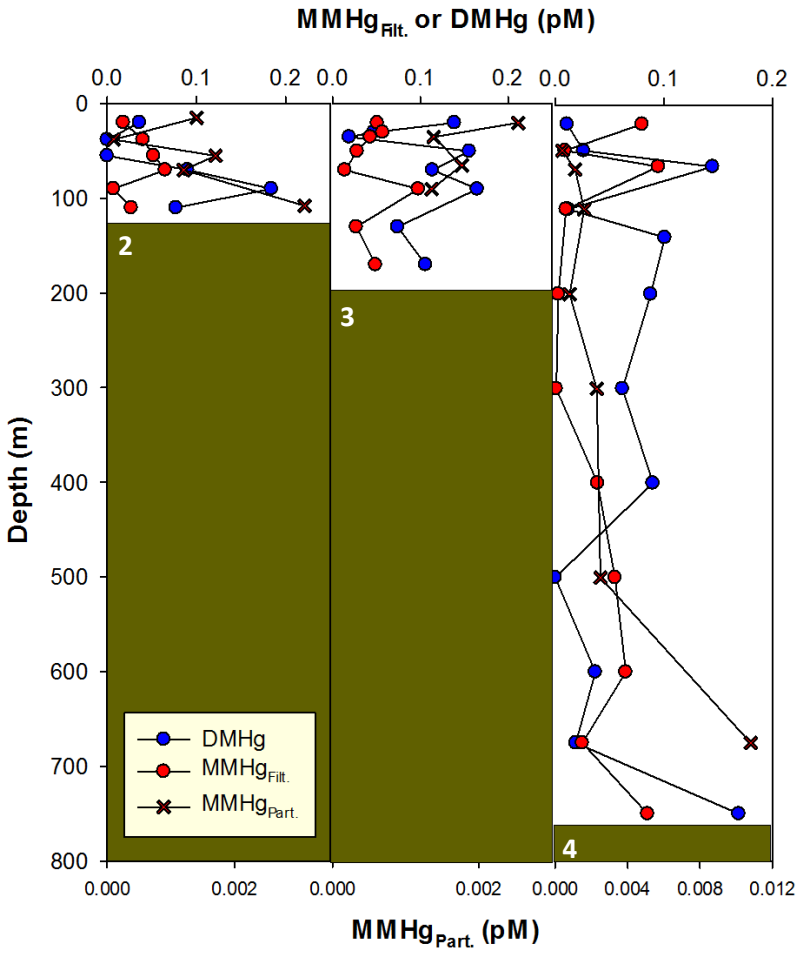

Figure 4.11. Filtered and particulate MMHg, and DMHg in the water column on the continental shelf (Stations 2–3) and slope (Station 4) near Peru.

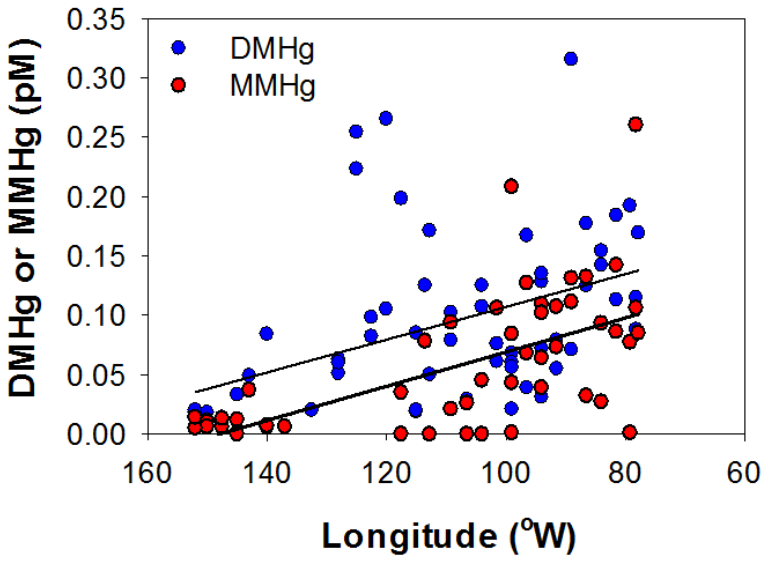

Figure 4.12. Filtered MMHg (r^2 = 0.2, *p* = 0.002) and DMHg (r^2 = 0.4, p < 0.0001) appear to decrease in AAIW (700–1000 m) moving west across the section (slope = –0.0001 for both DMHg and MMHg).

.

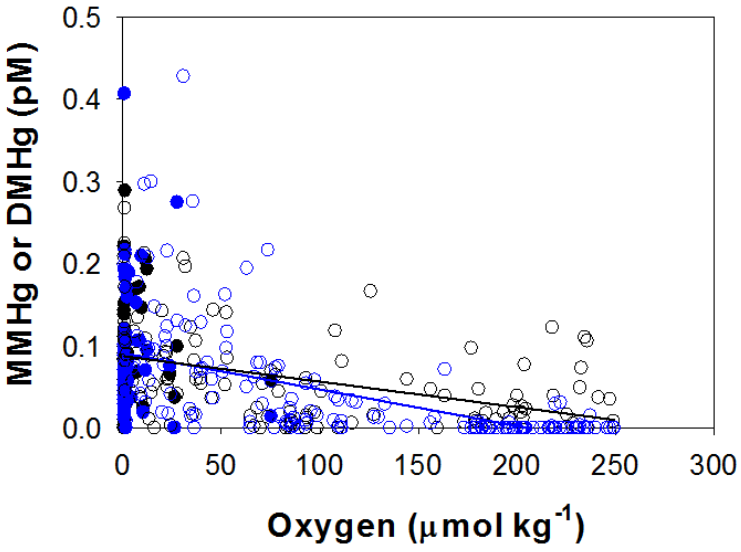

Figure 4.13. DMHg and filtered MMHg concentrations related to dissolved oxygen (DMHg, $r^2 = 0.3$, $p < 0.0001$; MMHg, $r^2 = 0.2$, $p < 0.0001$) in thermocline waters (100–700 m). Closed circles are upwelling Stations 1–9 and open circles are non-upwelling Stations 10–36.

5. THE BEHAVIOR AND DISTRIBUTION OF METHYLATED MERCURY COMPARED BETWEEN THE NORTH ATLANTIC AND EASTERN TROPICAL SOUTH PACIFIC OCEANS

Abstract

Monomethylmercury (MMHg) and dimethylmercury (DMHg) are present in the ocean at femtomolar concentrations, making their detection and separation challenging. Using methods described in Chapter 2, high-resolution vertical profiles of MMHg and DMHg were obtained during two expansive sections in the North Atlantic and eastern tropical South Pacific Oceans, culminating in the largest data set of methylated Hg in the ocean. Increased concentrations of MMHg and DMHg were observed in the subsurface chlorophyll maximum and more commonly in low-oxygen thermocline waters. Dimethylmercury concentrations correlated with redox sensitive metals, increasing with Fe and Co reduction and decreasing with Mn reduction. In the Atlantic thermocline, Fe and Co correlated with decreasing MMHg and increasing DMHg, suggesting that MMHg is methylated to DMHg during Fe and Co reduction. In the thermocline of the Atlantic and Pacific Oceans, MMHg concentrations were typically two-fold greater than DMHg, Total methylated Hg (MMHg + DMHg) was related to apparent oxygen utilization, however, comparison between the two basins over a wide range of oxygen concentrations suggests that other factors may be of greater importance for controlling mercury methylation. Dimethylmercury was the dominant form of methylated Hg in most deep water masses and concentrations of both DMHg and MMHg increased in aging Pacific deep water. Increased concentrations of MMHg and DMHg in deep North Atlantic waters

may be related to anthropogenic mercury inputs. Analytical separation of methylated Hg species revealed unique and independent distributions of MMHg and DMHg. These data suggest that MMHg and DMHg are produced throughout the water column in oxygenated subsurface waters, low-oxygen thermocline waters, and likely in deep water masses during thermohaline circulation.

5.1. Introduction

Current knowledge of inorganic mercury (Hg) methylation originates from incubation experiments conducted with sediment and pore water (Compeau and Bartha, 1985; Gilmour et al., 1992; Benoit et al., 2003; Hammerschmidt et al., 2004, 2008), pure cultures of microbes (Wood et al., 1968; King et al., 2000; Kerin et al., 2006; Hamelin et al., 2011; Schaefer et al., 2011; Parks et al., 2013; Gilmour et al., 2013), and seawater (Celo et al., 2006; Monperrus et al., 2007; Lehnherr et al., 2011; Munson, 2014). The most extensively studied medium is anoxic sediment, where sulfate-reducing bacteria (SRB) are the primary methylators (Compeau and Bartha, 1985; Gilmour et al., 1992; Benoit et al., 2003), and production of monomethylmercury (MMHg) appears to be limited by the availability and speciation of inorganic Hg (Hammerschmidt and Fitzgerald, 2004; Hammerschmidt et al., 2008; Gilmour et al., 2013; Hsu-Kim et al., 2013). Neutrally charged complexes, such as HgS^0, are thought to be the most bioavailable forms of inorganic Hg (Benoit et al., 2003), however, facilitated diffusion and active transport across cell membranes may shuttle other forms of Hg into cells where methylation occurs (Hsu-Kim et al., 2013).

Cultures of SRB, iron-reducing bacteria, and methanogens have been observed to produce MMHg from inorganic Hg substrate (Wood et al., 1968; King et al., 2000; Kerin

et al., 2006; Hamelin et al., 2011; Schaefer et al., 2011; Gilmour et al., 2013). Inside the cell, MMHg production has been linked to the reductive acetyl-coenzyme A (CoA) pathway, a biochemical process involving the synthesis of methylcobalamin (vitamin B12; Choi et al., 1994). More recently, and upon discovery of the *hgcAB* gene cluster responsible for Hg methylation in SRB (Parks et al., 2013), a more diverse group of anaerobic microorganisms has been observed to methylate Hg, including fermentative, acetogenic, and cellulolytic microorganisms (Gilmour et al., 2013). The *hgcA* gene encodes a corrinoid-dependent protein (HgcA) similar to the corrinoid iron-sulfur protein required for methyltransferase in the acetyl-CoA pathway. Methyl transfer reactions can occur only after cobalt within the HgcA protein is reduced (Co^{2+} to Co^{+}), and this is thought to be facilitated by the HgcB ferrodoxin protein encoded by *hgcB* (Choi et al., 1994; Parks et al., 2013). Transfer of a methyl group to inorganic Hg is presumed to occur during these methyl transfer reactions.

Microorganisms identified as potential methylators in pore water and bacteria cultures require anoxic conditions for their metabolism to be thermodynamically favorable, however, seawater incubation tests with isotopically enriched ^{199}Hg and ^{198}Hg have demonstrated MMHg production under oxic conditions (Monperrus et al., 2007; Lehnherr et al., 2011). Methylation in oxic water may result from either abiotic reactions (Celo et al., 2006), biotic reactions involving anaerobic bacteria in hypoxic microenvironments (e.g., suspended particles), or by other microbes with an undiscovered ability to methylate inorganic Hg. In Arctic Ocean waters, the rate of MMHg decomposition measured using $CH_3{}^{201}Hg$ was two orders of magnitude greater than the methylation rate, resulting in a fast approach to steady-state concentrations (4–10

d; Lehnherr et al., 2011). In waters of the Mediterranean Sea, $CH_3{}^{201}Hg$ decomposition was observed under both light and dark incubation conditions, suggesting decomposition by both photochemical and microbial demethylation pathways (Monperrus et al., 2007).

Oceanographic field observations have consistently revealed elevated concentrations of methylated Hg in low-oxygen regions of the water column, particularly oxygen minimum zones (OMZ) that persist in the thermocline (Mason et al., 2012). Multiple studies have observed significant correlations between either MMHg, dimethylmercury (DMHg), or total methylated Hg (MMHg + DMHg) and apparent oxygen utilization (AOU; Mason and Fitzgerald, 1991; Mason and Sullivan, 1999; Kirk et al., 2008; Sunderland et al., 2009; Heimbürger et al., 2010; Cossa et al., 2011; Lehnherr et al., 2011), a proxy for heterotrophic microbial activity. Other studies, however, have reported elevated concentrations of methylated Hg in the well-oxygenated subsurface chlorophyll maximum in addition to the OMZ, apparently negating the dependence of Hg methylation on low-oxygen conditions (Heimbürger et al., 2010; Heimbürger et al., in review; Bowman et al., 2014). Seminal investigations of methylated Hg in the ocean were limited by a lack of measurements in deep water, analytical challenges including high detection limits, and the determination of total methylated Hg instead of independent measurements of MMHg and DMHg. Seawater incubation tests observed production of DMHg from Hg(II) and from methylation of MMHg, but at rates much slower than the production of MMHg (Lehnherr et al., 2011). While DMHg has been reported as the dominant species of methylated Hg in the deep ocean (Cossa et al., 1997; Mason and Sullivan, 1999; Mason et al., 1995), its production and interaction with MMHg has been understudied.

Results from the U.S. GEOTRACES North Atlantic Zonal Transect (Chapter 3, Atlantic, GA03) and Eastern Pacific Zonal Transect (Chapter 4, Pacific, GP16) were used to examine the behavior of MMHg and DMHg in upper water column, thermocline, and deep waters of these two ocean basins.

5.2. Results

5.2.1 Subsurface chlorophyll maximum

A subsurface chlorophyll maximum is often located at the lower boundary of the euphotic zone, where either upwelling or vertical diffusion delivers dissolved nutrients from depth and there is sufficient sunlight to support primary production (Feely et al., 2004). Subsurface maxima of methylated Hg have been reported previously in the Mediterranean Sea, where they were associated with the microbial loop and active nano- and picophytoplankton (Heimbürger et al., 2010). Maxima of MMHg also were observed near the subsurface chlorophyll maximum in both the Atlantic and Pacific Oceans. Few DMHg maxima were observed at the subsurface chlorophyll maximum in the Atlantic Ocean, but were found commonly in the upwelling region of the eastern equatorial Pacific Ocean (Chapters 3–4). In the oxygenated subsurface chlorophyll maximum, MMHg concentrations were greater than those of DMHg. Below the subsurface chlorophyll maximum, rates of net primary production decrease and both DMHg and MMHg increase with decreasing oxygen (Fig. 5.1). In the surface mixed layer (<100 m depth), concentrations of DMHg correlated with redox-sensitive iron (Fe), manganese (Mn), and cobalt (Co), and these relationships were strongest in the upwelling region of the eastern Pacific Ocean (Fig. 5.2). In suboxic areas of the Pacific upwelling region, Fe(III) is used as a terminal electron acceptor and concentrations of DMHg and filtered

Fe were positively correlated. DMHg concentrations also increased with filtered Co in the mixed layer of the Pacific, which is indicative of Co reduction from highly insoluble Co^{3+} to Co^{2+} (Saito et al., 2004). DMHg was unrelated to Co in the Atlantic, where greater concentrations of oxygen in the Atlantic surface waters may have precluded Co reduction. These findings are consistent with microbial culture studies that link microbial Fe- and Co-reduction to methylation of inorganic Hg (Choi et al., 1994; Kerin et al., 2006; Ekstrom and Morel, 2008; Gilmour et al., 2013). In contrast to relationships with Fe and Co, concentrations of DMHg were inversely related to filtered Mn, which suggests electrochemical reduction of Mn (increasing filtered Mn) decreases DMHg. Potential demethylation during Mn reduction is a unique observation – Mn oxides are known to bind MMHg which can be released during Mn reduction (Desauziers et al., 1997) and would more likely be associated with increasing rather than decreasing concentrations of methylated Hg. There were no significant correlations between MMHg and redox-sensitive metals, suggesting that redox conditions favor the production of DMHg more than that of MMHg.

5.2.2 Thermocline waters

Concentrations of filtered total methylated Hg (MMHg + DMHg) were maximum in Atlantic thermocline waters (100–1000 m), and changes in the MMHg:DMHg molar ratio with depth suggest that MMHg is methylated to DMHg under low-oxygen conditions. Suspended particles in the Atlantic contained <1% of total MMHg in the water column and were not included in this analysis. There was a weak but significant correlation between total methylated Hg and AOU, and the relationship was best fit by a second-order polynomial function, similar to results in the North Pacific (Sunderland et

al, 2009; Fig. 5.3a). The highest concentrations of methylated Hg were observed between 100–150 μmol kg^{-1} AOU. Where oxygen consumption in the thermocline was relatively low (AOU < 50 μmol kg^{-1}), MMHg concentrations were up to 80× greater than those of DMHg, potentially from MMHg production in overlying water (e.g., subsurface chlorophyll maximum) and vertical transport into the thermocline (Fig. 5.3b). Alternatively, MMHg production may be favored relative to that of DMHg when AOU is low. Where AOU was greater than 75 μmol kg^{-1} in the thermocline, MMHg:DMHg molar ratios decreased to an average of 2 ± 2 (n = 60).

Dimethylmercury was positively correlated with AOU (r^2 = 0.1, p < 0.0001) as well as Co and Fe in the Atlantic thermocline (Fig.5. 4a). Concentrations of dissolved oxygen were >50 μmol kg^{-1} in the OMZ of the North Atlantic, which is inconsistent with methylation by anaerobic microbes. However, anoxic/hypoxic microenvironments in sinking particles may harbor microbes that reduce Co and Fe and produce DMHg. Correlations between DMHg, Co, and Fe in the thermocline are consistent with increasing DMHg under reducing conditions at the subsurface chlorophyll maximum (Fig. 2), but inconsistent with decreasing DMHg associated with Mn reduction (p = 0.07). Concentrations of MMHg were not correlated with AOU in thermocline waters of the North Atlantic (p = 0.7) and were related inversely with those of Co and Fe (Fig. 5.4b), in contrast to DMHg. Concentrations of total methylated Hg were unrelated to either filtered Co (p = 0.9) or Fe (p = 0.2). Decreasing MMHg with increasing DMHg suggests that pre-formed MMHg is methylated to DMHg during Co and Fe reduction in the thermocline of the North Atlantic. These results suggest that DMHg produced under oxic and low-

oxygen conditions drives the correlation between total methylated Hg and AOU in Atlantic thermocline waters.

Total methylated Hg also was maximum in the Pacific thermocline and related to AOU by a second-order function (Fig. 5.3c), similar to the relationship observed in the Atlantic (Fig. 5.3a), although the maximum inflection point in the Pacific was shifted toward higher AOU. Suspended particles in the Pacific also contained minimal concentrations of MMHg (≤1% total methylated Hg) and only filtered concentrations were used for this comparison. High primary production in the upwelling region of the eastern Pacific stimulated greater oxygen consumption in the thermocline, and maximum concentrations of total methylated Hg were observed between 150–200 μmol kg^{-1} AOU. Unlike in the Atlantic where MMHg:DMHg ratios varied 80-fold when AOU was < 50 μmol kg^{-1}, MMHg:DMHg ratios in the Pacific varied by less than an order of magnitude and averaged 2 ± 3 (n = 146). Where AOU concentrations were >100 μmol kg^{-1}, MMHg:DMHg molar ratios in the thermocline were similar between the North Atlantic and eastern South Pacific (Mann-Whitney Rank Sum, p = 0.5). Unlike in the Atlantic, the correlation between total methylated Hg and AOU in the Pacific was driven by MMHg (r^2 = 0.1, p < 0.0001 for MMHg vs. AOU; p = 0.7 for DMHg vs. AOU). Monomethylmercury (r^2 = 0.03, p = 0.02) and DMHg (r^2 = 0.1, p < 0.0001 DMHg) were related positively to filtered Co, but unrelated to either Fe or Mn in the Atlantic thermocline. The lack of correlation between total methylated Hg and other redox-sensitive metals in the Pacific may result from efficient metal scavenging in productive upwelling waters.

In the thermocline of both the North Atlantic and eastern South Pacific Oceans, concentrations of filtered DMHg and MMHg were related positively to filtered total Hg (HgT), and the slopes for each species were similar between basins (Fig. 5.5). These relationships suggest that in thermocline waters, on average about 10% of total Hg is as DMHg and 5–6% as MMHg, which is inconsistent with average MMHg:DMHg molar ratios in the thermocline (2 ± 2 in Atlantic, n = 60; 2 ± 3 in Pacific, n = 146). Weak correlation coefficients (Fig. 5.5) and relatively high variability of MMHg:DMHg ratios (± 100–150%) highlight the fact that while we can make generalizations, the behavior of MMHg and DMHg in thermocline waters is often unpredictable. Filtered total Hg was positively correlated with AOU in the Atlantic and Pacific thermoclines (Fig. 5.6), but unlike methylated Hg the relationship was linear. The decrease of total methylated at AOU >150-200 μmol kg^{-1}, coincident with a continued increase of filtered HgT, suggests that methylation rates may decrease beyond a certain point after depletion of bioavailable forms of inorganic Hg or exhaustion of organic molecules needed to sustain the metabolisms of specific methylating microorganisms.

Concentrations of filtered HgT, MMHg, and DMHg in thermocline waters were not significantly different between the eastern Pacific upwelling region and the North Atlantic (Kruskal-Wallis One Way ANOVA, $p < 0.05$), however, the sources of Hg were different. Lamborg and colleagues (2014) found a 1:1 pmol/μmol ratio of filtered HgT to remineralized phosphorus ($Hg:P_{remin}$) in waters unaffected by anthropogenic Hg inputs that receive Hg and P from decomposing biological material. In the Pacific upwelling region, Hg scavenged at the surface is released during recycling and remineralization processes in the thermocline and the $Hg:P_{remin.}$ ratio was 0.7 ± 0.3 (n = 60). This suggests

that while filtered HgT concentrations in the upwelling region were elevated relative to non-upwelling thermocline waters in the section (Table 5.1), the Hg originated from a natural source. In younger waters of the Atlantic thermocline the $Hg:P_{remin.}$ ratio was 2 ± 1 (n = 258) indicating that there is excess Hg present due to anthropogenic inputs. While Hg originated from different sources, similar concentrations of HgT in the Atlantic and Pacific upwelling thermoclines resulted in similar concentrations of MMHg and DMHg (Kruskal-Wallis One Way ANOVA, $p < 0.05$; Table 5.1).

5.2.3 Deep waters

Aging deep water in the Pacific accumulated both MMHg and DMHg (Table 5.2) and in the Atlantic, deep water contains significantly more methylated Hg due to anthropogenic inputs (Fig. 5.6a). Deep water in the Atlantic (North Atlantic Deep Water, NADW and Antarctic Bottom Water, AABW) was impacted by anthropogenic Hg inputs ($Hg:P_{remin} > 1$; Lamborg et al., 2014), and total methylated Hg increased with the $Hg:P_{remin}$ ratio (Fig. 5.7a). Dimethylmercury and MMHg were independently correlated with $Hg:P_{remin}$ ($r^2 = 0.07$, $p = 0.006$ for DMHg; $r^2 = 0.3$, $p < 0.0001$ for MMHg). Atlantic thermocline waters also contain anthropogenic Hg ($Hg:P_{remin} > 1$; Lamborg et al., 2014), but there was no correlation with $Hg:P_{remin}$ ($p = 0.2$; Fig. 5.7b). Demethylation in thermocline waters may have removed excess MMHg and DMHg (Lehnherr et al., 2011) produced from inputs of anthropogenic Hg while slower demethylation rates in deep water, due to the absence of sunlight (Monperrus et al., 2007), preserved greater concentrations of methylated Hg. Overall, deep water in the Atlantic had 1.4× more total methylated Hg, on average, than deep water in the Pacific that did not receive anthropogenic Hg inputs.

In Pacific deep water masses unaffected by anthropogenic Hg, concentrations of MMHg and DMHg increased with age (Lower Circumpolar Deep Water (LCDW) < Pacific Deep Water (PDW) < Modified PDW (PDW_M); Kruskal-Wallis One Way ANOVA, $p < 0.05$), with MMHg and DMHg in similar proportions to each other (Table 5.2). The only exception was MMHg which was similar between LCDW and PDW ($p > 0.05$). In the Pacific section, no external sources of MMHg or DMHg to deep water masses were identified; MMHg in suspended particles was too low (< 0.001 pM at depths > 2000 m) to release notable amounts of filtered MMHg, and there was no increase in either MMHg or DMHg at the sediment-water interface near abyssal sediments, or within the buoyant hydrothermal vent plume released from the East Pacific Rise (Chapter 4). Methylation of inorganic Hg in deep water masses has not been studied, however, these results suggest that deep water methylation likely occurs.

Dimethylmercury was the dominant form of methylated Hg in NADW, PDW, and PDW_M, and concentrations of DMHg and MMHg were similar in LCDW and AABW (Table 5.2). Greater concentrations of DMHg relative to MMHg may result from increased stability of DMHg in cold, deep water masses (Mason and Fitzgerald, 1993; Mason et al, 1998). Methylation of MMHg to DMHg was not likely a source of increased DMHg because methylation rates measured in polar surface waters were 1–2 orders of magnitude slower for DMHg (produced from Hg(II) and MMHg) compared to methylation of Hg(II) to MMHg (Lehnherr et al., 2011). Net methylation of MMHg would have to be sufficient enough to replace what is lost to demethylation while still accumulating greater concentrations with age. The MMHg:DMHg molar ratios of deep water masses may be influenced by the original composition of the water mass prior to

subduction. For example, in the Arctic Ocean, Andersson and colleagues (2008) found elevated concentrations of dissolved gaseous Hg (DMHg + Hg^0) in ice covered waters. Seasonal ice cover at subduction regions may prevent evasion of DMHg, causing polar surface waters to accumulate DMHg in excess of MMHg.

5.3. Conclusions

High vertical and horizontal resolution sampling, sufficiently low detection limits, and separation of MMHg and DMHg have resulted in this being the most comprehensive data set of methylated Hg in the ocean. Distributions of MMHg and DMHg across two expansive ocean sections suggest that MMHg and DMHg are produced throughout the entire water column; in oxygenated subsurface waters, low-oxygen thermocline waters, and likely in deep water masses. At the subsurface chlorophyll maximum, DMHg correlated with redox-sensitive metals, increasing in concentration concomitantly with Fe and Co reduction and decreasing as Mn is reduced. Positive correlations between DMHg, Fe, and Co were also found in the Atlantic thermocline and correlated inversely with MMHg, suggesting that methylation of MMHg was a source of DMHg under low-oxygen conditions. Monomethylmercury was typically 2-fold greater than DMHg in the thermocline of the Atlantic and Pacific Oceans.

There was some correlation between total methylated Hg and AOU, however, concentrations of methylated Hg decreased as remineralization progressed, despite a continued increase in filtered HgT. This pattern may reflect the exhaustion of bioavailable forms of inorganic Hg and organic molecules needed to sustain the metabolism of methylating microorganisms. Methylated Hg correlates with oxygen consumption in thermocline waters of multiple ocean basins (Mason et al, 2012),

suggesting that the greatest concentrations of MMHg and DMHg would be found in highly productive, suboxic thermocline waters. However, this is not true due to inputs of anthropogenic Hg. Concentrations of MMHg and DMHg were similar between Atlantic thermocline waters affected by anthropogenic Hg inputs and highly productive upwelling waters in the eastern Pacific, despite substantial differences in oxygen concentrations (Pacific upwelling OMZ <10 μM O_2, Atlantic OMZ >50 μM O_2). Enrichment of MMHg and DMHg in waters affected by anthropogenic Hg needs to be considered when comparing oceanographic surveys and building budgets of methylated Hg in the global ocean.

Monomethylmercury and DMHg were increased significantly in Atlantic deep water containing greater concentrations of anthropgoenic Hg compared to deep waters in the Pacific. In the Pacific, where deep water was not affected by anthropogenic Hg, methylated Hg increased with water mass age. Dimethylmercury was often the dominant form of methylated Hg in deep water masses. In order for DMHg to excede MMHg in the deep ocean, methyation dynamics would have to be signifiacntly different from surface waters. Alternatively, the MMHg:DMHg ratio in deep water masses may reflect the original compositon of the water mass at the surface prior to subduction and thermohaline circulation.

Acknowledgements

I thank Pete Sedwick and Bettina Sohst for Fe data, Joe Resing, Mariko Hatta, and Chris Measures for Mn data, and Mak Saito, Abigail Noble, and Nick Hawco for Co data.

References

Benoit, J.M., Gilmour, C.C., Heyes, A., Mason, R.P. 2003. Geochemical and biological conrols over methylmercury production and degradation in aquatic ecosystems. In American Chemical Society (Ed.), Biogeochemistry of Environmentally Important Trace Elements (Chp. 19, pp 262–297).

Bowman, K.L., Hammerschmidt, C.R., Lamborg, C.H., Swarr, G. 2014. Mercury in the North Atlantic Ocean: The U.S. GEOTRACES zonal and meridional sections. Deep-Sea Res. II. DOI: 10.1016/j.dsr2.2014.07.004.

Celo, V., Lean, D. R. S., Scott, S. L. 2006. Abiotic methylation of mercury in the aquatic environments. Sci. Tot. Environ. 368, 126–137.

Choi, S., Chase, T. Jr., Bartha, R. 1994. Metabolic pathways leading to mercury methylation in *Desulfovibrio desulfuricans*. Appl. Environ. Microbiol. 60: 4072-4077.

Compeau, G., Bartha, R. 1985. Sulfate-reducing bacteria: principal methylators of mercury in anoxic estuarine sediments. Appl. Environ. Microbiol. 50, 498–502.

Cossa, D., Heimbürger, L.-E., Lannuzel, D., Rintoul, S.R., Butler, E.C.V., Bowie, A.R., et al. 2011. Mercury in the Southern Ocean. Geochim. Cosmochim. Ac. 75, 4037–4052.

Cossa, D., Martin, J.-M., Takayanagi, K., Sanjuan, J. 1997. The distribution and cycling of mercury species in the western Mediterranean Sea. Deep-Sea Res. II. 44, 721–740.

Desauziers, V., Castre, N., Cloirec, P.L. 1997. Sorption of methylmercury by clays and mineral oxides. Environ. Technol. 18, 1009–1018.

Ekstrom, E.B., Morel, F.M.M. 2008. Cobalt limitation of growth and mercury methylation in sulfate-reducing bacteria. Environ. Sci. Technol. 42, 93–99.

Feely, R.A., Sabine, C.L., Schlitzer, R., Bullister, J., mecking, S., Greeley, D. 2004. Oxygen utilization and organic carbon remineralization in the upper water column of the Pacific Ocean. J. Oceanography. 60, 45–52.

Gilmour, C.C., Henry, E.A., Mitchell, R. 1992. Sulfate stimulation of mercury methylation in freshwater sediments. Environ. Sci. Technol. 26, 2281–2288.

Gilmour, C.C., Podar, M., Bullock, A.L., Graham, A.M., Brown, S.D., Somenahally, A.C., et al. 2013. Mercury methylation by novel microorganisms from new environments. Environ. Sci Technol. 47, 11810–11820.

Hamelin, S., Amyot, M., Barkay, T., Wang, Y., Planas, D. 2011. Methanogens: Principal methylators of mercury in lake periphyton. Environ. Sci. Technol. 45, 7693–7700.

Hammerschmidt, C.R., Fitzgerald, W.F., Balcom, P.H., Visscher, P.T. 2008. Organic matter and sulfide inhibit methylmercury production in sediments of New York/New Jersey Harbor. Mar. Chem. 109, 165–182.

Hammerschmidt, C.R., Fitzgerald, W.F., Lamborg, C.H., Balcom, P.H., Visscher, P.T. 2004. Biogeochemistry of methylmercury in sediments of Long Island Sound. Mar. Chem. 90, 31–52.

Heimbürger, L.-E., Cossa, D., Marty, J.-C., Migon, C., Averty, B., Dufour, A., Ras, J. 2010. Methyl mercury distributions in relation to the prescence of nano- and

picophytoplankton in an oceanic water column (Ligurian Sea, North-western Mediterranean). Geochim. Cosmochim. Acta 74, 5549–5559.

Heimbürger, L.-E., Sonke, J., Cossa, D., Point, D., Lagane, C., Laffont, L., et al. 2014. Shallow methylmercury production in the marginal sea ice zone of the central Arctic Ocean, in review.

Hsu-Kim, H., Kucharzyk, K.H., Zhang, T., Deshusses, M.A. 2013. Mechanisms regulating mercury bioavailability for methylating microorganisms in the aquatic environment: A critical review. Environ. Sci. Technol. 47, 2441–2456.

Kerin, E.J., Gilmour, C.C., Roden, E., Suzuki, M.T., Coates, J.D., Mason, R.P. 2006. Mercury methylation by dissimilatory iron-reducing bacteria. Appl. Environ. Microbiol. 72, 7919– 7921.

King, J.K., Kostka, J.E., Frischer, M.E., Saunders, F.M. 2000. Sulfate-reducing bacteria methylate mercury at variable rates in pure culture and in marine sediments. Appl. Environ. Microbiol. 66, 2430–2437.

Kirk, J.L., St. Louis, V.L., Hintelmann, H., Lehnherr, I., Else, B., Poissant, L. 2008. Methylated mercury species in marine waters of the Canadian High and Sub Arctic. Environ. Sci. Technol. 42, 8367–8373.

Lehnherr, I., St. Louis, V.L., Hintelmann, H., Kirk, J.L. 2011. Methylation of inorganic mercury in polar marine waters. Nat. Geosci. 4, 298–302.

Mason, R.P., Choi, A.L., Fitzgerald, W.F., Hammerschmidt, C.R., Lamborg, C.H., Soerensen, A.L., Sunderland, E.M. 2012. Mercury biogeochemical cycling in the ocean and policy implications. Environ. Res. 119, 101–117.Monperrus, M.,

Tessier, E., Amouroux, D., Leynaert, A., Huonnic, P., Donard, O.F.X. 2007. Mercury methylation, demethylation and reduction rates in coastal and marine surface waters of the Mediterranean Sea. Mar. Chem. 107, 49–63.

Mason, R.P, Fitzgerald, W.F. 1991. Mercury speciation in open ocean waters. Water Air Soil Poll. 56, 779–798.

Mason, R.P, Fitzgerald, W.F. 1993. The distribution and biogeochemical cycling of mercury in the equatorial Pacific Ocean. Deep-Sea Res. I. 40, 1897–1924.

Mason, R.P., Rolfhus, K.R., Fitzgerald, W.F. 1995. Methylated and elemental mercury cycling in surface and deep ocean waters of the North Atlantic. Water Air Soil Pollut. 80, 665–677.

Mason, R.P., Rolfhus, K.R., Fitzgerald, W.F. 1998. Mercury in the North Atlantic. Mar. Chem. 61, 37–53.

Mason, R.P., Sullivan, K.A. 1999. The distribution and speciation of mercury in the South and equatorial Atlantic. Deep-Sea Res. II 46, 937–956.

Monperrus, M., Tessier, E., Amouroux, D., Leynaert, A., Huonnic, P., Donard, O.F.X. 2007. Mercury methylation, demethylation and reduction rates in coastal and marine surface waters of the Mediterranean Sea. Mar. Chem. 107, 49–63.

Munson, K. M. 2014. Transformations of mercury in the marine water column. (Doctoral dissertation). Retrieved from Massachusetts Institute of Technology Libraries. http://hdl.handle.net/1721.1/87513.

Parks, J. M., A. Johs, M. Podar, R. Bridou, R. A. Hurt, S. D. Smith, S. J., et al. 2013. The genetic basis for bacterial mercury methylation. Science, 339, 1332–1335.

Saito, M.A., Moffett, J.W., DiTullio, G.R. 2004. Cobalt and nickel in the Peru upwelling region: A major flux of labile cobalt utilized as a micronutrient. Global Biogeochem. Cy. 18, GB4030, doi: 10.1029/2003GB002216.

Schaefer, J.K., Rocks, S.S., Zheng, W., Liang, L., Gu, B., Morel, F.M.M. 2011. Active transport, substrate specificity, and methylation of Hg(II) in anaerobic bacteria. Proc. Natl. Acad. Sci. USA. 108, 8714–8719.

Sunderland, E.M., Krabbenhoft, D.P., Moreau, J.W., Strode, S.A., Landing, W.A. 2009. Mercury sources, distribution, and bioavailability in the North Pacific Ocean: Insights from data and models. Global Biogeochem. Cycles 23, GB2010.

Wood, J.M., Kennedy, F.S., Rosen, C.G. 1968. Synthesis of methyl-mercury compounds by extracts of a methanogenic bacterium. Nature. 220, 174–174.

Table 5.1. Mean (± SD) concentrations (pM) of filtered HgT, MMHg, and DMHg in thermocline waters of the North Atlantic (100–1000 m), and equatorial South Pacific (100–700 m) Oceans at upwelling (Stations 1–9) and non-upwelling (Stations 10–36) locations. The number of measured concentrations is in parentheses.

Region	HgT	MMHg	DMHg
Atlantic	0.9 ± 0.3 (296)	0.11 ± 0.10 (189)	0.09 ± 0.11 (207)
Pacific upwelling (St.1–9)	1.0 ± 0.4 (69)	0.09 ± 0.06 (67)	0.09 ± 0.07 (70)
Pacific non-upwelling (St.10–36)	0.5 ± 0.3 (190)	0.06 ± 0.06 (118)	0.04 ± 0.07 (156)

Table 5.2. Mean (± SD) concentrations (pM) of filtered MMHg and DMHg in deep water masses of the North Atlantic (North Atlantic Deep Water, NADW; Antarctic Bottom Water, AABW), and equatorial South Pacific Oceans (Lower Circumpolar Deep Water, LCDW; Pacific Deep Water, PDW; Modified Pacific Deep Water, PDW_M). The number of measured concentrations is in parentheses. The Mann-Whitney Rank Sum test was used to compare concentrations of MMHg and DMHg in each water mass.

Water mass	MMHg	DMHg	MMHg:DMHg	MMHg vs. DMHg (*p*-value)
NADW	0.087 ± 0.096 (94)	0.14 ± 0.11 (88)	1.3 ± 1.4 (47)	<0.001
AABW	0.13 ± 0.10 (14)	0.16 ± 0.11 (20)	0.85 ± 0.90 (10)	0.3
LCDW	0.012 ± 0.0075 (7)	0.017 ± 0.011 (8)	1.3 ± 1.2 (7)	0.3
PDW	0.049 ± 0.055 (114)	0.074 ± 0.068 (208)	1.2 ± 1.4 (100)	<0.001
PDW_M	0.089 ± 0.057 (49)	0.12 ± 0.068 (56)	0.93 ± 1.0 (36)	<0.001

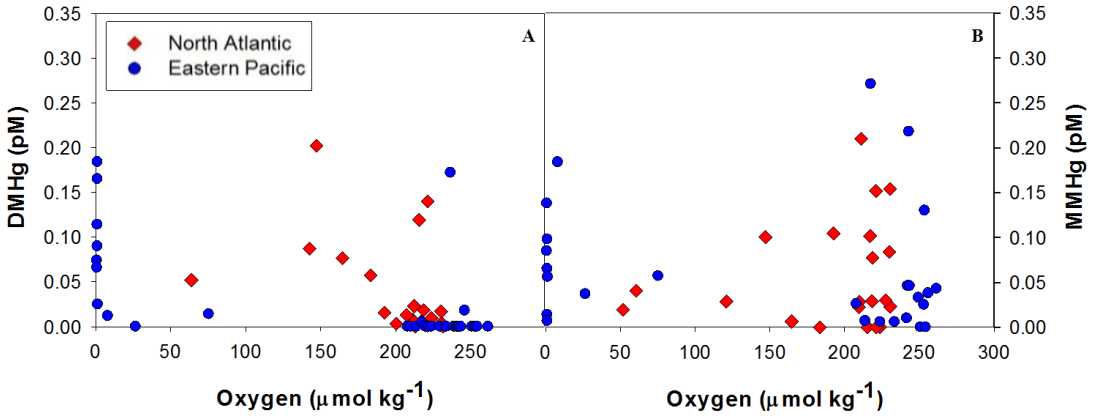

Figure 5.1. DMHg (panel A) and MMHg (panel B) maxima are found in oxygenated and low-oxgyen waters at depths near the subsurface cholorophyll maximum (70–100 m). Red diamonds are data from the North Atlantic Zonal Transect (North Atlantic) and blue circles are data from the Eastern Pacific Zonal Transect (Eastern Pacific).

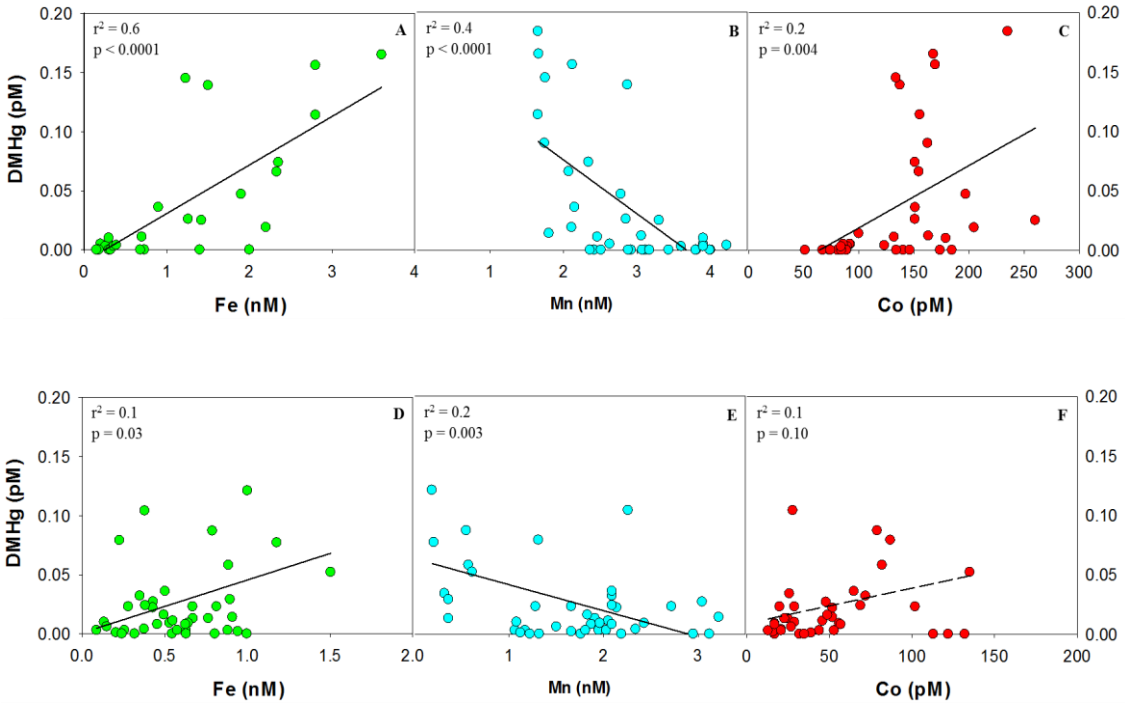

Figure 5.2. Correlations between DMHg and filtered Fe, Mn, and Co in the upper water column (< 100 m depth) in the Pacific upwelling region (panels A–C) and North Atlantic Ocean (panels D–F). Unpublished Fe, Mn, and Co data was obtained with permission from the National Science Foundation Biological & Chemical Oceanography Data Management Office (www.bco-dmo.org).

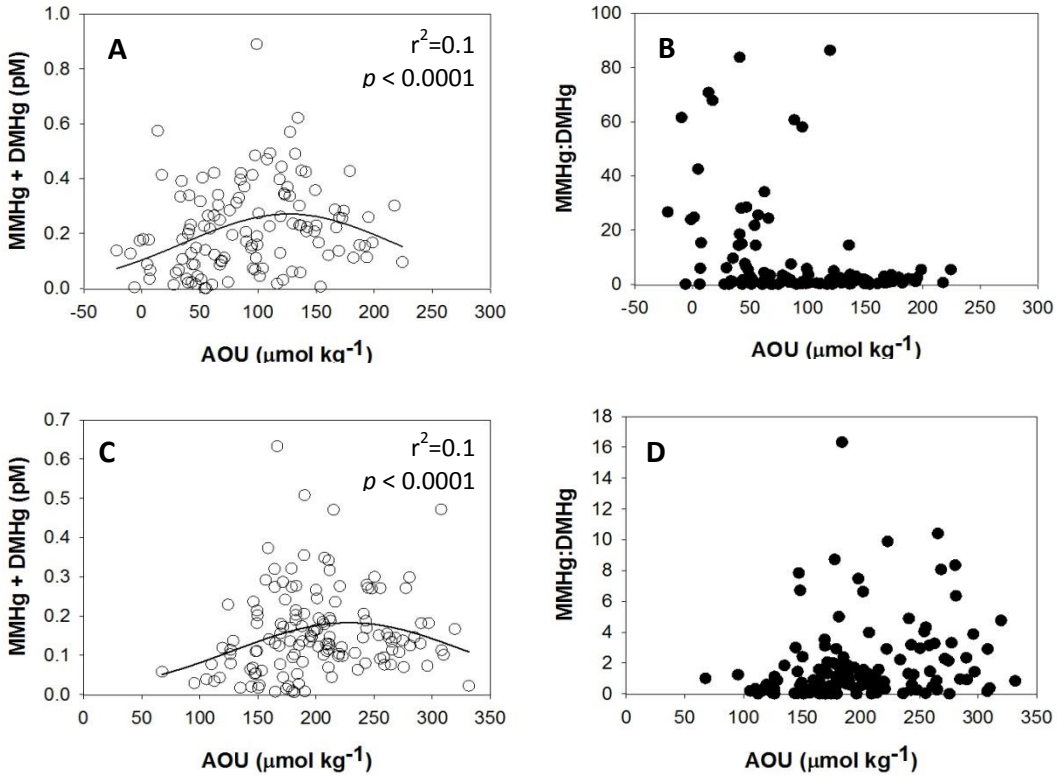

Figure 5.3. Total methylated Hg (MMHg + DMHg) was correlated with AOU in the thermocline of the North Atlantic (panel A; 100–1000 m) and eastern Pacific Oceans (panel C; 100–700 m). The MMHg:DMHg molar ratios in the thermocline of the Atlantic (panel B) and Pacific Oceans (panel D).

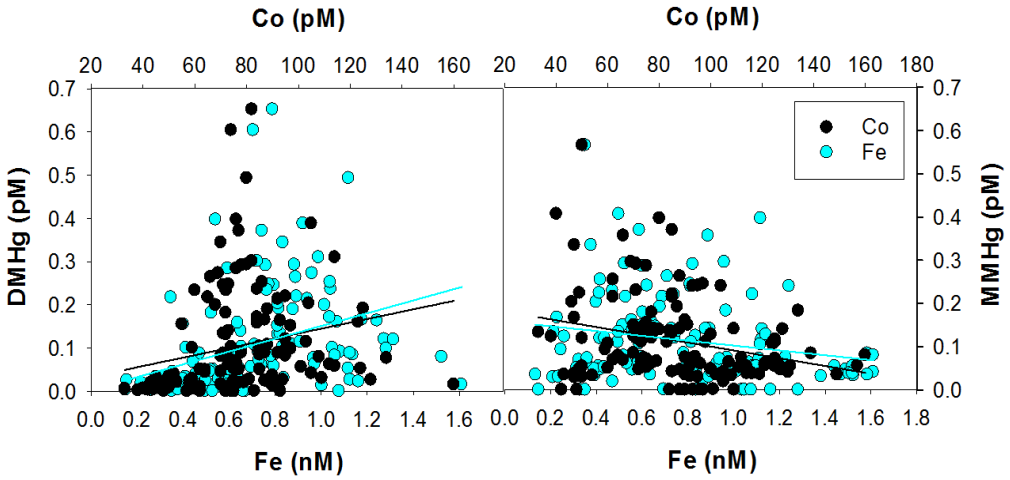

Figure 5.4. Dimethylmercury (panel A) was postively correlated with filtered Co (r^2 = 0.05, p = 0.009) and Fe (r^2 = 0.1, p < 0.0001) in Atlantic thermocline waters (100–1000 m). Methylmercury (panel B) was inversely related to filtered Co (r^2 = 0.1, p < 0.0001) and Fe (r^2 = 0.04, p = 0.02).

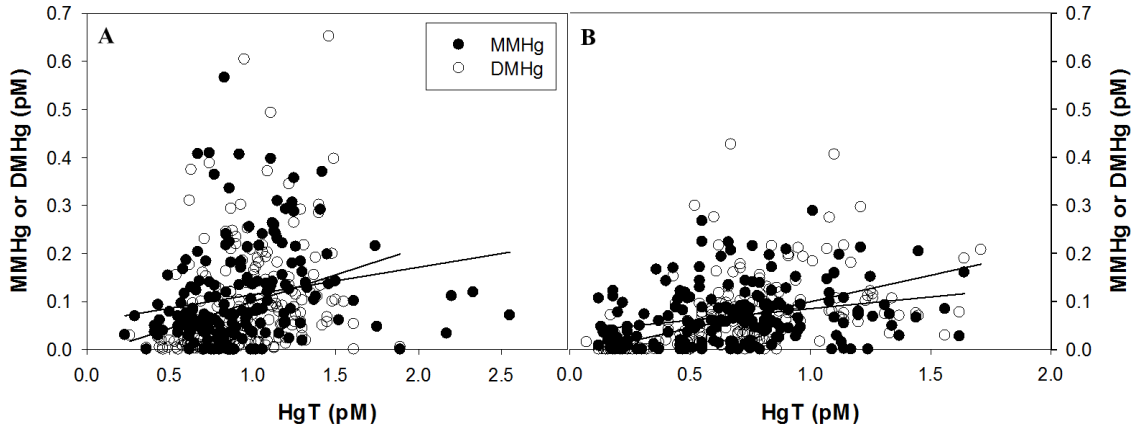

Figure 5.5. MMHg and DMHg were positively correlated with total Hg in thermocline waters of the North Atlantic (panel A, 100–1000 m) and equatorial South Pacific Oceans (panel B, 100–700 m). Linear regression statistics: Atlantic ($r^2 = 0.04$, $p = 0.006$), Atlantic ($r^2 = 0.1$, $p < 0.0001$), Pacific MMHg ($r^2 = 0.1$, $p = 0.0002$), Pacific DMHg ($r^2 = 0.3$, $p < 0.0001$). Linear regression slopes were similar for MMHg (0.06 ± 0.02 Atlantic, 0.05 ± 0.01 Pacific) and DMHg (0.1 ± 0.03 Atlantic, 0.1 ± 0.1 Pacific). for both Atlantic and Pacific).

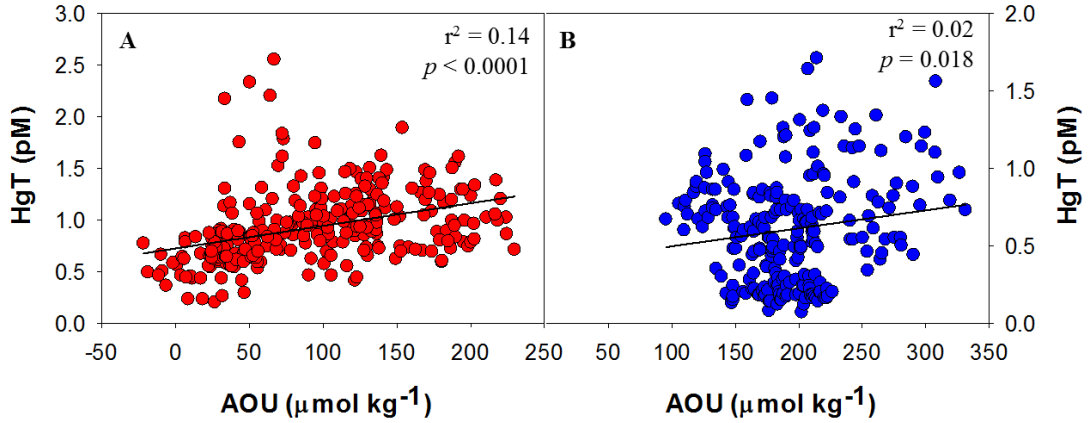

Figure 5.6. Total Hg was positively correlated with AOU in the thermocline of the North Atlantic (panel A; 100–1000 m) and eastern Pacific Oceans (panel B; 100–700 m).

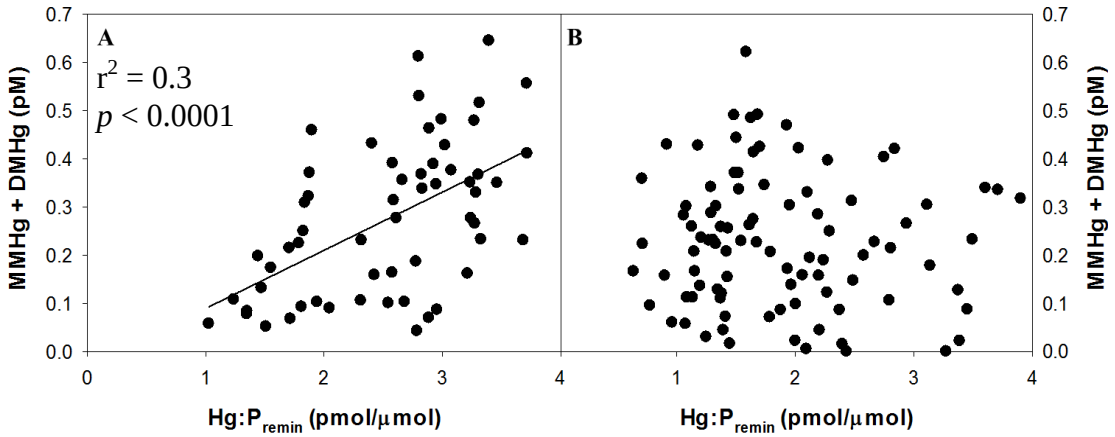

Figure 5.7. Total methylated Hg (MMHg + DMHg) concentrations increase with the Hg:P_{remin} ratio in deep waters (>1500 m) of the North Atlantic (NADW and AABW, panel A). Results from Station 16 were not included because of external inputs from the TAG hydrothermal vent field. There is no significant correlation between methyatled Hg and Hg:P_{remin} (p = 0.2) in Atlantic thermocline waters (panel B; 100–1000 m).

Appendix A. Storage bottle material and cleaning for determination of total mercury in seawater

Hammerschmidt, C.R., Bowman, K.L., Tabatchnick, M.D., Lamborg, C.H. 2011. Storage bottle material and cleaning for determination of total mercury in seawater. Limnol. Oceanogr.-Methods 9, 426–431.

Abstract

Accurate determinations of trace levels of mercury (Hg) in water require scrupulously clean sampling equipment and storage bottles. To avoid Hg contamination during storage, it has been presumed that water samples must be stored in either glass or Teflon® bottles cleaned with a rigorous method, such as submersion in hot acid. These cleaning procedures are hazardous, and use of Teflon® bottles can be cost prohibitive for major oceanographic programs. We investigated the suitability of alternative cleaning procedures and bottle materials for storage of seawater containing sub-picomolar levels of Hg. We found that a simple technique with detergent, dilute acid, and bromine monochloride removes Hg from all bottle materials tested, which included FEP Teflon®, glass, polycarbonate (PC), low-density polyethylene (LDPE), and fluorinated polyethylene (FLPE). The technique is effective for bottles that are either new or used previously for trace-level oceanographic samples (total Hg < 10 pM). Stability of seawater Hg levels differed dramatically among storage bottle materials during a 74-week test. Hg in seawater stored in LDPE, FLPE, and FEP bottles increased within 15 weeks of storage at room temperature. In contrast, Hg levels in seawater stored in PC bottles were increased modestly only after 74 weeks of storage and those in glass bottles were unchanged throughout the test. We recommend future use of this new cleaning method and encourage greater utilization of glass and PC bottles for storage of waters containing low levels of Hg.

Introduction

Accurate determinations of trace metals in seawater require sensitive instrumentation, a clean analytical environment, and scrupulously clean sampling equipment and storage bottles (Patterson and Settle, 1976; Gill and Fitzgerald, 1985). Techniques for quantification of total mercury (Hg) in seawater are mature and well refined, including determination by cold-vapor atomic fluorescence spectrometry (CVAFS; Bloom and Fitzgerald, 1988) and inductively coupled plasma mass spectrometry (Haraldsson et al., 1989), and trace-metal clean techniques that ensure sample integrity during collection and processing have been known for decades (Gill and Fitzgerald, 1985). To avoid Hg contamination during storage, it has been presumed that water samples must be stored in either glass or Teflon® bottles cleaned with a rigorous method, such as submersion in hot acid (U.S. EPA, 2002). Although this cleaning method and bottle materials are known to be effective for long-term archival of waters having relatively high levels of total Hg (> 5 pM; Parker and Bloom, 2005), they are unproven for oligotrophic seawater, which contains commonly 0.2–2 pM total Hg (Fitzgerald et al., 2007). Moreover, bottles made of Teflon, typically fluorinated ethylene propylene (FEP), are about 10−100× more expensive than those made of other hydrocarbon polymers or glass, and such cleaning procedures are hazardous and limited by the number of bottles that can be cleaned simultaneously. These constraints are not conducive for large-scale oceanographic research programs, such as GEOTRACES, in which hundreds of water samples will be collected during each expedition and may be stored for an extended period prior to analysis.

Here, we examine two basic questions about bottles used to store seawater for Hg analysis: 1) By what alternative methods to hot acid, if any, can bottles made of FEP and other materials be cleaned so that they will not contaminate seawater with Hg? 2) Are Hg concentrations in seawater stable (i.e., no increase or decrease) during prolonged storage periods in FEP and other bottle materials? These questions were investigated during a 17-month laboratory test of bottle cleanliness and Hg stability in stored seawater. We found that a simple cleaning technique with detergent, dilute acid, and bromine monochloride (BrCl) removes Hg quantitatively from all bottle materials tested, which included FEP, borosilicate glass, polycarbonate (PC), low-density polyethylene (LDPE), and fluorinated high-density polyethylene (FLPE)—bottle materials used commonly for sampling trace metals in water. Moreover, and surprisingly, we found the stability of seawater Hg in FEP bottles to be inferior to that stored in either glass or PC vessels: Hg concentrations increased significantly in seawater stored at room temperature in FEP, LDPE, and FLPE during a 17-month storage period. Hence, the use of bottles made of either glass or PC is advised for storage of trace-level water samples intended for Hg determination.

Materials and procedures

Cleaning new bottles—A 4 × 5 factorial design was used to investigate the efficacy of four common cleaning methods for removing Hg from sample bottles made from five different materials. The four cleaning methods ranged from a presumably comprehensive approach for removing metals and organics (Method A) to a simple cleaning with 10% HCl (Method D). We tested the four following bottle cleaning methods:

Method A: 1) Wash bottle interior with Citranox® detergent and reagent-grade water (RGW, resistivity > 18 MΩ-cm) and rinse with hot tap water followed by 3× rinse with RGW, 2) fill with 1 N KOH (ACS grade) for 24 h followed by 3× rinse with RGW, 3) fill with 4 M HNO_3 (ACS grade) for 24 h followed by 3× rinse with RGW, and 4) fill with 0.6 M HCl (ACS grade) for 24 h followed by 5× rinse with RGW.

Method B: 1) Rinse bottle 2× with RGW, fill with Citranox®/RGW solution for 6 d, and rinse with RGW, 2) fill with 1.2 M HCl (Instra-analyzed, J.T. Baker) for 6 d and rinse 5× with RGW, 3) fill with 0.5% BrCl solution (Bloom and Crecelius, 1983) for 1 d followed by 3× rinse with 0.01 M HCl (Instra-analyzed) and 5× rinse with RGW.

Method C: Same as Method B only that the 1.2 M HCl treatment is followed by a 3× rinse with 0.01 M HCl and 5× rinse with RGW (i.e., no BrCl treatment).

Method D: Wash bottle interior with Citranox® detergent and hot tap water followed by 3× rinse with RGW, and 2) fill with 1.2 M HCl (ACS grade) for 24 h followed by 5× rinse with RGW.

Bottle cleaning was conducted inside a Class 100 clean room by personnel using "clean hands/dirty hands" techniques (U.S. EPA, 2002). Clean bottles were stored empty, with caps on, and double bagged in new zip-type polyethylene bags (2 mil).

The efficacy of each cleaning method was tested with new 250-mL bottles made of FEP (Nalgene, ethylene tetrafluoroethylene caps), borosilicate glass (Fisherbrand, polytetrafluoroethylene-lined polyethylene caps), PC (Nalgene, polypropylene cap), FLPE (Nalgene, fluorinated polypropylene cap), and LDPE (Nalgene, polypropylene cap). Three bottles made of each material were cleaned with each of the four methods described above. Afterward, the cleanliness of bottles was investigated by filling them

with 0.2 L of 0.1-µm filtered RGW, containing 0.10 ± 0.03 pM total Hg, to which was added 0.2 mL of BrCl (0.1% of sample volume). BrCl solution is acidic and a strong oxidant, and Hg has a relatively strong affinity for halide ligands. The Hg content of RGW in each bottle was measured after about 18 h of storage inside a HEPA-filtered laminar flow hood in a Class 100 clean room. Contamination from interior bottle surfaces was evaluated as the difference in total Hg concentration between direct analysis of RGW from the purifier and that from sample bottles, with reagent contributions monitored carefully and subtracted from both types of waters.

Storage—The stability of Hg in seawater stored at either room temperature or frozen was examined for each of the bottle materials tested above. Both freezer and room temperature storage conditions were tested because it is unknown whether Hg concentrations may be more stable in frozen seawater. Results from the cleaning methods component of this study (discussed below) indicated that Method B was the most efficacious for removing Hg from each of the bottle materials tested. Hence, new 250-mL bottles made of glass, FEP, PC, LDPE, and FLPE were cleaned with Method B and filled with 0.2 L of filtered (0.2 µm) seawater from the northwest Atlantic Ocean (38° 43' N, 70 °W, 10-m depth, salinity = 33.27, dissolved organic carbon = 70 µM) that had an initial Hg level of 0.91 ± 0.05 pM (n = 12). This concentration is within the range of those measured commonly in open-ocean waters (i.e., ~ 0.2−2 pM; Fitzgerald et al., 2007). Samples were acidified to 0.1% with high-purity HCl (Instra-analyzed), containing a relatively low level of Hg (measured, 10 pM in concentrated acid), and bottle caps were tightened by hand. All bottles were double bagged in new zip-type polyethylene bags (2 mil). Half of the bottles made of each plastic were stored in a

conventional freezer (≤ −20 °C) and the other half at room temperature in a darkened cabinet outside of the clean laboratory (~20 °C). Samples in glass bottles were stored only in the room-temperature cabinet. A potential source of Hg concentration instability in stored seawater is diffusion of Hg^0 through bottle materials (Bothner and Robertson, 1975; Parker and Bloom, 2005). Hg^0 in air of the room-temperature cabinet (Fitzgerald and Gill, 1979), measured 3× over a 24-h period, averaged 26 ± 17 ng m^{-3}, which is typical for indoor air (Carpi & Chen, 2001). Hg^0 was not determined inside the freezer, although it is presumed to be low given the temperature dependence of Hg volatility (Huber et al., 2006) and that the freezer was new and had not contained Hg-enriched materials. Seawater in each of the five bottle types was measured for total Hg after 1, 3, 15, 32, and 74 weeks of storage.

Hg analysis—Total Hg was measured by dual Au amalgamation CVAFS (Fitzgerald and Gill, 1979; Bloom and Fitzgerald, 1988). Water samples (0.2 L) were digested with 0.2 mL BrCl solution for 12−18 h and pre-reduced with 0.1 mL of 12% (wt:vol) NH_2OH prior to transferring to a 400-mL gas-liquid separator. Sample Hg^{2+} was reduced to Hg^0 in the gas-liquid separator with 0.1 mL of 50% (wt:vol) $SnCl_2$ and purged from solution with Hg-free N_2. Analyses of total Hg were calibrated versus Hg^0 taken from the headspace over pure liquid (Gill and Fitzgerald, 1987) and verified by comparison to determinations of Hg^{2+} from a solution traceable to the U.S. National Institute of Standards and Technology. Recovery of 100 pg Hg^{2+} additions to seawater (about 2.5 pM) averaged 100 ± 7% (± 1 SD, n = 28).

Assessment and discussion

Cleaning new bottles—The efficacy of tested cleaning methods for removing Hg varied among bottle materials (Figure 1). Each of the four methods resulted in little or no residual Hg in bottles made of either glass or PC. Method A, the seemingly most rigorous of the four, removed Hg from all bottle interiors except those made of FEP, which suggests that FEP was the dirtiest of the four tested polymers. In contrast to Method A, Hg was removed from FEP bottles by each of the three other methods. Methods C and D, while effective for glass, FEP, and PC, did not remove Hg completely from the two types of polyethylene bottles.

Method B cleaned Hg from each of the five bottle materials tested (Figure 1). It appears that BrCl is a key agent for effective cleaning of bottles used for trace-level Hg determination. The only difference between Methods B and C was that Method B included a final treatment with 0.5% BrCl. Use of BrCl had no effect on the cleanliness of glass, FEP, and PC bottles, but it made a substantial difference on removal of Hg from LDPE and FLPE bottles. Our laboratories have found that sample oxidation with 0.1−0.2% BrCl, in the original sample bottle, is sufficient to liberate Hg quantitatively in seawater containing relatively low levels of dissolved organic carbon (DOC, < 100 µM C). Cleaning sample bottles with either an equal or greater concentration of BrCl should remove any contaminant Hg that might be mobilized from the material during sample oxidation with BrCl. The relative ease and safety of this bottle cleaning procedure, compared to treatment with hot acids, as prescribed by the U.S. Environmental Protection Agency Method 1631 (U.S. EPA, 2002), lends itself favorably as an alternative for routine laboratory use.

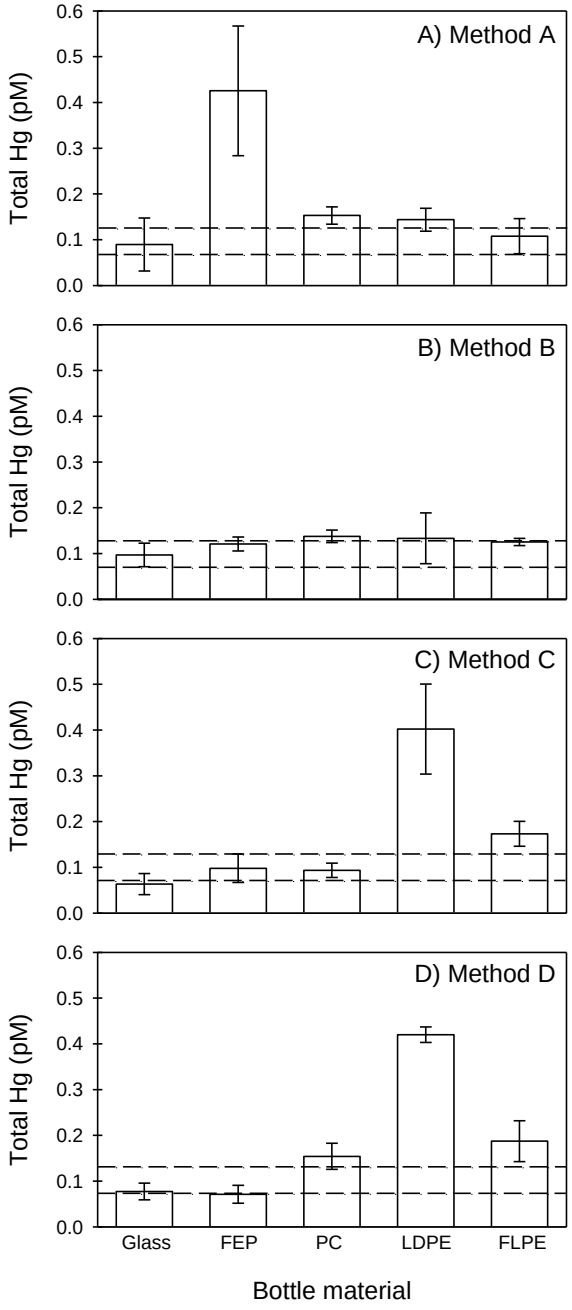

Fig. 1. Total Hg in reagent-grade water after 18 h of storage with 0.1% BrCl in bottles made of borosilicate glass, fluorinated ethylene propylene (FEP), polycarbonate (PC), low-density polyethylene (LDPE), and fluorinated high-density polyethylene (FLPE) cleaned with four different methods (A–D). Three bottles were tested for each bottle material type and cleaning method; error bars are one standard deviation of the mean. Dashed lines delineate the range of total Hg in reagent-grade water only.

Cleaning contaminated bottles—The efficacy of cleaning Method B also was tested with previously used bottles. Our initial test examined only new bottles that had not been subject to potential contamination with Hg and ligands from prior use. Natural organic matter, for example, can adsorb to bottle surfaces, complex sample Hg, and thereby potentially bias measured Hg levels (Parker and Bloom, 2005). An important and useful question is whether previously used bottles, especially those that have contained water with high levels of Hg and organic matter, can be cleaned again for re-use without predisposing an artifact to the next sample. The effectiveness of Method B was tested by filling bottles made of glass, FEP, PC, LDPE, and FLPE with filtered (0.2 µM) seawater from Vineyard Sound, Massachusetts (DOC = 210 µM) that was amended with Hg to about 10 pM, a concentration substantially greater than that of total Hg in open-ocean seawater (Fitzgerald et al., 2007). To intentionally dope bottle interiors with Hg and natural ligands, the samples were allowed to stand for two weeks (unacidified, room temperature) before water was discarded and bottles cleaned again with Method B. After cleaning, and similar to our test with new bottles, bottles were filled with 0.2 L of RGW, oxidized with 0.1% BrCl, and total Hg was measured in the water. No contaminant Hg was detected in the RGW. Total Hg (pM, ± 1 SD) averaged 0.10 ± 0.04 in FEP, 0.06 ± 0.03 in glass, 0.11 ± 0.02 in PC, 0.11 ± 0.06 in LDPE, and 0.08 ± 0.02 in FLPE, levels that were similar to those in RGW only (0.10 ± 0.03 pM).

Fresh and estuarine waters often contain Hg and DOC at levels far greater than those in open-ocean seawater (Fitzgerald and Lamborg, 2003). Moreover, our experience is that the same sample bottles used for freshwater or near-shore research are often re-used during oceanographic expeditions. Accordingly, we were interested in knowing

whether sample bottles exposed to highly contaminated freshwater could be cleaned sufficiently by Method B for oceanographic studies. This was tested by filling clean bottles made of glass, FEP, PC, LDPE, and FLPE with filtered (0.2 μm) water from the Little Miami River, Ohio, (pH = 8.3; DOC = 500 μM) that was amended with Hg^{2+} (as $HgCl_2$) to 100 pM. The Hg content of this water is about 100× greater than open-ocean waters, but within the range of some contaminated estuaries (Fitzgerald and Lamborg, 2003) and streams (e.g., Hurley et al., 1995). Bottles were left undisturbed and unacidified for two weeks at room temperature before solutions were discarded and bottles cleaned with Method B. After cleaning, bottles were filled with 0.2 L of RGW, water oxidized with 0.1% BrCl, and total Hg determined.

In contrast to the test with Hg-amended Vineyard Sound water, contaminant Hg was evident in RGW from all bottle materials except glass, which had a Hg content (0.15 ± 0.07 pM) that was not significantly different from direct analysis of RGW (0.10 ± 0.03 pM). Hg concentrations (pM, ± 1 SD) were substantially greater in RGW from bottles made of other materials: 0.51 ± 0.45 in FEP, 0.52 ± 0.12 in PC, 1.85 ± 0.37 in LDPE, and 0.60 ± 0.31 in FLPE. While contamination was evident, the fraction of Hg from the original sample (100 pM) that carried over and was detected in the RGW was small (0.4−1.8%) and would be neither of concern nor discernable if waters having comparable Hg levels were sampled subsequently. However, this finding indicates that Method B should not be used for routine cleaning of bottles re-used for sampling of both highly contaminated and open-ocean waters. Our laboratories clean all sample bottles with Method B but keep oceanographic bottles segregated from others.

Storage—The stability of Hg in seawater stored at room temperature differs dramatically among storage bottle materials (Table 1). Under the conditions of our study, Hg concentrations in seawater were very stable in glass and PC bottle: Levels in bottles made of either material were unchanged during the 74-week storage period with the exception of a modest increase in PC bottles at the end of the test. LDPE proved to be an inferior bottle material for storage of seawater for Hg determination; levels increased 5-fold during the initial week of storage, which is consistent with results of prior studies (Bothner and Robertson, 1975; Parker and Bloom, 2005). Mean concentrations of total Hg in seawater increased as a function of storage time in FEP ($r^2 = 0.81$, $p = 0.01$) and FLPE ($r^2 = 0.99$, $p < 0.01$), and levels were significantly greater than the original water (i.e., 0.91 ± 0.05 pM) within 15 and 3 weeks of storage, respectively. Fitzgerald and Lyons (1975) also found Hg to be stable in seawater stored in FEP bottles up to eight weeks, the maximum extent of their test. Hence, FEP and FLPE may be suitable for relatively short-term, but not prolonged, storage of seawater containing low-pM levels of Hg. The finding that aqueous Hg levels are not stable in FEP over prolonged storage is in contrast to results published previously (Parker and Bloom, 2005), although the prior study examined waters having substantially greater initial concentrations of Hg (5–15 pM).

Freezer storage minimizes Hg contamination of seawater stored in plastic bottles (Table 2). Freezer storage resulted in no discernable level of Hg contamination of seawater in FEP bottles, in contrast to those stored at room temperature (Table 1). Frozen storage of seawater in LDPE and FLPE bottles reduced the magnitude of contamination compared to room-temperature storage; however, Hg levels were

Table 1. Total Hg (± 1 SD) in acidified (0.1% HCl), 0.2-µm filtered seawater stored at room temperature in bottles made of borosilicate glass, fluorinated ethylene propylene (FEP), polycarbonate (PC), low-density polyethylene (LDPE), and fluorinated high-density polyethylene (FLPE, n = 3 each). Mean initial Hg concentration in the seawater was 0.91 ± 0.05 pM.

	Total Hg (pM)				
Time (weeks)	Glass	FEP	PC	LDPE	FLPE
0	0.89 ± 0.07	0.86 ± 0.04	0.93 ± 0.05	0.85 ± 0.03	0.89 ± 0.01
1	0.88 ± 0.02	0.93 ± 0.01	0.98 ± 0.09	4.26 ± 0.35	0.94 ± 0.05
3	0.88 ± 0.02	0.95 ± 0.06	0.89 ± 0.01	5.11 ± 1.62	1.28 ± 0.12
15	0.93 ± 0.09	1.27 ± 0.07	1.01 ± 0.07	45.6 ± 12.1	3.62 ± 1.08
32	0.85 ± 0.06	1.96 ± 0.65	0.93 ± 0.13	6.18 ± 1.76	4.54 ± 0.17
74	0.90 ± 0.09	2.01 ± 0.87	1.21 ± 0.12	15.4 ± 4.72	10.5 ± 1.45

Table 2. Total Hg (± 1 SD) in acidified (0.1% HCl), 0.2-µm filtered seawater stored frozen in bottles made of fluorinated ethylene propylene (FEP), polycarbonate (PC), low-density polyethylene (LDPE), and fluorinated high-density polyethylene (FLPE, *n* = 3 each). Mean initial Hg concentration in the seawater was 0.91 ± 0.05 pM.

	Total Hg (pM)			
Time (weeks)	FEP	PC	LDPE	FLPE
0	0.84 ± 0.01	0.92 ± 0.07	0.85 ± 0.03	0.85 ± 0.03
1	0.91 ± 0.05	0.93 ± 0.02	2.22 ± 0.21	0.90 ± 0.06
3	0.88 ± 0.09	0.87 ± 0.01	2.23 ± 1.35	1.00 ± 0.03
15	1.11 ± 0.09	0.89 ± 0.03	1.26 ± 0.13	2.63 ± 1.15
32	1.04 ± 0.18	1.07 ± 0.11	0.87 ± 0.03	3.12 ± 1.24
74	1.16 ± 0.25	1.26 ± 0.12	1.29 ± 0.10	4.00 ± 2.28

increased substantially compared to the initial concentration and often with relatively high degrees of variability among replicate bottles (Table 2). Hence, freezer storage minimizes Hg contamination of seawater stored in FEP bottles but it does not completely ameliorate problems associated polyethylene bottles. Seawater Hg levels in PC bottles were uncompromised for at least eight months, whether stored frozen or at room temperature.

In none of our tests with acidified seawater (0.1% HCl) were there detectable losses of Hg during storage at either room temperature or –20 °C (Tables 1 and 2). Measured Hg levels after storage were either similar to or greater than the initial concentration. This indicates that significant losses of Hg did not occur as a result of either adsorption of ionic species to bottle walls or diffusion of dissolved Hg^0 from water through the bottle material. In contrast, many seawater samples, particularly those stored in FEP, LDPE, and FLPE bottles, experienced a significant increase of Hg during the storage test. We speculate that the source of Hg contamination is diffusion of Hg^0 through bottle materials with subsequent oxidation and accumulation as Hg^{2+} in the acidified solution (Parker and Bloom, 2005). This hypothesis is consistent with the temperature dependence of Hg diffusivity and volatility (Huber et al., 2006) and that, for a particular bottle material, seawater stored at −20 °C had less Hg contamination than those stored at ~20 °C.

Comments and recommendations

As an alternative to submersion in hot acid, we found that a relatively simple method employing detergent and dilute HCl and BrCl effectively cleaned Hg from the

five bottle materials tested. Our two laboratories have cleaned bottles with this method (Method B) for more than two years and it was used to prepare bottles for the U.S. GEOTRACES Intercalibration for Hg. We recommend its use for investigations in both freshwater and marine systems, but caution against interchangeable use of bottles between systems with relatively high and low Hg levels; 1% carryover of Hg from contaminated freshwater can result in significant bias to pristine open-ocean samples. We also have found that repeated BrCl cleaning of bottles made of PC, unlike FEP and glass, results in a gradual yellowing of the polymer, although we have not detected any functional deficiencies related to sample storage for total Hg analysis.

The superb, long-term stability of Hg in glass bottles was expected, and so was the poor stability in bottles made of LDPE. However, seawater stored in FEP and PC bottles provided surprises. Of the four hydrocarbon polymers tested, PC was the only bottle material in which seawater Hg levels were not compromised during a storage period of ≥ 8 months. To our knowledge, PC bottles are not used commonly by aquatic Hg researchers, who (we included) often use FEP bottles when a plastic is preferred to glass, such as in a shipboard laboratory. The strong bias toward Teflon® likely extends from past practice, a U.S. EPA method indicating its suitability (U.S. EPA, 2002), and from Teflon® polymers being amenable to repeated submersion in hot acid for cleaning. However, we have presented a new method for bottle cleaning that does not require hot acid. In contrast to PC, acidified seawater stored in FEP bottles at room temperature showed significant contamination after storage for 15 weeks. Such contamination calls into question the accuracy of seawater Hg determinations made on samples stored in FEP bottles for extended periods under conditions similar to those used in this test. While

glass bottles are superior, we encourage greater use of PC bottles for Hg sampling because they cost about 10-fold less than those made of FEP and are better than Teflon® in maintaining the integrity of low-Hg seawater during prolonged storage.

Acknowledgment

We thank the captain and crew of the R/V *Endeavor* (EN-452) for help with seawater collection. Jaclyn Klaus and Deepthi Nalluri assisted with bottle cleaning. This research was supported by the U.S. National Science Foundation (OCE-0825108).

References

Bloom, N. S., and E. A. Crecelius. 1983. Determination of mercury in seawater at sub-nanogram per liter levels. Mar. Chem. 14:49−59 [doi: 10.1016/0304-4203(83)90069-5].

Bloom, N. S., and W. F. Fitzgerald. 1988. Determination of volatile mercury species at the picogram level by low-temperature gas chromatography with cold-vapor atomic fluorescence detection. Anal. Chim. Acta. 208:151−161 [doi: 10.1016/S0003-2670(00)80743-6].

Bothner, M. H., and D. E. Robertson. 1975. Mercury contamination of sea water samples stored in polyethylene containers. Anal. Chem. 47:592–595 [doi: 10.1021/ac60353a012].

Carpi, A., and Y.-F. Chen. 2001. Gaseous elemental mercury as an indoor air pollutant. Environ. Sci. Technol. 35:4170−4173 [doi: 10.1021/es010749p].

Fitzgerald, W. F., and W. B. Lyons. 1975. Mercury concentrations in open-ocean waters: sampling procedure. Limnol. Oceanogr. 20:468−471.

Fitzgerald, W. F., and G. A. Gill. 1979. Subnanogram determination of mercury by two-stage gold amalgamation applied to atmospheric analysis. Anal. Chem. 51:1714−1720 [doi: 10.1021/ac50047a030].

Fitzgerald, W. F., and C. H. Lamborg. 2003. Geochemistry of mercury in the environment, p. 107–148. *In* B. Sherwood-Lollar [ed.], Treatise on geochemistry. Elsevier.

Fitzgerald, W. F., C. H. Lamborg, and C. R. Hammerschmidt. 2007. Marine

biogeochemical cycling of mercury. Chem. Rev. 107:641–662 [doi: 10.1021/cr050353m].

Gill, G. A., and W. F. Fitzgerald. 1985. Mercury sampling of open ocean waters at the picomolar level. Deep Sea Res. A 32:287–297 [doi: 10.1016/0198-0149(85)90080-9].

Gill, G. A., and W. F. Fitzgerald. 1987. Picomolar mercury measurements in seawater and other materials using stannous chloride and two-stage amalgamation with gas phase detection. Mar. Chem. 20:227–243 [doi: 10.1016/0304-4203(87)90074-0].

Haraldsson, C., S. Westerlund, and P. Ohman. 1989. Determination of mercury in natural samples at the sub-nanogram level using inductively coupled plasma mass spectrometry after reduction to elemental mercury. Anal. Chim. Acta 221:77−84 [doi: 10.1016/S0003-2670(00)81940-6].

Huber, M. L., A. Laesecke, and D. G. Friend. 2006. Correlation for the vapour pressure of mercury. Ind. Eng. Chem. Res. 45:7351−7361 [doi: 10.1021/ie060560s].

Hurley, J. P., J. M. Benoit, C. L. Babiarz, M. M. Shafer, A. W. Andren, J. R. Sullivan, R. Hammond, and D. A. Webb. 1995. Influences of watershed characteristics on mercury levels in Wisconsin rivers. Environ. Sci. Technol. 29:1867−1875 [doi: 10.1021/es00007a026].

Parker, J. L., and N. S. Bloom. 2005. Preservation and storage techniques for low-level aqueous mercury speciation. Sci. Tot. Environ. 337:253–263 [doi: 10.1016/j.scitotenv.2004.07.006].

Patterson, C. C., and D. M. Settle. 1976. The reduction of orders of magnitude errors in lead analyses of biological material and natural waters by evaluating and controlling the extent and sources of industrial lead contamination introduced during sample collection, handling and analysis. *In* P. D. LaFleur [ed.] Accuracy in trace analysis: sampling, sample handling, and analysis. U.S. National Bureau of Standards Special Publication 422, Washington, D.C.

U.S. Environmental Protection Agency. 2002. Method 1631, revision E: Mercury in water by oxidation, purge and trap, and cold vapor atomic fluorescence spectrometry. EPA-821-R-02-019. U.S. Environmental Protection Agency, Office of Water, Washington, DC.

Appendix B. Vertical methylmercury distribution in the subtropical North Pacific Ocean

Hammerschmidt, C.R., Bowman, K.L. 2012. Vertical methylmercury distribution in the subtropical North Pacific Ocean. Mar. Chem. 132–133, 77–82.

Abstract

Humans are exposed to toxic and bioaccumulative monomethylmercury (MMHg) principally by consuming seafood. However, knowledge of the sources of MMHg to surface-dwelling marine organisms has been hampered by a paucity of information on its vertical distribution in the open ocean. Here, we report the first complete high-resolution profile of MMHg, from sea surface to bottom water, in the Pacific Ocean. Filtered water and suspended particles were sampled at the SAFe station (140 °W, 30 °N) during the U.S. GEOTRACES Intercalibration. Distributions of MMHg and dimethylmercury suggest that both are synthesized in low-oxygen and oxic strata of the water column and that deep-sea sediments are not an important source. Scaling estimates imply that a majority of MMHg in phytoplankton and, by extension, the pelagic food web at this location results from production in the mixed layer, which is impacted by anthropogenic mercury inputs and thus may be affected by future changes in emissions to the atmosphere.

1. Introduction

A principal concern with mercury (Hg) in the environment is human exposure to toxic monomethylmercury (MMHg) by consumption of fish (Mergler et al., 2007). Most of the fish eaten by humans are of marine origin (U.S. EPA, 2002; Sunderland, 2007). Major sources of MMHg in the ocean and, by extension, seafood have been suggested to include production in sediments on the continental margin (Hammerschmidt and Fitzgerald, 2006a), deep-sea deposits and hydrothermal vents (Kraepiel et al., 2003; Lamborg et al., 2006), and formation in oxic and low-oxygen regions of the water column, presumably through heterotrophic microbial activity (Mason and Fitzgerald, 1993; Monperrus et al., 2007; Cossa et al., 2009, 2011; Sunderland et al., 2009; Heimbürger et al, 2010; Lehnherr et al., 2011). However, knowledge of the sources of MMHg to surface-dwelling marine organisms, including many fishes consumed by humans, has been hampered by a paucity of information on its vertical distribution in the open ocean (Fitzgerald et al., 2007).

To better understand the biogeochemistry and sources of MMHg in the ocean, we determined the vertical distribution of methylmercury species at the SAFe station (Sampling and Analysis of Iron; 140 °W, 30 °N) in the North Pacific Ocean during the 2009 U.S. GEOTRACES Intercalibration cruise. This location, which is about mid-way between Hawaii and California, has full ocean depth (~5000 m) with multiple subsurface water masses, and it is within the expansive gyre of oligotrophic surface water in the subtropical North Pacific. Accordingly, the vertical distribution and associated cycling of MMHg and dimethylmercury (DMHg) at the SAFe site may be representative of that in other comparable oceanic environs.

2. Materials and methods

2.1. Sampling

Seawater was sampled with a trace-metal clean rosette and Teflon-coated GO-Flo bottles from 20 water depths at the SAFe site in the North Pacific Ocean in May 2009. Promptly after sampling, seawater was filtered through a pre-rinsed capsule (0.2 μm; Pall AcroPak-200, polyethersulfone membrane) and silicone tubing as it was decanted from a rosette bottle into a 2-L FEP Teflon® bottle, a technique we have found to result in no measureable loss of DMHg (Bowman and Hammerschmidt, 2011). Suspended particles also were sampled from eight depths with a multiple-unit large-volume in situ filtration system (Bishop et al., 1985) onto pre-cleaned quartz filters that collect a size fraction between 1 and 51 μm. Water volumes filtered through filter punches analyzed for MMHg ranged from 0.07 m^3 at the surface to about 0.24 m^3 at 850 m depth. Trace-metal clean techniques were used during sampling, preparation, and analysis of the samples (Hammerschmidt et al., 2011; Lamborg et al., 2012).

2.2. Methylmercury determination

DMHg and MMHg were extracted from filtered seawater and analyzed with methods detailed elsewhere (Bowman and Hammerschmidt, 2011). Briefly, 2-L sample bottles containing seawater were fitted with a multi-port cap (Omnifit Q-series; Danbury, CT) and impinger with a fine-pore frit at the bottom of the bottle. DMHg was purged from solution with 30 L of N_2 (0.8 L min^{-1}) and concentrated on Tenax TA (23% graphitized carbon, 20/35 mesh, Alltech), a resin used by others to quantify DMHg (e.g.,

Mason and Sullivan, 1999; Horvat et al., 2003). The N_2 was of ultra-high purity and cleansed of Hg by passage through Au-coated glass beads and graphitized carbon prior to the impinger. Purged waters were prepared for MMHg extraction by reaction with H_2SO_4 (1% sample volume) for 12–24 h, neutralized with KOH, and adjusted to pH 4.9 with 4 M acetate buffer prior to addition of cold sodium tetraethylborate and purging of the ethylated derivative of MMHg (methylethylmercury) from solution onto a Tenax column. Both DMHg and MMHg (as methylethylmercury) were quantified by gas-chromatographic, cold-vapor atomic fluorescence spectrometry (CVAFS; Bloom, 1989; Tseng et al., 2004) in a shipboard laboratory.

All equipment and containers used for sample collection, storage, and analysis were cleaned rigorously with acid and rinsed with either reagent-grade water (resistivity, > 18 MΩ-cm) or surface seawater prior to use. Sample DMHg and MMHg were quantified after each Tenax column was calibrated individually with aliquots of an aqueous MMHg standard that was derivatized and purged from solution in the same bottles used for samples. Aqueous MMHg standards were standardized versus an aqueous Hg(II) solution traceable to the U.S. National Institute of Standards and Technology. Precision of determinations averaged 15% relative difference between duplicate samples for both DMHg (n = 14 duplicates) and MMHg (n = 2). Recovery of known MMHg additions from sample matrixes averaged 91% (n = 10). The method detection limit, based on analysis of reagent blanks (3σ), was about 2 fM for MMHg and similar to the instrument detection limit for DMHg in a 2-L sample.

MMHg was extracted from particles (1–51 µm) by leaching quartz filters with high-purity 2 N HNO_3 for 4 h in a 60 °C water bath at Wright State University

(Hammerschmidt and Fitzgerald, 2006b). Sample MMHg was quantified by gas-chromatographic CVAFS after calibration with a standardized solution.

2.3. Total Hg in filtered seawater

Total Hg was measured in 0.2-L aliquots of filtered (0.2 µm) water that were separate from those used for methylmercury determination but collected from the same GO-Flo bottles. Water for total Hg analysis was acidified to 0.2% with high-purity HCl and stored in rigorously cleaned 250-mL FEP Teflon® bottles (Hammerschmidt et al., 2011) until analysis at Wright State University, about six weeks after sampling. Analyses of reagent-grade water that was stored in FEP bottles and transported with the samples indicated no discernable Hg contamination during storage (i.e., trip blanks). Samples were oxidized with BrCl solution (0.1% sample volume) for > 12 h and subsequently pre-reduced with NH_2OH. Sample Hg was reduced to Hg^0 with $SnCl_2$ and quantified by dual Au-amalgamation CVAFS (Fitzgerald and Gill, 1979; Bloom and Fitzgerald, 1988). Total Hg measurements were calibrated versus Hg^0 gas standards. Recoveries of known Hg(II) additions to sample matrixes averaged 99% (n = 7) and the precision of one procedurally duplicated sample was 10% relative difference, which was comparable to the precision of seawater determinations of total Hg in a companion study (mean = 4% relative difference; range = 0.5–20%; n = 70). The method detection limit for total Hg (3σ reagent blanks) was about 0.05 pM for a 0.2-L sample.

3. Results and discussion

MMHg and DMHg have two well-defined and corresponding subsurface maxima in the water column of the eastern North Pacific at 500 and 1000 m depth (Figure 1a). These maxima correspond with the core of oxygenated North Pacific Intermediate Water (NPIW; ~300–700 m depth) and oxygen minimum zone (800–1000 m). Filtered MMHg is low in the surface mixed layer presumably as a result of photochemical decomposition (Monperrus et al., 2007; Whalin et al., 2007) and uptake by phytoplankton, while gaseous DMHg is lost most likely by evasion to the atmosphere (Black et al., 2009). Deeper waters have homogeneous distributions of MMHg (24 ± 4 fM) and DMHg (13 ± 1 fM) with no increase near the seafloor, which suggests that deep-sea sediments are not a significant source. Cossa and colleagues drew a similar conclusion based on profiles in the open Mediterranean Sea and Southern Ocean (Cossa et al., 2009, 2011). This is the first high-resolution profile of MMHg concentrations below 1000 m in the Pacific Ocean, although methylated Hg has been measured in the upper 1000 m of water at other locations in the Pacific (Mason and Fitzgerald, 1990; Sunderland et al., 2009). Levels of methylmercury in the upper 1000 m at SAFe are 2–6× less than those measured at a station about 1000 km to the west-(Sunderland et al., 2009). A similar degree of variability of methylated Hg concentrations has been observed among locations in the Mediterranean Sea and Southern Ocean (Cossa et al., 2009, 2011).

The vertical distribution of total Hg in filtered water at SAFe is different from the methylmercury species (Figure 1b). Total Hg has a transient, atmospherically enhanced level of 0.40 pM at the sea surface and a minimum of 0.25 pM at greater depths in the surface mixed layer (upper ~130 m). Total Hg increases with depth through the

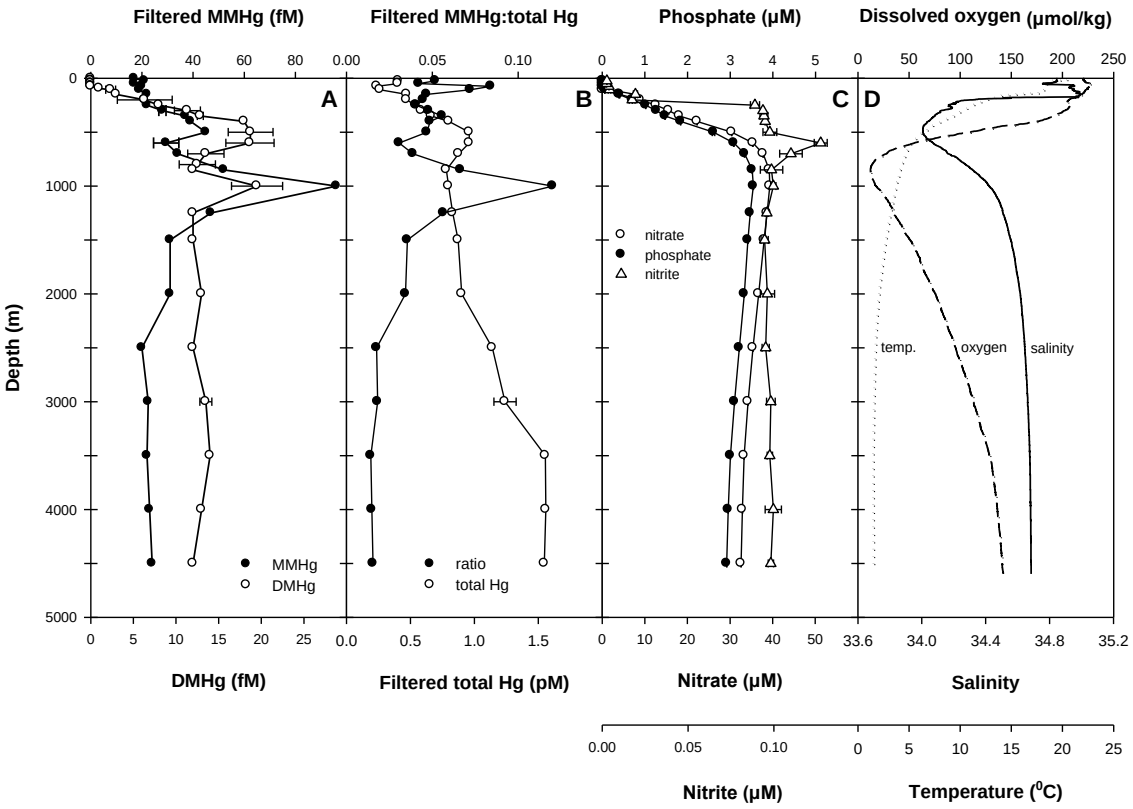

Fig. 1. Vertical distribution of mercury species at the SAFe station in the North Pacific; a) DMHg and filtered MMHg, b) filtered total Hg and MMHg:total Hg ratio, c) nutrients, and d) physicochemistry. Error bars for Hg concentrations are the difference between duplicate samples.

thermocline, with a maximum at 500 m in NPIW, and greater concentrations in bottom water. Levels of total Hg in filtered water at the SAFe station are 50–100% less than those at a station about 1000 km to the west (Sunderland et al., 2009), but the vertical distribution of total Hg is comparable to that at other locations in the open North Pacific (Laurier et al., 2004) and controlled by mixing and particle scavenging (Figure 2).

Elevated total Hg in North Pacific Bottom Water (≥ 3500 m) can be attributed to long-term accumulation associated with soft-tissue remineralization processes superimposed on oceanic abyssal circulation (i.e., thermohaline). Broadly, the amounts of many biological active substances (e.g., NO_3^-, PO_4^{3-}, CO_2) increase at depth as water ages in transit from source regions in the North Atlantic to the northeast Pacific, where the oldest deep water is found. We recently measured total Hg in North Atlantic Deep Water (NADW) as part of the U.S. GEOTRACES North Atlantic zonal section. At a station in the northwest Atlantic about midway between Cape Cod and Bermuda (35.4 °N, 66.5 °W), deep water (1500–4000 m) contained 0.93 ± 0.10 pM total Hg and 18 µM NO_3^- (unpublished data). The increase of total Hg between NADW at this station and NPBW at SAFe (≥ 3500 m; 1.55 ± 0.01 pM total Hg, 33 µM NO_3^-) is a factor of 1.7 and nearly identical that of NO_3^-, which has a horizontal enrichment of 1.8. This inter-basin comparison, while limited to just the two end members of the thermohaline cycle, implies that Hg accumulation in deep waters results from remineralization of biological soft tissues and provides a useful tool for predicting total Hg in deep waters elsewhere in the ocean.

Methylmercury is commonly enriched in low-oxygen seawater associated with increased microbial remineralization of organic material (Mason and Fitzgerald, 1990,

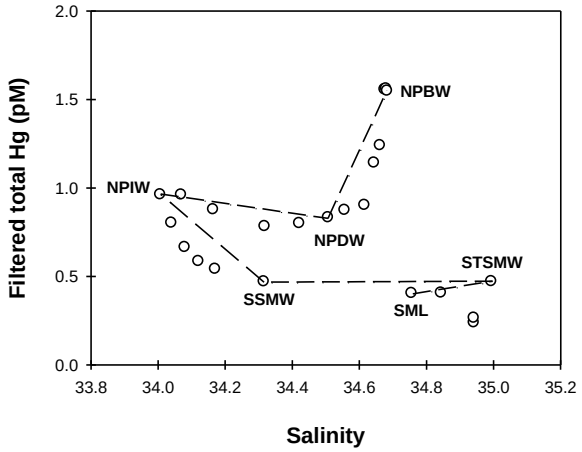

Fig. 2. Property–property plot of filtered total Hg versus salinity at the SAFe site. Dashed lines indicate conservative mixing between water masses: Surface Mixed Layer (SML; upper ~130 m), Subtropical Salinity Maximum Water (STSMW; σ_θ = 24.0, centered at ~ 150 m), Subsurface Salinity Minimum Water (SSMW; σ_θ = 25.8, centered at ~ 200 m), NPIW (σ_θ = 26.8, centered at ~ 500 m), North Pacific Deep Water (NPDW; σ_θ = 27.4, centered at ~ 1300 m), and North Pacific Bottom Water (NPBW; σ_θ = 27.8, > 3000m) (Talley, 1985, 1993; Sabine et al., 1995).

1993; Mason and Sullivan, 1999; Cossa et al., 2009; Sunderland et al., 2009; Heimbürger et al., 2010). This has been attributed to in situ methylation of inorganic Hg by heterotrophic microorganisms. Such an in situ source is a likely explanation for the MMHg and DMHg focused around 1000 m in the oxygen minimum at SAFe (Mason and Fitzgerald, 1993), where the fraction of filtered total Hg as MMHg also is maximum (Figure 1b). This is supported by the absence of similar features in distributions of either total Hg or nutrients (Figure 1b,c), which suggest isopycnal transport at these depths is not a major source. MMHg production at 1000 m depth can be estimated as the product of a vertical eddy diffusion coefficient for deep water (K_V = 2–4 $\times 10^{-4}$ m^2 s^{-1}; Hogg et al., 1982; Gargett, 1984) and concentration gradient between 1000 m (96 fM) and both 700 m (34 fM) and 1500 m (31 fM). This approximation yields a flux of 6–12 pmol m^{-2} d^{-1} in the oxygen minimum zone, which is within the range of fluxes from sediments on the remote continental shelf (Hammerschmidt and Fitzgerald, 2006a; Hollweg et al., 2010).

The reason for the MMHg and DMHg maxima in NPIW is less clear. Potential sources of methylated mercury in NPIW at the SAFe station include release from sinking particles, isopycnal transport, and *in situ* production. The vertical distribution of particulate MMHg is similar to that of particulate organic carbon (POC) in surface and intermediate waters at SAFe (Figure 3). MMHg in particles is 2.8 fM at the surface and decreases exponentially with depth to 0.7 fM at 220 m. This concentration, near the upper boundary of NPIW, is comparable to that at the lower boundary of the water mass, which means that sinking particles add little MMHg to NPIW. An increase in the ratio of particulate MMHg:POC with depth suggests that MMHg is either more refractory than

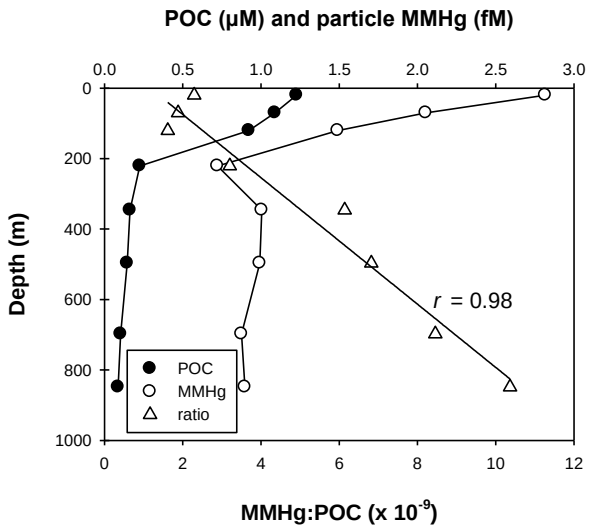

Fig. 3. Vertical distributions of particle-specific MMHg, particulate organic carbon (POC), and the particulate MMHg:POC ratio at the SAFe station.

bulk POC or that it is scavenged by, or produced within, sinking particles (Figure 3). The mass-normalized concentration of MMHg in particles at 20 m depth (e.g., phytoplankton) is about 0.8 ng g^{-1} wet weight, assuming that the particles are composed entirely of organic matter (no hard parts), Redfield stoichiometry of the material, and a water content of 95% (Knauer and Martin, 1972). MMHg in surface particles at SAFe is comparable to that in phytoplankton of Long Island Sound (0.5 ng g^{-1}; Hammerschmidt and Fitzgerald, 2006b), the New England continental shelf (0.3 ng g^{-1}; Hammerschmidt and Fitzgerald, 2006a), and Monterey Bay (1.3–4.5 ng g^{-1}; Knauer and Martin, 1972).

Another potential explanation for methylmercury species in NPIW is that they were pre-formed in source waters and advected horizontally to the SAFe site, just as total Hg is increased in this water mass. NPIW is formed by cabbeling of deep shelf water from the Sea of Okhotsk with Oyashio and Kuroshio water in the western Pacific (Talley, 1997; You, 2003a). Water from the Sea of Okhotsk has contact with benthic deposits (Shcherbina et al.,2003) that could be a source of MMHg and DMHg to NPIW. MMHg is mobilized from shelf sediments to overlying water (Hammerschmidt and Fitzgerald, 2006a; Hollweg et al., 2010), and we have observed recently a DMHg efflux from deposits on the margin of the northwest Atlantic Ocean (unpublished results). Water from the Sea of Okhotsk is a known source of organic carbon (Hernes and Benner, 2002) and trace metals (Nishioka et al., 2007) to the ocean interior. The estimated water-mass age of NPIW at SAFe is 20–70 y (Warner et al., 1996; You, 2003b). Accordingly, for DMHg and MMHg in NPIW to be derived from the Sea of Okhotsk, they would require a lifetime of 20+ years. Little is known about the lifetime of methylmercury species in subsurface seawater, but that of DMHg has been estimated to be 0.3–30 years (Mason

and Fitzgerald, 1993). It is unclear if lateral transport is a significant source of methylmercury in NPIW at the SAFe site; however, if it were, this would be a remarkable vector for distributing MMHg from the margins to the interior ocean.

In situ production is the other potential source of methylmercury in NPIW. Methylation within the water mass has been posited by Sunderland and colleagues (2009) to be a source of methylated Hg in NPIW. Here, we show the speciation of methylated Hg in NPIW and the significant presence of DMHg (Figure 1a). If the methylmercury species were produced in situ by microbial activity, then the methylation process was probably aerobic (Monperrus et al., 2007), because oxygen was relatively high (55–175 μmol O_2 kg^{-1}) in the region where MMHg and DMHg were maximal (400–600 m depth). Alternatively, methylation could be mediated by anaerobic microorganisms associated with anoxic microenvironments, such as decomposing remains of plankton (Heimbürger et al., 2010). A nitrite maximum at 600 m (Figure 1c) suggests that either denitrification or ammonium oxidation co-occurs within NPIW, although it is unknown if either process is related to Hg methylation.

The ratio of MMHg:DMHg is about two throughout much of the subsurface water column at the SAFe station (Figure 4). MMHg:DMHg is 2.3 ± 0.4 in NPIW, 4.4 ± 0.5 near the oxygen-minimum zone, and 1.9 ± 0.4 in water below 1500 m. With the exception of the oxygen-minimum region, the relative constancy of the ratio indicates that a steady state condition may exist between MMHg and DMHg, because neither molecule behaves conservatively. This would require an active exchange of methyl groups between the molecules, as observed recently by Lehnherr and colleagues in polar seawater (Lehnherr et al., 2011). The ratio of methyl groups associated with MMHg and

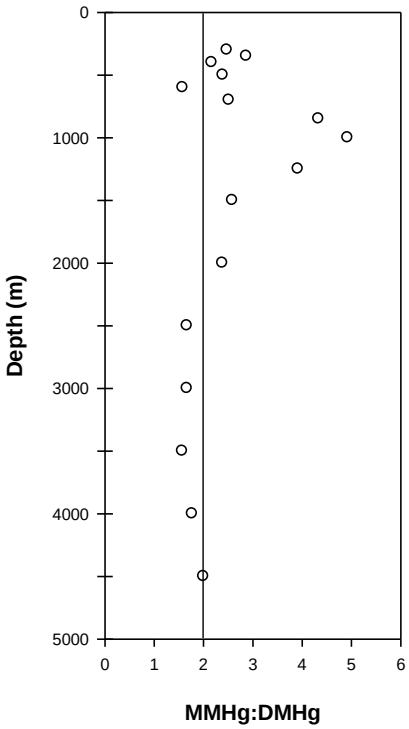

Fig. 4. Vertical distribution of monomethylmercury:dimethylmercury (MMHg:DMHg) molar ratios in subsurface water at the SAFe site.

DMHg is near unity throughout much of the water column. A greater MMHg:DMHg ratio in the oxygen minimum zone suggests involvement of different processes (possibly ones that are associated with hypoxia and employ different methylation mechanisms) that result in the establishment of a different steady state. The maximum MMHg:DMHg ratio around 1000 m depth (Figure 4) corresponds with a peak in the MMHg:total Hg ratio (Figure 1b). This suggests that low oxygen conditions maximize the net production of methylated mercury and the fraction as MMHg.

NPIW is a source of methylmercury species to the mixed layer. The flux of DMHg from NPIW can be estimated as the product of a vertical eddy diffusion coefficient for surface water (K_V = 0.5–1 × 10^{-4} m^2 s^{-1}; Fiadeiro and Craig, 1978; Gargett, 1984) and concentration gradient between 500 m (19 fM) and 100 m (2 fM). This approximation yields a flux of 0.2–0.4 pmol m^{-2} d^{-1}. The same estimate for MMHg between 500 m (45 fM) and 100 m (19 fM) depths suggests an efflux of 0.3–0.6 pmol m^{-2} d^{-1}.

The vertical diffusive flux of MMHg from NPIW to the mixed layer (~0.3–0.6 pmol m^{-2} d^{-1}) at SAFe is trivial compared to bioaccumulation of about 4–7 pmol m^{-2} d^{-1} by primary producers. This bioaccumulation estimate is based on a particulate MMHg:carbon ratio of 2 × 10^{-9} (Figure 2) and assumes net community production is about 0.7–1.3 mol C m^{-2} y^{-1} in the mixed layer at SAFe. The estimate of net community production, which is considerably less than that of gross primary production (~6 mol C m^{-2} y^{-1}; Behrenfeld and Falkowski, 1997), assumes upward diffusion of NO_3^- into the mixed layer (0.1–0.2 mol NO_3^- m^{-2} y^{-1}) limits growth of phytoplankton that have 6.6 C:N Redfield stoichiometry. The vertical nitrate flux is the product of the thermocline NO_3^-

gradient (Figure 1c; 76 µmol m^{-4}) and vertical eddy diffusivity coefficient (0.5–1 × 10^{-4} m^2 s^{-1}). Photochemical decomposition of MMHg in surface seawater (k ~ 0.08–0.4 d^{-1}; Monperrus et al., 2007; Whalin et al., 2007) is estimated to consume an additional 8–40 pmol m^{-2} d^{-1} if the process were limited to the extent of ultraviolet radiation penetration (Lehnherr and St. Louis, 2009), which is about 5 m in the North Pacific (Goes et al., 1995). MMHg also may be decomposed by biological processes in the mixed layer. Accordingly, diffusion-advection of MMHg from water beneath the mixed layer is at least an order of magnitude less than the amounts bioaccumulated and decomposed photochemically at the SAFe station. This suggests that MMHg in the mixed layer at SAFe must be either transported horizontally by surface currents or, more likely, produced there. A Hg methylation rate constant of only 0.0003–0.0012 d^{-1} in the mixed layer would be sufficient to balance estimated MMHg losses to bioaccumulation and photochemical decomposition at SAFe. Such rates of Hg methylation are considerably less than those measured in surface waters of the Canadian Archipelago (0.006 ± 0.002 d^{-1}; Lehnherr et al., 2011). For the losses to bioaccumulation and photodecomposition to be balanced by atmospheric inputs of MMHg, rainwater would need to contain 0.4–1.7 pM MMHg (assuming 1 m rain y^{-1}), a concentration that is at least 10-fold greater than that in rain over the Pacific Ocean (< 0.05 pM; Mason et al., 1992).

Our results imply that both MMHg and DMHg are produced in oxic and low-oxygen regions throughout the marine water column. We observed subsurface peaks of MMHg and DMHg in both the oxygen minimum zone (~ 1000 m depth; 12–18 µmol O_2 kg^{-1}) and in more oxygenated (55–175 µmol kg^{-1}) North Pacific Intermediate Water. Vertical distributions of both methylated species differ considerably from that of total

Hg, which implies that production of MMHg and DMHg is influenced by environmental factors that control availability of ionic Hg and activities of microbial functional groups that may differ with depth. Our simple, one-dimensional scaling estimates suggest that a majority of MMHg in phytoplankton at the SAFe station results from production in the mixed layer, although we cannot rule out MMHg inputs from surface currents. About half of the ionic Hg in the mixed layer is from anthropogenic sources and delivered by atmospheric transport and deposition (Lamborg et al., 2002). If MMHg production in the mixed layer were limited by availability of ionic Hg, as it appears to be in sediments (Hammerschmidt and Fitzgerald, 2004; Fitzgerald et al., 2007), then future changes in Hg inputs, including atmospheric deposition, may influence levels of MMHg in pelagic food webs.

Acknowledgements

We thank Phoebe Lam and Jim Bishop for providing filtered particles and POC results; Greg Cutter for sharing nutrient and CTD data; captain, crew, and scientific party of the 2009 U.S. GEOTRACES Intercalibration cruise for help sampling water; and Gary Gill, Alyson Santoro, Pete Morton, Bill Fitzgerald, and Carl Lamborg for thoughtful discussions of our findings. This research was supported by the U.S. National Science Foundation (OCE-0825108).

References

Behrenfeld, M.J., Falkowski, P.G., 1997. Photosynthetic rates derived from satellite-based chlorophyll concentration. Limnology and Oceanography 42, 1–20.

Bishop, J.K.B., Schupack, D., Sherrell, R.M., Conte, M., 1985. A multiple-unit large-volume in-situ filtration system (MULVFS) for sampling oceanic particulate matter in mesoscale environments. In: Zirino, A (Ed.), Mapping Strategies in Chemical Oceanography, Advances in Chemistry Series, Vol. 209. American Chemical Society, Washington, DC, pp. 155–175.

Black F.J., Conaway, C.H., Flegal, A.R., 2009. Stability of dimethyl mercury in seawater and its conversion to monomethyl mercury. Environmental Science and Technology 43, 4056–4062.

Bloom, N.S., 1989. Determination of picogram levels of methylmercury by aqueous phase ethylation, followed by cryogenic gas chromatography, with cold vapour atomic fluorescence detection. Canadian Journal of Fisheries and Aquatic Sciences 46, 1131–1140.

Bloom, N.S., Fitzgerald, W.F., 1988. Determination of volatile mercury species at the picogram level by low-temperature gas chromatography with cold-vapor atomic fluorescence detection. Analytica Chimica Acta 208, 151−161.

Bowman, K.L., Hammerschmidt, C.R., 2011. Extraction of monomethylmercury from seawater for low-femtomolar determination. Limnology and Oceanography Methods 9, 121–128.

Cossa, D., Averty, B., Pirrone, N., 2009. The origin of methylmercury in open Mediterranean waters. Limnology and Oceanography 54, 837–844.

Cossa, D., Heimbürger, L.-E., Lannuzel, D., Rintoul, S.R., Butler, E.C.V., Bowie, A.R., Averty, B., Watson, R.J., Remenyi, T., 2011. Mercury in the Southern Ocean. Geochimica et Cosmochimica Acta 75, 4037–4052.

Fiadeiro, M.E.; Craig, H., 1978. Three-dimensional modeling of tracers in the deep Pacific Ocean: I. Salinity and oxygen. Journal of Marine Research 36, 323–355.

Fitzgerald, W.F., Gill, G.A., 1979. Subnanogram determination of mercury by two-stage gold amalgamation applied to atmospheric analysis. Analytical Chemistry 51, 1714−1720.

Fitzgerald W.F., Lamborg, C.H., Hammerschmidt, C.R., 2007. Marine biogeochemical cycling of mercury. Chemical Reviews 107, 641–662.

Gargett, A.E., 1984. Vertical eddy diffusivity in the ocean interior. Journal of Marine Research 42, 359–393.

Goes, J.I., Handa, N., Taguchi, S., Hama, T., 1995. Changes in the patterns of biosynthesis and composition of amino acids in a marine phytoplankter exposed to ultraviolet-B: nitrogen limitation implicated. Photochemistry and Photobiology 62, 703–710.

Hammerschmidt, C.R., Fitzgerald, W.F., 2004. Geochemical controls on the production and distribution of methylmercury in near-shore marine sediments. Environmental Science and Technology 38, 1487–1495.

Hammerschmidt, C.R., Fitzgerald, W.F., 2006a. Methylmercury cycling in sediments on the continental shelf of southern New England. Geochimica et Cosmochimica Acta 70, 918–930.

Hammerschmidt, C.R., Fitzgerald, W.F., 2006b. Bioaccumulation and trophic transfer of methylmercury in Long Island Sound. Archives of Environmental Contamination and Toxicology 51, 416–424.

Hammerschmidt, C.R., Bowman, K.L., Tabatchnick, M.D., Lamborg, C.H., 2011. Storage bottle material and cleaning for determination of total mercury in seawater. Limnology and Oceanography Methods 9, 426–431.

Heimbürger L.-E., Cossa, D., Marty, J.-C., Migon, C., Averty, B., Dufour, A., Ras, J., 2010. Methyl mercury distributions in relation to the presence of nano- and picophytoplankton in an oceanic water column (Ligurian Sea, North-western Mediterranean). Geochimica et Cosmochimica Acta 74, 5549–5559.

Hernes, P.J., Benner, R., 2002. Transport and diagenesis of dissolved and particulate terrigenous organic matter in the North Pacific Ocean. Deep-Sea Research I 49, 2119–2132.

Hollweg, T.A., Gilmour, C.C., Mason, R.P., 2010. Mercury and methylmercury cycling in sediments of the mid-Atlantic continental shelf and slope. Limnology and Oceanography 55, 2703–2722.

Hogg, N., Biscaye, P., Gardner, W., Schmitz, Jr., W.J., 1982. On the transport and modification of Antarctic Bottom Water in the Vema Channel. Journal of Marine Research 40, 231–263.

Horvat, M., Kotnik, J., Logar, M., Fajon, V., Zvonaric, T., Pirrone, N., 2003. Speciation of mercury in surface and deep-sea waters in the Mediterranean Sea. Atmospheric Environment 37, S93–S108.

Knauer, G.A., Martin, J.H., 1972. Mercury in a marine pelagic food web. Limnology and Oceanography 17, 868–876.

Kraepiel, A.M., Keller, K., Chin, H.B., Malcolm, E.G., Morel, F.M.M., 2003. Sources and variations of mercury in tuna. Environmental Science and Technology 37, 5551–5558.

Lamborg, C.H., Fitzgerald, W.F., O'Donnell, J., Torgersen, T., 2002. A non-steady-state compartmental model of global-scale mercury biogeochemistry with interhemispheric atmospheric gradients. Geochimica et Cosmochimica Acta 66, 1105–1118.

Lamborg, C.H., Von Damm, K.L., Fitzgerald, W.F., Hammerschmidt, C.R., Zierenberg, R., 2006. Mercury and monomethylmercury in fluids from Sea Cliff submarine hydrothermal field, Gorda Ridge. Geophysical Research Letters 33, L17606.

Lamborg, C.H., Hammerschmidt, C.R., Gill, G.A., Mason, R.P., Gichuki, S., 2012. An intercomparison of procedures for the determination of total mercury in seawater

and recommendations regarding mercury speciation during GEOTRACES cruises. Limnology and Oceanography Methods

Laurier, F.J.G., Mason, R.P., Gill, G.A., Whalin, L., 2004. Mercury distributions in the North Pacific Ocean—20 years of observations. Marine Chemistry 90, 3–19.

Lehnherr, I., St. Louis, V.L., 2009. Importance of ultraviolet radiation in the photodemethylation of methylmercury in freshwater ecosystems. Environmental Science and Technology 43, 5692–5698.

Lehnherr, I., St. Louis, V.L., Hintelmann, H., Kirk, J.L., 2011. Methylation of inorganic mercury in polar marine waters. Nature Geoscience 4, 298–302.

Lewis, B.L., Froelich, P.N., Andreae, M.O., 1985. Methylgermanium in natural waters. Nature 313, 303–305.

Mason, R.P., Fitzgerald, W. F., 1990. Alkylmercury species in the equatorial Pacific. Nature 347, 457-459.

Mason, R.P., Fitzgerald, W.F., 1993. The distribution and biogeochemical cycling of mercury in the equatorial Pacific Ocean. Deep-Sea Research I 40, 1897−1924.

Mason, R.P., Sullivan, K.A., 1999. The distribution and speciation of mercury in the South and equatorial Atlantic. Deep-Sea Research II 46, 937−956.

Mason, R.P., Fitzgerald, W.F., Vandal, G.M., 1992. The sources and composition of mercury in Pacific Ocean rain. Journal of Atmospheric Chemistry 14, 489–500.

Mergler, D., Anderson, H.A., Chan, L.H.M., Mahaffey, K.R., Murray, M., Sakamoto, M., Stern, A.H., 2007. Methylmercury exposure and health effects in humans: A worldwide concern. Ambio 36, 3–11.

Monperrus, M., Tessier, E., Amouroux, D., Leynaert, A., Huonnic, P., Donard, O.F.X., 2007. Mercury methylation, demethylation and reduction rates in coastal and marine surface waters of the Mediterranean Sea. Marine Chemistry 107, 49–63.

Nishioka, J., Ono, T., Saito, H., Nakatsuka, T., Takeda, S., Yoshimura, T., Suzuki, K., Kuma, K., Nakabayashi, S., Tsumune, D., Mitsudera, H., Johnson, W.K., Tsuda, A., 2007. Iron supply to the western subarctic Pacific: importance of iron export from the Sea of Okhotsk. Journal of Geophysical Research 112, C10012.

Sabine, C.L., Mackenzie, F.T., Winn, C., Karl, D.M., 1995. Geochemistry of carbon dioxide in seawater at the Hawaii Ocean Time series station, ALOHA. Global Biogeochemical Cycles 9, 637–651.

Shcherbina, A.Y., Talley, L.D., Rudnick, D. L., 2003. Direct observations of North Pacific ventilation: brine rejection in the Okhotsk Sea. Science 302, 1952−1955.

Sunderland, E.M., 2007. Mercury exposure from domestic and imported estuarine and marine fish in the U.S. seafood market. Environmental Health Perspectives 115, 235–242.

Sunderland, E.M., Krabbenhoft, D.P., Moreau, J.W., Strode, S.A., Landing, W.M., 2009. Mercury sources, distribution, and bioavailability in the North Pacific Ocean: insights from data and models. Global Biogeochemical Cycles 23, GB2010.

Talley, L.D., 1985. Ventilation of the subtropical North Pacific: the shallow salinity minimum. Journal of Physical Oceanography 15, 633–649.

Talley, L.D., 1993. Distribution and formation of North Pacific Intermediate Water. Journal of Physical Oceanography 23, 517–537.

Talley, L.D., 1997. North Pacific Intermediate Water transports in the mixed water region. Journal of Physical Oceanography 27, 1795–1803.

Tseng, C.-M., Hammerschmidt, C.R., Fitzgerald, W.F., 2004. Determination of methylmercury in environmental matrixes by on-line flow injection and atomic fluorescence spectrometry. Analytical Chemistry 76, 7131−7136.

U.S. Environmental Protection Agency, 2002. Estimated per capita fish consumption in the United States, August 2002. EPA-821-C-02-003, U.S. Environmental Protection Agency, Washington, DC.

Warner, M.J., Bullister, J.L., Wisegarver, D.P., Gammon, R.H., Weiss, R.F., 1996. Basin-wide distribution of chlorofluorocarbons CFC-11 and CFC-12 in the North Pacific: 1985–1989. Journal of Geophysical Research 101, 20525–20542.

Whalin, L., Kim, E.-H., Mason, R., 2007. Factors influencing the oxidation, reduction, methylation and demethylation of mercury species in coastal waters. Marine Chemistry 107, 278–294.

You, Y., 2003a. Implications of cabbeling on the formation and transformation mechanism of North Pacific Intermediate Water. Journal of Geophysical Research Oceans 108, 3134.

You, Y., 2003b. The pathway and circulation of North Pacific Intermediate Water. Geophysical Research Letters 30, 2291.

Appendix C. Mercury in the anthropocene ocean

Lamborg, C., Bowman, K., Hammerschmidt, C., Gilmour, C., Munson, K., Selin, N., Tseng, C.-M. 2014. Mercury in the Anthropocene ocean. Oceanography 27, 76–87.

Mercury in the Anthropocene Ocean

By Carl Lamborg, Katlin Bowman, Chad Hammerschmidt, Cindy Gilmour, Kathleen Munson, Noelle Selin, and Chun-Mao Tseng

Carl Lamborg (clamborg@whoi.edu) is Associate Scientist, Department of Marine Chemistry and Geochemistry, Woods Hole Oceanographic Institution, Woods Hole, MA, USA. **Katlin Bowman** is a graduate student in the Department of Earth and Environmental Sciences, Wright State University, Dayton, OH, USA. **Chad Hammerschmidt** is Associate Professor, Department of Earth and Environmental Sciences, Wright State University, Dayton, OH, USA. **Cindy Gilmour** is Senior Scientist, Smithsonian Environmental Research Center, Edgewater, MD, USA. **Kathleen Munson** is a Joint Program student, Department of Marine Chemistry and Geochemistry, Woods Hole Oceanographic Institution, Woods Hole, MA, USA. **Noelle Selin** is Assistant Professor, Engineering Systems Division and Department of Earth, Atmospheric and Planetary Sciences, Massachusetts Institute of Technology, Cambridge, MA, USA. **Chun-Mao Tseng** is Associate Professor, Institute of Oceanography, National Taiwan University, Taiwan.

ABSTRACT

Mercury is a toxic metal present at trace levels in the ocean, but it accumulates in fish at concentrations high enough to pose a threat to human and environmental health. Human activity has dramatically altered the global mercury cycle, resulting in loadings to the ocean that have increased by at least a factor of three from pre-anthropogenic levels. Loadings are likely to continue to increase as a result of higher atmospheric emissions and others factors related to global environmental change. The impact that these loadings will have on the production of methylated mercury (the form that accumulates in fish) is unclear. In this report, we summarize the biogeochemistry of mercury in the ocean and use this information to examine past impacts that human activity has had on the cycling

of this toxic metal. We also highlight ways in which the mercury cycle may continue to be affected and its potential impact on mercury in fish.

INTRODUCTION

Mercury is a notoriously toxic trace metal that has received global attention since the poisoning of thousands of people in southern Japan (Minamata and Niigata) in the mid-1950s. Ingestion of fish laden with monomethylmercury (CH_3Hg^+) caused those tragic circumstances and inspired researchers worldwide to examine mercury toxicity to humans and wildlife, measure concentrations in terrestrial and aquatic biota, and understand the biogeochemical cycling of the element's multiple forms.

Mercury would be of little toxicological concern if it were not for its microbial and abiotic transformation to CH_3Hg^+, which is the form that most readily bioaccumulates and biomagnifies in marine food webs. These processes result in CH_3Hg^+ concentrations in predatory fish and marine mammal species, including many species eaten by humans (e.g., tuna, swordfish, shark, pilot whale) that regularly exceed guidelines for safe consumption. Indeed, 5–10% of US women of childbearing age having blood CH_3Hg^+ levels that increase the risk of neurodevelopmental problems in their children (Mahaffey et al., 2009), presumably as a result of eating seafood (Selin et al., 2010). While the effects of current mercury exposures may not be as overt as those experienced in Minamata, the size of the worldwide population exposed to potentially harmful levels of CH_3Hg^+ via seafood consumption is likely in the hundreds of millions.

In addition to the impact on human health, we are just beginning to understand how elevated concentrations of mercury in food webs can affect their health and

sustainability. Several studies documented developmental and behavioral effects of CH_3Hg^+ on fish and other animals at concentrations commonly found in the environment (Scheuhammer et al., 2007) but at levels well below those causing acute toxicity. Indeed, some studies have suggested that the sustainability of some animal populations may already be threatened by impaired reproductive success as a result of mercury exposure (e.g., Tartu et al., 2013).

These disturbing ecological findings come in the context of geochemical research that indicates human activities have significantly perturbed the mercury cycle on local, regional, and global scales. Mercury loadings to the atmosphere, for example, have increased at least three-fold since the Industrial Revolution and are expected to continue to rise (e.g., Driscoll et al., 2013). Some research even suggests that anthropogenic impacts on the mercury cycle extend well before industrialization, largely as a result of its use in gold and silver mining.

Here, we review the environmental pathways of mercury from its introduction to the ocean to its accumulation in seafood, focusing on what is known and unknown about key microbial transformations of mercury in the sea, and how this cycle may change in the future.

Mercury Species Concentrations and Transformations in the Ocean

Mercury exists primarily as four chemical species in the ocean: elemental Hg (Hg^0), mercuric ion (Hg^{2+}, also written as Hg(II)) in a variety of inorganic and organic complexes, and methylated forms that include both CH_3Hg^+ and dimethylmercury ($(CH_3)_2Hg$; Table 1; Figure 1). As with most trace metals, both biological and physical

Table 1. Summary of Hg species in the ocean.

Species	Typical Concentration/ Percent of Total	Note
Total Hg	< 0.1–10 pM	
Hg^{2+}	50–100%	Generally dominant form
Hg^{0}	< 5–50%	Majority in atmosphere, dissolved gas in ocean
CH_3Hg^{+}	< 20%	Species that bioaccumulates in food webs
$(CH_3)_2Hg$	< 20%	Dissolved gas, origin unknown

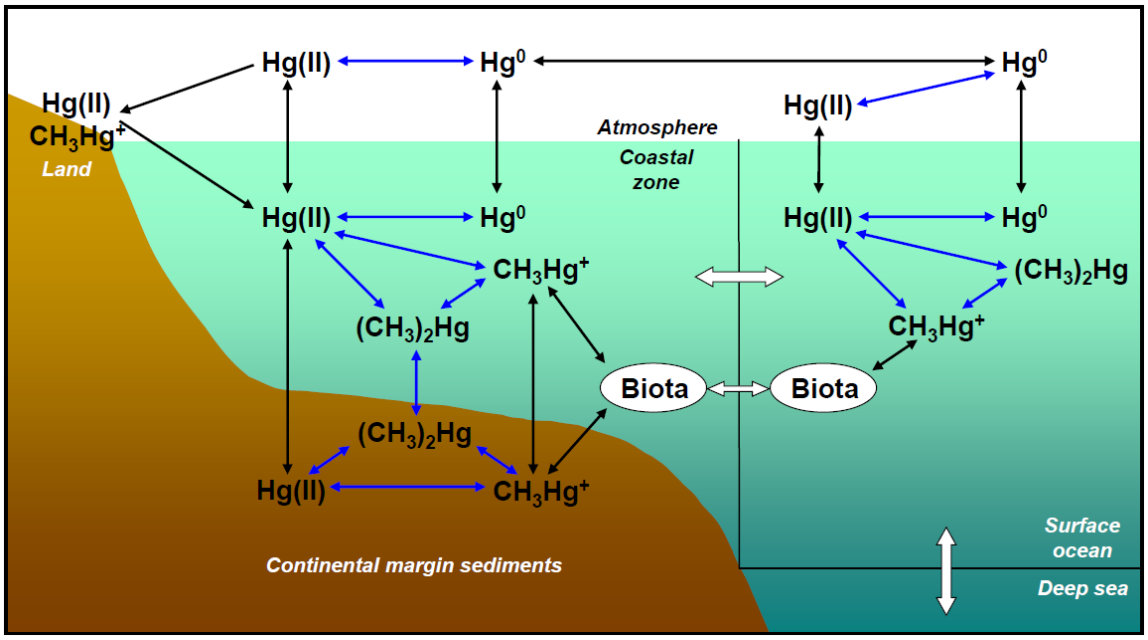

Figure 1. Conceptual model of mercury biogeochemical cycling in the ocean. Gaseous elemental mercury (Hg^0) is oxidized in the atmosphere to complexes of divalent mercury (Hg(II), also written as Hg(II)) and deposited to land and the surface ocean. Hg(II) can be either reduced to Hg^0 or methylated to form monomethylmercury (CH_3Hg^+) and dimethylmercury ($(CH_3)_2Hg$). Blue arrows highlight biogeochemical transformations of mercury. Black arrows denote fluxes among the atmosphere, water, sediments, and biota. All of the mercury species can be transported hydrologically between the coastal zone, surface ocean, and deep sea, with bioaccumulative CH_3Hg^+ also transported by bioadvection (white arrows; Fitzgerald et al., 2007).

processes govern the distribution of total mercury in the ocean. Combined influences of bioaccumulation and organic matter remineralization, as well as inputs from the atmosphere, scavenging, and horizontal advection, result in mercury displaying nutrient- and scavenged-type profiles with depth in the ocean. At any location, the profile will be dependent upon the relative strength of each of these processes (e.g., Mason et al., 2012). Figure 2 shows some representative vertical profiles of total dissolved mercury and Hg^0 concentrations from open-ocean stations that illustrate these behaviors. Bioaccumulation in surface water and release during remineralization of soft tissues in the thermocline likely cause nutrient-type distributions of mercury, as often observed for trace metals that are biologically essential (e.g., zinc, cobalt, cadmium). Thus, increased concentrations of total dissolved mercury in the thermocline are a result of vertical transport from above and a slow rate of removal by either scavenging or microbial uptake.

Although distributions of total mercury are important to establish, the story of mercury cycling in the ocean is fundamentally connected to its proclivity to change chemical and physical forms. Natural and anthropogenic sources emit elemental Hg (as well as a lesser amount of gaseous Hg(II)). Direct atmospheric deposition is presumed to be the principal source of Hg(II) (mercury is oxidized to Hg(II) in the atmosphere) to most of the ocean (e.g., Driscoll et al., 2013), although rivers and groundwater can be more important in nearshore systems and the confined Arctic Ocean. This flux amounts to about 7 Mmole yr^{-1} in the net (Amos et al., 2013). Once in the marine environment, Hg(II) has a complex biogeochemistry, resulting in one of three fates (Figure 1): (1)

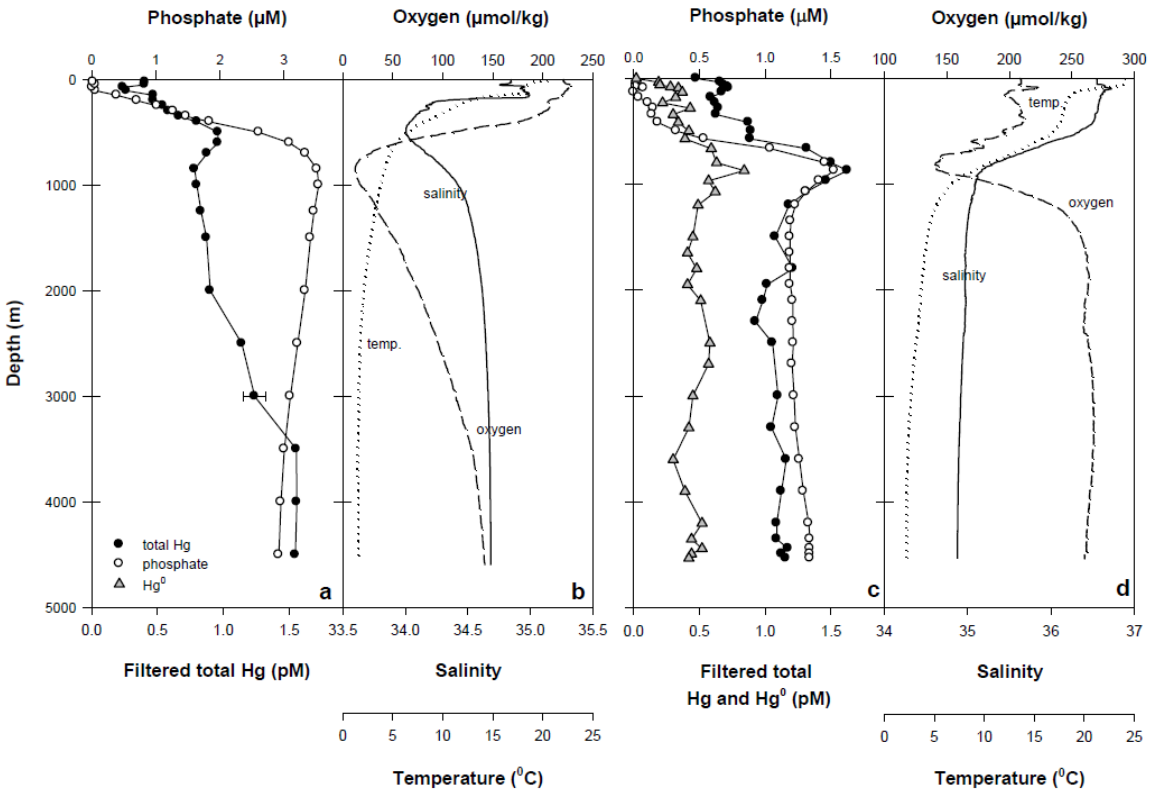

Figure 2. Vertical profiles of filtered total mercury, nutrients, and physicochemical parameters that illustrate different vertical mercury distributions in the ocean. (a and b) SAFe (Sampling and Analysis of Fe) program site in the North Pacific Ocean (Hammerschmidt and Bowman, 2012). (c and d) Station 10 (31.8°N, 64.2°W) in the western North Atlantic Ocean sampled during the recent US GEOTRACES zonal section (recent work of author Bowman).

reduction to Hg^0 and evasion to the atmosphere, (2) methylation to either CH_3Hg^+ or $(CH_3)_2Hg$, and (3) scavenging from the water column.

Reduction

Net reduction of Hg(II) to Hg^0 proceeds strongly enough that Hg^0 is often supersaturated in seawater with respect to the atmosphere (Mason et al., 2012). Subsequent evasion of Hg^0 to the atmosphere is half of the air-sea cycling loop and is a unique aspect of the biogeochemistry this metal. The reduction and evasion process is a major component of the marine Hg cycle, with evasion fluxes removing 50–80% of gross loadings from the atmosphere. Mercury reduction in seawater is thought to occur rapidly and to include both abiotic (photochemical) reactions as well as reduction by biota. Most mercury reduction in productive coastal waters is likely by a biological mechanism, driven by any one of several mercury-reducing bacteria. In contrast, photochemical reduction is more likely the dominant pathway in the open ocean, where light penetration is deeper and biological productivity less.

Methylation and Demethylation

Sediments

External sources of the methylated forms of mercury are too low to explain the concentrations and fluxes of it in the ocean (e.g., Fitzgerald et al., 2007), suggesting that the primary source is internal production in sediments or the water column. In nearshore environments and likely for continental shelves, in situ sediment production accounts for most of the CH_3Hg^+ present. Other significant sources of CH_3Hg^+ to nearshore systems include tidal marshes, waste water treatment facilities, submarine groundwater discharge,

and mangroves that have exceptionally high rates of mercury methylation (e.g., Driscoll et al., 2013). Principal losses of CH_3Hg^+ from these waters include sedimentation, photochemical decomposition, harvesting of seafood, and export to the wider ocean.

In a recent breakthrough, Parks et al. (2013) identified two genes (*hgcA* and *hgcB*) that are responsible for mercury methylation in some cultured anaerobic bacteria. These genes have also been found in other organisms that were not yet known to be mercury methylators, and from a more diverse group of anaerobic bacteria than previously observed (Gilmour et al., 2011; Parks et al., 2013). This finding reveals that the effect of microbial population structure in methylation is still poorly understood beyond the presence/absence of the general classes of microbes that contribute to methylation. Moreover, the microbial mechanism of mercury methylation is unknown, although it is thought to occur by an intracellular process. Examination of the genes in greater detail should reveal much about the biochemistry of mercury methylation and aid in our understanding of its occurrence in the environment.

The genetic basis of Hg methylation not withstanding, net production of CH_3Hg^+ in coastal sediments appears to be influenced more by Hg(II) bioavailability than the activity of methylating microbes. Supply of electron acceptors (e.g., SO_4^{2-} or Fe(III)) as well as labile organic matter appear to be sufficient to fuel organisms' mercury methylation even in the sandiest of marine deposits. Accordingly, geochemical factors that influence the sediment-water partitioning and chemical speciation of Hg(II) substrate greatly affect benthic production of CH_3Hg^+. Maximum rates of CH_3Hg^+ production are observed in coastal sediments that have relatively low levels of both solid-phase organic matter and sulfide, which favors partitioning of Hg(II) species into pore water and

therefore uptake by microbes (Fitzgerald et al., 2007). In contrast, CH_3Hg^+ production can be inhibited in sediments with enhanced levels of either organic matter (greater particle binding) or sulfide, which shifts speciation of dissolved Hg−S species to ionically charged complexes that are less bioavailable (e.g., Benoit et al., 1999). Therefore, Hg methylation is most effective at redox transition zones, where sulfate-reducing bacteria are present, but their sulfide by-product is not so abundant as to sequester Hg in sediments.

Microbial demethylation also significantly influences net production of CH_3Hg^+; however, the mechanisms and rates of degradation remain a large gap in our understanding of CH_3Hg^+ biogeochemistry in marine sediments. Multiple functional groups of anaerobic microorganisms have the ability to demethylate CH_3Hg^+ by either an oxidative process where CO_2 and Hg(II) are the end products or use of the organomercurial lyase protein, MerB, encoded on the mer operon (Barkay et al., 2003). However, microbial demethylation via the mer operon is likely not the dominant mechanism of CH_3Hg^+ loss in anoxic sediment.

Water Column

Hg(II) also can be methylated to CH_3Hg^+ and $(CH_3)_2Hg$ in the marine water column (Figure 1; the sum of the two species denoted as $\sum CH_3Hg$). The most striking feature of the vertical distribution of $\sum CH_3Hg$ is the ubiquitous maximum in the OMZ, typically from 500–1,000 m depth (Figure 4). Maxima of $\sum CH_3Hg$ in OMZs have been widely attributed to in situ methylation fueled by microbial remineralization of organic matter (e.g., Mason and Fitzgerald, 1993), the process that also is partly responsible for the

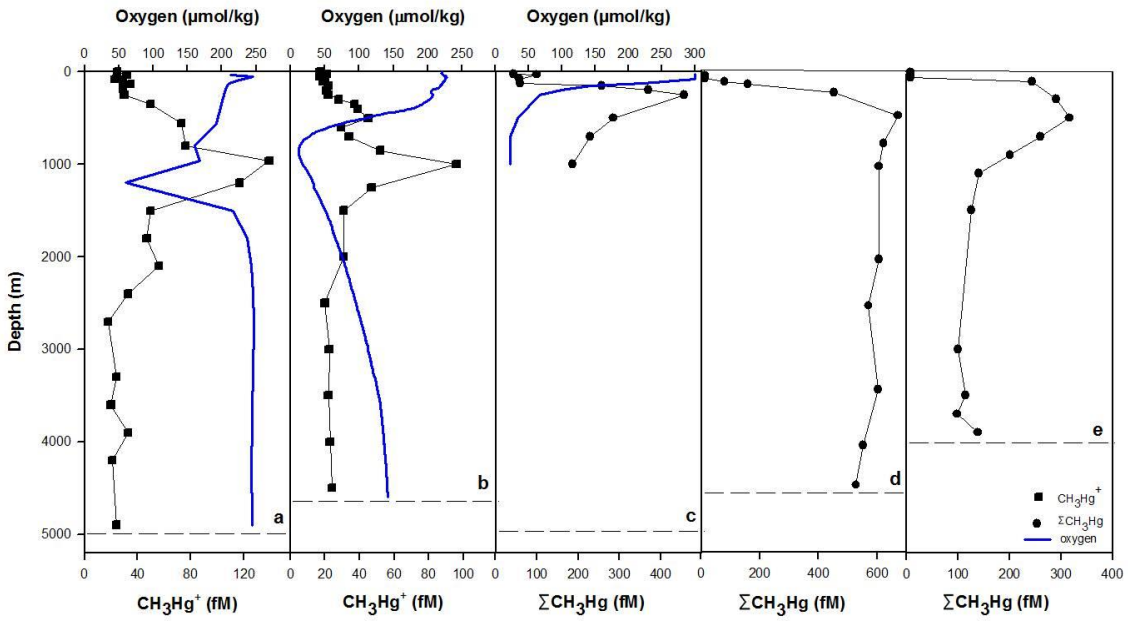

Figure 4. Representative profiles of monomethylmercury (CH_3Hg^+) and total methylated mercury ($\sum CH_3Hg$) in seawater, illustrating a connection to dissolved oxygen distributions. Filtered CH_3Hg^+ in (a) Northeast Atlantic Ocean (unpublished data of author Bowman) and (b) subtropical North Pacific Ocean (Hammerschmidt and Bowman, 2012). $\sum CH_3Hg$ in unfiltered water of the (c) sub-Arctic North Pacific (Sunderland et al., 2009), (d) Southern Ocean (Cossa et al., 2011), and (e) Mediterranean Sea (Cossa et al., 2009). Dashed lines denote the depth of the sediment-water interface.

oxygen minimum, in addition to a slow rate of ventilation in the thermocline. Sectional oceanographic studies have observed associations between methylated mercury species and either apparent oxygen utilization (AOU) or organic carbon remineralization rate (Sunderland et al., 2009), which suggests that production of methylated mercury in the marine water column is limited by methylation potential more than it is by Hg(II) availability.

Much of the previous research describing mercury methylation under anoxic conditions may be of little use in understanding CH_3Hg^+ dynamics in the open ocean. Although strains of iron- and sulfate-reducing bacteria methylate mercury in anoxic sediments (Gilmour et al., 2011), neither functional group is active in the marine water column except under conditions of extreme suboxia associated with some OMZs and microenvironments in sinking particles. The prevalence of CH_3Hg^+ and $(CH_3)_2Hg$ throughout the oxic ocean and active rates of mercury methylation in oxic surface waters (Mason et al., 2012) implies that the ability to methylate mercury is widespread among microorganisms, including aerobes.

Burial

On time scales of tens of thousands of years and more, the ultimate sink for mercury is burial in marine sediments (e.g., Fitzgerald et al., 2007; Amos et al., 2013). Unfortunately, there is not a great deal of data for the concentration of mercury in deep-sea sediments. As a result, we do not have well-constrained estimates for the rate at which sedimentation removes mercury from the ocean. We can make a first order estimate using studies that observed correlations between mercury and organic matter in

sediments (e.g., Fitzgerald et al., 2007) along with estimates for the amount of organic carbon buried on continental shelves and the abyssal ocean. This approach suggests that about 1 Mmol yr^{-1} of mercury is buried in global abyssal sediments, while almost 2 Mmol yr^{-1} are buried on continental shelves. This mercury eventually makes its way back into the global cycle through subduction of marine sediments at active margins, reappearing as mercury volatilized from volcanoes and associated deposits. However, it is clear that more Hg is going into the ocean each year (approximately 7 Mmole yr^{-1} net from atmosphere and rivers; e.g., Amos et al., 2013) than leaving through burial, leading to inevitable increases.

The Anthropogenic Load Timing and Magnitude

As mentioned earlier, human activity has significantly increased the amount of mercury present in biologically active reservoirs at a variety of scales. At present, there is conflicting information regarding the amount of pollution mercury released, the timing of the releases, and fate of that material. What is clear, and as a result of complex biogeochemistry and resulting mobility, is that previously released pollution mercury remains active and contributes to the amount found in active environmental reservoirs (e.g., Amos et al., 2013). Thus, there is a reservoir of "legacy" mercury in the ocean, atmosphere, and soils that must be tracked to adequately assess pollution impacts and that will necessarily result in lags between corrective actions (such as reducing emissions) and subsequent declines in the environment. A critical area of research in environmental mercury biogeochemistry is to assess the scope of mercury perturbations in time and space and to include such information in models that will allow predictions to be made.

Our recent research as part of the GEOTRACES program (Anderson et al., 2014, in this issue; http://www.geotraces.org) has allowed us to estimate the amount of anthropogenic mercury in the ocean from direct oceanographic measurements. We compared the concentration of total mercury to that of remineralized phosphate in deep and intermediate waters from around the world, with an emphasis on the North and South Atlantic. Interestingly, mercury concentrations correlate well with remineralized phosphate in all deep waters except the North Atlantic, indicating that mercury under non-pollution conditions is behaving much like a macronutrient: it increases in concentration as it is swept along the oceanic conveyor belt through the deep Atlantic, into the deep Southern Ocean, then into the deep Indian, and eventually the deep North Pacific. In contrast, mercury-to-remineralized phosphate ratios were greatly increased in NADW of the North Atlantic and some intermediate waters, indicating anthropogenic impact. The excess anthropogenic mercury accounts for about 300 Mmoles present in the ocean today, which has increased concentrations in the surface ocean, permanent thermocline, and deep ocean regions by about 250%, 160%, and 10%, respectively.

Our estimated amount of anthropogenic mercury in the ocean is consistent with the amounts predicted by previous modeling efforts, in particular, with that of Sunderland and Mason (2007). Their model is one of the few to explicitly include deepwater formation when considering the fate of mercury in the ocean. They found about 49% of total anthropogenic mercury resides below 1,500 m depth, similar to our measurements. The model highlights the importance that deepwater formation plays in the fate of anthropogenic Hg in the short term (century to millennium time scale); if this process did not occur, our results suggest that almost twice as much mercury would currently reside

in the surface ocean. This dynamic also has something to tell us about the future of Hg in the ocean. It is predicted that in the next 50 years, as much Hg could be released from industry as has been released in the previous 150 (Streets et al., 2009). However, of the future Hg added to the ocean, a larger proportion will be found in shallower water and will therefore be potentially available for inclusion in the marine food web. In short, not only will Hg concentrations in the surface ocean continue to rise along with emissions, but that rise could be at a faster rate than emissions. Because the residence time of mercury in the mixed layer is only 0.5-1 years, if we reduce atmospheric mercury inputs to the open ocean, there should be a proportional and immediate reduction of mercury concentrations in pelagic food webs.

Historical archives provide compelling evidence of mercury concentration increases in biologically important reservoirs in the ocean. They suggest 200–500% increases of CH_3Hg^+ concentration in the ocean since industrialization. Such an increase of CH_3Hg^+ in seabirds is consistent with the GEOTRACES-based estimate of Hg(II) increases (e.g., Mason et al., 2012). It is possible that changes in the recent past and in some locations may very well be different from global averages. Thus, a conservative description of the state-of-the-science is that many studies support the hypothesis that increased emissions of Hg result in higher Hg concentrations in fish in the ocean, but that there is still much we do not know.

The response of CH_3Hg^+ production in sediments on the continental margin is likely to influence future changes in Hg(II) loadings from either the atmosphere or rivers because surface sediments in nearshore and remote continental shelf regions have accumulated massive reservoirs of Hg(II) since the beginning of human Hg loadings.

Benthic infauna mix this pool of "legacy" mercury throughout the upper 10+ cm of surface sediment. Its burial and removal from active zones of methylation (upper few centimeters) will occur only after centimeters of new sediment are added, which will take decades to centuries in most systems. Future changes in CH_3Hg^+ production and bioaccumulation in coastal ecosystems are most likely to result from alterations of water quality that is hypothesized to influence Hg(II) bioavailability, benthic CH_3Hg^+ flux, and the size and composition of the biological pool into which CH_3Hg^+ is accumulated, but these effects are poorly constrained (Driscoll et al., 2013; Amos et al., 2013).

Global Change Impact on the Mercury Cycle

In addition to the possibility of increased mercury loadings to the ocean in the future, other changes in the marine mercury cycle could occur as a result of changes in climate, ocean physics, and productivity, as well as land use and terrestrial mercury cycling. Several studies have contemplated the potential impact that global change might have on the mercury cycle (e.g., AMAP, 2011; Amos et al., 2013; Krabbenhoft and Sunderland, 2013; UNEP, 2013). However, our current understanding of the dependencies of various aspects of mercury biogeochemistry on these various forcings is too limited to make firm predictions. For example, Table 3 shows a few of the forcings that have been considered, some of which display competing impacts on the mercury cycle. Thus, and as with many aspects of global change science, the impact on the mercury cycle is very uncertain and that realization complicates the job of planning for or mitigating the impact of future mercury loadings to the ocean.

Regional Impact Case Studies

The future of human impacts on the ocean regarding Hg can already be seen in some locations. Below, we highlight two case studies: the South China Sea, which is directly downwind and downriver from the region of largest current anthropogenic Hg emissions, and the Arctic, where a changing climate and unusual atmospheric dynamics combine to threaten people and food webs.

South China Sea

The South China Sea (SCS) receives riverine and atmospheric loadings of Hg from China and surrounding areas, which are among the highest emitters of Hg at present. As a result, the concentrations of Hg found in the SCS are unusually high for a large marginal sea, ranging from 3–10 pM (Fu et al., 2010; Tseng et al., 2012). In contrast, the Mediterranean Sea, which is nearly the same size as the SCS, exhibits Hg concentrations that are about five times less and receives a total areal Hg load that is less than half that of the SCS. Indeed, the SCS is closer in areal loading to urbanized embayments like Long Island Sound than the Mediterranean (Table 2). So much Hg is in the air over the SCS that in winter, when winds are from the northwest, Hg^0 invades the sea in a situation rarely observed anywhere else (evasion is the norm; Tseng et al., 2013). At most times of the year, the evasional flux of Hg from the SCS is virtually the same as that from the Mediterranean and other ocean regions, implying that evasion may not be proportional to total Hg as is frequently assumed (e.g., Amos et al., 2013). If this is the case, then progressively larger percentages of Hg loadings to the wider ocean can be expected to remain there than current models would predict. If the future of most ocean regions is

Table 2. First-order total Hg mass balances for several embayments and marginal seas. Fluxes in nmol m^{-2} yr^{-1}. Data are from Fitzgerald et al. (2007), Rajar et al. (2007), Fu et al. (2010), and Tseng et al. (2012).

Term	NY/NJ Harbor (500 km^2)	San Francisco Bay (1,236 km^2)	Long Island Sound (3,250 km^2)	Chesapeake Bay (12,000 km^2)	Mediterranean Sea (2,510,000 km^2)	South China Sea (3,500,000 km^2)
Sources						
Atmospheric Dep.	40	16.2	40	108	46	186
River/Watershed	4500	977	298	177	26	49
Water Treat. Facilities	460	15.4	18.5	n/a	37*	n/a
Sinks						
Evasion	120	2.4	123	48	99	108
Net Ocean Export	3460	415	25	90	3	102
Burial	1420	592	209	158	22	24
Total Load	5000	1009	357	300	109	235

anything like the SCS, the impact of human emissions may be more serious than we currently appreciate.

The Arctic

There are two reasons that the Arctic is of concern with respect to global mercury change. First, during springtime, so-called Arctic Mercury Depletion Events regularly occur, where a large fraction of lower tropospheric Hg is oxidized and deposited to snow and ice. The chemistry behind this process is not perfectly understood, but likely involves reactive halogen species that are generated during polar sunrise. The result is a large deposition of Hg to the surface in a short period of time and could threaten Arctic ecosystems were it to remain. However, there is chemistry that occurs in snow and ice that results in the reduction and evasion of a substantial fraction of this deposited Hg, lowering the net effect of Depletion Events. The events themselves may not be new phenomena (Drevnick et al., 2012), but with the loss of sea ice in the Arctic, the process of re-emission of Hg deposited by Depletion Events may decrease in the future, dramatically increasing the net load to the Arctic Ocean (assuming snow is better at reducing/evading Hg than the ocean).

A second cause for concern is the impact that global change is having on Hg loadings to the Arctic Ocean from rivers. The Arctic Ocean is a uniquely river-influenced basin, and warming appears to have resulted in a dramatic increase in riverine flow into this stretch of ocean. Much of this increased freshwater is thought to arise from the melting of permafrost and releases a substantial amount of organic carbon in the process. Mercury stored in permafrost soils is also released during this process, and modeling

estimates have suggested that the result could be a substantial increase in Hg loadings from rivers in the coming years (Fisher et al., 2012). The impact of all these forces might already be having an effect, as certain populations of two Arctic animals appear to be threatened by Hg-induced loss of fecundity (Tartu et al., 2013), and others are likely to follow (AMAP, 2011). As with global warming, the Arctic may be the "canary in the coal mine" for the impact of our past, present, and future releases of mercury to the environment.

What Can Be Done?

The future trajectory of ocean mercury depends on socioeconomic and technological factors. Historically, dramatic increases in mercury emission associated with industrialization have increased mercury loading to the ocean. While efforts in several developed countries (including the United States and Europe) have resulted in emissions decreases there, rapidly industrializing countries are currently the main source of atmospheric mercury emission. Depending on how countries industrialize, and what controls are put in place, particularly in Asia, anthropogenic mercury emissions in 2050 could increase by 96%, or decrease by 4%, or anything in between, relative to 2006 emissions (Streets et al., 2009). Under the highest emission scenario, net deposition to the global ocean is projected to increase by 33% (Corbitt et al., 2011).

As present-day anthropogenic sources represent only a fraction (about one-third) of the global emission of mercury to the atmosphere, quantifying the time scales of legacy emission are critical to determining the future of ocean mercury. Importantly, mercury released now is tomorrow's legacy mercury. Global simulations have shown that

future increases in legacy mercury substantially add to estimates of changes in atmospheric deposition under policy scenarios (Amos et al., 2013; Sunderland and Selin, 2013). Thus, controlling emissions today has a long-term benefit.

Policy actions at national, regional, and global scales have addressed mercury pollution sources. In the United States, the recent Mercury and Air Toxics Standards mandate mercury emissions reductions for the first time from power generation sources, in particular, coal-fired power plants. Globally, the Minamata Convention is a new, legally binding international agreement with a goal of protecting human health and the environment from anthropogenic emissions and releases of mercury. The Convention, signed in October 2013, takes a life-cycle approach, addressing mercury production, use, trade, and emissions. Provisions that could have the largest impact on the global ocean are those on atmospheric emissions, releases to land and water, and artisanal and small-scale gold mining (ASGM). On emissions, the Convention requires the application of best available techniques and best environmental practices (BAT/BEP) for new sources, starting five years after the treaty's entry into force (which will likely be 2015 at the earliest). The concept of BAT/BEP takes into account both technical and economic feasibility of controls. For existing sources, parties are required to choose from a variety of measures to control, and where feasible reduce emissions, starting 10 years after entry into force.

Convention provisions on ASGM could also impact future deposition to the ocean. Though previous mercury emission inventories identified stationary combustion as the largest global atmospheric emission sector, the most recent inventory by the United Nations Environment Programme estimates that ASGM is largest (UNEP, 2013). While

there is much uncertainty in the ASGM inventory, and the quantification of how much mercury enters the global atmosphere where it might affect the open ocean and/or remain in local waterways, reducing this source will have benefits on both local and global scales. Under the Minamata Convention, parties with more than insignificant ASGM are required to develop a national action plan and take steps to reduce, and where feasible eliminate, the use and release of mercury in these activities.

Taken together, Minamata Convention provisions could, optimistically, result in emissions trajectory at the low end of those projected for 2050, with implementation of basic emissions controls on a large range of sources (Sunderland and Selin, 2013). These actions would result in avoiding the large increases projected under business-as-usual, but little change from today to 2050 in the amount of mercury in the ocean. This scenario suggests that environmental improvements would require more aggressive action in the future, and that the initial importance of the Minamata Convention may be in raising awareness legally and politically about mercury as a global environmental contaminant.

Moving forward, several lessons emerge for future mercury policy. Experience with regional mercury management suggests that future policy should take into account transboundary influences, coordinate across environmental media, and better assess human and ecological impacts in regulatory analyses. With the new Minamata Convention, coordinating policies across scales—ensuring that national, regional, and international actions are consistent and reinforcing—will become more important. In addition, because mercury is a legacy pollutant, population risks could be further minimized by improved adaptive measures such as fish advisories, before the benefits of international policy are fully realized.

Acknowledgements

We thank Elsie Sunderland, Rob Mason, Ken Johnson, and Bill Landing for helpful discussions. The US GEOTRACES research reported herein was supported by the US National Science Foundation Chemical Oceanography program.

References

AMAP. 2011. *AMAP Assessment 2011: Mercury in the Arctic*. Oslo, Norway, 193 pp. Available online at: http://www.amap.no/documents/doc/amap-assessment-2011-mercury-in-the-arctic/90 (accessed December 8, 2013).

Amos, H.M., D.J. Jacob, D.G. Streets, and E.M. Sunderland. 2013. Legacy impacts of all-time anthropogenic emissions on the global mercury cycle. *Global Biogeochemical Cycles* 27:410–421.

Anderson, R.F., E. Mawji, G.A. Cutter, C.I. Measures, and C. Jeandel. 2014. GEOTRACES – Changing the way we explore ocean chemistry. *Oceanography* 27(1):XX–XX, http://dx.doi.org/XXX.

Barkay, T., S.M. Miller, and A.O. Summers. 2003. Bacterial mercury resistance from atoms to ecosystems. *FEMS Microbiology Reviews* 27:355–384, http://dx.doi.org/10.1016/S0168-6445(03)00046-9.

Benoit, J.M., C.C. Gilmour, R.P. Mason, and A. Heyes. 1999. Sulfide controls on mercury speciation and bioavailability to methylating bacteria in sediment pore waters. *Environmental Science & Technology* 33:951–957, http://dx.doi.org/10.1021/es9808200.

Corbitt, E.S., D.J. Jacob, C.D. Holmes, D.G. Streets, and E.M. Sunderland. 2011. Global source-receptor relationships for mercury deposition under present-day and 2050 emissions scenarios. *Environmental Science & Technology* 45:10,477–10,484.

Cossa, D., B. Averty, and N. Pirrone. 2009. The origin of methylmercury in open Mediterranean waters. *Limnology and Oceanography* 54:837–844.

Cossa, D., L.E. Heimburger, D. Lannuzel, S.R. Rintoul, E.C.V. Butler, A.R. Bowie, B. Averty, R.J. Watson, and T. Remenyi. 2011. Mercury in the Southern Ocean. *Geochimica et Cosmochimica Acta* 75:4,037–4,052.

Dijkstra, J.A., K.L. Buckman, D. Ward, D.W. Evans, M. Dionne, and C.Y. Chen. 2013. Experimental and natural warming elevates mercury concentrations in estuarine fish. *Plos ONE* 8(3):e58401, http://dx.doi.org/10.1371/journal.pone.0058401.

Drevnick, P.E., H. Yang, C.H. Lamborg, and N.L. Rose. 2012. Net atmospheric mercury deposition to Svalbard: Estimates from lacustrine sediments. *Atmospheric Environment* 59:509–513, http://dx.doi.org/10.1016/j.atmosenv.2012.05.048.

Driscoll, C.T., R.P. Mason, H.M. Chan, D.J. Jacob, and N. Pirrone. 2013. Mercury as a global pollutant: Sources, pathways, and effects. *Environmental Science & Technology* 47: 4,967–4,983.

Fisher, J.A., D.J. Jacob, A.L. Soerensen, H.M. Amos, A. Steffen, and E.M. Sunderland. 2012. Riverine source of Arctic Ocean mercury inferred from atmospheric observations. *Nature Geoscience* 5:499–504.

Fitzgerald, W.F., C.H. Lamborg, and C.R. Hammerschmidt. 2007. Marine biogeochemical cycling of mercury. *Chemical Reviews* 107:641–662.

Fu, X.W., X. Feng, G. Zhang, W. Xu, X. Li, H. Yao, P. Liang, J. Li, J. Sommar, R. Yin, and N. Liu. 2010. Mercury in the marine boundary layer and seawater of the South China Sea: Concentrations, sea/air flux, and implication for land outflow. *Journal of Geophysical Research* 115, D06303, http://dx.doi.org/10.1029/2009jd012958.

Gilmour, C.C., D.A. Elias, A.M. Kucken, S.D. Brown, A.V. Palumbo, C.W. Schadt, and J.D. Wall. 2011. Sulfate-teducing bacterium *Desulfovibrio desulfuricans* ND132 as a model for understanding bacterial mercury methylation. *Applied and Environmental Microbiology* 77:3,938–3,951.

Hammerschmidt, C.R., W.F. Fitzgerald, P.H. Balcom, and P.T. Visscher. 2008. Organic matter and sulfide inhibit methylmercury production in sediments of New York/New Jersey Harbor. *Marine Chemistry* 109:165–182.

Hammerschmidt, C.R., and K.L. Bowman. 2012. Vertical methylmercury distribution in the subtropical North Pacific. *Marine Chemistry* 132–133:77–82.

Krabbenhoft, D.P., and E.M. Sunderland. 2013. Global change and mercury. *Science* 341:1,457–1,458.

Mahaffey, K.R., R.P. Clickner, and R.A. Jeffries. 2009. Adult women's blood mercury concentrations vary regionally in the United States: Association with patterns of fish consumption (NHANES 1999–2004). *Environmental Health Perspectives* 117:47–53, http://dx.doi.org/10.1289/ehp.11674.

Mason, R.P., and W.F. Fitzgerald. 1993. The distribution and biogeochemical cycling of mercury in the Equatorial Pacific Ocean. *Deep Sea Research Part I* 40:1,897–1,924, http://dx.doi.org/10.1016/0967-0637(93)90037-4.

Mason, R.P., A.L. Choi, W.F. Fitzgerald, C.R. Hammerschmidt, C.H. Lamborg, A.L. Soerensen, and E.M. Sunderland. 2012. Mercury biogeochemical cycling in the ocean and policy implications. *Environmental Research* 119:101–117, http://dx.doi.org/10.1016/j.envres.2012.03.013.

Parks, J.M., A. Johs, M. Podar, R. Bridou, R.A. Hurt Jr., S.D. Smith, S.J. Tomanicek, Y. Qian, S.D. Brown, C.D. Brandt, and others. 2013. The genetic basis for bacterial mercury methylation. *Science* 339:1,332–1,335, http://dx.doi.org/10.1126/science.1230667.

Rajar, R., M. Cetina, M. Horvat, and D. Zagar. 2007. Mass balance of mercury in the Mediterranean Sea. *Marine Chemistry* 107:89–102.

Scheuhammer, A.M., M.W. Meyer, M.B. Sandheinrich, and M.W. Murray. 2007. Effects of environmental methylmercury on the health of wild birds, mammals, and fish. *Ambio* 36:12–18, http://dx.doi.org/10.1579/0044-7447(2007)36[12:EOEMOT]2.0.CO;2.

Selin, N.E., E.M. Sunderland, C.D. Knightes, and R.A. Mason. 2010. Sources of mercury exposure for US seafood consumers: Implications for policy. *Environmental Health Perspectives* 118:137–143, http://dx.doi.org/10.1289/ehp.0900811.

Selin, N.E. 2013. Global change and mercury cycling: Challenges for implementing a global mercury treaty. *Environmental Toxicology and Chemistry* http://dx.doi.org/10.1002/etc.2374.

Streets, D.G., Q. Zhang, and Y. Wu. 2009. Projections of global mercury emissions in 2050. *Environmental Science & Technology* 43:2,983–2,988, http://dx.doi.org/10.1021/es802474j.

Sunderland, E.M., and R.P. Mason. 2007. Human impacts on open ocean mercury concentrations. *Global Biogeochemical Cycles* 21, GB4022, http://dx.doi.org/10.1029/2006GB002876.

Sunderland, E.M., D.P. Krabbenhoft, J.W. Moreau, S.A. Strode, and W.M. Landing. 2009. Mercury sources, distribution, and bioavailability in the North Pacific Ocean: Insights from data and models. *Global Biogeochemical Cycles* 23, GB2010, http://dx.doi.org/10.1029/2008GB003425.

Sunderland, E.M., and N.E. Selin. 2013. Future trends in environmental mercury concentrations: Implications for prevention strategies. *Environmental Health* 12:2, http://dx.doi.org/10.1186/1476-069x-12-2.

Tartu, S., A. Goutte, P. Bustamante, F. Angelier, B. Moe, C. Clément-Chastel, C. Bech, G.W. Gabrielsen, J.O. Bustnes, and O. Chastel. 2013. To breed or not to breed:

Endocrine response to mercury contamination by an Arctic seabird. *Biology Letters* 9(4), http://dx.doi.org/10.1098/rsbl.2013.0317.

Tseng, C.M., C.S. Liu, and C. Lamborg. 2012. Seasonal changes in gaseous elemental mercury in relation to monsoon cycling over the northern South China Sea. *Atmospheric Chemistry and Physics* 12:7,341–7,350, http://dx.doi.org/10.5194/acp-12-7341-2012.

Tseng, C.-M., C.H. Lamborg, and S.-C. Hsu, 2013. A unique seasonal pattern in dissolved elemental mercury in the South China Sea, a tropical and monsoon-dominated marginal sea. *Geophysical Research Letters*, 40, 167–172, doi: 10.1029/2012GL054457.

UNEP. 2013. *Global Mercury Assessment 2013: Sources, Emissions, Releases and Environmental Transport*. UNEP Chemicals Branch, Geneva, Switzerland, 42 pp.

Appendix D. A global ocean inventory of anthropogenic mercury based on water column measurements

Lamborg, C.H., Hammerschmidt, C.R., Bowman, K.L., Swarr, G.J., Munson, K.M., Ohnemus, D.C., Lam, P.J., Heimbürger, L.-E., Rijkenberg, M.J.A., Saito, M.A. 2014. A global ocean inventory of anthropogenic mercury based on water column measurements. Nature 512, 65–68.

A global ocean anthropogenic mercury inventory based on water column measurements

Carl H. Lamborg[1], Chad R. Hammerschmidt[2], Katlin L. Bowman[2], Gretchen J. Swarr[1], Kathleen M. Munson[1], Daniel C. Ohnemus[1], Phoebe J. Lam[1], Lars-Eric Heimbürger[3], Micha J.A. Rijkenberg[4] and Mak A. Saito[1]

[1]*Department of Marine Chemistry and Geochemistry, Woods Hole Oceanographic Institution, Woods Hole, MA 02543 USA*

[2]*Department of Earth and Environmental Sciences, Wright State University, Dayton, OH 45435 USA*

[3]*Observatoire Midi-Pyrénées, Laboratoire Géosciences Environnement Toulouse, CNRS/IRD/Université Paul-Sabatier, 14, avenue Édouard Belin, 31400 Toulouse, France*

[4]*Department of Biological Oceanography, Royal Netherlands Institute for Sea Research, Den Burg, 1790 AB, The Netherlands*

Mercury (Hg) is a toxic, bioaccumulating trace metal whose emissions to the environment have increased significantly as a result of anthropogenic activities such as mining and fossil fuel combustion[1,2]. Several recent models have estimated that these emissions have increased the oceanic Hg inventory by 36-1313 Mmoles since the 1500's[2-9]. Such predictions have remained largely untested due to a lack of appropriate historical data and natural archives. Here we show oceanographic measurements of Hg and related parameters from several recent expeditions to the Atlantic, Pacific, Southern and Arctic Oceans. We find that deep North Atlantic waters and most intermediate waters are anomalously enriched in Hg relative to deep waters of the South Atlantic, Southern and Pacific Oceans, likely as a result of the incorporation of anthropogenic Hg. We estimate the total amount of anthropogenic Hg present in the global ocean to be 290±80 Mmoles, with almost two thirds residing in water shallower than 1000 m. Our findings suggest that anthropogenic perturbations to the global Hg cycle have led to a ~150% increase in

the amount of Hg in thermocline waters and have more than tripled the Hg content of surface waters. This information may aid our understanding of the processes and the depths at which inorganic Hg species are converted into toxic methylmercury and subsequently bioaccumulated in marine food webs.

Mercury is emitted to the atmosphere by natural and human sources primarily as Hg^o, which is unusually volatile for a metal[1]. The elemental form is removed from the atmosphere after oxidation to Hg^{2+} which is then deposited to land and ocean. Within the ocean, Hg^{2+} is readily reduced to Hg^o, resulting in surface waters being supersaturated in the elemental form with respect to the atmosphere. With an atmospheric lifetime between a few months and a year as well as the evasion of Hg^o from the ocean to the atmosphere, Hg from any source can be widely dispersed across the globe[5]. Hg in the ocean is also subject to bioaccumulation and scavenging by organic-rich particles. Such particles eventually sink out of the surface ocean and are respired at deeper depths, transporting carbon, nutrients and metals like Hg in the process. In this way, Hg is very much like CO_2 in that it is a biologically active gas that exhibits wide dispersal in the atmosphere, vigorous air-sea exchange and vertical transport in the ocean as a result of the particulate "biological carbon pump[10]." Like the other Group 12 elements (Zn and Cd)[11] we might expect that Hg distributions in the ocean should mimic macronutrients like PO_4^{3-} (low in the surface, increasing through the thermocline, higher in the deep Pacific than deep Atlantic). As can be seen in some representative vertical profiles of Hg concentrations (Figure 1), this general trend is indeed observed.

However, oceanic Hg distributions are a combination of pre-anthropogenic, nutrient-like and transient signals resulting from human activities over the past several centuries.

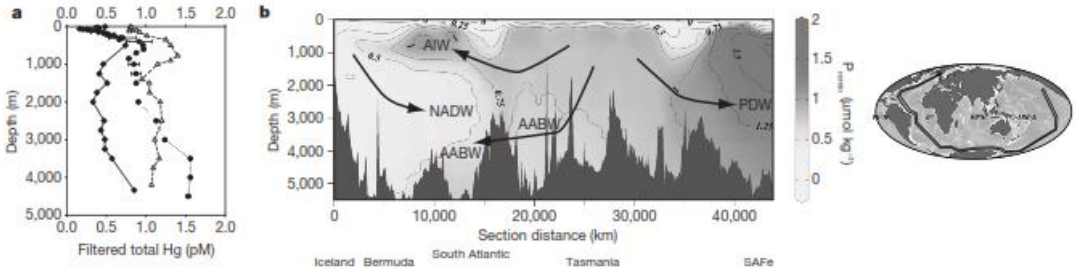

Figure 1. **Mercury and P_{remin} distributions in the Ocean.** Panel a, representative profiles of total dissolved Hg from the North Atlantic near Bermuda (triangles), from the South Atlantic (circles) and NE Pacific Ocean (the "SAFe" station) as well as (Panel b) world-wide vertical distribution of P_{remin} as interpolated from WOCE data (www.ewoce.org).

Figure 2 shows the concentrations of Hg and dissolved phosphate released during organic matter remineralization (P_{remin}=AOU/170) measured in a variety of water masses from GEOTRACES cruises to the North and South Atlantic Oceans, the Pacific sector of the Southern Ocean, a GEOTRACES Intercalibration cruise to the subtropical NE Pacific Ocean and non-GEOTRACES cruises to the tropical Pacific (the "Metalloenzyme Cruise"), the North Pacific (CLIVAR Repeat P16), and the central Arctic Ocean (2011 Polarstern cruise TransArc ARK XXIV/3) [12-17]. In the water masses other than Northern Hemisphere North Atlantic Deep Water and recently subducted Antarctic Bottom Water (henceforth referred to as "un-impacted" deep waters), a striking correlation between Hg and P_{remin} is seen (the reduced major axis regression line in Figure 2). This correlation offers several important insights: 1) these water masses possess little anthropogenic Hg delivered by the biological pump, otherwise a good correlation along and a y-intercept that is essentially zero (-0.07± 0.03 μmole Hg) would not have been observed (see supplemental material for more discussion); 2) the slope of the line is an expression of the Hg/P ratio in sinking organic matter formed in surface waters from before the anthropogenic impact (1.02 ± 0.03 μmole Hg/mole P); 3) the relationship allows us to use it as a benchmark against which water masses that do contain anthropogenic Hg can be compared.

The impact of anthropogenic Hg emissions in the deep North Atlantic and various thermocline water masses is evident in Figure 2, with data points that lie above the unimpacted deep water regression line showing evidence of anthropogenic Hg contributions, and the vertical distance between the data and the line representing the amount of Hg in that water mass contributed from human sources. It is immediately

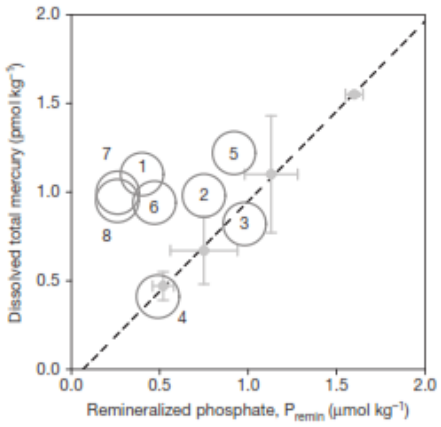

Figure 2. **The concentration of Hg and P_{remin} in various water masses**. The gray symbols are the data from deep waters (>1000 m depth) not suspected of possessing anthropogenic Hg. The remaining symbols include North Atlantic Deep Water in the North Atlantic (1), Antarctic Bottom Water sampled between Tasmania and Antarctica (2), and thermocline waters from the North Atlantic (6), South Atlantic (4), the southern Ocean between Tasmania and Antarctica (8), the Arctic Ocean (7), the Northeast Pacific (5) and tropical Pacific (3).

apparent, however, that the degree of Hg perturbation for each water mass is not equal. This can be explored further by dividing the amount of anthropogenic Hg in each water mass by a tracer, preferably a pollutant that has a similar emissions history. This will allow the derived amount of Hg_{anth} to be cross-checked against expectations as well as greatly simplify the conversion of our measurements to a scaled-up estimate of the total amount of pollutant Hg in the ocean. For this purpose, we have selected the amount of CO_{2anth} present in each water mass (Table 1). The CO_{2anth} estimates were derived with the □C* method of Gruber and colleagues[18] from a variety of data sets,[19] and then gridded over the whole ocean (the GLODAP database).[20] The Hg_{anth}/CO_{2anth} ratios in most of the water masses are not statistically different from either each other or the Hg/CO_2 ratio in primary anthropogenic atmospheric emissions (9.6-12.4 Mmole Hg/y; 0.79±0.04 Pmole C/y; Hg/C=14±2 nmole/mole).[21-23] However, shallower water masses appear to have smaller mean Hg_{anth}/CO_{2anth} ratios than either North Atlantic Deep Water (NADW) or Antarctic Bottom Water (AABW), which contain mean Hg_{anth}/CO_{2anth} ratios that exceed those in most known emissions sources[22]. The cause of this higher ratio is unclear, but it may be attributed to either high localized rates of atmospheric Hg deposition due to high rates of precipitation (Southern Ocean), enrichment caused by salt rejection during ice formation[14], proximity to historically strong regions of Hg emissions in North America and Europe (North Atlantic) or the prevalence of coal burning as a source of CO_2 early in the Industrial Revolution. For example, surface waters near Iceland (the site of NADW formation) and Antarctica (AABW) are enriched in Hg (~2 pM)[14,24] with respect to average surface waters (0.6 pM; see below), which is consistent with greater mean Hg/CO_2 ratios in these deep waters. Some alteration in Hg_{anth}/CO_{2anth} ratios should also

Table 1. Summary of Hg, P_{remin} and CO_{2anth} data.

Basin/Water Mass	Hg (pmole kg^{-1})	P_{remin} (µmole kg^{-1})	Hg_{anth} (pmole kg^{-1})	CO_{2anth} (µmole kg^{-1})	$(Hg/CO_2)_{anth}$ (nmole $mole^{-1}$)
Unimpacted deep waters					
South Atlantic/NADW[a]	0.47±0.08	0.52±0.06	0	0	---
South Atlantic/AABW[b]	0.67±0.19	0.75±0.19	0	0	---
Tropical Pacific/PDW and PBW[c]	1.10±0.33	1.13±0.15	0	0	---
Subtropical Northeast Pacific/ PDW and PBW[d]	1.55±0.01	1.60±0.05	0	0	---
Impacted deep waters					
North Atlantic/NADW[a]	1.1±0.2	0.40±0.05	0.72±0.17	10.2±9.7	58±29
Southern Ocean/AABW[g]	0.98±0.17	0.75±0.10	0.29±0.20	5±4	76±8
Thermocline waters					
South Atlantic/thermocline[e]	0.41±0.14	0.49±0.35	-0.02±0.28	25±13	---
Tropical Pacific/thermocline[e]	0.82±0.35	0.98±0.48	-0.10±0.60	16±16	---
North Atlantic/thermocline[e]	0.94±0.27	0.47±0.30	0.52±0.21	42±14	15±8
Northeast Pacific/thermocline[e]	1.22±0.39	0.92±0.72	0.35±0.59	25±14	23±18
Arctic Ocean/thermocline[f]	1.00±0.11	0.26±0.03	0.80±0.12	~30	~27
Southern Ocean/thermocline[g]	0.95±0.057	0.47±0.33	0.66±0.57	22±12	37±24

Hg, P_{remin} and CO_{2anth} values are water mass averages. The Hg_{anth} and $(Hg/CO_2)_{anth}$ values shown are averages of sample-by-sample calculations.

Selection criteria:

[a]all stations from section, depths between 1500 and 4000 m.

[b]all stations from section, depths below 4000 m.

[c]all stations from section, depths below 1000 m.

[d]one station, depths below 1000 m.

[e]all stations, depths 100-1000 m.

[f]two stations, depths 200-1000 m.

[g]all stations south of 50^{o} S, depths 100-1000 m.

be expected from the differential behaviors in the ocean between these two biologically active gases (Hg_{anth} will be moved into the thermocline and mode waters by both the biological as well as the solubility pump,[10] while CO_{2anth} will not be pumped biologically as oceanic primary productivity is not C limited).

We used the observed Hg_{anth}/CO_{2anth} ratios in each impacted water mass to estimate the inventory of Hg_{anth} in the ocean as a whole by multiplying these ratios by the estimated amount of CO_{2anth} in the ocean (9.8 ± 1.6 Pmole C)[19]. Given the still small and evolving amount of oceanographic Hg data available, we chose to use one Hg_{anth}/CO_{2anth} ratio for intermediate waters (100–1000 m; 25 ± 11 nmole/mole) and another for the deep North Atlantic (66 ± 14 nmole/mole), and use the GLODAP model estimate for the percentage of CO_{2anth} in each ocean layer: 15% in surface water, 71% in intermediate waters, and 16% in deep. This calculation suggests that there is about 170 ± 80 Mmoles of anthropogenic Hg between 100 and 1000 m depth and about 100 ± 20 Mmoles deeper than 1000 m.

Identifying the anthropogenic impact on Hg in waters shallower than 100 m using P_{remin} is not appropriate because atmospheric deposition is the primary source of Hg to the surface ocean, not particle remineralization. Alternatively, we estimated Hg_{anth} in surface waters by comparing the slope of the regression in Figure 2 with the Hg/P ratio in contemporary suspended particulate matter. The Hg/P ratio was derived from analysis of Hg and P in mixed-layer particulate matter collected by *in situ* pumping performed during both the North Atlantic GEOTRACES and tropical Pacific Metalloenzyme cruises. This ratio is 3.4 ± 1.3 μmole Hg/mole P, indicating a factor of 3.4 ± 1.3 increase in the concentration of Hg in microseston since industrialization. This degree of secular

change of Hg in surface waters is consistent with archives of atmospheric Hg deposition that indicate a 2–5× increase worldwide since industrialization[25]. The data presented here suggest that the total amount of Hg in the top 100 m of the ocean is about 22 Mmole (an average concentration of 0.6 pM). Accordingly, Hg_{anth} in this layer is about 16 ± 6 Mmoles.

Our overall estimate of 290 ± 80 Mmoles (rounded to 2 significant figures) of Hg_{anth} in the ocean is in reasonable agreement with a number of model-based predictions,[4,7,8,26] but suggests the highest and lowest estimates are implausible. On the high end is the prediction of Streets and colleagues,[2] who estimated an amount of Hg_{anth} in the ocean of 1313 Mmoles, which required a major contribution from artisanal and small-scale gold mining currently and in the past. This particular inventory is important to test as it has featured prominently in recent negotiations concerning international efforts to curb emissions of Hg to the environment.[27] Our measurements and calculations here suggest that either the Streets estimate for past Hg anthropogenic releases are too high, or that much of the Hg they predicted to be in the ocean resides elsewhere, such as in soils. Recent work by Lyatt Jaegle, Yanxu Zhang and colleagues has provided support for this as well using modeling fits to water column profiles that also suggest loadings to the ocean are lower than those of Streets and colleagues.[28] It should be noted that the estimate for total CO_{2anth} to which we have indexed[19] is for the year 1994. Estimates for more recent times and with different methods suggest greater CO_{2anth} (e.g., 12.9 Pmole[29]) which would predict higher values of Hg_{anth} as well (380 Mmole). However, this higher estimate is still much less than that of Streets et al.

As noted, we found that about a third of anthropogenic Hg loadings to the ocean are in deep water, particularly NADW. One model with which our results agree quite well is that of Sunderland and Mason[7], who used a multi-box model that explicitly included deep water formation in the North Atlantic. In their simulation, 129 Mmoles of Hg_{anth} reside shallower than 1500 m in the ocean, with another 124 Mmoles in deeper waters. Thus, the prevalence of anthropogenic Hg in deep waters of the North Atlantic indicate the importance, as captured by the Sunderland and Mason model, of deep water formation for sequestration of surface Hg on millennial timescales. This observation also leads to the conclusion, given that Hg emissions from anthropogenic sources are predicted to increase at a rate faster than in the previous few centuries,[21] that future loadings may somewhat overwhelm the deep water formation sink. Thus, we should expect that the rate of increase of Hg in surface waters in the next few decades should be greater than the rate of increase in emissions during the same time period.

The impact of anthropogenic loadings on the oceanic Hg reservoir can be estimated with knowledge of the total amount of Hg in the ocean. Using the North and South Atlantic concentration profiles to each represent a quarter of the whole ocean and the Pacific profiles to represent the other half, we estimated that the ocean contains 1390 Mmoles of dissolved total Hg, with 22 Mmoles in the 0–100 m surface ocean, 292 Mmoles in the 100–1000 m intermediate depths and 1260 Mmoles in waters deeper than 1000 m (the average concentration in these three layers being 0.6, 0.9 and 1.0 pM, respectively[13-15,17,30]). These amounts are less than most previous estimates; for example, Sunderland and Mason[7] estimated 666 Mmoles shallower than 1500 m and 1095 Mmoles in deeper water. Thus, analysis of the new data presented here suggests that the relative

impact of human Hg emissions on the ocean is greater than previously thought: waters shallower than 1000 m appear to have contained 120 Mmole in the pre-industrial past, and exhibit a factor of 2.6× increase, while the ocean as a whole has experienced a 1.1× increase.

As our analysis reveals, and as has been noted elsewhere,[26] the impact of human Hg emissions is not uniform within the ocean. Therefore, the extent to which methylmercury concentrations in fish have changed since industrialization, and might change in response to further perturbation (perhaps as much as a 5× increase over pre-industrial by 2050)[21] can be determined only following studies of the vertical patterns in Hg methylation dynamics as well as basin-scale controls on methylation of anthropogenic Hg.

References

1 Fitzgerald, W. F. & Lamborg, C. H. in *Treatise on Geochemistry* Vol. Vol. 9, Chp. 4 eds Heinrich D. Holland & Karl K. Turekian) 1-47 (Pergamon, 2003).

2 Streets, D. G. *et al.* All-Time Releases of Mercury to the Atmosphere from Human Activities. *Environ Sci Technol* **45**, 10485-10491, doi:10.1021/es202765m (2011).

3 Mason, R. P., Fitzgerald, W. F. & Morel, F. M. M. The biogeochemical cycling of elemental mercury - anthropogenic influences. *Geochim Cosmochim Acta* **58**, 3191-3198 (1994).

4 Lamborg, C. H., Fitzgerald, W. F., O'Donnell, J. & Torgersen, T. A non-steady-state compartmental model of global-scale mercury biogeochemistry with interhemispheric atmospheric gradients. *Geochim Cosmochim Acta* **66**, 1105-1118 (2002).

5 Selin, N. E. *et al.* Global 3-D land-ocean-atmosphere model for mercury: Present-day versus preindustrial cycles and anthropogenic enrichment factors for deposition. *Glob Biogeochem Cycles* **22**, GB2011, doi:2010.1029/2007GB003040 (2008).

6 Soerensen, A. L. *et al.* An Improved Global Model for Air-Sea Exchange of Mercury: High Concentrations over the North Atlantic. *Environ Sci Technol* **44**, 8574-8580, doi:10.1021/es102032g (2010).

7 Sunderland, E. M. & Mason, R. P. Human impacts on open ocean mercury concentrations. *Glob Biogeochem Cycles* **21**, GB4022 (2007).

8 Strode, S., Jaegle, L. & Emerson, S. Vertical transport of anthropogenic mercury in the ocean. *Glob Biogeochem Cycles* **24**, doi:Gb4014/10.1029/2009gb003728 (2010).

9 Amos, H. M., Jacob, D. J., Streets, D. G. & Sunderland, E. M. Legacy impacts of all-time anthropogenic emissions on the global mercury cycle. *Glob Biogeochem Cycles*, n/a-n/a, doi:10.1002/gbc.20040 (2013).

10 Volk, T. & Hoffert, M. in *The Carbon Cycle and Atmospheric CO_2: Natural Variations Archean to Present.* eds E. Sundquist & W.S. Broecker) 99-110 (American Geophysical Union, 1985).

11 Morel, F. M. M., Milligan, A. J. & Saito, M. A. in *Treatise on Geochemistry - Volume 6: The Oceans and Marine Geochemistry* (ed H. Elderfield) 113-143 (Elsevier, Inc., 2003).

12 Anderson, L. A. & Sarmiento, J. L. Redfield ratios of remineralization determined by nutrient data-analysis. *Glob Biogeochem Cycles* **8**, 65-80, doi:10.1029/93gb03318 (1994).

13 Bowman, K. L., Hammerschmidt, C. R., Lamborg, C. H. & Swarr, G. J. Mercury in the North Atlantic Ocean: The U.S. GEOTRACES zonal and meridional sections. *Deep Sea Research Part II* (in review).

14 Cossa, D. *et al.* Mercury in the Southern Ocean. *Geochim Cosmochim Acta* **75**, 4037-4052, doi:10.1016/j.gca.2011.05.001 (2011).

15 Hammerschmidt, C. R. & Bowman, K. L. Vertical methylmercury distribution in the subtropical North Pacific *Marine Chemistry* **132-133**, 77-82 (2012).

16 Munson, K. M., Lamborg, C. H., Swarr, G. & Saito, M. A. Mercury species concentrations and fluxes in the equatorial and southern Pacific Ocean. (in preparation).

17 Sunderland, E. M., Krabbenhoft, D. P., Moreau, J. W., Strode, S. A. & Landing, W. M. Mercury sources, distribution, and bioavailability in the North Pacific Ocean: Insights from data and models. *Glob Biogeochem Cycles* **23**, GB2010 (2009).

18 Gruber, N., Sarmiento, J. L. & Stocker, T. F. An improved method for detecting anthropogenic CO2 in the oceans. *Glob Biogeochem Cycles* **10**, 809-837, doi:10.1029/96gb01608 (1996).

19 Sabine, C. L. *et al.* The oceanic sink for anthropogenic CO2. *Science* **305**, 367-371 (2004).

20 Key, R. M. *et al.* A global ocean carbon climatology: Results from Global Data Analysis Project (GLODAP). *Glob Biogeochem Cycles* **18**, - (2004).

21 Streets, D. G., Zhang, Q. & Wu, Y. Projections of Global Mercury Emissions in 2050. *Environ Sci Technol* **43**, 2983-2988 (2009).

22 Pacyna, E. G. *et al.* Global emission of mercury to the atmosphere from anthropogenic sources in 2005 and projections to 2020. *Atmospheric Environment* **44**, 2487-2499, doi:10.1016/j.atmosenv.2009.06.009 (2010).

23 Le Quéré, C. *et al.* The global carbon budget 1959-2011. *Earth Syst. Sci. Data Discuss.* **5**, 1107-1157, doi:10.5194/essdd-5-1107-2012 (2012).

24 Mason, R. P., Rolfhus, K. R. & Fitzgerald, W. F. Mercury in the North Atlantic. *Marine Chemistry* **61**, 37-53 (1998).

25 Lamborg, C. H. *et al.* Modern and historic atmospheric mercury fluxes in both hemispheres: Global and regional mercury cycling implications. *Glob Biogeochem Cycles* **16**, 1104, doi: 1110.1029/2001GB001847 (2002).

26 Mason, R. P. *et al.* Mercury biogeochemical cycling in the ocean and policy implications. *Environmental Research* **119**, 101-117, doi:10.1016/j.envres.2012.03.013 (2012).

27 Selin, N. E. Global change and mercury cycling: Challenges for implementing a global mercury treaty. *Environmental Toxicology and Chemistry*, n/a-n/a, doi:10.1002/etc.2374 (2013).

28 Jaegle, L. *et al.* in *11th International Conference on Mercury as a Global Pollutant* (Edinburgh, Scotland, 2013).

29 Khatiwala, S. *et al.* Global ocean storage of anthropogenic carbon. *Biogeosciences* **10**, 2169-2191, doi:10.5194/bg-10-2169-2013 (2013).

30 Swarr, G., Lamborg, C. H., Rijkenberg, M. & Hammerschmidt, C. R. Total dissolved Hg on a meridional transect in the SW Atlantic Ocean. (in preparation).

Acknowledgements We thank the Captains and crews of all cruises as well as Pete Morton, Jess Fitzsimmons, Rachel Shelley, Ana Aquilar-Islas, Randi Bundy, Paul Morris, Stephanie Owens, Kuanbo Wang, Sylvain Rigaud and Steve Pike for sample collection during the North Atlantic GEOTRACES cruise, Lennart Groot, Dominik Weiss, Patrick Laan, Jeroen de Jong, Rob Middag, Leo Pena, Alison Hartman, José Marcus Godoy, Loes Gerringa, Marie Boyé and Jonathan Dérot for sample collection during the South Atlantic GEOTRACES cruise and Tyler Goepfert, Erin Bertrand and Dawn Moran for sampling during the Metalloenzyme cruise and Michiel Rutgers van der Loeff and Ben Galfond for providing samples from the 2011 Polarstern cruise to the central Arctic Ocean. We also very grateful to Daniel Cossa and Elsie Sunderland for providing digital versions of their Southern Ocean and P16 data. Thanks also to Helen Amos, Lyatt Jaegle, Bror Jonsson, Rob Mason, Elsie Sunderland and Yanxu Zhang for helpful discussions and three anonymous reviewers and Daniel Cossa for important comments. This work was supported by NSF grants: OCE-0825108, -0825157, -0927274, -0928191, -1031271, -1132480, and -1132515, and we thank co-PI's, Robert Mason and Gary Gill.

Author Contributions CHL, CRH, KLB, GS, DCO, LEH, MJAR and MAS participated in GEOTRACES, Metalloenzyme and Tara cruises; CHL, CRH, KLB, GS and LEH performed Hg analyses; DCO and PJL designed the particulate sampling experiments and performed P analyses; CHL, CRH, MJAR, MAS and LEH designed the Hg-related experiments; CHL, CRH, KLB, GS, KMM and LEH interpreted the data; all authors contributed to manuscript preparation.

Methods

Dissolved water samples were collected using ultra-clean techniques,[31] including the use of a largely metal-free collection system and pressure filtration to 0.45 μm of water samples directly from the sampling GO-Flo bottles. Aliquots for total dissolved Hg were collected in 250-mL, acid-washed, borosilicate glass bottles, digested with BrCl and analyzed by Cold Vapor Atomic Fluorescence Spectrometry following $SnCl_2$ reduction and gold-trap pre-concentration[32-34].

P_{remin} was calculated according to Anderson and Sarmiento[12] as P_{remin} = AOU / 170±10, where AOU is the apparent oxygen utilization and is calculated as $[O_2]_{sat} - [O_2]_{obs}$, where $[O_2]_{sat}$ is determined from depth, temperature and salinity[35].

Particulate Hg and P were determined from subsamples of QMA or polyethersulfone (PES) filters loaded with suspended matter (<51 μm) using McLane pumps. For Hg, the filter aliquots were digested with 2 M HNO_3, and the digest treated as dissolved samples[36]. For P, PES filter subsamples were digested in a 3:1 sulfuric acid:hydrogen peroxide solution to oxidize and dissolve the PES filter, dried down, and then particles were digested in a 4N HCl/HNO_3/HF mixture[37]. The digest was analyzed for multiple elements including P on a high resolution Inductively Coupled Plasma Mass Spectrometer and standardized using multi-element external standards (similar to Lamborg et al.[38]).

Water masses were defined primarily based on depth (as noted in Table 1), in accordance with those suggested by Talley and colleagues.[39] This definition represents an

approximation for more refined definitions made of the basis of temperature, salinity and basin.

Appendix E. Permission to reprint

2. Extraction of monomethylmercury from seawater for low-femtomolar determination

To: Ms. Katlin L Bowman,
On behalf of the Association for the Sciences of Limnology and Oceanography, we are happy to grant permission to use the figures from Limnology & Oceanography per your application. We are granting this one time use for your PhD dissertation which is not to be sold.

When reproducing the article/figure(s), please cite according to the references that follow:

All copyrighted works, whether displayed electronically or in print, should be properly acknowledged as follows:

"Copyright (Year) by the Association for the Sciences of Limnology and Oceanography, Inc."

Once permission is granted to use an article or any part thereof of a work from L&O, the full citation must include:
1. Name(s) of the author(s);
2. Journal title (Association for the Sciences of Limnology & Oceanography or L&O)
3. Publication date
4. Volume number
5. Issue number
6. Chapter or article name
7. Pages on which the articles, data, and/ or figure(s) appear

For your records, the Association for the Sciences of Limnology and Oceanography is a nonprofit organization. (Taxpayer I.D. Number: 38-1710020)

If you have additional requests or have any questions in regard to this request, you can contact me directly via e-mail at jdavis@sgmeet.com.

Sincerely,

Jo Davis
ASLO Business Office
Database Supervison

3. Mercury in the North Atlantic Ocean: The U.S. GEOTRACES zonal and meridional sections

ELSEVIER LICENSE
TERMS AND CONDITIONS

Nov 12, 2014

This is a License Agreement between Katlin L. Bowman ("You") and Elsevier ("Elsevier") provided by Copyright Clearance Center ("CCC"). The license consists of your order details, the terms and conditions provided by Elsevier, and the payment terms and conditions.

All payments must be made in full to CCC. For payment instructions, please see information listed at the bottom of this form.

Supplier	Elsevier Limited The Boulevard,Langford Lane Kidlington,Oxford,OX5 1GB,UK
Registered Company Number	1982084
Customer name	Katlin L. Bowman
Customer address	425 Dayton Towers Drive DAYTON, OH 45410
License number	3487900268955
License date	Oct 14, 2014
Licensed content publisher	Elsevier
Licensed content publication	Deep Sea Research Part II: Topical Studies in Oceanography
Licensed content title	Mercury in the North Atlantic Ocean: The U.S. GEOTRACES zonal and meridional sections
Licensed content author	Katlin L. Bowman,Chad R. Hammerschmidt,Carl H. Lamborg,Gretchen Swarr
Licensed content date	Available online 24 July 2014
Licensed content volume number	n/a
Licensed content issue number	n/a
Number of pages	1
Start Page	None
End Page	None

Type of Use	reuse in a thesis/dissertation
Intended publisher of new work	other
Portion	full article
Format	both print and electronic
Are you the author of this Elsevier article?	Yes
Will you be translating?	No
Title of your thesis/dissertation	Mercury distributions and cycling in the North Atlantic and Eastern Tropical South Pacific Oceans
Expected completion date	Dec 2014
Estimated size (number of pages)	
Elsevier VAT number	GB 494 6272 12
Permissions price	0.00 USD
VAT/Local Sales Tax	0.00 USD / 0.00 GBP
Total	0.00 USD

(Appendix A) Storage bottle material and cleaning for determination of total mercury in seawater

To: Ms Katlin L Bowman

On behalf of the Association for the Sciences of Limnology and Oceanography, we are happy to grant permission to use the figures fromLimnology & Oceanography per your application below.

When reproducing the article/figure(s), please cite according to the references that follow:

All copyrighted works, whether displayed electronically or in print, should be properly acknowledged as follows:

"Copyright 2014 by the Association for the Sciences of Limnology and Oceanography, Inc."

Once permission is granted to use an article or any part thereof of a work from L&O, the full citation must include:
1. Name(s) of the author(s);
2. Journal title (Association for the Sciences of Limnology & Oceanography or L&O)
3. Publication date
4. Volume number
5. Issue number
6. Chapter or article name
7. Pages on which the articles, data, and/ or figure(s) appear

For your records, the Association for the Sciences of Limnology and Oceanography is a nonprofit organization. (Taxpayer I.D. Number: 38-1710020)

If you have additional requests or have any questions in regard to this request, you can contact me directly via e-mail at jdavis@sgmeet.com.

Sincerely,

Jo Davis
ASLO Business Office
Database Supervisor

Will the copyrighted material appear in a for-profit publication? no

Will the copyrighted material appear in a not-for-profit publication?
yes
Proposed Publication Date: December 2013

REQUESTOR INFORMATION
Requestor: Ms Katlin L Bowman
Contact's Name (if different):
Institution: Wright State University
Department: Earth & Environmental Sciences Mailing Address:
425 Dayton Towers Drive Apt. 12Q
Dayton, Ohio 45410
United States
Telephone: 3302611039
Fax:
Email: bowman.49@wright.edu

INTENDED USE
Publication in which material will appear:
PhD Dissertation
Publisher: Wright State University

MATERIAL TO BE USED
Author(s) Name(s): Chad R. Hammerschmidt, Katlin L. Bowman, Melissa D. Tabatchnick, Carl H. Lamborg Journal Title: Limnology and Oceanography: Methods Publication Date: 2011
Volume: 9
Issue:
Chapter, article or figure name or title: Storage bottle material and cleaning for determination of total mercury in seawater Pages on which articles, data or figures appear: 426-431
Special notes:

(Appendix B) Vertical methylmercury distribution in the subtropical North Pacific Ocean

ELSEVIER LICENSE
TERMS AND CONDITIONS

Nov 12, 2014

This is a License Agreement between Katlin L. Bowman ("You") and Elsevier ("Elsevier") provided by Copyright Clearance Center ("CCC"). The license consists of your order details, the terms and conditions provided by Elsevier, and the payment terms and conditions.

All payments must be made in full to CCC. For payment instructions, please see information listed at the bottom of this form.

Supplier	Elsevier Limited The Boulevard,Langford Lane Kidlington,Oxford,OX5 1GB,UK
Registered Company Number	1982084
Customer name	Katlin L. Bowman
Customer address	425 Dayton Towers Drive DAYTON, OH 45410
License number	3485100289287
License date	Oct 09, 2014
Licensed content publisher	Elsevier
Licensed content publication	Marine Chemistry
Licensed content title	Vertical methylmercury distribution in the subtropical North Pacific Ocean
Licensed content author	Chad R. Hammerschmidt,Katlin L. Bowman
Licensed content date	20 March 2012
Licensed content volume number	132
Licensed content issue number	n/a
Number of pages	6
Start Page	77
End Page	82
Type of Use	reuse in a thesis/dissertation

Portion	full article
Format	both print and electronic
Are you the author of this Elsevier article?	Yes
Will you be translating?	No
Title of your thesis/dissertation	Mercury distributions and cycling in the North Atlantic and Eastern Tropical South Pacific Oceans
Expected completion date	Dec 2014
Estimated size (number of pages)	200
Elsevier VAT number	GB 494 6272 12
Permissions price	0.00 USD
VAT/Local Sales Tax	0.00 USD / 0.00 GBP
Total	0.00 USD

(Appendix C) Mercury in the anthropocene ocean

(Appendix D) A global ocean inventory of anthropogenic mercury based on water column measurements

Author Requests

If you are the author of this content (or his/her designated agent) please read the following. Since 2003, ownership of copyright in in original research articles remains with the Authors*, and provided that, when reproducing the Contribution or extracts from it, the Authors acknowledge first and reference publication in the Journal, the Authors retain the following non-exclusive rights:

a. To reproduce the Contribution in whole or in part in any printed volume (book or thesis) of which they are the author(s).

b. They and any academic institution where they work at the time may reproduce the Contribution for the purpose of course teaching.

c. To reuse figures or tables created by them and contained in the Contribution in other works created by them.

d. To post a copy of the Contribution as accepted for publication after peer review (in Word or Tex format) on the Author's own web site, or the Author's institutional repository, or the Author's funding body's archive, six months after publication of the printed or online edition of the Journal, provided that they also link to the Journal article on NPG's web site (eg through the DOI).

NPG encourages the self-archiving of the accepted version of your manuscript in your funding agency's or institution's repository, six months after publication. This policy complements the recently announced policies of the US National Institutes of Health, Wellcome Trust and other research funding bodies around the world. NPG recognizes the efforts of funding bodies to increase access to the research they fund, and we strongly encourage authors to participate in such efforts.
Authors wishing to use the published version of their article for promotional use or on a web site must request in the normal way.
If you require further assistance please read NPG's online author reuse guidelines.
Note: *British Journal of Cancer* maintains copyright polices of its own that are different from the general NPG policies. Please consult this journal to learn more.
* Commissioned material is still subject to copyright transfer condition.